

# Perturbation and operator methods for solving Stokes flow and heat flow problems

**Citation for published version (APA):**

Chandra, T. D. (2002). *Perturbation and operator methods for solving Stokes flow and heat flow problems*. [Phd Thesis 1 (Research TU/e / Graduation TU/e), Mathematics and Computer Science]. Technische Universiteit Eindhoven. <https://doi.org/10.6100/IR554634>

**DOI:**

[10.6100/IR554634](https://doi.org/10.6100/IR554634)

**Document status and date:**

Published: 01/01/2002

**Document Version:**

Publisher's PDF, also known as Version of Record (includes final page, issue and volume numbers)

**Please check the document version of this publication:**

- A submitted manuscript is the version of the article upon submission and before peer-review. There can be important differences between the submitted version and the official published version of record. People interested in the research are advised to contact the author for the final version of the publication, or visit the DOI to the publisher's website.
- The final author version and the galley proof are versions of the publication after peer review.
- The final published version features the final layout of the paper including the volume, issue and page numbers.

[Link to publication](#)

**General rights**

Copyright and moral rights for the publications made accessible in the public portal are retained by the authors and/or other copyright owners and it is a condition of accessing publications that users recognise and abide by the legal requirements associated with these rights.

- Users may download and print one copy of any publication from the public portal for the purpose of private study or research.
- You may not further distribute the material or use it for any profit-making activity or commercial gain
- You may freely distribute the URL identifying the publication in the public portal.

If the publication is distributed under the terms of Article 25fa of the Dutch Copyright Act, indicated by the "Taverne" license above, please follow below link for the End User Agreement:

[www.tue.nl/taverne](http://www.tue.nl/taverne)

**Take down policy**

If you believe that this document breaches copyright please contact us at:

[openaccess@tue.nl](mailto:openaccess@tue.nl)

providing details and we will investigate your claim.

**Perturbation and Operator Methods  
for Solving Stokes Flow and Heat Flow Problems**



**Perturbation and Operator Methods  
for Solving Stokes Flow and Heat Flow Problems**

PROEFSCHRIFT

ter verkrijging van de graad van doctor aan de  
Technische Universiteit Eindhoven, op gezag van de  
Rector Magnificus, prof.dr. R.A. van Santen, voor een  
commissie aangewezen door het College voor  
Promoties in het openbaar te verdedigen  
op woensdag 22 mei 2002 om 16:00 uur

door

**Tjang Daniel Chandra**

geboren te Malang, Indonesië

Dit proefschrift is goedgekeurd door de promotoren:

prof.dr.ir. J. de Graaf  
en  
prof.dr. J. Molenaar

Copromotor:  
dr. S.W. Rienstra

CIP-DATA LIBRARY TECHNISCHE UNIVERSITEIT EINDHOVEN

Chandra, Tjang Daniel

Perturbation and operator methods for solving Stokes flow and heat flow problems / by Tjang Daniel Chandra. - Eindhoven : Technische Universiteit Eindhoven, 2002.

Proefschrift. - ISBN 90-386-0542-0

NUGI 811

Subject headings : elliptic partial differential equations / differential equations ; perturbation methods

2000 Mathematics Subject Classification : 35Q30

Printed by University Press Facilities, Eindhoven University of Technology

*Dedicated to my wife Kezia Sri Juliati  
and  
my son Stefanus Albert Chandra*



# Contents

<b>Introduction</b>	<b>1</b>
<b>I Perturbation methods</b>	<b>7</b>
1 Introduction . . . . .	7
2 Preliminary definitions . . . . .	8
3 Regular and singular perturbations . . . . .	13
3.1 Regular perturbations . . . . .	13
3.2 Singular perturbation of boundary layer type . . . . .	15
4 Method of slow variation . . . . .	23
4.1 Examples . . . . .	24
5 Method of slight variation . . . . .	39
5.1 Example . . . . .	40
6 The Stokes equation . . . . .	42
6.1 Example . . . . .	44
<b>II Analytical approximations to the viscous glass flow problem in the mould–plunger pressing process, including an investigation of boundary conditions</b>	<b>49</b>
1 Introduction . . . . .	50
2 Governing equations . . . . .	51
3 Slender-geometry approximation . . . . .	52
4 The temperature problem . . . . .	54
5 Boundary conditions . . . . .	56
5.1 Boundary conditions on the plunger . . . . .	56
5.2 Boundary conditions on the mould . . . . .	58
5.3 The free surface . . . . .	58
6 Some auxiliary results . . . . .	59
6.1 The flux . . . . .	59
6.2 The total force on the plunger . . . . .	60
7 Results . . . . .	61
7.1 The velocity and pressure field . . . . .	61
7.2 The force on the plunger . . . . .	62
7.3 A prescribed force or velocity of the plunger . . . . .	63
8 Examples . . . . .	64
8.1 A given plunger velocity . . . . .	64



8.2	A given plunger force . . . . .	67
8.3	Numerical method . . . . .	69
9	Conclusions . . . . .	70
<b>III On an operator equation for Stokes boundary value problems</b>		<b>73</b>
1	Introduction . . . . .	73
2	General Theory . . . . .	74
2.1	The Dirichlet problem . . . . .	74
2.2	The Neumann problem . . . . .	75
2.3	A parameterized class of solutions . . . . .	76
2.4	The operator equation on the boundary $\partial\Omega$ . . . . .	76
3	Applications . . . . .	77
3.1	The interior of the unit disk . . . . .	77
3.2	The interior of the unit ball . . . . .	79
<b>IV Further illustrations of the operator method</b>		<b>85</b>
1	Introduction . . . . .	85
2	The exterior of the unit disk . . . . .	85
2.1	The operator equation . . . . .	86
2.2	Solution . . . . .	87
3	The exterior of the unit ball . . . . .	88
3.1	The operator equation . . . . .	89
3.2	Solution . . . . .	90
4	An inhomogeneous SBVP in the unit disk . . . . .	91
4.1	Subproblems . . . . .	91
4.2	Solution . . . . .	96
5	A Half-space . . . . .	98
5.1	The operator equation . . . . .	98
5.2	Solution . . . . .	101
6	An infinite strip . . . . .	101
6.1	The operator equation . . . . .	102
6.2	Solution . . . . .	105
7	An infinite wedge . . . . .	106
7.1	The Dirichlet problem . . . . .	106
7.2	The Neumann problem . . . . .	108
7.3	The operator equation . . . . .	108
7.4	Solution . . . . .	110
<b>V The effect of spatial inhomogeneity in thermal conductivity on the formation of hot-spots</b>		<b>111</b>
1	Introduction . . . . .	111
2	Governing equations . . . . .	113
3	Analysis of the reduced equation . . . . .	115
3.1	Behaviour of solutions . . . . .	115

3.2	Fundamental mode approximation . . . . .	118
3.3	Steady-state solution for a unit slab geometry . . . . .	119
4	Formation of hot-spots in a three-layer finite slab . . . . .	120
4.1	Formulation of the problem . . . . .	121
4.2	Steady-state solutions . . . . .	122
5	Numerical results . . . . .	125
6	Concluding remarks . . . . .	127
	<b>Bibliography</b>	<b>129</b>
	<b>Index</b>	<b>132</b>
	<b>Summary</b>	<b>134</b>
	<b>Acknowledgements</b>	<b>135</b>
	<b>Curriculum Vitae</b>	<b>136</b>



# Introduction

One of the branches of mathematics is applied mathematics. In this field, the mathematics is studied that originates from applications. Here, we restrict ourselves to physical applications. One usually translates the physical problem into ordinary or partial differential equations and their initial and boundary conditions. This process is called mathematical modelling. In many cases, the governing equations can not be solved exactly. Therefore, one looks for an approximate solution. There are two approaches for obtaining approximate solutions : an analytical and a numerical one. As a first step in the modelling process, the governing equations are made dimensionless. This process often yields one or more small dimensionless parameters. After comparing the order of magnitudes of terms in the governing equations, we can neglect the terms that are apparently too small to be of relevance. If the remaining model still contains a small parameter ( $\varepsilon$ ), we can utilise perturbation methods. Based on this parameter, we assume that the solution of the governing equations can be expanded into an asymptotic expansion. After substitution of the expansion into the governing equations, each coefficient of  $\varepsilon$  must vanish and a sequence of differential equations results that has to be solved successively. In some cases, the geometry (the domain of interest) of the problem leads to the small parameter. For example, if there are two different length scales and their ratio is small, then we have this ratio as a small parameter.

In this thesis, we apply the above procedure to the modelling of glass flow and heat flow problems. The former modelling leads to Stokes flow, while the latter is related to a heat conduction model problem, and a microwave heating problem. We will consider two different approaches to solve the Stokes flow problem, namely perturbation and operator methods. To solve the heat conduction problem, we use perturbation methods. Finally, using a fundamental-mode approximation of an eigenfunction expansion, we consider the microwave heating problem. First, we will discuss the glass flow problem.

Glass is a widely used packing material, for example in the form of jars and bottles in the food industry. The production of glass forms like jars goes more or less as follows. First, grains and additives, like soda, are heated in a tank. Here, gas burners or electric heaters provide the heat necessary to warm the material up to about 1200°C. At one end the liquid glass comes out and is led to a pressing or blowing machine. To obtain a glass form a two-stage process is often used. First, a blob of hot glass called a gob falls into a configuration consisting of a *mould* and *plunger*. As soon as the gob has fallen into this mould, the plunger starts moving to press the glass. This process is called *pressing* (see Figure 0.1). At the end, the glass drop is reshaped into the preform of a bottle or a jar called a *parison*. After a short period of time, for cooling purposes (the mould is kept at 500°C), the parison is blown to its

final shape in another mould. This process is called *blowing* (see Figure 0.2). In this thesis we only consider the glass flow during the pressing phase.

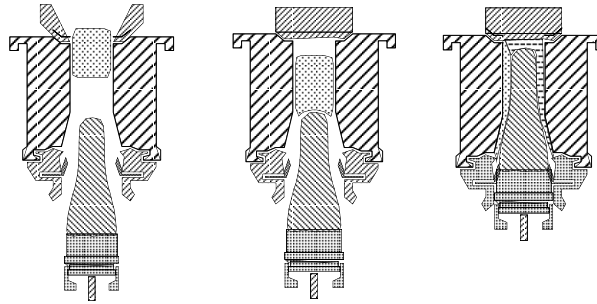


Figure 0.1: Pressing phase

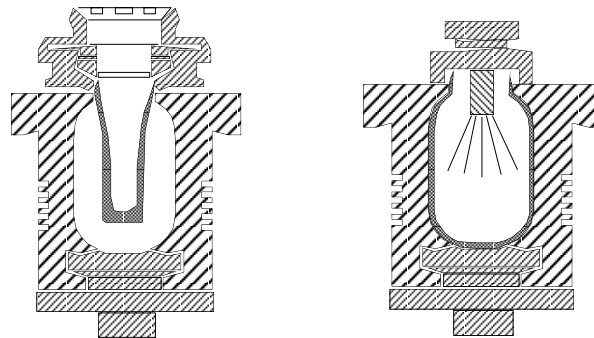


Figure 0.2: Blowing phase

The glass flow at temperatures above  $600^{\circ}\text{C}$  can be described by the Navier-Stokes equations for incompressible Newtonian fluids. Moreover, in view of the geometry of plunger and mould, we choose axisymmetric cylindrical coordinates. Therefore we have a two-dimensional problem in the  $(r, z)$  plane. Next, we make the Navier-Stokes equations dimensionless using appropriate scalings. Note that we concentrate our analysis on the glass flow in the narrow annular duct between plunger and mould, in other words, the annular duct is slender. Therefore, we have two relevant length scales, namely the wall thickness of the parison ( $D$ ) and the length of the plunger ( $L$ ), with  $D \ll L$ . So, we can introduce a small parameter  $\varepsilon = D/L$ . There are two ways of scaling :

1. We scale both  $z$  and  $r$  with  $D$ . Using the characteristic data of the glass flow such as velocity, viscosity, length scale, etc, we obtain that the glass flow is highly viscous (the Reynolds number is small). Therefore, we can ignore the inertia terms of the Navier-Stokes equations and we arrive at the Stokes equations. To proceed, we make a rescaling  $Z = \varepsilon z$  and assume that the velocity and the pressure can be expanded into asymptotic expansions based on  $\varepsilon$ .
2. We scale  $z$  with  $L$  and  $r$  with  $D$ . Next, we expand the velocity and the pressure into asymptotic expansion to obtain a set of equations called Reynolds lubrication-flow equations. This approach is still valid if the Reynolds number ( $Re$ ) is  $O(1)$ , because  $Re$  occurs only in the combination  $\varepsilon Re$ .

Since we assume that there are no more length scales in the  $z$  direction, we can use both scalings. To solve the system of equations completely, we need to consider the boundary conditions.

During the formation process of glass, a lubricant like graphite powder is extensively used in order to improve the sliding conditions of the glass inside the mould. Lack of lubrication will affect the final quality of the glass product. The presence of this lubricant suggests us to consider slip-type boundary conditions. This means that the tangential component of the glass velocity  $\mathbf{v}$  at the wall differs from the wall velocity  $\mathbf{v}_w$ , the difference being called the slip velocity. In this research, we consider Navier's slip condition, which assumes that the slip velocity is proportional to the tangential (shear) stress. The slip factor ( $s$ ) measures the amount of slip. There is no slip if  $s = 0$ , while there is no friction if  $s = \infty$ . The other boundary conditions describe that the walls of plunger and mould are solid. This implies that, the normal component of the velocity is zero. To determine the velocity completely, we have to know the pressure gradient. This pressure gradient can be found, if we know the value of the flux for every level  $z$ . As shown in Figure 0.1, as the plunger goes down, it causes the glass to move upward through a varying cross section such that the volume flux for every level  $z$  is not constant. Using Gauss' theorem, we can determine the value of this flux. Finally, we can determine the velocity and the pressure gradient of the glass flow analytically. Further, using the results obtained, we can derive a formula for the total force on the plunger.

Next, we discuss two examples. In the first one, we use simple parabolic profiles for the plunger and the mould, while the velocity of the plunger is given. We find a good agreement between the velocity obtained analytically and numerical results from the Finite Element Method. Using the given velocity of the plunger, we calculate the total force on the plunger. In the second example, we use a geometry of a real plunger and mould, while the plunger force is prescribed. Using this force, we can determine semi-analytically both the velocity of the plunger and the position of the top of the plunger as a function of time.

Now, we consider the second approach to solve Stokes boundary value problem. We use the method described in Padmavathi et al [40] and Sheng and Zhong [46] to translate the Stokes equations into an operator equation on the boundary  $\partial\Omega$  of the domain  $\Omega$  with a tangent vector field  $\boldsymbol{\alpha}$  on the boundary  $\partial\Omega$  as unknown. To obtain the operator equation, we have to solve Dirichlet and Neumann problems. This operator equation leads to the solution of the Stokes boundary value problem that can be parameterized by  $\boldsymbol{\alpha}_\mathcal{H}$ , the *harmonic extension* of  $\boldsymbol{\alpha}$  to the interior of the domain  $\Omega$ .

As an application of the above method, we give some examples of solving Stokes boundary value problems for some simple domains such as the interior and the exterior of the unit disk and of the unit ball, a half space, an infinite strip, etc.

Besides of the Stokes flow, in this thesis we also consider heat flow problems. First, we discuss heat conduction in correspondence with the type of the geometry of the problem, and second, nonlinear heat conduction related to microwave heating. Following van Dyke [13,14], we investigate two types of geometry, a slowly and a slightly varying geometry. In the former geometry, the variation of the length scale in one direction is slower than in the other direction. Mathematically, we write the boundary as  $y = R(\varepsilon x)$ . We solve this problem by rescaling  $X = \varepsilon x$ . In the latter geometry, the boundary varies a little but not slowly. We write the boundary (typically) as  $y = \varepsilon R(x)$ . For each geometry we present examples of heat conduction problem to describe the difference of both geometries.

Next, we consider the microwave heating problem. Recently microwave radiation for heating is more and more applied, with applications like cooking, melting, sintering, and drying. This heating technique has advantages over the use of a conventional heating, such as speed of heating, the potential to heat the material without heating its surroundings, etc. However, the widespread industrial application of microwave heating faces the formation of hot-spots, that is small regions of very high temperature relative to the surroundings. Such a phenomenon can either be desirable, such as in metal melting, or undesirable, such as in ceramic sintering.

In general, the modelling of the microwave heating involves a coupling of electromagnetic and thermal phenomena. These phenomena can be expressed mathematically as a system of a damped wave equation derived from Maxwell's equations governing the propagation of the microwave radiation and a forced heat equation governing the heat flow. In this research, we assume a temperature independent of the electrical conductivity of the material and microwave speed. Therefore, we may solve the damped wave equation separately, which leads to a single forced heat equation governing the heat flow. Next, we focus on solving the heat problem to investigate the effect of the inhomogeneity of conductivity on the formation of a hot-spot. The governing equation is

$$\frac{\partial \theta}{\partial t} = \nabla \cdot (k(\theta) \nabla \theta) + \delta |E|^2 f(\theta),$$

with  $\theta$  the temperature,  $k(\theta)$  thermal conductivity of the material,  $\delta$  a positive parameter related to the intensity of electric field,  $|E|$  is the amplitude of the electric field, and  $f(\theta)$  the rate of the microwave energy absorption by the material. Here, we take it to be of Arrhenius type. We consider a one-dimensional unit slab consisting of three layers of material with different thermal conductivity. We assume the thermal conductivity of the form  $k(\theta) = \mu e^{\nu \theta}$ , where  $\theta$  is the temperature, while the parameter  $\mu$  has different values in each of the three layers. This  $\mu$  measures the magnitude of the thermal conductivity of the material and the inner layer has the smallest value of the parameter  $\mu$ . To simplify the problem, we consider only the steady-state solution and use the Dirichlet boundary conditions on each layer. The other boundary conditions require that both the temperature and the heat flux are continuous across the layers.

To solve the problem, we use an eigenfunction expansion based on the Galerkin method and we consider only the fundamental-mode approximation. In [1], Andonowati has shown numerically that this fundamental mode is dominant for some geometries such as a unit sphere, a finite cylinder, a rectangular block and for Dirichlet boundary conditions. Therefore, we focus on this fundamental mode. For three layers, we obtain a system of equations that is solved numerically.

First, as an example, we consider a unit slab geometry. In this geometry, we show that the bifurcation diagram of possible steady-states of the temperature  $\theta$  and  $\delta$  is S-shaped. This means that there is an interval with three solutions, two of which are stable. So, there are critical values  $\delta_{cr}$  and  $\delta^{cr}$ , for which a slight change in  $\delta$  yields a catastrophic increase or decrease in the temperature. Next, we consider a unit slab consisting of three layers of material with different thermal conductivity ( $\mu$ ). We assume the inner layer has the smallest value of  $\mu$ . We find the temperature in this layer is higher than that in other layers. It means that a smaller  $\mu$  yields a higher temperature. The larger the difference of  $\mu$  in the inner and outer layers, the larger the discrepancy of the temperature between the inner layer and the rest of the region will be. Further, we consider only the inner layer. For fixed value of  $\delta$ , we get a temperature jump near some values of  $\mu$ . This jump shows that there is a critical value of  $\mu$  and indicates the formation of a hot-spot.

Let us briefly outline the structure of this thesis. Chapters I and II present the perturbation method. Chapter I contains some notions from the perturbation method such as the symbol  $O$  and  $o$ , asymptotic expansion, regular and singular perturbations of boundary layer type. We discuss two types of geometry, the slowly and slightly varying geometry. Finally, we close this chapter by investigating the Stokes equations in a semi-infinite slowly varying geometry. This investigation gives a motivation to derive a general theory for solving the Stokes boundary value problems.

In chapter II, we discuss the modelling of the glass flow including an investigation of the boundary conditions. We solve the glass flow problem using asymptotic expansions based on the slowly varying geometry of the plunger and the mould. This (slightly adapted) chapter appeared in the Journal of Engineering Mathematics 39:241-259, 2001.

Chapters III - IV present the operator method. In chapter III, we derive the operator equation from the Stokes boundary value problems. Some examples of solving the problems are presented for domains such as the interior of a disk and of a ball. This (slightly adapted) chapter is accepted to be included into the Proceedings of 4<sup>th</sup> European Conference on Elliptic and Parabolic Problems, Rolduc, June 18-22, 2001.

Next, further application of the operator method for solving Stokes boundary value problems with as domains such as the exterior of the unit disk and of the unit ball, a half-space, an infinite strip, etc, are discussed in Chapter IV.

Finally, in chapter V, we consider a simplified model of the microwave heating of a one-dimensional unit slab. Using an eigenfunction expansion for the problem based on the Galerkin method with a fundamental-mode approximation, we investigate the effect of thermal conductivity on the formation of hot-spots. This chapter appeared in the Journal of Engineering Mathematics 38:101-118, 2000.





# Chapter I

## Perturbation methods

### 1 Introduction

The mathematical solution of a “real world” problem starts with the modelling phase, where the problem is described in a mathematical representation of its primitive elements and their relations. As the solution is not served by unnecessary complexity, we are interested in an adequate mathematical description with the lowest number of essentially independent parameters and variables.

A very important aspect in the modelling is therefore the introduction of a hierarchy of importance: to distinguish the important, a little bit important, and unimportant effects. Based on this hierarchy it is decided which aspects can be included and which can be neglected in the model.

For exactly this reason some effects in any modelling will be small: sometimes small but not small enough to be ignored, and sometimes small but in a non-uniform way such that they are important locally.

For an efficient solution, and to obtain qualitative insight, it makes sense to utilize this “smallness”. Methods that systematically exploit such inherent smallness are called “perturbation methods”.

Perturbation methods have a long history. Before the time of numerical methods and computers, perturbation methods were the only way to increase the applicability of available exact solutions to difficult, and otherwise intractable problems. Nowadays, perturbation methods have their use as a natural step in the process of systematic modelling, since they provide insight in the nature of singularities occurring in the problem and in typical parameter dependencies, and sometimes they increase the speed of practical calculations.

We will consider here a class of perturbation problems connected to Stokes flow (flow of high Newtonian viscosity) confined by slightly deformed simple geometries. The problem is inspired by glass flow, which is an important problem of such flows, although of course there are other types of confined Stokes flow, *e.g.* lubrication flow in bearings.

To illustrate the methods we will sometimes consider the simpler problem of stationary heat flow, which amounts to solving the more easily accessible Laplace equation. Both problems are, however, of elliptic type, and therefore the heat problem may serve as a suitable model problem.

## 2 Preliminary definitions

In this section, we discuss some definitions that will be used frequently in the subsequent sections. First, since we are only interested in comparing the behaviour of functions  $f(\varepsilon)$  with a gauge function  $\phi(\varepsilon)$  as a parameter  $\varepsilon \rightarrow 0$ , we introduce order symbols to define an asymptotic approximation. For example,  $f(\varepsilon) = \varepsilon^3$  tends to zero faster than  $\phi(\varepsilon) = \varepsilon$  as  $\varepsilon \rightarrow 0$ . The following definitions describe a notation for this behaviour.

**Definition 2.1.** ( Large  $O$  )

1. For a given  $\varepsilon$ -interval  $I = \{\varepsilon \mid 0 < \varepsilon \leq \varepsilon_1\}$ , we say that

$$f(\varepsilon) = O(\phi(\varepsilon)) \text{ as } \varepsilon \rightarrow 0, \quad (2.1)$$

if there exists a positive number  $k$  independent of  $\varepsilon$  and a neighbourhood  $N$  of  $\varepsilon = 0$  such that

$$|f(\varepsilon)| \leq k |\phi(\varepsilon)| \text{ for all } \varepsilon \text{ in } N \cap I. \quad (2.2)$$

Note that if the limit

$$\lim_{\varepsilon \rightarrow 0} \frac{f(\varepsilon)}{\phi(\varepsilon)} \quad (2.3)$$

exists and is finite then  $f(\varepsilon) = O(\phi(\varepsilon))$  as  $\varepsilon \rightarrow 0$ .

2. Similarly, for a given domain  $D \subset \mathbb{R}^n$  and  $\varepsilon$ -interval  $I$ , we say that

$$f(\mathbf{x}; \varepsilon) = O(\phi(\mathbf{x}; \varepsilon)) \text{ as } \varepsilon \rightarrow 0, \quad (2.4)$$

if for each  $\mathbf{x} \in D$ , there exist a positive number  $k(\mathbf{x})$  and a neighbourhood  $N(\mathbf{x})$  of  $\varepsilon = 0$  such that

$$|f(\mathbf{x}; \varepsilon)| \leq k(\mathbf{x}) |\phi(\mathbf{x}; \varepsilon)| \text{ for all } \varepsilon \text{ in } N(\mathbf{x}) \cap I. \quad (2.5)$$

**Definition 2.2.** (Uniformity)

$f(\mathbf{x}; \varepsilon) = O(\phi(\mathbf{x}; \varepsilon))$  is uniformly valid in  $D$  if in (2.5) both  $k$  and  $N$  are independent of  $\mathbf{x}$ .

**Definition 2.3.** ( Small  $o$  )

1. We say that

$$f(\varepsilon) = o(\phi(\varepsilon)) \text{ as } \varepsilon \rightarrow 0, \quad (2.6)$$

if for any given  $\delta > 0$ , there exists an  $\varepsilon$ -interval  $I(\delta) = \{\varepsilon \mid 0 < \varepsilon \leq \varepsilon_1(\delta)\}$  such that

$$|f(\varepsilon)| \leq \delta |\phi(\varepsilon)| \text{ for all } \varepsilon \text{ in } I. \quad (2.7)$$

Note that if

$$\lim_{\varepsilon \rightarrow 0} \frac{f(\varepsilon)}{\phi(\varepsilon)} = 0 \quad (2.8)$$

then  $f(\varepsilon) = o(\phi(\varepsilon))$  as  $\varepsilon \rightarrow 0$ .

2. Similarly, for a given domain  $D \subset \mathbb{R}^n$ , we say that

$$f(\mathbf{x}; \varepsilon) = o(\phi(\mathbf{x}; \varepsilon)) \text{ as } \varepsilon \rightarrow 0 \quad (2.9)$$

if for each  $\mathbf{x} \in D$  and any given  $\delta > 0$ , there exist an  $\varepsilon$ -interval  $I(\mathbf{x}, \delta) = \{\varepsilon \mid 0 < \varepsilon \leq \varepsilon_1(\mathbf{x}, \delta)\}$  such that

$$|f(\mathbf{x}; \varepsilon)| \leq \delta |\phi(\mathbf{x}; \varepsilon)| \text{ for all } \varepsilon \text{ in } I. \quad (2.10)$$

**Definition 2.4.** (Uniformity)

$f(\mathbf{x}; \varepsilon) = o(\phi(\mathbf{x}; \varepsilon))$  is uniformly valid in  $D$  if in (2.10)  $\varepsilon_1$  depends only on  $\delta$  but not on  $\mathbf{x}$ .

Note that  $f = o(\phi)$  implies  $f = O(\phi)$  but the converse is not true. We write  $f = O_s(\phi)$  if  $f = O(\phi)$  but  $f \neq o(\phi)$  (see Example 2.5).

**Example 2.5**

We have

$$\varepsilon \cos(\varepsilon) = O(\varepsilon) \text{ as } \varepsilon \rightarrow 0, \quad (2.11)$$

since  $|\varepsilon \cos(\varepsilon)| \leq |\varepsilon|$  for all  $\varepsilon > 0$ . At the same time,  $\varepsilon \cos(\varepsilon) \neq o(\varepsilon)$ , and therefore  $= O_s(\varepsilon)$ .

**Example 2.6**

$$\frac{\varepsilon}{\varepsilon^\varepsilon - 1} = O\left(\frac{1}{\ln(\varepsilon)}\right) \text{ as } \varepsilon \rightarrow 0, \quad (2.12)$$

because  $\lim_{\varepsilon \rightarrow 0} \frac{\varepsilon \ln(\varepsilon)}{\varepsilon^\varepsilon - 1} = 1$ .

**Example 2.7**

We have

$$\varepsilon^\alpha = o(1) \text{ where } \alpha > 0, \text{ as } \varepsilon \rightarrow 0, \quad (2.13)$$

since for any given  $\delta > 0$ , (2.7) holds provided that  $\varepsilon \in I(\delta) = \{\varepsilon \mid 0 < \varepsilon \leq \delta^{1/\alpha}\}$ .

**Example 2.8**

Since

$$e^{-1/\varepsilon} = o(\varepsilon^n), \text{ as } \varepsilon \rightarrow 0, \text{ for any } n, \quad (2.14)$$

$e^{-1/\varepsilon}$  is called a transcendentally small term (TST) or an exponentially small term (EST) and can be ignored asymptotically against any power of  $\varepsilon$ .

**Example 2.9**

Let  $D = \{x \mid 0 < x < 1\}$ . We have  $\cos(\frac{x}{\varepsilon}) = O(1)$  as  $\varepsilon \rightarrow 0$  uniformly valid in  $D$  since we can choose  $k = 1.1$  such that  $|\cos(\frac{x}{\varepsilon})| \leq k$  for all  $x \in D$ . However,  $\cos(\frac{x}{\varepsilon}) = O(x)$  as  $\varepsilon \rightarrow 0$  is not uniformly valid in  $D$  since there is no constant  $k$  such that  $|\cos(\frac{x}{\varepsilon})| \leq kx$  for all  $x \in D$ .

**Example 2.10**

Let  $D = \{x \mid 0 < x < 1\}$ . Then,  $x^2 + e^{-x/\varepsilon} = O(x^2)$  as  $\varepsilon \rightarrow 0$  in  $D$ , since  $k(x) = 1 + \frac{1}{x^2}$  such that

$$|x^2 + e^{-x/\varepsilon}| \leq (1 + \frac{1}{x^2})x^2, \text{ for all } x \in D. \quad (2.15)$$

There is no  $k(x)$  possible independent of  $x$ , so this is not uniformly. On the other hand, for  $D_A = \{x \mid 0 < A < x < 1\}$ , we can choose  $\varepsilon_1 = A/\ln A^{-2}$  and  $k = 2$  such that now

$$|x^2 + e^{-x/\varepsilon}| = x^2(1 + x^{-2}e^{-x/\varepsilon}) \leq x^2(1 + A^{-2}e^{-A/\varepsilon}) \leq 2x^2 \text{ for all } x \in D_A, \quad (2.16)$$

and  $x^2 + e^{-x/\varepsilon} = O(x^2)$  uniformly on  $D_A$ .

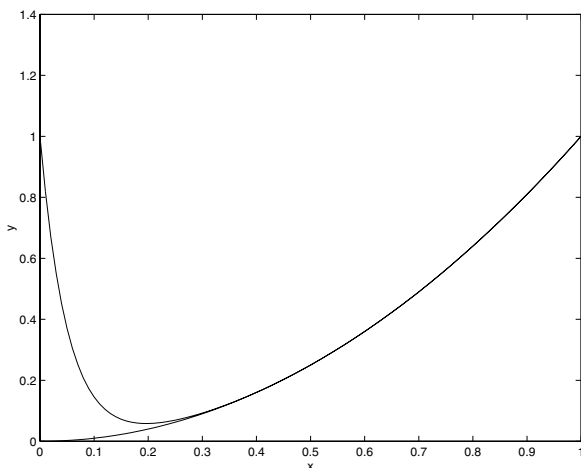


Figure 2.1: Comparison between  $y(x; \varepsilon) = x^2 + e^{-x/\varepsilon}$  and its asymptotic approximation  $x^2$  for  $\varepsilon = 0.1$ .

Figure (2.1) shows the graph of  $y(x; \varepsilon) = x^2 + e^{-x/\varepsilon}$  and its asymptotic approximation  $x^2$  for  $\varepsilon = 0.1$ . It appears that the approximation is good for  $x$  not near 0. For  $x$  too close to zero,  $x^2$  does not approximate  $y(x; \varepsilon)$  asymptotically, no matter how small  $\varepsilon$  is. The region  $x$  near zero is an example of a boundary layer. We will discuss boundary layers in more detail in the next section.

**Example 2.11**

Let  $D = \{x \mid x > 0\}$ . Then

$$x\varepsilon^\alpha = o(x^2) \text{ where } \alpha > 0, \text{ as } \varepsilon \rightarrow 0, \quad (2.17)$$

since for any given  $\delta > 0$ , (2.10) holds provided that  $\varepsilon \in I(x, \delta) = \{\varepsilon \mid 0 < \varepsilon \leq (x\delta)^{1/\alpha}\}$ . Since this interval depends on  $x$ , (2.17) is not uniformly valid in  $D$ . However, if we restrict  $D$  to  $D_1 = \{x \mid 0 < x \leq X_1\}$  with  $X_1$  is a fixed constant, then (2.17) is uniformly valid in  $D_1$  since the interval becomes  $I(\delta) = \{\varepsilon \mid 0 < \varepsilon \leq (X_1\delta)^{1/\alpha}\}$ , which does not depend anymore on  $x$ .

Next, we give the definitions of asymptotic sequence and asymptotic expansion. This expansion can be either uniform or non uniform. Those definitions play an important role in perturbation methods that we will discuss in next section.

**Definition 2.12.** (Asymptotic Sequence)

A sequence  $\{\mu_n(\varepsilon)\}_{n=1}^{\infty}$  is called an asymptotic sequence, if  $\mu_{n+1}(\varepsilon) = o(\mu_n(\varepsilon))$ , as  $\varepsilon \rightarrow 0$ , for each  $n = 1, 2, \dots$ .

**Example 2.13**

The following are examples of asymptotic sequences (as  $\varepsilon \rightarrow 0$ )

$$\begin{aligned} \mu_n(\varepsilon) = \varepsilon^n, \quad \mu_n(\varepsilon) = \varepsilon^{n/2}, \quad \mu_n(\varepsilon) = \tan^n(\varepsilon), \quad \mu_n(\varepsilon) = \ln(\varepsilon)^{-n}, \\ \mu_n(\varepsilon) = \varepsilon^p \ln(\varepsilon)^q \text{ where } p = 0, 1, 2, \dots, \quad q = 0 \dots p \text{ and } n = \frac{1}{2}p(p+3) - q. \end{aligned} \quad (2.18)$$

In terms of asymptotic sequences, we can define asymptotic expansions as follows

**Definition 2.14.** (Asymptotic Expansion)

Let  $f(\mathbf{x}; \varepsilon)$  be defined in some domain  $D$  and some neighbourhood of  $\varepsilon = 0$ . Let  $\{\mu_n(\varepsilon)\}_{n=1}^{\infty}$  be a given asymptotic sequence. Then  $f(\mathbf{x}; \varepsilon)$  has an asymptotic expansion to  $N$  terms as  $\varepsilon \rightarrow 0$  with respect to this asymptotic sequence given by

$$f(\mathbf{x}; \varepsilon) \sim \sum_{n=1}^N f_n(\mathbf{x})\mu_n(\varepsilon), \quad (2.19)$$

if

$$f(\mathbf{x}; \varepsilon) - \sum_{n=1}^M f_n(\mathbf{x})\mu_n(\varepsilon) = o(\mu_M) \text{ as } \varepsilon \rightarrow 0, \quad (2.20)$$

for each  $M = 1, 2, \dots, N$ .

Another definition of an asymptotic expansion which is equivalent to (2.20) is

$$f(\mathbf{x}; \varepsilon) - \sum_{n=1}^M f_n(\mathbf{x})\mu_n(\varepsilon) = O(\mu_{M+1}) \text{ as } \varepsilon \rightarrow 0, \quad (2.21)$$

for each  $M = 1, 2, \dots, N - 1$ .

We call  $f_n(\mathbf{x})$  a shape-function, and by definition it is independent of  $\varepsilon$ . The expansion (2.19) is called a Poincaré, classical, or straightforward asymptotic approximation (see [24], p. 25). If  $\mu_n(\varepsilon) = \varepsilon^n$ , we call the expansion an asymptotic power series. In ([15], p. 16) the expansion (2.19) is called regular expansion or Poincaré expansion. Different from ([15]), we define a regular expansion as a uniform Poincaré expansion (see Definition 3.1).

The dependence of the form of a Poincaré expansion on the choice of independent variable  $\mathbf{x}$  cannot be overstated. This is illustrated by the following examples

**Example 2.15**

- $\sin(x + \varepsilon + \varepsilon^2) = \sin(x) + \varepsilon \cos(x) + O(\varepsilon^2)$ , but  $\sin(\xi + \varepsilon^2) = \sin(\xi) + O(\varepsilon^2)$  if we introduce  $\xi = x + \varepsilon$ .
- $\sin(\varepsilon x + \varepsilon) = \varepsilon x + \varepsilon + O(\varepsilon^3)$ , but  $\sin(X + \varepsilon) = \sin(X) + O(\varepsilon)$  if we introduce  $X = \varepsilon x$ . Note that in either expansion  $x$  and  $X$  are taken fixed. This means, for example, that if  $X$  is fixed, effectively  $x = O(\varepsilon^{-1})$ .
- $e^{-x/\varepsilon} = 0 + o(\varepsilon^n)$ , while  $x > 0$ , but  $e^{-\xi} = O(1)$  if we introduce  $\xi = x/\varepsilon$ .

Note that in asymptotic expansions, we only consider a fixed ( $N$ ) number of terms, since for  $N \rightarrow \infty$ , the series can be either convergent or divergent (see Example 2.17). Also, it is not necessary that a convergent asymptotic expansion converges to the expanded function (see Example 2.18).

For a given asymptotic sequence  $\{\mu_n(\varepsilon)\}_{n=1}^{\infty}$ ,  $f_n(\mathbf{x})$  can be determined uniquely by the following formulas (we assume that  $\mu_n$  are nonzero for  $\varepsilon$  near zero and that each of the limits below exist)

$$f_1(\mathbf{x}) = \lim_{\varepsilon \rightarrow 0} \frac{f(\mathbf{x}; \varepsilon)}{\mu_1(\varepsilon)}, \quad (2.22a)$$

$$f_2(\mathbf{x}) = \lim_{\varepsilon \rightarrow 0} \frac{f(\mathbf{x}; \varepsilon) - f_1(\mathbf{x})\mu_1(\varepsilon)}{\mu_2(\varepsilon)}, \quad (2.22b)$$

$$\begin{aligned} & \vdots \\ & f_n(\mathbf{x}) = \lim_{\varepsilon \rightarrow 0} \frac{f(\mathbf{x}; \varepsilon) - \sum_{k=1}^{n-1} f_k(\mathbf{x})\mu_k(\varepsilon)}{\mu_n(\varepsilon)}. \end{aligned} \quad (2.22c)$$

We will give some examples of asymptotic expansions for  $\varepsilon \rightarrow 0$ .

**Example 2.16**

Given some different asymptotic sequences, a function may have different asymptotic expansions.

$$\tanh(\varepsilon) = \varepsilon - \frac{1}{3}\varepsilon^3 + \frac{2}{15}\varepsilon^5 + O(\varepsilon^7), \quad (2.23a)$$

$$= \sinh(\varepsilon) - \frac{1}{2}\sinh^3(\varepsilon) + \frac{3}{8}\sinh^5(\varepsilon) + O(\sinh^7(\varepsilon)) \quad (2.23b)$$

$$= \varepsilon \cos(\varepsilon) + \frac{1}{6}(\varepsilon \cos(\varepsilon))^3 + \frac{41}{120}(\varepsilon \cos(\varepsilon))^5 + O((\varepsilon \cos(\varepsilon))^7). \quad (2.23c)$$

In fact, re-expanding the expansions (2.23b, 2.23c) into Taylor series around  $\varepsilon = 0$  will yield the expansions (2.23a). We say that two functions  $f$  and  $g$  are asymptotically equal, to  $N$  terms, if  $f - g = o(\mu_N)$  as  $\varepsilon \rightarrow 0$ .

**Example 2.17**

If  $\varepsilon \neq 0$  then the asymptotic expansion  $\sum_{n=1}^N n\varepsilon^n$  diverges as  $N \rightarrow \infty$ .

**Example 2.18**

Two different functions may have the same asymptotic expansion.

$$\cos(\varepsilon) = 1 - \frac{1}{2}\varepsilon^2 + \frac{1}{24}\varepsilon^4 + O(\varepsilon^6). \quad (2.24a)$$

$$\cos(\varepsilon) + e^{-1/\varepsilon} = 1 - \frac{1}{2}\varepsilon^2 + \frac{1}{24}\varepsilon^4 + O(\varepsilon^6). \quad (2.24b)$$

Note that the asymptotic expansion in (2.24b) converges to  $\cos(\varepsilon)$  instead of  $\cos(\varepsilon) + e^{-1/\varepsilon}$ .

### 3 Regular and singular perturbations

#### 3.1 Regular perturbations

In applied mathematics, one usually formulates a mathematical model for a physical problem by establishing the governing equations. These equations usually consist of a (system of) differential equation(s)  $L(f, \mathbf{x}; \varepsilon) = 0$  and boundary conditions  $B(f; \varepsilon) = 0$ , where  $\varepsilon$  is a parameter or a parameter vector. For the moment we will consider just a single parameter and this parameter is assumed to be small. As discussed in the introduction, the occurrence of at least one small parameter is very natural in any result of modelling, because the process of modelling is essentially a distinction between main effects that should be included, and effects that are too small to be included. Therefore, in this hierarchy there will almost always be effects that are relatively small but not small enough to be ignored.

For example, in a fluid flow problem, the (dimensionless) viscosity may be small, but without viscosity an airfoil would not have drag or lift, and therefore viscosity cannot be discarded from the modelling.

The usual situation is that the resulting equations can not be solved exactly, and we need to seek for approximations of the solution. Generally speaking, there are two major methods to obtain approximate solutions, namely numerical methods and perturbation methods. Perturbation methods are analytical in nature, but not all analytical methods to construct a solution are of perturbation type. Some analytical methods produce explicit solutions in the form of integrals or infinite series, but since these will have to be evaluated numerically we will for simplicity categorize them among the numerical methods.

This section will be about perturbation methods. They are based on the smallness of the problem parameter  $\varepsilon$ . We assume that the solution  $f(\mathbf{x}; \varepsilon)$  of the governing equation will be expanded into a Poincaré expansion. This expansion can be either uniform or non uniform.

**Definition 3.1.** If  $f(\mathbf{x}; \varepsilon)$  can be expanded into a Poincaré expansion (2.19) and the expansion holds uniformly in  $\mathbf{x} \in D$  (uniformly valid in  $D$ ), we say that  $f(\mathbf{x}; \varepsilon)$  has a regular perturbation expansion in  $D$ . Otherwise,  $f(\mathbf{x}; \varepsilon)$  has a singular perturbation expansion in  $D$ .



Below, we give two examples to illustrate this notion of uniform expansion.

**Example 3.2**

Consider an asymptotic expansion below with  $D = \mathbb{R}$ ,

$$\begin{aligned}\cos(x + \varepsilon) &= \cos(x) \cos(\varepsilon) - \sin(x) \sin(\varepsilon) \\ &= \cos(x) \left(1 - \frac{1}{2}\varepsilon^2 + O(\varepsilon^4)\right) - \sin(x) \left(\varepsilon - \frac{1}{6}\varepsilon^3 + O(\varepsilon^5)\right) \\ &= \cos(x) - \varepsilon \sin(x) - \frac{1}{2}\varepsilon^2 \cos(x) + \frac{1}{6}\varepsilon^3 \sin(x) + O(\varepsilon^4).\end{aligned}$$

Since  $|\cos(x)|$  and  $|\sin(x)|$  are bounded ( $\leq 1$ ) for all  $x \in \mathbb{R}$ , it follows that the above asymptotic expansion is uniformly valid for all  $x \in \mathbb{R}$ .

**Example 3.3**

$$\begin{aligned}\cos(x + \varepsilon x) &= \cos(x) \cos(\varepsilon x) - \sin(x) \sin(\varepsilon x) \\ &= \cos(x) \left(1 - \frac{1}{2}\varepsilon^2 x^2 + O(\varepsilon^4 x^4)\right) - \sin(x) \left(\varepsilon x - \frac{1}{6}\varepsilon^3 x^3 + O(\varepsilon^5 x^5)\right) \\ &= \cos(x) - \varepsilon x \sin(x) - \frac{1}{2}\varepsilon^2 x^2 \cos(x) + \frac{1}{6}\varepsilon^3 x^3 \sin(x) + O(\varepsilon^4 x^4).\end{aligned}$$

Note that each coefficient of  $\varepsilon^n$  is bounded in interval  $0 \leq x \leq X(\varepsilon)$  provided that  $X(\varepsilon) = O(1)$  as  $\varepsilon \rightarrow 0$ . Therefore, the asymptotic expansion is uniformly valid for in this interval. Consider the second term. The value  $x \sin(x)$  oscillates but increases linearly with  $x$ . As a result,  $\varepsilon x \sin(x)$  will become  $O(1)$ . Consequently the asymptotic expansion is not uniformly in an interval  $0 \leq x \leq X(\varepsilon)$ , with  $X(\varepsilon) = O(\frac{1}{\varepsilon})$ .

After assuming an asymptotic sequence of order functions  $\{\mu_n(\varepsilon)\}$ , and formally expanding  $f(\mathbf{x}; \varepsilon)$  into the corresponding Poincaré expansion

$$f(\mathbf{x}; \varepsilon) = \mu_0(\varepsilon) f_0(\mathbf{x}) + \mu_1(\varepsilon) f_1(\mathbf{x}) + \dots, \quad (3.25)$$

we substitute this expansion into both  $L(f, \mathbf{x}; \varepsilon) = 0$  and  $B(f; \varepsilon) = 0$ , and again formally expand the equations into a Poincaré expansion based on the same order functions

$$L(f, \mathbf{x}; \varepsilon) = \mu_0(\varepsilon) L_0(f_0, \mathbf{x}) + \mu_1(\varepsilon) L_1(f_1, f_0, \mathbf{x}) + \dots = 0 \quad (3.26)$$

(Note that  $L$  or  $B$  may have to be rescaled, but this is unimportant as the right-hand side is zero anyway). Since each term in such an expansion is independent of  $\varepsilon$ , each term must vanish and we obtain a sequence of governing equations  $L_n = 0$ , yielding  $f_n(\mathbf{x})$ , which can be solved successively.

It should be noted that the problem formulation usually presents at least one natural choice of independent variable  $\mathbf{x}$ , for example by the interval considered, or any given  $x$ -dependent source term or coefficient.

The following example illustrates the above sketched iterative procedure to solve an algebraic equation. Finding a suitable sequence of order functions is especially crucial.

**Example 3.4**

We would like to find an asymptotic expansion for the solution of

$$x^3 + x^2 - x - 1 + \varepsilon = 0, \varepsilon \rightarrow 0. \quad (3.27)$$

Note that for  $\varepsilon = 0$ , the roots of (3.27) are  $x = 1, -1, -1$  (of order 1). As the corrections seem to be  $O(\varepsilon)$ , we assume an expansion of the form

$$x = x_0 + \varepsilon x_1 + \varepsilon^2 x_2 + O(\varepsilon^3). \quad (3.28)$$

Substituting the expansion (3.28) into (3.27), and equating the coefficients of like powers of  $\varepsilon$  yields

$$O(1) : x_0^3 + x_0^2 - x_0 - 1 = 0 \quad (3.29a)$$

$$O(\varepsilon) : 3x_0^2 x_1 + 2x_0 x_1 - x_1 + 1 = 0, \dots \quad (3.29b)$$

We obtain  $x_0 = 1, -1, -1$  and  $x_1 = \frac{-1}{3x_0^2 + 2x_0 - 1}$ . For  $x_0 = 1$ , then  $x_1 = -\frac{1}{4}$ . Therefore, we obtain the asymptotic expansion of the solution of (3.27) is

$$x = 1 - \frac{1}{4}\varepsilon + O(\varepsilon^2). \quad (3.30)$$

For  $x_0 = -1$ , however,  $x_1$  is undefined. Therefore, we reconsider our assumption of a power series expansion, and re-expand the expansion (3.28) into

$$x = -1 + \varepsilon^\alpha x_1 + O(\varepsilon^{2\alpha}), \quad (3.31)$$

to obtain

$$-2\varepsilon^{2\alpha-1} x_1^2 + x_1^3 \varepsilon^{3\alpha-1} + 1 = 0. \quad (3.32)$$

Considering the balance between the terms in (3.32), there are several possible values for  $\alpha$ .

1. For  $\alpha = \frac{1}{3}$ , we obtain  $x_1 = 0$ . Considering the next order,  $O(\varepsilon^{2/3})$ , leads to  $1 = 0$ . Therefore, we neglect this possibility.
2. For  $\alpha = \frac{1}{2}$ , it follows that  $x_1 = \pm \frac{1}{2}\sqrt{2}$  and the asymptotic expansions for the solution of (3.27) are

$$x = -1 + \frac{1}{2}\sqrt{2}\sqrt{\varepsilon} + O(\varepsilon), \quad (3.33a)$$

$$x = -1 - \frac{1}{2}\sqrt{2}\sqrt{\varepsilon} + O(\varepsilon). \quad (3.33b)$$

### 3.2 Singular perturbation of boundary layer type

In this section, we will consider a phenomenon that is sometimes associated to a singular perturbation, namely a boundary layer which is a narrow region where the solution of the governing equations changes rapidly. It means that there is a nonuniformity in that region. Some examples of physical processes where boundary layers may occur are viscous fluid flow near a solid wall, the temperature of a fluid near a solid wall, etc.

To illustrate the procedure to solve this problem, we consider, for example, the differential equation

$$\mathcal{L}(\Phi''(x; \varepsilon), \Phi'(x; \varepsilon), \Phi(x; \varepsilon), x, \varepsilon) = 0, \quad x \in D = [0, 1], \quad \varepsilon \rightarrow 0, \quad (3.34)$$

with boundary conditions  $\Phi(0) = A$  and  $\Phi(1) = B$ , where  $A$  and  $B$  are constants of  $O(1)$ . Mathematically, we can anticipate the existence of boundary layers if small parameter  $\varepsilon$  is multiplied with the highest derivative (here, the second derivative) in the differential equation (see [9], p. 145). As the order of the equation reduces when  $\varepsilon \rightarrow 0$ , not all boundary conditions can be satisfied and another Poincaré expansion, based on another choice of independent variable, is locally necessary.

We assume here just one boundary layer, located at  $x = 0$ , and we assume that  $\Phi(x; \varepsilon)$  can be expanded into an asymptotic expansion. Because of the boundary layer,  $\Phi(x; \varepsilon)$  does not have a regular expansion on the whole of  $[0, 1]$ . Therefore, we divide the interval  $[0, 1]$  into 2 asymptotically overlapping subintervals. In the subinterval called outer region, we introduce a regular expansion (called outer expansion) using the original variable. Next, for the other subinterval called inner region, we introduce an expansion (called inner expansion) describing the rapid changes using a magnified scale. Finally, to match those asymptotic expansions, it is necessary that they have the same functional form on the overlap region. Hence, we find an asymptotic approximation (but not a Poincaré expansion) to the solution that is uniformly valid over the whole interval  $[0, 1]$ .

First, we consider the outer region  $[D_1, 1]$  for any fixed  $D_1 > 0$ , with  $x = O(1)$ . We assume  $\Phi(x; \varepsilon)$  can be expanded as

$$\Phi(x; \varepsilon) = \sum_{n=1}^{N-1} \mu_n(\varepsilon) \Phi_n(x) + O(\mu_N), \quad (3.35)$$

with  $\mu_1(\varepsilon) = 1$  since the boundary conditions are of  $O(1)$ . Substitute this outer expansion (3.35) into the differential equation (3.34). Since the second derivative is multiplied by  $\varepsilon$ , we obtain for each  $n$ , a first order differential equation. Therefore in general,  $\Phi_n(x; \varepsilon)$  can not satisfy both boundary conditions. Since the boundary layer is located at  $x = 0$ , we consider the boundary condition at  $x = 1$  to obtain  $\Phi_n(x)$ .

Now, we consider the inner region  $[0, D_2\delta(\varepsilon)]$  for fixed  $D_2 > 0$ . Here we introduce the inner variable  $\xi = \frac{x}{\delta(\varepsilon)}$ ,  $x = O(\delta(\varepsilon))$ , where  $\delta(\varepsilon)$  represents the thickness of the boundary layer. (If the boundary layer is at  $x = 1$ , we rescale  $x$  as  $x = 1 + \delta(\varepsilon)\xi$ ). In this inner region, besides the independent variable, we also rescale the dependent variables as

$$\Phi(\delta(\varepsilon)\xi; \varepsilon) = \lambda(\varepsilon)\Psi(\xi; \varepsilon). \quad (3.36)$$

If we assume the outer expansion is of  $O(1)$  as  $x \rightarrow 0$  and since the boundary condition at  $x = 0$  is of  $O(1)$ , we have the inner expansion is also of  $O(1)$ . Therefore, we get  $\lambda = 1$ . By introducing (3.36) into the differential equation (3.34), we obtain a differential equation, say,

$$\mathcal{L}^*(\Psi''(\xi; \varepsilon), \Psi'(\xi; \varepsilon), \Psi(\xi; \varepsilon), \xi, \delta(\varepsilon); \varepsilon) = 0. \quad (3.37)$$

We solve this differential equation (3.37) together with the boundary condition at  $x = 0$ . But, first we have to determine  $\delta(\varepsilon)$ . We choose  $\delta(\varepsilon)$  such that the differential equation (3.37) has the richest structure, that is, it contains the largest number of terms that satisfy the boundary condition and matching condition with the outer expansion. Recall that in the outer solution, the second order differential equation is reduced to the first order differential

equation. Therefore, the differential equation (3.37) should also contain the missing term (here, the second derivative) of the differential equation (3.34) in the leading order of the outer expansion. This principle to find the  $\delta(\varepsilon)$  is called the principle of the least degeneracy (see [12], p. 86). The chosen  $\delta(\varepsilon)$  that has this property is called a distinguished limit or significant degeneration.

Next, we assume the inner expansion of the form

$$\Psi(\xi; \varepsilon) = \sum_{n=1}^{N-1} \zeta_n(\varepsilon) \Psi_n(\xi) + O(\zeta_N), \tag{3.38}$$

with  $\zeta_1 = 1$ , since the inner expansion is of  $O(1)$ . Substituting this expansion into (3.37) and considering the boundary condition at  $x = 0$ , we obtain  $\Psi_n(\xi)$ . For each  $n$ , we have a second order differential equation with only one boundary condition. Therefore the solutions  $\Psi_n(\xi)$  will contain one undetermined constant. To obtain this constant and to obtain a uniform solution for the whole interval  $[0, 1]$ , the inner and the outer expansions are matched over the overlap region. Figure (3.2) represents a boundary layer phenomenon.

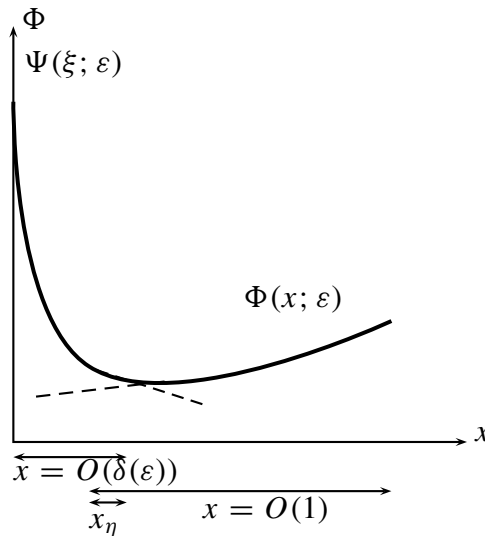


Figure 3.2: Boundary layer

There are two common matching principles, *viz.*

1. Matching by an intermediate variable (see [25], p. 52, or [31], p. 24). We introduce an intermediate variable  $x_\eta = \frac{x}{\eta(\varepsilon)}$  that is located in the transition region or overlap region between the outer region  $O(1)$  and the inner region  $O(\varepsilon)$ . As an Ansatz, usually we take  $\eta(\varepsilon) = \varepsilon^n$  with  $0 < n < 1$ . Next, we follow the procedure below

- (a) Substitute the intermediate variable  $x_\eta$  into the outer solution and assume there is an  $\eta_1(\varepsilon)$  so that it is still an asymptotic approximation of outer solution for any  $\eta(\varepsilon)$  that satisfies  $\eta_1(\varepsilon) \ll \eta(\varepsilon) \ll 1$ .
  - (b) Similarly, substitute the intermediate variable  $x_\eta$  into the inner solution and assume there is an  $\eta_2(\varepsilon)$  so that it is still an asymptotic approximation of inner solution for any  $\eta(\varepsilon)$  that satisfies  $\varepsilon \ll \eta(\varepsilon) \ll \eta_2(\varepsilon)$ .
  - (c) Assume that there is an overlap between the outer and the inner region, that is  $\eta_1(\varepsilon) \ll \eta_2(\varepsilon)$ , where the outer and the inner solution have the same functional form.
2. Matching by Van Dyke's rule (see [12], p. 90). In this technique, we rewrite the outer expansion in the inner variable and the inner expansion in the outer variable as follows

$$\begin{aligned} & \text{the } m\text{-term inner expansion of (the } n\text{-term outer expansion)} \\ & = \text{the } n\text{-term outer expansion of (the } m\text{-term inner expansion),} \end{aligned} \quad (3.39)$$

where  $m$  and  $n$  are any two integers which may be equal or not. Usually,  $m$  is chosen as either  $n$  or  $n + 1$ . For the left-hand side of (3.39), we rewrite the first  $n$ -terms of the outer expansion in inner variable, expand it for  $\varepsilon \rightarrow 0$  with the inner variable fixed, and consider the first  $m$ -terms of the resulting expansion. Next, we do conversely for the right-hand side of (3.39). Finally, a single uniformly valid expansion, called a composite expansion, can be formed as follows

$$\begin{aligned} \text{composite expansion} &= \text{outer expansion} + \text{inner expansion} \\ & \quad - \text{outer expansion rewritten in inner variable,} \end{aligned} \quad (3.40)$$

or

$$\begin{aligned} \text{composite expansion} &= \text{outer expansion} + \text{inner expansion} \\ & \quad - \text{inner expansion rewritten in outer variable.} \end{aligned} \quad (3.41)$$

### Example 3.5

We start with an algebraic example that illustrates the search for distinguished limits. Suppose we would like to find the asymptotic expansion for the solution of a quadratic equation

$$\varepsilon x^2 - x + 2 = 0, \quad \varepsilon \rightarrow 0. \quad (3.42)$$

Note that (3.42) is a quadratic equation and therefore has two roots although  $\varepsilon$  is very small. For  $\varepsilon = 0$ , however, (3.42) reduces into a linear equation which only has one root. So, (3.42) behaves differently when  $\varepsilon \rightarrow 0$  and when  $\varepsilon = 0$ . This phenomenon leads to a singular perturbation problem. A similar phenomenon occurs in solving a differential equation when the highest derivative is multiplied by a small parameter (see Example (3.6)).

In a similar way as in Example (3.4), we assume the expansion of the form

$$x = x_0 + \varepsilon x_1 + O(\varepsilon^2), \quad (3.43)$$

to obtain

$$O(1) : x_0 = 2, \quad (3.44a)$$

$$O(\varepsilon) : x_1 = x_0^2 = 4, \dots \quad (3.44b)$$

Therefore, we obtain the asymptotic expansion for the solution of (3.42) as

$$x = 2 + 4\varepsilon + O(\varepsilon^2). \quad (3.45)$$

To obtain the other root, we make a rescaling  $x = \frac{\bar{x}}{\delta(\varepsilon)}$ . As an Ansatz, we choose  $\delta(\varepsilon) = \varepsilon^n$ . Substitute this rescaling into (3.42) yields

$$\varepsilon^{1-2n}\bar{x}^2 - \varepsilon^{-n}\bar{x} + 2 = 0. \quad (3.46)$$

Note that, using the expansion (3.43), the quadratic equation (3.42) is reduced to a linear equation (3.44a). Therefore, we have to choose  $n$  such that (3.46) contains the largest number of terms and includes the missing quadratic term. Considering the balance between terms in (3.46), we observe that there are 3 candidates for the distinguished limits, viz.  $n = 0$ ,  $n = \frac{1}{2}$ , and  $n = 1$ . Geometrically, those candidates are the intersection points of the graphs of the powers of  $\varepsilon$  in (3.46) that is  $1 - 2n$ ,  $-n$ , and 0 (see Figure (3.3)).

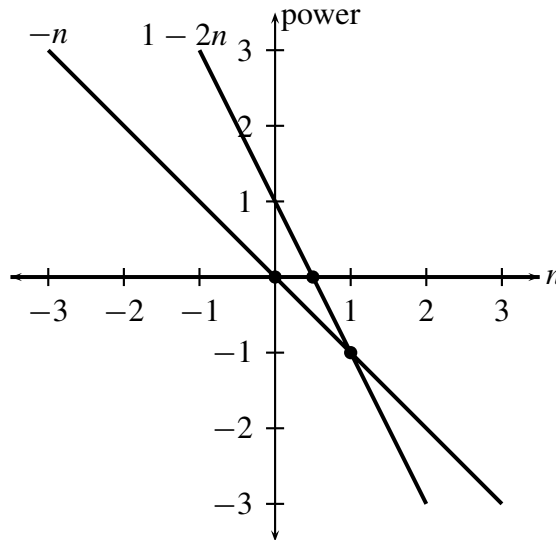


Figure 3.3: The candidates for distinguished limits

We will analyse each of the candidates to determine the distinguished limit as follows

1. For  $n = 0$ , we get  $\bar{x} = 2$ , which is the same solution as (3.45). Therefore, we ignore this possibility.

2. For  $n = \frac{1}{2}$ , the term  $\varepsilon^{-1/2}\bar{x}$  dominates, which yields  $\bar{x} = 0$ . It means that the non-trivial leading order term is not  $O(\varepsilon^{-1/2})$ . Therefore, we also ignore this possibility. Geometrically, this could be seen directly from the Figure (3.3), because below the intersection point  $(\frac{1}{2}, 0)$ , there is another line.
3. For  $n = 1$ , we get

$$\bar{x}^2 - \bar{x} = 0, \quad (3.47)$$

which yields  $\bar{x} = 0$  or  $\bar{x} = 1$ . For similar reasons as above, we ignore the possibility of  $\bar{x} = 0$ . Next, for  $\bar{x} = 1$ , we assume the expansion

$$x = \frac{\bar{x}}{\varepsilon} = \frac{1}{\varepsilon} (1 + \varepsilon\bar{x}_1 + O(\varepsilon^2)) = \frac{1}{\varepsilon} + \bar{x}_1 + O(\varepsilon). \quad (3.48)$$

Substituting this expansion into (3.42) yields  $\bar{x}_1 = -2$ . Therefore, the other asymptotic expansion of the solution of (3.42) is

$$x = \frac{1}{\varepsilon} - 2 + O(\varepsilon). \quad (3.49)$$

Note that, geometrically, it seems that the lowest intersection point yields the best candidates for the distinguished limit.

### Example 3.6

Next, we consider a problem described by a differential equation, which exemplifies more the types of problem we will be dealing with. We consider the boundary value problem

$$\varepsilon y'' + y' = x \text{ as } \varepsilon \rightarrow 0, \quad y(0) = 0, \quad y(1) = 1. \quad (3.50)$$

Note that, for  $\varepsilon = 0$ , the order of the differential equation (3.50) reduces from 2 to 1. Therefore, it can not satisfy both boundary conditions and we may anticipate a boundary layer at either end. Since the coefficient of  $y'$  is positive throughout  $0 < x < 1$ , it follows that the boundary layer is located at  $x = 0$  (see [9], p. 155)<sup>1</sup>. If the boundary layer were at  $x = 1$ , one would obtain an unbounded inner expansion as  $\varepsilon \rightarrow 0$ , which would not match with the outer expansion which appears to be of  $O(1)$ . Now, we consider the outer expansion by assuming an expansion of the form

$$y(x; \varepsilon) = y_0(x) + \varepsilon y_1(x) + O(\varepsilon^2). \quad (3.51)$$

Since the boundary layer is located at  $x = 0$ , we use the boundary condition  $y(1) = 1$ . Introducing the expansion (3.51) into the differential equation (3.50) yields

$$O(1) : y_0' = x, \quad y_0(1) = 1, \quad (3.52a)$$

$$O(\varepsilon) : y_1' = -y_0''(x), \quad y_1(1) = 0, \quad (3.52b)$$

$$O(\varepsilon^2) : y_2' = -y_1''(x), \quad y_2(1) = 0, \dots \quad (3.52c)$$

Solving the above differential equations, we obtain the outer expansion

$$y(x; \varepsilon) = \frac{1}{2}x^2 + \frac{1}{2} + \varepsilon(1 - x) + O(\varepsilon^2). \quad (3.53)$$

---

<sup>1</sup>if the coefficient of  $y'$  is negative throughout  $0 < x < 1$ , then the boundary layer is located at  $x = 1$ .

Next, we consider the inner expansion. We rescale  $x = \varepsilon^n \xi$ . Since both the boundary conditions and the outer expansion are of  $O(1)$ , we rescale the dependent variable as  $y(\varepsilon^n \xi; \varepsilon) = Y(\xi; \varepsilon)$ . Introducing these rescalings into the differential equation (3.50), we arrive at

$$\varepsilon^{1-2n} \frac{d^2 Y}{d\xi^2} + \varepsilon^{-n} \frac{dY}{d\xi} = \varepsilon^n \xi. \quad (3.54)$$

Using the similar analysis as in Example (3.5), we have to choose  $n$  such that (3.54) contains the largest number of terms and the second derivative  $\frac{d^2 Y}{d\xi^2}$ . Considering the balance between terms of (3.54), we find a boundary layer thickness of order  $O(\varepsilon)(n = 1)$ . Therefore, (3.54) turns into

$$\frac{d^2 Y}{d\xi^2} + \frac{dY}{d\xi} = \varepsilon^2 \xi. \quad (3.55)$$

It is easily verified that the other possibility of  $n$  leads to an inner expansion that will not match with the outer expansion. Next, we assume an inner expansion of the form

$$Y(\xi; \varepsilon) = Y_0(\xi) + \varepsilon Y_1(\xi) + \varepsilon^2 Y_2(\xi) + O(\varepsilon^3), \quad (3.56)$$

to obtain

$$O(1) : \frac{d^2 Y_0}{d\xi^2} + \frac{dY_0}{d\xi} = 0, \quad Y_0(0) = 0, \quad (3.57a)$$

$$O(\varepsilon) : \frac{d^2 Y_1}{d\xi^2} + \frac{dY_1}{d\xi} = 0, \quad Y_1(0) = 0, \quad (3.57b)$$

$$O(\varepsilon^2) : \frac{d^2 Y_2}{d\xi^2} + \frac{dY_2}{d\xi} = \xi, \quad Y_2(0) = 0, \dots \quad (3.57c)$$

We obtain the inner expansion

$$Y(\xi; \varepsilon) = A(1 - e^{-\xi}) + \varepsilon B(1 - e^{-\xi}) + \varepsilon^2 \left( C(1 - e^{-\xi}) + \frac{1}{2} \xi^2 - \xi \right) + O(\varepsilon^3). \quad (3.58)$$

To obtain an expansion that is uniformly valid for the whole interval, we make a matching between the outer expansion (3.53) and the inner expansion (3.58). We use Van Dyke's matching rule. First, we rewrite the outer expansion (3.53) in the inner variable ( $\xi = \frac{x}{\varepsilon}$ ) to obtain

$$y(x; \varepsilon) = \frac{1}{2} x^2 + \frac{1}{2} + \varepsilon(1 - x) + O(\varepsilon^2) = \frac{1}{2} + \varepsilon + \frac{1}{2} \varepsilon^2 \xi^2 - \varepsilon^2 \xi + O(\varepsilon^2). \quad (3.59)$$

Next, we rewrite the inner expansion (3.58) in the outer variable  $x = \varepsilon \xi$  to obtain

$$\begin{aligned} Y(\xi; \varepsilon) &= A(1 - e^{-x/\varepsilon}) + \varepsilon B(1 - e^{-x/\varepsilon}) + \varepsilon^2 \left( C(1 - e^{-x/\varepsilon}) + \frac{1}{2} \xi^2 - \xi \right) + O(\varepsilon^3) \\ &= A + \varepsilon B + \varepsilon^2 C + \frac{1}{2} \varepsilon^2 \xi^2 - \varepsilon^2 \xi + O(\varepsilon^3) \quad \text{as } \varepsilon \rightarrow 0. \end{aligned} \quad (3.60)$$

Comparing (3.59) and (3.60), we see that both expressions are functionally identical if  $A = \frac{1}{2}$ ,  $B = 1$ , and  $C = 0$ . Therefore, the inner expansion (3.58) becomes

$$Y(\xi; \varepsilon) = \frac{1}{2} (x^2 + 1 - e^{-x/\varepsilon}) + \varepsilon (-x + 1 - e^{-x/\varepsilon}) + O(\varepsilon^2). \quad (3.61)$$



Before we proceed with the composite expansion, we try another matching principle, *viz.* matching by intermediate variable to find the constants  $A$  and  $B$ . We introduce the intermediate variable  $x_\eta = \frac{x}{\eta(\varepsilon)}$ , with  $\eta(\varepsilon) = \varepsilon^n$  and  $0 < n < 1$ . This interval for  $n$  emerges from the fact that the intermediate variable should lie between the outer variable,  $n = 0$  and the inner variable,  $n = 1$ . Since  $x = \varepsilon\xi$ , it follows that  $\xi = \frac{x_\eta}{\varepsilon^{1-n}}$ . Substituting this intermediate variable into the outer solution (3.53) yields

$$\begin{aligned} y(x; \varepsilon) &= \frac{1}{2}x^2 + \frac{1}{2} + \varepsilon(1 - x) + O(\varepsilon^2) \\ &= \frac{1}{2} + \frac{1}{2}\varepsilon^{2n}x_\eta^2 + \varepsilon - \varepsilon^{n+1}x_\eta + O(\varepsilon^2), \end{aligned} \quad (3.62)$$

which is still an asymptotic approximation of the outer solution for  $n < \frac{1}{2}$ . Here, we can choose, for example,  $\eta_1(\varepsilon) = \varepsilon^{3/8}$ . Next, in a similar way, the inner solution (3.58) becomes

$$\begin{aligned} Y(\xi; \varepsilon) &= A(1 - e^{-\xi}) + \varepsilon B(1 - e^{-\xi}) + \varepsilon^2(C(1 - e^{-\xi}) + \frac{1}{2}\xi^2 - \xi) + O(\varepsilon^3) \\ &= A\left(1 - e^{-x_\eta/(\varepsilon^{1-n})}\right) + \varepsilon B\left(1 - e^{-x_\eta/(\varepsilon^{1-n})}\right) + \varepsilon^2 C\left(1 - e^{-x_\eta/(\varepsilon^{1-n})}\right) \\ &\quad + \frac{1}{2}x_\eta^2\varepsilon^{2n} - \varepsilon^{n+1}x_\eta + O(\varepsilon^3) \\ &= A + \frac{1}{2}x_\eta^2\varepsilon^{2n} + \varepsilon B - \varepsilon^{n+1}x_\eta + \varepsilon^2 C + O(\varepsilon^3), \text{ as } \varepsilon \rightarrow 0, \end{aligned} \quad (3.63)$$

which is still an asymptotic approximation of the inner solution for all  $0 < n < 1$ . Therefore, we can choose, for example,  $\eta_2(\varepsilon) = \varepsilon^{1/8}$ . Since  $\eta_1(\varepsilon) \ll \eta_2(\varepsilon)$ , indeed, there is an overlap region. Hence, we can take  $\eta(\varepsilon)$  from the overlap region, for example,  $\eta(\varepsilon) = \varepsilon^{1/4}$ . Next, comparing (3.62) and (3.63) again we obtain  $A = \frac{1}{2}$ ,  $B = 1$  and  $C = 0$ .

Finally, using the outer expansion (3.53) and the inner expansion (3.61), we obtain the composite expansion is

$$y^c(x; \varepsilon) = \frac{1}{2}x^2 + \frac{1}{2} - \frac{1}{2}e^{-x/\varepsilon} + \varepsilon(1 - x - e^{-x/\varepsilon}) + O(\varepsilon^2). \quad (3.64)$$

Note that, the differential equation (3.50) has an exact solution, *viz.*

$$\begin{aligned} y^e(x; \varepsilon) &= \frac{1}{2}x^2 - \varepsilon x + \left(\frac{\varepsilon + \frac{1}{2}}{1 - e^{-1/\varepsilon}}\right)(1 - e^{-x/\varepsilon}) \\ &= \frac{1}{2}x^2 + \frac{1}{2} - \frac{1}{2}e^{-x/\varepsilon} + \varepsilon(-x + 1 - e^{-x/\varepsilon}) + TST, \end{aligned} \quad (3.65)$$

which is the same as the composite function (3.64).

Figure (3.4) represents a comparison between the outer expansion (3.53), the inner expansion (3.61), and the exact solution (3.65) for  $\varepsilon = 0.05$ . It can be seen that, the outer expansion (3.53) agrees with the exact solution (3.65), except in a small interval near  $x = 0$ .

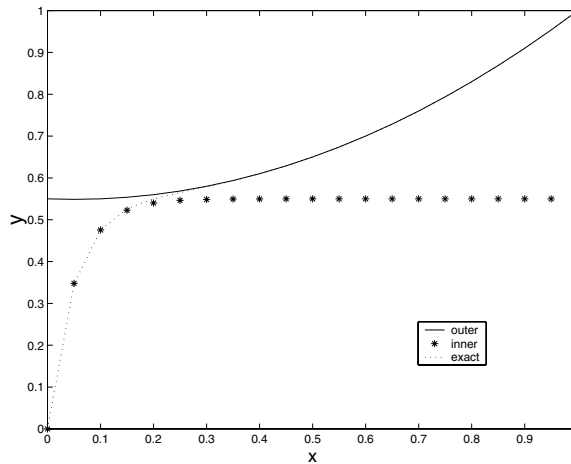


Figure 3.4: Comparison between the outer, the inner, and the exact solution for  $\varepsilon = 0.05$ .

## 4 Method of slow variation

As we noted above, the choice of the independent coordinate is very important when constructing an approximate solution in the form of a Poincaré expansion. This is particularly true when we deal with a problem in more than one dimension, and described by a partial differential equation. If the geometry is slender such that the prevailing length scale in one direction is much longer than in the other, then it is very likely that the solution follows this behaviour, and varies in the “long” direction much slower than in the “short” direction. This will be the case if there are no other lengths scales inherent in the problem, like a source, a wave length, or abrupt variations in geometry. The effects of the outer ends may be of this type, and have to be accounted for if the ends determine the solution. We will come back to this type of problem in an example below.

In this section, we consider a slender geometry with variations in the long direction that are much slower than in the other direction(s). Following Van Dyke [13,14], this will be called a slowly varying geometry. (If the variations are small, but not slow, the geometry is called slightly varying. See the next section.)

In a slowly varying geometry, the boundary and possibly other properties of the geometry vary in one direction much more slowly than in the other. If we take  $x$  to be the slow direction, the derivatives in  $x$  direction are small. Assume that the characteristic length scale in  $y$  direction is  $D$  and the characteristic length scale in  $x$  is  $L$ , while  $D \ll L$ , and no other (shorter) length scales are present. Usually,  $D$  is the width and  $L$  is the length of the region of interest. If we scale all lengths on  $D$ , the small parameter  $\varepsilon = \frac{D}{L}$  appears naturally in the problem, and geometry (or other properties) will be functionally dependent on the combination  $(\varepsilon x, y)$  (in 2 dimensions). For example, the boundary may be described by  $y = F(\varepsilon x)$ .

A method to solve the slowly varying geometry is by rescaling the slow coordinate to  $X = \varepsilon x$ , and then introduce an assumed Poincaré expansion with shape functions in  $X$  and  $y$ . It should be noted (we will come back to this in the next section) that after introducing the slow variable  $X$ , the  $x$ -derivatives in the equations will be multiplied by powers of  $\varepsilon$ . In the perturbation scheme these derivatives will be dropped, and therefore any approximate solution will fail to satisfy the boundary conditions at the ends. As we will see, this will have to be repaired by local approximations in  $x$ ; these are essentially boundary layers in  $X$ .

Example (4.1.1) below shows that following a naive approach, without a rescaling, the solution will be valid only for fixed  $x$ , and it will break down for large  $x$ , *i.e.*  $x = O(\frac{1}{\varepsilon})$ . So, in some sense we might say that the slowly varying problem in its original variables is a singular perturbation problem and the rescaling transforms the singular problem into a regular problem. Of course, this is not entirely true, because there is in general still a region of non-uniformity near the ends, but at least the region of validity of the solution has become much bigger and is now almost the whole domain.

Common examples of this method (or rather: the results of this method) are lubrication theory of highly viscous flow in bearings [18], quasi one-dimensional gas flow in slowly varying ducts [32], Webster's equation for sound waves in horns [43], and the Bernoulli-Euler theory of the bending of slender beams [17].

Often, the respective theories are derived without taking explicit notice of the implied small parameter. Sometimes, like in lubrication theory (see [18], p. 83) the  $x$  and  $y$  coordinates are scaled right from the start with length scale  $L$  and  $D$  respectively. Especially when dealing with more than one length scales in  $x$ , or when higher order corrections are of interest, the more systematic approach of above is probably preferable.

## 4.1 Examples

Here, we will consider two examples of heat conduction problems, to illustrate the above method of slow variation. Both problems are kept relatively simple, in order to allow us to calculate the solutions explicitly and in detail. The first example is a two-dimensional one and concerns an infinite symmetric strip with Dirichlet boundary conditions. This example illustrates both the failure of the naive approach, and the success of the above method of slow variation. The second example is more complicated, as it deals with a completely arbitrary (albeit slender) three-dimensional geometry of finite length, with Neumann boundary conditions (insulated) on the surface. Furthermore, the effects of the ends are considered in great detail by deriving the full solution (up to second order) in the boundary layers at the ends.

### 4.1.1 Heat conduction problem

In this example we consider a heat conduction problem in a domain  $\Omega_1$ , which is an infinite symmetric strip that is bounded by the boundaries  $y = \pm DR \left(\frac{x}{L}\right)$ ,  $D \ll L$ . We prescribe

the temperature at the boundaries and assume the temperature to be bounded as  $|x| \rightarrow \infty$ .

$$\Delta T(x, y) = 0, (x, y) \in \Omega_1, \quad (4.66a)$$

$$T\left(x, \pm DR\left(\frac{x}{L}\right)\right) = \pm T_a, \quad (4.66b)$$

$$T(x, y) \text{ is bounded for } |x| \rightarrow \infty, \quad (4.66c)$$

where  $T_a$  is the characteristic temperature.

At first, we make the heat problem (4.66a-4.66c) dimensionless by scaling  $x := Dx$ ,  $y := Dy$ ,  $T := T_a T$ , to obtain (see Figure (4.5))

$$\Delta T(x, y) = 0, (x, y) \in \Omega_1^*, \quad (4.67a)$$

$$T(x, \pm R(\varepsilon x)) = \pm 1, \varepsilon = \frac{D}{L} \ll 1, \quad (4.67b)$$

$$T(x, y) \text{ is bounded for } |x| \rightarrow \infty, \quad (4.67c)$$

where  $\Omega_1^*$  is the dimensionless version of  $\Omega_1$ , bounded by  $y = \pm R(\varepsilon x)$ .

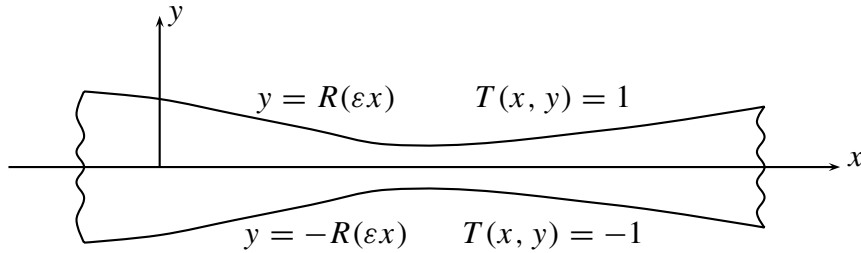


Figure 4.5: Slowly varying infinite symmetric strip

As mentioned above, the first step to solve the slowly varying geometry problem is by rescaling  $X = \varepsilon x$ . Before that, however, we will discuss the naive solution that would have been obtained without rescaling. This solution is not incorrect, but just limited as it is valid only on a scale of  $x = O(1)$ . We assume a perturbation expansion in powers of  $\varepsilon$ :

$$T(x, y; \varepsilon) = T_0(x, y) + \varepsilon T_1(x, y) + \varepsilon^2 T_2(x, y) + O(\varepsilon^3). \quad (4.68)$$

Introducing this expansion into the heat conduction equation (4.67a), we have to solve  $\Delta T_n(x, y) = 0$ . Since the parameter  $\varepsilon$  occurs implicitly and explicitly, we expand the boundary  $y = R(\varepsilon x)$  as

$$R(\varepsilon x) = R(0) + \varepsilon x R'(0) + \frac{1}{2} \varepsilon^2 x^2 R''(0) + O(\varepsilon^3). \quad (4.69)$$

Next, we expand the temperature  $T_n(x, y)$  about  $y = \pm R(0)$  to obtain the boundary condi-

tions for  $n = 0, 1, 2$ , respectively,

$$\begin{aligned} T_0(x, \pm R(0)) &= \pm 1, & T_1(x, \pm R(0)) &= \mp x R'(0) \frac{\partial T_0}{\partial y}(x, \pm R(0)), \\ T_2(x, \pm R(0)) &= \mp x R'(0) \frac{\partial T_1}{\partial y}(x, \pm R(0)) \mp \frac{1}{2} x^2 R''(0) \frac{\partial T_0}{\partial y}(x, \pm R(0)) - \\ &\quad \frac{1}{2} x^2 R'(0)^2 \frac{\partial^2 T_0}{\partial y^2}(x, \pm R(0)). \end{aligned}$$

The resulting solution, (bounded in  $x$ ) is now

$$T(x, y) = \frac{y}{R(0)} - \varepsilon x y \frac{R'(0)}{R(0)^2} + \frac{1}{6} \varepsilon^2 y (3x^2 - y^2 + R(0)^2) \frac{2R'(0)^2 - R''(0)R(0)}{R(0)^3} + O(\varepsilon^3). \quad (4.70)$$

Note that for  $x = O(\frac{1}{\varepsilon})$ , the second term becomes of order 1 and the solution (4.70) will not satisfy asymptotically the boundary conditions. Therefore, the solution (4.70) is no longer valid for  $x = O(\frac{1}{\varepsilon})$ . This, however, is the interesting length scale. To remedy the disadvantage of the solution (4.70) and incorporate the part of the solution that scales on  $x = O(\frac{1}{\varepsilon})$ , we rescale the  $x$ -coordinate to  $X = \varepsilon x$ . Then the problems (4.67a, 4.67b) adopt the form

$$\varepsilon^2 \frac{\partial^2 T}{\partial X^2} + \frac{\partial^2 T}{\partial y^2} = 0, \quad T(X, \pm R(X)) = \pm 1. \quad (4.71)$$

Note that as  $\varepsilon$  tends to zero, the boundaries remain  $y = \pm R(X)$ , but the governing equation does not remain the heat conduction equation. As  $\varepsilon^2$  appears to be the essential small parameter, we assume<sup>2</sup> the perturbation expansion in power of  $\varepsilon^2$

$$T(X, y; \varepsilon) = T_0(X, y) + \varepsilon^2 T_1(X, y) + \varepsilon^4 T_2(X, y) + O(\varepsilon^6). \quad (4.72)$$

After introducing (4.72) into (4.71) and equating like powers of  $\varepsilon$ , we obtain

$$\frac{\partial^2 T_0}{\partial y^2} = 0, \quad T_0 = \pm 1, \quad \text{at } y = \pm R(X), \quad (4.73)$$

$$\frac{\partial^2 T_n}{\partial y^2} = -\frac{\partial^2 T_{n-1}}{\partial X^2}, \quad T_n = 0, \quad \text{at } y = \pm R(X), \quad \text{for } n \geq 1. \quad (4.74)$$

Solving (4.73, 4.74), we find the solution

$$T(X, y) = \frac{y}{R(X)} - \frac{1}{6} \varepsilon^2 y (y^2 - R(X)^2) \frac{d^2}{dX^2} \left( \frac{1}{R(X)} \right) + O(\varepsilon^4). \quad (4.75)$$

Note that this solution is now still valid for  $X = O(1)$ , but at the same time incorporates the previous solution (4.70), as straightforward Taylor expansion would show.

---

<sup>2</sup>This is not necessarily true! See the next example.

### 4.1.2 A generalized heat conduction problem, including boundary layers

In this example, we further generalize the heat conduction problem to three dimensions inside the domain  $\Omega_2 \subset \mathbb{R}^3$  being a finite cylinder ( $0 \leq x \leq L$ ) that is bounded by the boundary  $r = DR\left(\frac{x}{L}, \theta\right)$ ,  $D \ll L$ , with a cross section of arbitrary shape. We prescribe an insulated boundary condition at the “long” boundaries and prescribe the temperature at the ends  $x = 0$  and  $x = L$ .

$$\Delta T(r, \theta, x) = 0 \quad \text{for } (r, \theta, x) \in \Omega_3, \quad (4.76a)$$

$$\frac{\partial T}{\partial n}(r, \theta, x) = 0 \quad \text{at } S = r - DR\left(\frac{x}{L}, \theta\right) = 0, \quad (4.76b)$$

$$T(r, \theta, 0) = T_a T_c\left(\frac{r}{D}, \theta\right) + T_\infty, \quad (4.76c)$$

$$T(r, \theta, L) = T_a T_d\left(\frac{r}{D}, \theta\right) + T_\infty, \quad (4.76d)$$

where  $T_a$  and  $T_\infty$  are characteristic and reference temperatures.

First, we make the heat conduction problem (4.76 a-d) dimensionless by scaling  $r := Dr$ ,  $x := Dx$ ,  $S := DS$ ,  $T := T_a T + T_\infty$ , to obtain

$$\Delta T = 0 \quad \text{for } (r, \theta, x) \in \Omega_3^*, \quad (4.77a)$$

$$\nabla_\perp T \cdot \nabla_\perp S = \varepsilon R_X(\varepsilon x, \theta) \frac{\partial T}{\partial x} \quad \text{at } S = r - R(\varepsilon x, \theta) = 0, \quad (4.77b)$$

$$T = T_c(r, \theta) \quad \text{at } x = 0, \quad (4.77c)$$

$$T = T_d(r, \theta) \quad \text{at } x = \varepsilon^{-1}, \quad (4.77d)$$

where  $\Omega_2^*$  is the dimensionless version of  $\Omega_2$ , bounded by  $r = R(\varepsilon x, \theta)$ , with  $\varepsilon = \frac{D}{L} \ll 1$ . We introduced the transversal coordinate  $\mathbf{x}_\perp = \mathbf{x} - (\mathbf{x} \cdot \mathbf{e}_x)\mathbf{e}_x$ , and the transversal gradient  $\nabla_\perp = \frac{\partial}{\partial r}\mathbf{e}_r + \frac{1}{r}\frac{\partial}{\partial \theta}\mathbf{e}_\theta$ , such that at  $S = 0$  we have  $\nabla_\perp S = \mathbf{e}_r - \frac{R_\theta}{R}\mathbf{e}_\theta$ . Note that  $\nabla S$  at  $S = 0$  is outward normal to the surface  $r = R$ , but the transversal gradient  $\nabla_\perp S$  is directed in a cross-sectional plane  $\mathcal{A} = \mathcal{A}(\varepsilon x)$ , so it is normal to the  $x$ -axis and to the cylinder circumference given by  $S = 0$ ,  $x$  is constant (see Figure 4.6).

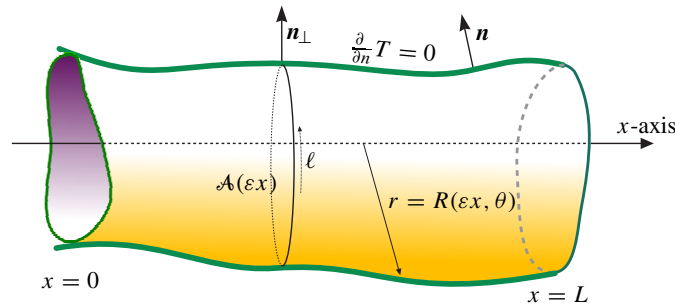


Figure 4.6: Sketch of geometry of the general heat conduction problem

Similar to the previous example, we introduce a rescaling  $X = \varepsilon x$  to obtain

$$\Delta_{\perp} T + \varepsilon^2 \frac{\partial^2 T}{\partial X^2} = 0, \quad (4.78a)$$

$$\nabla_{\perp} T \cdot \nabla_{\perp} S = \varepsilon^2 R_X(X, \theta) \frac{\partial T}{\partial X}, \quad (4.78b)$$

$$T(r, \theta, 0) = T_c(r, \theta), \quad (4.78c)$$

$$T(r, \theta, 1) = T_d(r, \theta). \quad (4.78d)$$

where evidently  $\Delta_{\perp} = \nabla_{\perp} \cdot \nabla_{\perp}$ .

Before we proceed to solving this problem, it is instructive to consider for comparison the following fluid mechanical phenomenon. If a viscous incompressible fluid, driven by a pressure difference, enters a pipe of constant cross section, the velocity profile will change gradually from the values at the entrance to the so-called fully developed velocity profile at a sufficient distance from the entrance (see [36], p. 226). This change is necessary because the viscosity causes the particles next to the wall to stick to the wall, so the flow velocity is zero at the wall. On the other hand, for steady flow the flux of flow is constant, so the fluid near the axis of the pipe must be accelerated (causing again friction), until a balance is achieved between the constraints of the wall and the applied pressure difference. Therefore, the initial velocity profile changes until its final form is established. Here, we can say that there is a boundary layer at the entrance (in axial direction, not in radial direction, since the flow is in axial direction).

Although our problem is on heat flow, rather than fluid flow, the diffusive effects are similar, suggesting that also in our problem boundary layers will occur at the ends  $X = 0$  and  $X = 1$  where the temperature distribution adapts itself to a “stationary state”, *i.e.* where the temperature field is balanced by the geometrical constraints of the wall and the applied temperature difference.

In Section 3.2, we have discussed that there are two expansions, the outer expansion and the inner expansion, that are used to solve the problem. We start here with the outer expansion.

### 4.1.3 Outer expansion

Since the boundary layers are assumed at  $X = 0$  and at  $X = 1$ , we solve the problem (4.78) without considering the boundary conditions at  $X = 0$  and at  $X = 1$ . In view of the occurrence of  $\varepsilon^2$  in (4.78a) and (4.78b), it seems to make sense to assume that the temperature  $T(r, \theta, X)$  can be expanded into an asymptotic expansion in powers of  $\varepsilon^2$ . It will turn out later, however, that due to the geometry, the correction terms of the inner expansion is of  $O(\varepsilon)$ , which requires via the matching conditions terms of the same order in the outer expansion. Therefore, we have to assume an outer expansion in powers of  $\varepsilon$ .

Introducing this expansion

$$T(r, \theta, X; \varepsilon) = T_0(r, \theta, X) + \varepsilon T_1(r, \theta, X) + \varepsilon^2 T_2(r, \theta, X) + O(\varepsilon^3) \quad (4.79)$$

into (4.78) and equating the coefficients of like power, we obtain for  $n = 0, 1, 2, 3$ , respectively,

$$\frac{\partial^2 T_0}{\partial r^2} + \frac{1}{r} \frac{\partial T_0}{\partial r} + \frac{1}{r^2} \frac{\partial^2 T_0}{\partial \theta^2} = 0, \quad \nabla_{\perp} T_0 \cdot \nabla_{\perp} S = 0, \quad \text{at } r = R(X, \theta), \quad (4.80)$$

$$\frac{\partial^2 T_1}{\partial r^2} + \frac{1}{r} \frac{\partial T_1}{\partial r} + \frac{1}{r^2} \frac{\partial^2 T_1}{\partial \theta^2} = 0, \quad \nabla_{\perp} T_1 \cdot \nabla_{\perp} S = 0, \quad \text{at } r = R(X, \theta), \quad (4.81)$$

$$\frac{\partial^2 T_2}{\partial r^2} + \frac{1}{r} \frac{\partial T_2}{\partial r} + \frac{1}{r^2} \frac{\partial^2 T_2}{\partial \theta^2} = -\frac{\partial^2 T_0}{\partial X^2}, \quad \nabla_{\perp} T_2 \cdot \nabla_{\perp} S = R_X(X, \theta) \frac{\partial T_0}{\partial X}, \quad \text{at } r = R(X, \theta), \quad (4.82)$$

$$\frac{\partial^2 T_3}{\partial r^2} + \frac{1}{r} \frac{\partial T_3}{\partial r} + \frac{1}{r^2} \frac{\partial^2 T_3}{\partial \theta^2} = -\frac{\partial^2 T_1}{\partial X^2}, \quad \nabla_{\perp} T_3 \cdot \nabla_{\perp} S = R_X(X, \theta) \frac{\partial T_1}{\partial X}, \quad \text{at } r = R(X, \theta). \quad (4.83)$$

Note that after the slow-variable scaling,  $S$  and  $R$  are independent of  $\varepsilon$ .

By inspection we see that a solution is  $T_0 \equiv 0$ ,  $T_1 \equiv 0$ . Since the Neumann problems (4.80), (4.81) have unique solutions up to a constant, we have the general solution

$$T_0(r, \theta, X) = T_0(X), \quad T_1(r, \theta, X) = T_1(X). \quad (4.84)$$

To obtain  $T_0(X)$ , we have to solve (4.82). Write (4.82) as

$$\Delta_{\perp} T_2 + \frac{d^2 T_0}{dX^2} = 0. \quad (4.85)$$

Integrate (4.85) over a cross-section  $\mathcal{A}$  of area  $A(X)$  and use Gauss' theorem to obtain

$$0 = \iint_{\mathcal{A}} \left( \Delta_{\perp} T_2 + \frac{d^2 T_0}{dX^2} \right) d\sigma = \iint_{\mathcal{A}} \left( \nabla \cdot \nabla_{\perp} T_2 + \frac{d^2 T_0}{dX^2} \right) d\sigma = \int_{\partial \mathcal{A}} \nabla_{\perp} T_2 \cdot \mathbf{n}_{\perp} d\ell + \frac{d^2 T_0}{dX^2} A(X),$$

where  $d\ell = \sqrt{R^2 + \left(\frac{\partial R}{\partial \theta}\right)^2} d\theta$ ,  $A(X) = \int_0^{2\pi} \frac{1}{2} R^2(X, \theta) d\theta$ , and  $\frac{dA(X)}{dX} = \int_0^{2\pi} R R_X d\theta$ . Since

$$\nabla_{\perp} T_2 \cdot \mathbf{n}_{\perp} = \nabla_{\perp} T_2 \cdot \frac{\nabla_{\perp} S}{|\nabla_{\perp} S|} = \frac{\frac{dT_0}{dX} R R_X}{\sqrt{R^2 + \left(\frac{\partial R}{\partial \theta}\right)^2}}, \quad (4.86)$$

it follows that

$$\frac{d^2 T_0}{dX^2} A(X) + \int_0^{2\pi} \frac{dT_0}{dX} R R_X d\theta = 0, \quad (4.87)$$

or

$$\frac{d^2 T_0}{dX^2} A(X) + \frac{dT_0}{dX} \frac{dA}{dX} = \frac{d}{dX} \left( \frac{dT_0}{dX} A(X) \right) = 0. \quad (4.88)$$

The solution of (4.88) is

$$T_0(X) = C_0 \int_0^X \frac{d\tilde{X}}{A(\tilde{X})} + D_0. \quad (4.89)$$



In a similar way, we obtain for  $T_1$ ,

$$T_1(X) = C_1 \int_0^X \frac{d\tilde{X}}{A(\tilde{X})} + D_1. \quad (4.90)$$

Higher order terms require the solution of the inhomogeneous Laplace equation in  $r$  and  $\theta$  on any cross-section. This becomes more and more complicated and at the same time less interesting. So we will stop here in our expansion, with the outer solution up to second order given by

$$T(r, \theta, X; \varepsilon) = (C_0 + \varepsilon C_1) \int_0^X \frac{d\tilde{X}}{A(\tilde{X})} + D_0 + \varepsilon D_1 + O(\varepsilon^2). \quad (4.91)$$

#### 4.1.4 Boundary layer at $X = 0$

Here, we consider the boundary layer at  $X = 0$ . Later, in a similar way, we will discuss the boundary layer at  $X = 1$ . We introduce the inner variable  $x = \frac{X}{\varepsilon}$  and we rename  $T(r, \theta, X; \varepsilon) = \Theta(r, \theta, x; \varepsilon)$  into (4.78) to obtain

$$\frac{\partial^2 \Theta}{\partial r^2} + \frac{1}{r} \frac{\partial \Theta}{\partial r} + \frac{1}{r^2} \frac{\partial^2 \Theta}{\partial \theta^2} + \frac{\partial^2 \Theta}{\partial x^2} = 0, \quad (4.92a)$$

$$\nabla_{\perp} \Theta \cdot \nabla_{\perp} S = \frac{\partial \Theta}{\partial r} - \frac{R_{\theta}}{R^2} \frac{\partial \Theta}{\partial \theta} = \varepsilon R_X(\varepsilon x, \theta) \frac{\partial \Theta}{\partial x} \quad \text{at } r = R(\varepsilon x, \theta), \quad (4.92b)$$

$$\Theta(r, \theta, 0) = T_c(r, \theta). \quad (4.92c)$$

Note that  $\Theta(r, \theta, x; \varepsilon) = Kx$ , where  $K$  is a constant, satisfies (4.92a) and satisfies ‘‘almost’’ (4.92b). As it is not immediately clear what the required behaviour for large  $x$  will have to be, we may have to include this solution in one of the expansions.

Next, the occurrence of  $\varepsilon$  in (4.92b) suggests us to assume the inner expansion as

$$\Theta(r, \theta, x; \varepsilon) = \Theta_0(r, \theta, x) + \varepsilon \Theta_1(r, \theta, x) + O(\varepsilon^2). \quad (4.93)$$

Since the parameter  $\varepsilon$  appears implicitly and explicitly, we expand the boundary conditions at  $r = R(\varepsilon x, \theta)$  and  $\Theta(R(\varepsilon x), \theta, x)$  about  $r = R(0, \theta)$  as follows

$$R(\varepsilon x, \theta) = R + \varepsilon x R_X + \frac{1}{2}(\varepsilon x)^2 R_{XX} + O((\varepsilon x)^3), \quad (4.94)$$

$$\Theta(R(\varepsilon x, \theta), \theta, x) = \Theta(R, \theta, x) + (\varepsilon x) R_X \frac{\partial \Theta}{\partial r}(R, \theta, x) + O((\varepsilon x)^2). \quad (4.95)$$

Furthermore, we have

$$\frac{R_{\theta}(\varepsilon x, \theta)}{R^2(\varepsilon x, \theta)} = \frac{R_{\theta}}{R^2} + \varepsilon x \frac{\partial}{\partial \theta} \left( \frac{R_X}{R^2} \right), \quad (4.96)$$

where  $R$  without argument denotes the values at  $X = 0$ .

So we have

$$\begin{aligned} \nabla_{\perp} \Theta \cdot \nabla_{\perp} S &= \frac{\partial \Theta}{\partial r} (R(\varepsilon x, \theta), \theta, x; \varepsilon) - \frac{R_{\theta}(\varepsilon x, \theta)}{R^2(\varepsilon x, \theta)} \frac{\partial \Theta}{\partial \theta} (R(\varepsilon x, \theta), \theta, x; \varepsilon) \\ &= \frac{\partial \Theta_0}{\partial r} - \frac{R_{\theta}}{R^2} \frac{\partial \Theta_0}{\partial \theta} + \varepsilon \left[ \frac{\partial \Theta_1}{\partial r} - \frac{R_{\theta}}{R^2} \frac{\partial \Theta_1}{\partial \theta} + x \frac{\partial^2 \Theta_0}{\partial r^2} R_X - x \frac{R_{\theta} R_X}{R^2} \frac{\partial^2 \Theta_0}{\partial r \partial \theta} - x \frac{\partial}{\partial \theta} \left( \frac{R_X}{R^2} \right) \frac{\partial \Theta_0}{\partial \theta} \right] \\ &= \varepsilon R_X \frac{\partial \Theta_0}{\partial x}, \quad (4.97) \end{aligned}$$

which means at  $r = R = R(0, \theta)$  we have

$$\nabla_{\perp} \Theta_0 \cdot \nabla_{\perp} S_0 = \frac{\partial \Theta_0}{\partial r} - \frac{R_{\theta}}{R^2} \frac{\partial \Theta_0}{\partial \theta} = 0, \quad (4.98)$$

$$\nabla_{\perp} \Theta_1 \cdot \nabla_{\perp} S_0 = \frac{\partial \Theta_1}{\partial r} - \frac{R_{\theta}}{R^2} \frac{\partial \Theta_1}{\partial \theta} = R_X \frac{\partial \Theta_0}{\partial x} - x \frac{\partial^2 \Theta_0}{\partial r^2} R_X + x \frac{R_{\theta} R_X}{R^2} \frac{\partial^2 \Theta_0}{\partial r \partial \theta} + x \frac{\partial}{\partial \theta} \left( \frac{R_X}{R^2} \right) \frac{\partial \Theta_0}{\partial \theta}, \quad (4.99)$$

where  $\nabla_{\perp} S_0 = \mathbf{e}_r - \frac{R_{\theta}}{R} \mathbf{e}_{\theta}$ . Using

$$\frac{d}{d\theta} \left( \frac{\partial \Theta_0}{\partial \theta} \right) = R_{\theta} \frac{\partial^2 \Theta_0}{\partial r \partial \theta} + \frac{\partial^2 \Theta_0}{\partial \theta^2}, \quad (4.100)$$

and the defining equation

$$-\frac{\partial^2 \Theta_0}{\partial r^2} = \frac{1}{R} \frac{\partial \Theta_0}{\partial r} + \frac{1}{R^2} \frac{\partial^2 \Theta_0}{\partial \theta^2} + \frac{\partial \Theta_0}{\partial x} = \frac{R_{\theta}}{R^3} \frac{\partial \Theta_0}{\partial \theta} + \frac{1}{R^2} \frac{\partial^2 \Theta_0}{\partial \theta^2} + \frac{\partial^2 \Theta_0}{\partial x^2}, \quad (4.101)$$

we see that (4.99) is equivalent to

$$\nabla_{\perp} \Theta_1 \cdot \nabla_{\perp} S_0 = \mathcal{Q}_0(x, \theta) \stackrel{\text{def}}{=} R_X \frac{\partial \Theta_0}{\partial x} + \frac{x}{R} \left[ R R_X \frac{\partial^2 \Theta_0}{\partial x^2} + \frac{d}{d\theta} \left( \frac{R_X}{R} \frac{\partial \Theta_0}{\partial \theta} \right) \right]. \quad (4.102)$$

Using the above boundary conditions, we obtain the following boundary value problem for the leading order ( $O(1)$ )

$$\Delta \Theta_0 = 0, \quad (4.103a)$$

$$\nabla_{\perp} \Theta_0 \cdot \nabla_{\perp} S_0 = \frac{\partial \Theta_0}{\partial r} - \frac{R_{\theta}}{R^2} \frac{\partial \Theta_0}{\partial \theta} = 0, \quad \text{at } r = R(0, \theta), \quad (4.103b)$$

$$\Theta_0(r, \theta, 0) = T_c(r, \theta), \quad (4.103c)$$

$$\Theta_0(r, \theta, x) \sim K_0 x + \text{constant} + \text{EST}, \quad \text{as } x \rightarrow \infty. \quad (4.103d)$$

where the linear term  $K_0 x$  anticipates a possible solution of this form.

The solution  $\Theta_0$  may be expressed by the eigenfunction expansion

$$\Theta_0(\mathbf{x}) = \sum_{n=0}^{\infty} A_n \psi_n(r, \theta) e^{-\lambda_n x} + \sum_{n=1}^{\infty} B_n \psi_n(r, \theta) e^{\lambda_n x} + K_0 x, \quad (4.104)$$

where  $\psi_n(r, \theta)$  satisfies the Sturm-Liouville problem

$$\frac{\partial^2 \psi_n}{\partial r^2} + \frac{1}{r} \frac{\partial \psi_n}{\partial r} + \frac{1}{r^2} \frac{\partial^2 \psi_n}{\partial \theta^2} + \lambda_n^2 \psi_n = 0, \quad (4.105a)$$

$$\nabla_{\perp} \psi_n \cdot \nabla_{\perp} S_0 = 0, \quad \text{at } r = R(0, \theta). \quad (4.105b)$$

Further on, we will for convenience take  $K_0$  and  $B_n$  to be zero. This is strictly speaking a result of the matching. The inner expansion would become infinite and cannot be matched with the outer solution.

Note that the eigenvalue  $\lambda_0 = 0$  corresponds to the eigenfunction  $\psi_0(r, \theta)$ , a constant. Assuming the orthonormality of  $\psi_n(r, \theta)$ , or  $\iint_{\mathcal{A}(0)} \psi_n(r, \theta)^2 d\sigma = 1$ , leads to  $\psi_0(r, \theta) =$

$A(0)^{-1/2}$ , where  $\mathcal{A}(0)$  denotes the cross-section  $x = 0$ , of area  $A(0)$ . The orthogonality of the eigenfunctions and the fact that  $\psi_0(r, \theta)$  is a constant imply that  $\iint_{\mathcal{A}(0)} \psi_n(r, \theta) d\sigma = 0$ , for  $n \neq 0$ .

Next, the boundary condition (4.103c) and the orthonormality of the eigenfunctions lead to

$$A_0 = A(0)^{-1/2} \iint_{\mathcal{A}(0)} T_c(r, \theta) d\sigma, \quad A_n = \iint_{\mathcal{A}(0)} T_c(r, \theta) \psi_n(r, \theta) d\sigma. \quad (4.106)$$

Since the cross-section of the cylinder is of arbitrary shape, we can not determine explicitly  $\psi_n(r, \theta)$ , except for  $n = 0$ . Based on the Sturm-Liouville theory, however, we know that the eigenvalues  $\lambda_n$  are nonnegative, countably infinite, and the corresponding eigenfunctions are complete and orthogonal. This verifies that we can indeed express the solution of heat equation (4.103) by a series of eigenfunctions (4.104).

Note that if  $R(\varepsilon x, \theta)$  does not depend on  $\theta$  (the cross section is a circle), the eigenfunctions  $\psi_n(r, \theta)$  are

$$\psi_n(r, \theta) = J_{\nu} \left( \frac{\alpha'_{\nu\mu}}{R(0)} r \right) e^{i\nu\theta}, \quad \nu \in \mathbb{Z}, \quad (4.107)$$

where  $\alpha'_{\nu\mu}$  are the real zeroes of the derivatives of Bessel functions,  $J'_{\nu}(\alpha'_{\nu\mu}) = 0$  and are ordered such that they are monotonically increasing. The corresponding eigenvalues are  $\lambda_n = \alpha'_{\nu\mu}/R(0)$ .

For the next order, *i.e.*  $O(\varepsilon)$ , we have to solve

$$\Delta \Theta_1 = 0, \quad (4.108a)$$

$$\nabla_{\perp} \Theta_1 \cdot \nabla_{\perp} S_0 = \mathcal{Q}_0, \quad \text{at } r = R(0, \theta), \quad (4.108b)$$

$$\Theta_1(r, \theta, 0) = 0, \quad (4.108c)$$

$$\Theta_1(r, \theta, x) \sim K_1 x + \text{constant} + \text{EST}, \quad \text{as } x \rightarrow \infty, \quad (4.108d)$$

where

$$\mathcal{Q}_0 = \sum_{n=1}^{\infty} A_n e^{-\lambda_n x} \left[ -R_X \lambda_n \psi_n + x R_X \lambda_n^2 \psi_n + \frac{x}{R} \frac{d}{d\theta} \left( \frac{R_X}{R} \frac{\partial \psi_n}{\partial \theta} \right) \right]_{r=R}.$$

To solve this problem, we introduce a Green's function  $G(\mathbf{x}; \boldsymbol{\xi})$  with  $\mathbf{x} = (r, \theta, x)$  and  $\boldsymbol{\xi} = (\rho, \eta, \xi)$  satisfying

$$\Delta_{\perp} G + \frac{\partial^2 G}{\partial x^2} = -\delta(\mathbf{x} - \boldsymbol{\xi}), \quad (4.109a)$$

$$\frac{\partial G}{\partial n} = 0, \text{ at } r = R(0, \theta), \quad (4.109b)$$

$$G(\mathbf{x}; \boldsymbol{\xi}) = 0, \text{ at } x = 0. \quad (4.109c)$$

$$G(\mathbf{x}; \boldsymbol{\xi}) \rightarrow \text{a constant}, \text{ as } x \rightarrow \infty. \quad (4.109d)$$

$$x \frac{\partial G}{\partial x}(\mathbf{x}; \boldsymbol{\xi}) \rightarrow 0, \text{ as } x \rightarrow \infty. \quad (4.109e)$$

We determine the Green's function by applying the Fourier Sine Transform<sup>3</sup> with respect to  $x$  ( $x \rightarrow k$ ) to equation (4.109a), and obtain

$$\Delta_{\perp} \hat{G} - k^2 \hat{G} = -\sqrt{\frac{2}{\pi}} \sin(k\xi) \delta(\mathbf{x}_{\perp} - \boldsymbol{\xi}_{\perp}). \quad (4.110)$$

Assuming that we can expand  $\hat{G} = \sum_{m=0}^{\infty} a_m \psi_m(r, \theta)$ , we obtain  $\Delta_{\perp} \hat{G} = -\sum_{m=0}^{\infty} a_m \lambda_m^2 \psi_m(r, \theta)$ . Substituting this into (4.110) yields<sup>3</sup>

$$\sum_{m=0}^{\infty} a_m \psi_m(r, \theta) (\lambda_m^2 + k^2) = \sqrt{\frac{2}{\pi}} \sin(k\xi) \delta(\mathbf{x}_{\perp} - \boldsymbol{\xi}_{\perp}). \quad (4.111)$$

Next, multiply (4.111) with  $\psi_n$  and integrate over a cross-section  $\mathcal{A}(0)$  of area  $A(0)$  to obtain

$$\iint_{\mathcal{A}(0)} \sum_{m=0}^{\infty} a_m \psi_n \psi_m (\lambda_m^2 + k^2) d\sigma = \sqrt{\frac{2}{\pi}} \iint_{\mathcal{A}(0)} \psi_n(r, \theta) \sin(k\xi) \delta(\mathbf{x}_{\perp} - \boldsymbol{\xi}_{\perp}) d\sigma. \quad (4.112)$$

Orthonormality of the base functions yields

$$a_m = \sqrt{\frac{2}{\pi}} \frac{\sin(k\xi)}{\lambda_m^2 + k^2} \psi_m(\rho, \eta). \quad (4.113)$$

Therefore,

$$\hat{G}(r, \theta, k; \rho, \eta, \xi) = \sqrt{\frac{2}{\pi}} \sum_{m=0}^{\infty} \frac{\sin(k\xi)}{\lambda_m^2 + k^2} \psi_m(\rho, \eta) \psi_m(r, \theta). \quad (4.114)$$

The inverse Fourier Sine Transform gives the solution

$$G(\mathbf{x}; \boldsymbol{\xi}) = \frac{2}{\pi} \sum_{m=0}^{\infty} \psi_m(\rho, \eta) \psi_m(r, \theta) \int_0^{\infty} \frac{\sin(kx) \sin(k\xi)}{\lambda_m^2 + k^2} dk, \quad (4.115)$$

---

<sup>3</sup>where  $\hat{f}(k) = \sqrt{\frac{2}{\pi}} \int_0^{\infty} \sin(kx) f(x) dx$ ,  $f(x) = \sqrt{\frac{2}{\pi}} \int_0^{\infty} \sin(kx) \hat{f}(k) dk$ .

where for  $\lambda_0 = 0$ , (see [21], p. 425)

$$\int_0^\infty \frac{\sin(kx) \sin(k\xi)}{k^2} dk = \frac{\pi}{2} \min(x, \xi), \quad (4.116)$$

and for  $\lambda_m > 0$ ,

$$\int_0^\infty \frac{\sin(kx) \sin(k\xi)}{\lambda_m^2 + k^2} dk = \frac{\pi}{2\lambda_m} e^{-\lambda_m \max(x, \xi)} \sinh(\lambda_m \min(x, \xi)). \quad (4.117)$$

Therefore, the Green's function becomes

$$G(x; \xi) = \begin{cases} \frac{x}{A(0)} + \sum_{m=1}^{\infty} \frac{\psi_m(\rho, \eta) \psi_m(r, \theta) e^{-\lambda_m \xi}}{\lambda_m} \sinh(\lambda_m x), & 0 \leq x \leq \xi, \\ \frac{\xi}{A(0)} + \sum_{m=1}^{\infty} \frac{\psi_m(\rho, \eta) \psi_m(r, \theta) e^{-\lambda_m x}}{\lambda_m} \sinh(\lambda_m \xi), & 0 \leq \xi \leq x. \end{cases} \quad (4.118)$$

Note that as  $x \rightarrow \infty$ ,  $G$  tends to  $\frac{\xi}{A(0)}$  and  $\frac{\partial G}{\partial x}$  tends to zero exponentially.

Using this Green's function, (4.108a), and (4.109a) we obtain

$$\Theta_1 \delta(\mathbf{x} - \xi) = G \Delta \Theta_1 - \Theta_1 \Delta G. \quad (4.119)$$

Note that the domain here is an infinite cylinder, therefore we consider a region  $\Omega$  with a finite length  $0 \leq \xi \leq X_0$ , where  $X_0$  is far enough from 0. Integrating (4.119) over the whole domain  $\Omega$  and using Green's second identity, (4.108), and (4.109), we get

$$\begin{aligned} \Theta_1(\xi) &= \iiint_{\Omega} (G \Delta \Theta_1 - \Theta_1 \Delta G) d\mathbf{x} \\ &= \iint_{x=0} \left( -G \frac{\partial \Theta_1}{\partial x} + \Theta_1 \frac{\partial G}{\partial x} \right) d\sigma + \iint_{r=R(0, \eta)} (G \nabla_{\perp} \Theta_1 - \Theta_1 \nabla_{\perp} G) \cdot \mathbf{n}_{\perp} d\sigma \\ &\quad + \iint_{x=X_0} \left( G \frac{\partial \Theta_1}{\partial x} - \Theta_1 \frac{\partial G}{\partial x} \right) d\sigma, \\ &= \iint_{r=R(0, \eta)} \frac{G \mathcal{Q}_0(x, \theta)}{|\nabla_{\perp} S|} d\ell d\xi + K_1 \xi, \end{aligned} \quad (4.120)$$

where  $|\nabla_{\perp} S| = \frac{1}{R} \sqrt{R^2 + R_{\theta}^2}$  and  $d\ell = \sqrt{R^2 + R_{\theta}^2} d\theta$ . Therefore, we obtain

$$\Theta_1(\xi) = \int_0^{2\pi} \int_0^{\infty} \mathcal{Q}_0(x, \theta) G(x; \xi) \Big|_{r=R} dx R d\theta + K_1 \xi. \quad (4.121)$$

To remove the  $x$ -integration, we calculate

$$\int_0^\infty e^{-\lambda_n x} G(\mathbf{x}; \boldsymbol{\xi})|_{r=R} dx = \frac{1 - e^{-\lambda_n \xi}}{A(0)\lambda_n^2} - \begin{cases} \sum_{m=1}^\infty \psi_m(R, \theta) \psi_m(\rho, \eta) \frac{e^{-\lambda_n \xi} - e^{-\lambda_m \xi}}{\lambda_n^2 - \lambda_m^2}, & \lambda_n \neq \lambda_m, \\ - \sum_{m=1}^\infty \psi_m(R, \theta) \psi_m(\rho, \eta) \frac{1}{2} \xi e^{-\lambda_n \xi}, & \lambda_n = \lambda_m, \end{cases} \quad (4.122)$$

and

$$\int_0^\infty x e^{-\lambda_n x} G(\mathbf{x}; \boldsymbol{\xi})|_{r=R} dx = \frac{2 - (2 + \lambda_n \xi) e^{-\lambda_n \xi}}{A(0)\lambda_n^3} - \begin{cases} \sum_{m=1}^\infty \psi_m(R, \theta) \psi_m(\rho, \eta) \frac{2\lambda_n(e^{-\lambda_n \xi} - e^{-\lambda_m \xi}) + \xi(\lambda_n^2 - \lambda_m^2)e^{-\lambda_n \xi}}{(\lambda_n^2 - \lambda_m^2)^2}, & \lambda_n \neq \lambda_m, \\ - \sum_{m=1}^\infty \psi_m(R, \theta) \psi_m(\rho, \eta) \frac{\xi e^{-\lambda_n \xi} (1 + \lambda_n \xi)}{4\lambda_n}, & \lambda_n = \lambda_m. \end{cases} \quad (4.123)$$

Therefore, after interchanging  $\mathbf{x}$  with  $\boldsymbol{\xi}$ , we obtain

$$\Theta_1(\mathbf{x}) = K_1 x + \sum_{n=1}^\infty A_n \int_0^{2\pi} \left[ -RR_X \lambda_n \psi_n \int_0^\infty e^{-\lambda_n \xi} G(\boldsymbol{\xi}; \mathbf{x}) d\xi + \left\{ RR_X \lambda_n^2 \psi_n + \frac{d}{d\eta} \left( \frac{R_X}{R} \frac{\partial \psi_n}{\partial \eta} \right) \right\} \int_0^\infty \xi e^{-\lambda_n \xi} G(\boldsymbol{\xi}; \mathbf{x}) d\xi \right] d\eta. \quad (4.124)$$

#### 4.1.5 Boundary layer at $X = 1$

Now, we consider the boundary layer at  $X = 1$ . We introduce the inner variable  $\bar{x} = \frac{1-X}{\varepsilon}$ , and since at the boundary  $T(r, \theta, 1) = O(1)$ , we rescale  $T(r, \theta, X; \varepsilon) = \Phi(r, \theta, \bar{x}; \varepsilon)$  into (4.78) to obtain

$$\Delta \Phi = 0, \quad (4.125a)$$

$$\nabla_\perp \Phi \cdot \nabla_\perp S = -\varepsilon R_X (1 - \varepsilon \bar{x}, \theta) \frac{\partial \Phi}{\partial \bar{x}}, \quad \text{at } r = R(1 - \varepsilon \bar{x}, \theta), \quad (4.125b)$$

$$\Phi(r, \theta, 0) = T_d(r, \theta), \quad (4.125c)$$

$$\Phi(r, \theta, \bar{x}) \sim L\bar{x} + \text{constant} + \text{EST}, \quad \text{as } \bar{x} \rightarrow \infty. \quad (4.125d)$$

In a similar way as before, we assume the inner expansion as

$$\Phi(r, \theta, \bar{x}; \varepsilon) = \Phi_0(r, \theta, \bar{x}) + \varepsilon \Phi_1(r, \theta, \bar{x}) + O(\varepsilon^2). \quad (4.126)$$

Using the same method of eigenfunction expansion and the Green's function, we obtain

$$\Phi_0(r, \theta, \bar{x}) = E_0 A(1)^{-1/2} + \sum_{n=1}^{\infty} E_n \phi_n(r, \theta) e^{-\mu_n \bar{x}} + L_0 \bar{x}, \quad (4.127)$$

$$\Phi_1(\xi) = \int_0^{2\pi} \int_0^{\infty} \bar{\mathcal{Q}}_0(\bar{x}, \theta) G(\mathbf{x}; \xi)|_{r=R} d\bar{x} R d\theta + L_1 \xi, \quad (4.128)$$

where

$$\begin{aligned} \bar{\mathcal{Q}}_0(\bar{x}, \theta) &= -\bar{R}_X \frac{\partial \Theta_0}{\partial \bar{x}} - \frac{\bar{x}}{\bar{R}} \left[ \bar{R} \bar{R}_X \frac{\partial^2 \Theta_0}{\partial \bar{x}^2} + \frac{d}{d\theta} \left( \frac{R_X}{R} \frac{\partial \Theta_0}{\partial \theta} \right) \right] \\ &= \sum_{n=1}^{\infty} E_n e^{-\mu_n \bar{x}} \left[ \bar{R}_X \mu_n \phi_n - \bar{x} \bar{R}_X \mu_n^2 \phi_n - \frac{\bar{x}}{\bar{R}} \frac{d}{d\theta} \left( \frac{\bar{R}_X}{\bar{R}} \frac{\partial \phi_n}{\partial \theta} \right) \right]_{r=\bar{R}}, \end{aligned}$$

where  $\bar{R}$  without argument denotes the values at  $X = 1$ .

After interchanging  $\mathbf{x}$  with  $\xi$ , we obtain

$$\begin{aligned} \Phi_1(\mathbf{x}) &= L_1 \bar{x} + \sum_{n=1}^{\infty} E_n \int_0^{2\pi} \left[ \bar{R} \bar{R}_X \mu_n \phi_n \int_0^{\infty} e^{-\mu_n \bar{x}} G(\xi; \mathbf{x}) d\xi \right. \\ &\quad \left. + \left\{ \bar{R} \bar{R}_X \mu_n^2 \phi_n - \frac{d}{d\eta} \left( \frac{R_X}{R} \frac{\partial \phi_n}{\partial \eta} \right) \right\} \int_0^{\infty} \xi e^{-\mu_n \xi} G(\xi; \mathbf{x}) d\xi \right] d\eta. \end{aligned} \quad (4.129)$$

#### 4.1.6 Matching

In this section, we discuss the matching between the outer solution (4.91) and the inner solutions (4.104), (4.124), (4.127), and (4.129). First, we consider the matching at  $X = 0$ . Applying Van Dyke's rule for matching, we rewrite the outer expansion (4.91) in inner variable  $x = \frac{X}{\varepsilon}$  to obtain

$$\begin{aligned} T(r, \theta, x; \varepsilon) &= (C_0 + \varepsilon C_1) \int_0^{\varepsilon x} \frac{d\tilde{X}}{A(\tilde{X})} + D_0 + \varepsilon D_1 + O(\varepsilon^2) \\ &= (C_0 + \varepsilon C_1) \frac{\varepsilon x}{A(0)} + D_0 + \varepsilon D_1 + O(\varepsilon^2) \\ &= D_0 + \varepsilon D_1 + \varepsilon x \frac{C_0}{A(0)} + \varepsilon^2 x \frac{C_1}{A(0)} + O(\varepsilon^2). \end{aligned} \quad (4.130)$$

Next we rewrite the inner expansion (4.104), (4.124) in the outer variable  $X$ . Since for  $\varepsilon \rightarrow 0$  the term  $e^{-\lambda_n \frac{X}{\varepsilon}}$  is EST, it can be ignored. Finally, we get

$$\Theta(r, \theta, X; \varepsilon) = A_0 A(0)^{-1/2} + \varepsilon x K_1 + \frac{\varepsilon}{A(0)} \sum_{n=1}^{\infty} \frac{A_n}{\lambda_n} \int_0^{2\pi} R R_X \psi_n d\eta + O(\varepsilon^2). \quad (4.131)$$

Comparing (4.130) and (4.131), we obtain

$$D_0 = A_0 A(0)^{-1/2}, \quad \frac{C_0}{A(0)} = K_1, \quad D_1 = \frac{1}{A(0)} \sum_{n=1}^{\infty} \frac{A_n}{\lambda_n} \int_0^{2\pi} R R_X \psi_n \, d\eta, \quad (4.132)$$

while  $C_0$  is still unknown and  $C_1$  is undetermined yet. To find these constants, we need another relationship which can be obtained from matching the outer expansion with the inner expansion at  $X = 1$ .

In a similar way, for matching at  $X = 1$ , we rewrite the outer solution (4.91) in inner variable  $\bar{x}$  to obtain

$$\begin{aligned} T(r, \theta, \bar{x}; \varepsilon) &= (C_0 + \varepsilon C_1) \int_0^{1-\varepsilon\bar{x}} \frac{d\tilde{X}}{A(\tilde{X})} + D_0 + \varepsilon D_1 + O(\varepsilon^2), \\ &\simeq (C_0 + \varepsilon C_1) \int_0^1 \frac{d\tilde{X}}{A(\tilde{X})} + (C_0 + \varepsilon C_1) \int_1^{1-\varepsilon\bar{x}} \frac{d\tilde{X}}{A(\tilde{X})} + D_0 + \varepsilon D_1, \\ &\simeq C_0 \int_0^1 \frac{d\tilde{X}}{A(\tilde{X})} + D_0 + \varepsilon \left[ C_1 \int_0^1 \frac{d\tilde{X}}{A(\tilde{X})} + D_1 \right] - \varepsilon\bar{x} \frac{C_0}{A(1)} - \varepsilon^2 \bar{x} \frac{C_1}{A(1)}. \end{aligned} \quad (4.133)$$

Next we rewrite the inner expansion (4.127), (4.129) in the outer variable  $X$  to obtain

$$\Phi(r, \theta, X; \varepsilon) = E_0 A(1)^{-1/2} + L_1 \varepsilon \bar{x} - \frac{\varepsilon}{A(1)} \sum_{n=1}^{\infty} \frac{E_n}{\mu_n} \int_0^{2\pi} \bar{R} \bar{R}_X \phi_n \, d\eta. \quad (4.134)$$

Comparing (4.133) and (4.134), we see that

$$C_0 \int_0^1 \frac{d\tilde{X}}{A(\tilde{X})} = E_0 A(1)^{-1/2} - D_0 = E_0 A(1)^{-1/2} - A_0 A(0)^{-1/2}, \quad (4.135)$$

$$\begin{aligned} C_1 \int_0^1 \frac{d\tilde{X}}{A(\tilde{X})} &= -D_1 - \frac{1}{A(1)} \sum_{n=1}^{\infty} \frac{E_n}{\mu_n} \int_0^{2\pi} \bar{R} \bar{R}_X \phi_n \, d\eta \\ &= -\frac{1}{A(0)} \sum_{n=1}^{\infty} \frac{A_n}{\lambda_n} \int_0^{2\pi} R R_X \psi_n \, d\eta - \frac{1}{A(1)} \sum_{n=1}^{\infty} \frac{E_n}{\mu_n} \int_0^{2\pi} \bar{R} \bar{R}_X \phi_n \, d\eta, \end{aligned} \quad (4.136)$$

$$L_1 = -\frac{C_0}{A(1)} = \frac{A_0 A(0)^{-1/2} - E_0 A(1)^{-1/2}}{A(1) \int_0^1 \frac{d\tilde{X}}{A(\tilde{X})}}. \quad (4.137)$$

Finally, we arrive at

$$K_1 = \frac{C_0}{A(0)} = \frac{E_0 A(1)^{-1/2} - A_0 A(0)^{-1/2}}{A(0) \int_0^1 \frac{d\tilde{X}}{A(\tilde{X})}}. \quad (4.138)$$



### 4.1.7 Heat Flux

In this section, we calculate the heat flux across a section  $X$ . Since the boundary  $r = R(\varepsilon x, \theta)$  is insulated we can show, by using Gauss' theorem, that the heat flux across each section is constant. Consider a portion of the finite cylinder with  $X_1 \leq X \leq X_2$ , then

$$0 = \iiint_V \Delta \Theta \, dx = \iiint_{\partial V} \nabla \Theta \cdot \mathbf{n} \, dS = - \iint_{\mathcal{A}(X_1)} \frac{\partial \Theta}{\partial x} \, d\sigma + \iint_{\mathcal{A}(X_2)} \frac{\partial \Theta}{\partial x} \, d\sigma. \quad (4.139)$$

Therefore, we get the flux

$$\mathcal{F} = \iint_{\mathcal{A}(X_1)} \frac{\partial \Theta}{\partial x} \, d\sigma = \iint_{\mathcal{A}(X_2)} \frac{\partial \Theta}{\partial x} \, d\sigma. \quad (4.140)$$

First we calculate the heat flux in the boundary layer, yielding

$$\begin{aligned} \iint_{\mathcal{A}(X)} \frac{\partial \Theta}{\partial x} \, d\sigma &= \int_0^{2\pi} \int_0^{R(X,\theta)} \frac{\partial \Theta}{\partial x} r \, dr d\theta = \int_0^{2\pi} \int_0^{R+\varepsilon x R_X} \left( \frac{\partial \Theta_0}{\partial x} + \varepsilon \frac{\partial \Theta_1}{\partial x} \right) r \, dr d\theta = \\ &= \int_0^{2\pi} \int_0^R \frac{\partial \Theta_0}{\partial x} r \, dr d\theta + \varepsilon \int_0^{2\pi} \int_0^R \frac{\partial \Theta_1}{\partial x} r \, dr d\theta + \varepsilon x \int_0^{2\pi} \frac{\partial \Theta_0}{\partial x} R_X R \, d\theta. \end{aligned} \quad (4.141)$$

As  $\psi_n$  ( $n \neq 0$ ) is orthogonal to a constant, we have indeed for the leading order

$$\int_0^{2\pi} \int_0^R \frac{\partial \Theta_0}{\partial x} r \, dr d\theta = - \sum_{n=1}^{\infty} \lambda_n A_n e^{-\lambda_n x} \int_0^{2\pi} \int_0^R \psi_n r \, dr d\theta = 0. \quad (4.142)$$

For the same reason, most of the terms in the second order disappear, and we get

$$\begin{aligned} \int_0^{2\pi} \int_0^R \frac{\partial \Theta_1}{\partial x} r \, dr d\theta &= K_1 A(0) + \sum_{n=1}^{\infty} A_n e^{-\lambda_n x} \int_0^{2\pi} \left[ -RR_X \psi_n \right. \\ &\quad \left. + \left\{ RR_X \lambda_n^2 \psi_n + \frac{d}{d\theta} \left( \frac{R_X}{R} \frac{\partial \psi_n}{\partial \theta} \right) \right\} \frac{1 + \lambda_n x}{\lambda_n^2} \right] d\theta. \end{aligned} \quad (4.143)$$

Using the periodicity of  $\psi_n$ , we obtain

$$\int_0^{2\pi} \int_0^R \frac{\partial \Theta_1}{\partial x} r \, dr d\theta = K_1 A(0) + \sum_{n=1}^{\infty} A_n \lambda_n x e^{-\lambda_n x} \int_0^{2\pi} RR_X \psi_n \, d\theta. \quad (4.144)$$

If we add the other term

$$x \int_0^{2\pi} \frac{\partial \Theta_0}{\partial x} R_X R \, d\theta = - \sum_{n=1}^{\infty} A_n e^{-\lambda_n x} x \lambda_n \int_0^{2\pi} R_X R \psi_n \, d\theta, \quad (4.145)$$

we obtain the flux as

$$\iint_{\mathcal{A}(X)} \frac{\partial \Theta}{\partial x} d\sigma = \varepsilon K_1 A(0). \quad (4.146)$$

which is indeed independent of  $x$ . Note that the heat flux is of  $O(\varepsilon)$ . This conservation of heat flux can be used to verify the matching (4.132). Consider the heat flux across  $X = \varepsilon x$  in the outer region. Using the outer solution (4.91), we obtain for the heat flux

$$\begin{aligned} \iint_{\mathcal{A}(X)} \frac{\partial T}{\partial X} d\sigma &= \iint_{\mathcal{A}(X)} \varepsilon \frac{\partial T}{\partial x} d\sigma = \iint_{\mathcal{A}(X)} \frac{\varepsilon}{A(X)} (C_0 + \varepsilon C_1) d\sigma \\ &= \varepsilon C_0 + O(\varepsilon^2). \end{aligned} \quad (4.147)$$

which is, again, indeed independent of  $X$ . This result confirms our previous matching result that  $K_1 A(0) = C_0$ .

It should be noted that the actual value of the heat flux, given from (4.138) as

$$\mathcal{F} = \varepsilon \frac{A(1)^{-1} \iint_{\mathcal{A}(1)} T_d d\sigma - A(0)^{-1} \iint_{\mathcal{A}(0)} T_c d\sigma}{\int_0^1 A(X)^{-1} dX}. \quad (4.148)$$

cannot be found from the outer or inner solution only, and we really need the combined information of outer and inner solution together.

## 5 Method of slight variation

In this section, we discuss the so-called slightly varying geometry (see [13,14]) where the geometry varies a little, but not slowly. In dimensionless coordinates, the boundary or any other property of the geometry is assumed to be of order 1 and it varies with deflections of order  $\varepsilon$ .

Mathematically, we may write the equation of the boundary as  $y = y_0 + \varepsilon G(x)$ ,  $G(x) = O(1)$ , together with, for example, the governing equation  $L(f(x, y; \varepsilon)) = 0$ . We solve this problem simply by expanding  $f(x, y; \varepsilon)$  into a regular perturbation expansion in power of  $\varepsilon$ . Unlike the slowly varying case, the parameter  $\varepsilon$  is still in the boundary condition and is not transformed into the governing equations. Therefore, the perturbation parameter  $\varepsilon$  occurs implicitly and explicitly in boundary conditions, for example,

$$f_0(x, y_0 + \varepsilon G(x)) + \varepsilon f_1(x, y_0 + \varepsilon G(x)) + \varepsilon^2 f_2(x, y_0 + \varepsilon G(x)) + \dots = 0.$$

Consequently, we can not directly expand the boundary condition into a Poincaré expansion. By expanding the boundary condition into a Taylor series about  $y = y_0$ ,

$$f_0(x, y_0 + \varepsilon G(x)) = f_0(x, y_0) + \varepsilon G(x) \frac{\partial f_0}{\partial y}(x, y_0) + \frac{1}{2} (\varepsilon G(x))^2 \frac{\partial^2 f_0}{\partial y^2}(x, y_0) + O(\varepsilon^3),$$

(etc. for  $f_1, f_2, \dots$ ), we render it into a Poincaré expansion (see [12], p. 14). Finally, we can solve the governing equations for each coefficient of  $\varepsilon$  successively.

Below, we give an example to illustrate the above method.

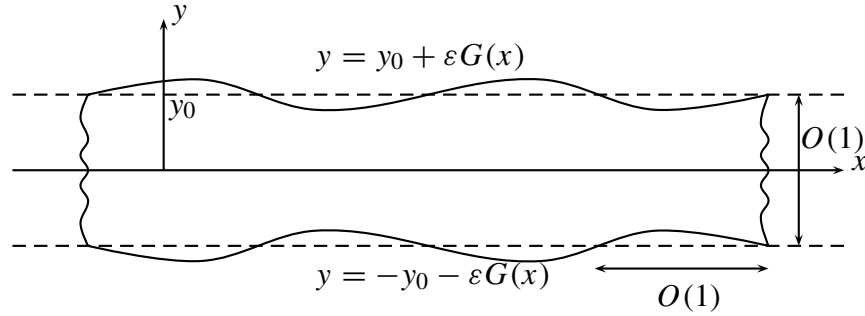


Figure 5.7: Slightly varying symmetric strip

## 5.1 Example

In this section, we discuss another heat conduction problem (similar to as Example (4.1.1)) but now the geometry is slightly varying. Although the problems in both examples are similar, the geometries are different, and we have to choose the appropriate method to solve each problem. In this example, we apply the above procedure.

### 5.1.1 Heat conduction problem

In this example, we consider a heat conduction problem  $\Delta T(x, y) = 0$  in an infinite strip  $\Omega_3$  that is bounded by  $y = \pm L \pm DG\left(\frac{x}{L}\right)$ ,  $D \ll L$ , where the temperature is prescribed. We assume the temperature is bounded as  $|x| \rightarrow \infty$ ,

$$\Delta T(x, y) = 0, (x, y) \in \Omega_3, \quad (5.149a)$$

$$T\left(x, \pm L \pm DG\left(\frac{x}{L}\right)\right) = \pm T_a, \quad (5.149b)$$

$$T(x, y) \text{ is bounded for } |x| \rightarrow \infty, \quad (5.149c)$$

where  $T_a$  is the characteristic temperature.

First, we make the problem (5.149) dimensionless, using scaling  $y := Ly$ ,  $x := Lx$ ,  $T := T_a T$  to obtain

$$\Delta T(x, y) = 0, (x, y) \in \Omega_3^*, \quad (5.150a)$$

$$T(x, \pm 1 \pm \epsilon G(x)) = \pm 1, \epsilon = \frac{D}{L} \ll 1, \quad (5.150b)$$

$$T(x, y) \text{ is bounded for } |x| \rightarrow \infty, \quad (5.150c)$$

where  $\Omega_3^*$  is the dimensionless version of  $\Omega_3$  that is bounded by  $y = \pm 1 \pm \epsilon G(x)$ .

We assume a regular perturbation expansion in powers of  $\epsilon$ ,

$$T(x, y; \epsilon) = T_0(x, y) + \epsilon T_1(x, y) + \epsilon^2 T_2(x, y) + O(\epsilon^3). \quad (5.151)$$

Introducing the expansion into the heat conduction equation (5.150a, 5.150b), we have

$$\Delta T_n(x, y) = 0, n = 0, 1, \dots, \quad (5.152)$$

and the boundary conditions at  $y = \pm 1 \pm \varepsilon G(x)$  turn into

$$T_0(x, \pm 1 \pm \varepsilon G(x)) + \varepsilon T_1(x, \pm 1 \pm \varepsilon G(x)) + \varepsilon^2 T_2(x, \pm 1 \pm \varepsilon G(x)) + \cdots = \pm 1. \quad (5.153)$$

Note that the perturbation parameter  $\varepsilon$  appears implicitly and explicitly. It means that the expansion (5.153) is not a Poincaré expansion. Therefore, it is impossible directly to equate like powers of  $\varepsilon$ . This can be solved by expanding the temperature  $T_n(x, y)$  into a Taylor series about  $y = \pm 1$  to render it into a Poincaré expansion (see [12], p. 14). We obtain

$$\begin{aligned} T_0(x, \pm 1) \pm \varepsilon G(x) \frac{\partial T_0}{\partial y}(x, \pm 1) + \frac{1}{2} \varepsilon^2 G(x)^2 \frac{\partial^2 T_0}{\partial y^2}(x, \pm 1) \pm \cdots \\ + \varepsilon T_1(x, \pm 1) \pm \varepsilon^2 G(x) \frac{\partial T_1}{\partial y}(x, \pm 1) + \frac{1}{2} \varepsilon^3 G(x)^2 \frac{\partial^2 T_1}{\partial y^2}(x, \pm 1) \pm \cdots \\ + \varepsilon^2 T_2(x, \pm 1) \pm \varepsilon^3 G(x) \frac{\partial T_2}{\partial y}(x, \pm 1) + \frac{1}{2} \varepsilon^4 G(x)^2 \frac{\partial^2 T_2}{\partial y^2}(x, \pm 1) \pm \cdots = \pm 1. \end{aligned}$$

Equating like powers of  $\varepsilon$ , we find the boundary conditions for  $n = 0, 1, 2$ ,

$$T_0(x, \pm 1) = \pm 1, \quad T_1(x, \pm 1) = \mp G(x) \frac{\partial T_0}{\partial y}(x, \pm 1), \quad (5.154)$$

$$T_2(x, \pm 1) = -\frac{1}{2} G(x)^2 \frac{\partial^2 T_0}{\partial y^2}(x, \pm 1) \mp G(x) \frac{\partial T_1}{\partial y}(x, \pm 1), \dots \quad (5.155)$$

For a particular example, we take  $G(x) = \sin(x)$  (see Figure (5.8)).

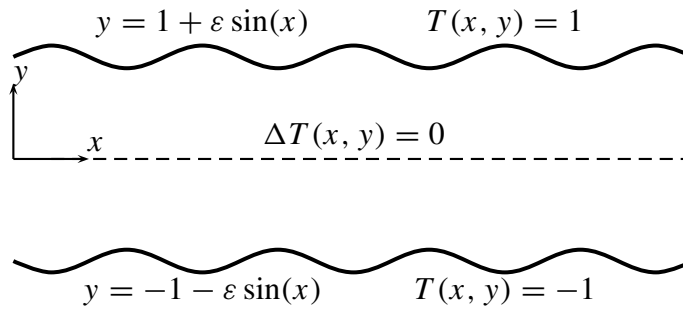


Figure 5.8: Sinus strip

Solving the heat conduction equation (5.152) with the boundary conditions (5.154, 5.155) yields the solution

$$T(x, y) = y - \varepsilon \frac{\sinh(y)}{\sinh(1)} \sin(x) + \frac{1}{2} \varepsilon^2 \coth(1) \left( y - \frac{\sinh(2y)}{\sinh(2)} \cos(2x) \right) + O(\varepsilon^3). \quad (5.156)$$

In Figure 5.9, we present a graph of solution (5.156) for  $\varepsilon = 0.25$  which confirms that the heat flows from the upper boundary to the lower almost linearly.

Below we discuss the derivation of the Stokes equation for highly viscous incompressible fluids. We investigate this problem in a semi-infinite slowly varying cylinder. The flow is

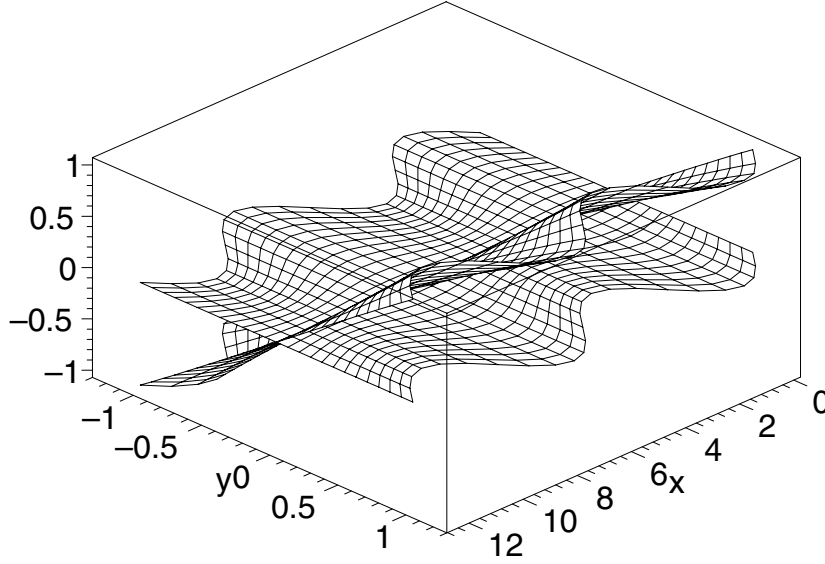


Figure 5.9: The graph of solution (5.156) for  $\varepsilon = 0.25$ .

driven by a given flux. Assuming there is a boundary layer in the entrance, we consider an outer and an inner expansion. We apply the procedure to solve the slowly varying geometry discussed in Section 4 to find the outer expansion. For the inner expansion, we expand the boundary conditions to a Taylor series. This expansion leads to the slightly varying geometry. Therefore, we apply the approach of Section 5. The resulting iteration yields a series of Stokes equations. This motivates the development of a theory to solve those equations for arbitrary geometry, source terms and boundary conditions.

## 6 The Stokes equation

In this section, we consider highly viscous fluids such as glass at high temperature. The governing equation is the Navier-Stokes equations. After making these equations dimensionless and using the Reynolds number is small, we arrive at the Stokes equations. In chapter II, we consider the same problem with different approach in scaling. We obtain a system of equations known as Reynold's lubrication-flow equations. In these equations, we have a multiplication between  $\varepsilon Re$  with the inertia terms, with  $\varepsilon$  is a dimensionless parameter. Therefore, in this approach, it is not necessary that the Reynolds number is of  $O(\varepsilon)$ .

The flow of incompressible viscous fluids is described by the Navier-Stokes equations

$$\rho \left( \frac{\partial \mathbf{v}}{\partial t} + \mathbf{v} \cdot \nabla \mathbf{v} \right) = \nabla \cdot \boldsymbol{\sigma} + \tilde{\mathbf{f}}, \quad (6.157a)$$

$$\nabla \cdot \mathbf{v} = h, \quad (6.157b)$$

where  $\mathbf{v}$  denotes the velocity field, and  $\rho$  the density. The vector field  $\tilde{\mathbf{f}}$  is a given external force density, the scalar field  $h$  is a given volume source distribution, and  $\boldsymbol{\sigma}$  is the fluid stress tensor given by

$$\boldsymbol{\sigma} = -p \mathbf{I} + \boldsymbol{\tau}, \quad \text{or} \quad \sigma_{ij} = -p \delta_{ij} + \tau_{ij}, \quad (6.158)$$

where  $p$  is the pressure,  $\mathbf{I} = (\delta_{ij})$  is the unit tensor, defined by  $\delta_{ij} = 1$  if  $i = j$ , and  $= 0$  otherwise, and  $\boldsymbol{\tau}$  is the deviatoric or viscous stress tensor. According to ([32], p. 45), for Newtonian fluid

$$\tau_{ij} = \eta \left( \frac{\partial v_i}{\partial x_j} + \frac{\partial v_j}{\partial x_i} - \frac{2}{3} \delta_{ij} \frac{\partial v_l}{\partial x_l} \right) + \zeta \delta_{ij} \frac{\partial v_l}{\partial x_l}, \quad (6.159)$$

where  $\eta$  is the dynamic viscosity and  $\zeta$  is the second viscosity. In general  $\eta$  and  $\zeta$  depend on temperature, and may vary in space and time, but if we assume a uniform temperature, then  $\eta$  and  $\zeta$  remain constant. Noting that

$$\nabla \cdot (\nabla \mathbf{v}) = \Delta \mathbf{v}, \quad \nabla \cdot (\nabla \mathbf{v})^T = \nabla (\nabla \cdot \mathbf{v}) = \nabla h,$$

$\nabla \cdot \boldsymbol{\sigma}$  reduces to  $-\nabla p + \eta \Delta \mathbf{v} + \eta \nabla h$ . As a result, (6.157 a,b) adopt the form

$$\rho \left( \frac{\partial \mathbf{v}}{\partial t} + \mathbf{v} \cdot \nabla \mathbf{v} \right) = -\nabla p + \eta \Delta \mathbf{v} + \mathbf{f}, \quad (6.160a)$$

$$\nabla \cdot \mathbf{v} = h. \quad (6.160b)$$

where we wrote  $\mathbf{f} = \tilde{\mathbf{f}} + (\frac{1}{3}\eta + \zeta)\nabla h$ . In order to investigate the hierarchy of small and large terms in (6.160 a,b), we have to make these equations dimensionless. We introduce a typical length scale  $D$  and a typical velocity  $V$ , and assume that the pressure gradient and both external force density and source fields are such that they are essentially balanced by the viscous forces density and the velocity divergence, respectively. Hence, we scale

$$\mathbf{v} := V \mathbf{v}, \quad p := \frac{\eta V}{D} p, \quad \mathbf{x} := D \mathbf{x}, \quad t := \frac{D}{V} t, \quad \mathbf{f} := \frac{\eta V}{D^2} \mathbf{f}, \quad h := \frac{V}{D} h. \quad (6.161)$$

As a result, we obtain the dimensionless form

$$Re \left( \frac{\partial \mathbf{v}}{\partial t} + \mathbf{v} \cdot \nabla \mathbf{v} \right) = -\nabla p + \Delta \mathbf{v} + \mathbf{f}, \quad \nabla \cdot \mathbf{v} = h,$$

where  $Re = \rho V D / \eta$  is the Reynolds number. If the term multiplied by the Reynolds number is uniformly small, we can ignore the inertia terms, and obtain the Stokes equations

$$\Delta \mathbf{v} - \nabla p = -\mathbf{f}, \quad (6.162a)$$

$$\nabla \cdot \mathbf{v} = h. \quad (6.162b)$$

This is the first part of our modelling hierarchy. Next, we will see how we can utilize the fact that the geometry actually considered is in some sense close to an other (simpler) geometry. If the considered geometry is in two dimensions and has two different length scales, for example the length scale for  $x$  is  $D$  and the length scale for  $y$  is  $L$ , with  $D \ll L$ , then we can produce another small parameter, *viz.*  $\varepsilon = \frac{D}{L} \ll 1$ , apart from the small parameter  $Re$ . If, however, we assume  $Re \ll \varepsilon \ll 1$ , it is only necessary to consider  $\varepsilon$ .

## 6.1 Example

In this example, we consider an incompressible fluid that is highly viscous ( $Re$  is small), such as glass at high temperature. Therefore, we will obtain the Stokes equation (6.162). We assume neither external force density nor volume source are given. The flow is driven by a given flux. We consider the Stokes boundary value problem

$$\Delta \mathbf{v} - \nabla p = \mathbf{0}, \mathbf{x} \in \Omega_4^*, \quad (6.163a)$$

$$\nabla \cdot \mathbf{v} = 0, \mathbf{x} \in \Omega_4^*, \quad (6.163b)$$

$$\mathbf{v}(x, \pm 1 \pm H(\varepsilon x)) = \mathbf{0}, \quad (6.163c)$$

$$\mathbf{v}(0, y) = (g(y), 0), \quad (6.163d)$$

$$\mathbf{v}(0, y) \text{ is bounded, as } x \rightarrow \infty, \quad (6.163e)$$

with  $\Omega_4^* = \{(x, y) \mid x > 0, -1 - H(\varepsilon x) < y < 1 + H(\varepsilon x)\}$  and  $\varepsilon = \frac{D}{L} \ll 1$  (see Figure 6.10). We prescribe at  $x = 0$ , a volume flux  $Q$  with  $Q = O(1)$ .

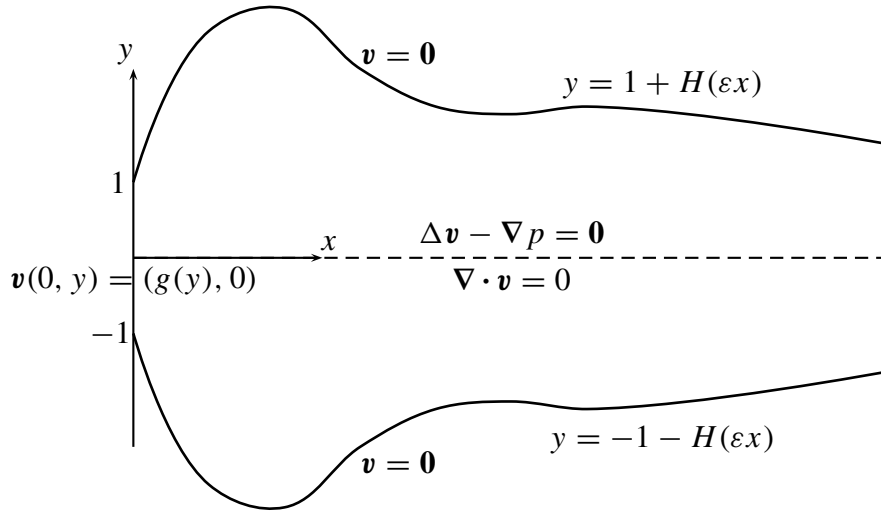


Figure 6.10: Semi-infinite strip with slowly varying diameter

Based on the slowly varying geometry approach, we make a rescaling  $X = \varepsilon x$ , and the Stokes equations (6.163) turn into

$$\varepsilon^2 \frac{\partial^2 u}{\partial X^2} + \frac{\partial^2 u}{\partial y^2} = \varepsilon \frac{\partial p}{\partial X}, \quad (6.164a)$$

$$\varepsilon^2 \frac{\partial^2 v}{\partial X^2} + \frac{\partial^2 v}{\partial y^2} = \frac{\partial p}{\partial y}, \quad (6.164b)$$

$$\varepsilon \frac{\partial u}{\partial X} + \frac{\partial v}{\partial y} = 0, \quad (6.164c)$$

$$\mathbf{v}(x, \pm 1 \pm H(X)) = \mathbf{0}. \quad (6.164d)$$

Similar to the Example 4.1.2, we assume there is a boundary layer at  $x = 0$ . At first, we consider the outer expansion.

### 6.1.1 Outer expansion

Here, we assume that  $u$ ,  $v$ , and  $p$  can be expanded into the series

$$u(X, y; \varepsilon) = u_0(X, y) + \varepsilon u_1(X, y) + \dots \quad (6.165)$$

$$v(X, y; \varepsilon) = v_0(X, y) + \varepsilon v_1(X, y) + \dots \quad (6.166)$$

$$p(X, y; \varepsilon) = \frac{1}{\varepsilon} p_{-1}(X, y) + p_0(X, y) + \dots \quad (6.167)$$

Here, we assume that  $p = O(\frac{1}{\varepsilon})$ , otherwise we would obtain  $u = v = 0$ , meaning there is no motion, which is obviously not what we want. Substituting the series (6.165-6.167) into (6.164) and equating coefficients of like powers of  $\varepsilon$ , we obtain

$$O(1) : \frac{\partial v_0}{\partial y} = 0, \quad \frac{\partial p_{-1}}{\partial y} = 0, \quad \frac{\partial^2 u_0}{\partial y^2} = \frac{\partial p_{-1}}{\partial X}, \quad (6.168)$$

$$O(\varepsilon) : \frac{\partial v_1}{\partial y} = -\frac{\partial u_0}{\partial X}, \quad \frac{\partial p_0}{\partial y} = \frac{\partial^2 v_0}{\partial y^2}, \quad \frac{\partial^2 u_1}{\partial y^2} = \frac{\partial p_0}{\partial X}, \quad (6.169)$$

$$O(\varepsilon^2) : \frac{\partial v_2}{\partial y} = -\frac{\partial u_1}{\partial X}, \quad \frac{\partial p_1}{\partial y} = \frac{\partial^2 v_1}{\partial y^2}, \quad \frac{\partial^2 u_2}{\partial y^2} = \frac{\partial p_1}{\partial X} - \frac{\partial^2 u_0}{\partial X^2}, \quad (6.170)$$

$$O(\varepsilon^n) : \frac{\partial v_n}{\partial y} = -\frac{\partial u_{n-1}}{\partial X}, \quad \frac{\partial p_{n-1}}{\partial y} = \frac{\partial^2 v_{n-1}}{\partial y^2} + \frac{\partial^2 v_{n-3}}{\partial X^2}, \quad \frac{\partial^2 u_n}{\partial y^2} = \frac{\partial p_{n-1}}{\partial X} - \frac{\partial^2 u_{n-2}}{\partial X^2}, \quad (6.171)$$

$$n = 3, 4, 5, \dots$$

We will investigate the leading order ( $O(1)$ ). Consider the first equation of (6.168). The boundary condition  $\mathbf{v}(X, \pm 1 \pm H(X)) = \mathbf{0}$  gives

$$v_0(X, y) = 0. \quad (6.172)$$

Next, since  $\frac{\partial p_{-1}}{\partial y} = 0$ , we have

$$p_{-1}(X, y) = p_{-1}(X). \quad (6.173)$$

Finally, using (6.173) and the boundary conditions, we get

$$u_0(X, y) = \frac{1}{2} \frac{\partial p_{-1}}{\partial X} \left( y^2 - (1 + H(X))^2 \right). \quad (6.174)$$

To obtain  $\frac{\partial p_{-1}}{\partial X}$ , we use the flux as follows

$$Q = \int_{-1-H(X)}^{1+H(X)} u(X, y) dy = \int_{-1-H(X)}^{1+H(X)} (u_0(X, y) + \varepsilon u_1(X, y) + \dots) dy. \quad (6.175)$$



Equating the coefficients of like power of  $\varepsilon$  yielding

$$O(1) : Q = \int_{-1-H(X)}^{1+H(X)} u_0(X, y) dy, \quad (6.176)$$

$$O(\varepsilon^n) : \int_{-1-H(X)}^{1+H(X)} u_n(X, y) dy = 0, n = 1, 2, 3, \dots. \quad (6.177)$$

Substitution of  $u_0(X, y)$  (6.174) into  $Q$  (6.176) yields

$$\frac{\partial p_{-1}}{\partial X}(X) = -\frac{3}{2} \frac{Q}{(1+H(X))^3}, \text{ or } p_{-1}(X) = \int^X -\frac{3}{2} \frac{Q}{(1+H(s))^3} ds. \quad (6.178)$$

Using (6.178), we obtain  $u_0(X, y)$  as

$$u_0(X, y) = -\frac{3}{4} Q \left[ \frac{y^2 - (1+H(X))^2}{(1+H(X))^3} \right]. \quad (6.179)$$

Now, we discuss the next order term ( $O(\varepsilon)$ ). Consider the first equation of (6.169)

$$\frac{\partial v_1}{\partial y} = -\frac{\partial u_0}{\partial X}. \quad (6.180)$$

Using  $u_0(X, y)$  (6.179) and the boundary conditions  $v_1(X, \pm 1 \pm H(X)) = 0$ , we obtain

$$v_1(X, y) = \frac{3}{4} Q \frac{H'(X)}{1+H(X)} \left[ y - \frac{y^3}{(1+H(X))^2} \right]. \quad (6.181)$$

Next, consider the second equation of (6.169). Since  $v_0(X, y) = 0$ , it follows that  $\frac{\partial p_0}{\partial y} = 0$ , or  $p_0(X, y) = p_0(X)$ . Finally, solving the last equation of (6.169) and using the boundary conditions  $u_1(X, \pm 1 \pm H(X)) = 0$ , we arrive at

$$u_1(X, y) = \frac{1}{2} \frac{\partial p_0}{\partial X} (y^2 - (1+H(X))^2). \quad (6.182)$$

Substitution of (6.182) into (6.177) yields

$$\frac{\partial p_0}{\partial X} = 0, \quad \text{and } u_1(X, y) = 0. \quad (6.183)$$

Therefore,  $p_0(X, y) = C$ , a constant.

So far we obtain the results as follows

$$u(X, y; \varepsilon) = -\frac{3}{4} Q \left[ \frac{y^2 - (1+H(X))^2}{(1+H(X))^3} \right] + O(\varepsilon^2), \quad (6.184)$$

$$v(X, y; \varepsilon) = \varepsilon \frac{3}{4} Q \frac{H'(X)}{1+H(X)} \left[ y - \frac{y^3}{(1+H(X))^2} \right] + O(\varepsilon^2), \quad (6.185)$$

$$p(X, y; \varepsilon) = \frac{1}{\varepsilon} \int^X -\frac{3}{2} \frac{Q}{(1+H(s))^3} ds + C + O(\varepsilon). \quad (6.186)$$

Using the above results, the boundary conditions  $\mathbf{v}(X, \pm 1 \pm H(X)) = \mathbf{0}$ , and (6.177), we can calculate further  $u_n, v_n, n = 2, 3, \dots$ , and  $p_n, n = 1, 2, \dots$ .

### 6.1.2 Inner expansion

Now, we consider the inner expansion by introducing the inner variable  $x = \frac{X}{\varepsilon}$  into (6.164 a-c) to obtain

$$\frac{\partial^2 u}{\partial x^2} + \frac{\partial^2 u}{\partial y^2} = \frac{\partial p}{\partial x}, \quad (6.187a)$$

$$\frac{\partial^2 v}{\partial x^2} + \frac{\partial^2 v}{\partial y^2} = \frac{\partial p}{\partial y}, \quad (6.187b)$$

$$\frac{\partial u}{\partial x} + \frac{\partial v}{\partial y} = 0, \quad (6.187c)$$

$$\mathbf{v}(x, \pm 1 \pm H(\varepsilon x)) = \mathbf{0}, \quad (6.187d)$$

$$\mathbf{v}(0, y) = (g(y), 0), \quad (6.187e)$$

$$\mathbf{v} \text{ is bounded as } x \rightarrow \infty. \quad (6.187f)$$

Next, we expand the boundary conditions  $y = 1 + H(\varepsilon x)$  into a Taylor series as follows

$$y = 1 + H(\varepsilon x) = 1 + \varepsilon x H'(0) + O(\varepsilon^2). \quad (6.188)$$

Note that the geometry of the boundary conditions in the inner region turns into a slightly varying geometry. Therefore, we use the procedure explained in Section 5. We assume that  $u, v$ , and  $p$ , can be expanded into series :

$$u(\varepsilon x, y; \varepsilon) = \psi(x, y; \varepsilon) = \psi_0(x, y) + \varepsilon \psi_1(x, y) + \dots \quad (6.189)$$

$$v(\varepsilon x, y; \varepsilon) = \varphi(x, y; \varepsilon) = \varphi_0(x, y) + \varepsilon \varphi_1(x, y) + \dots \quad (6.190)$$

$$p(\varepsilon x, y; \varepsilon) = \pi(x, y; \varepsilon) = \pi_0(x, y) + \varepsilon \pi_1(x, y) + \dots \quad (6.191)$$

Substituting the above series into (6.187) and using (6.188), we find that for each  $n = 0, 1, 2, \dots$ , we have to solve the Stokes equations

$$\frac{\partial^2 \psi_n}{\partial x^2} + \frac{\partial^2 \psi_n}{\partial y^2} = \frac{\partial \pi_n}{\partial x}, \quad (6.192a)$$

$$\frac{\partial^2 \varphi_n}{\partial x^2} + \frac{\partial^2 \varphi_n}{\partial y^2} = \frac{\partial \pi_n}{\partial y}, \quad (6.192b)$$

$$\frac{\partial \psi_n}{\partial x} + \frac{\partial \varphi_n}{\partial y} = 0, \quad (6.192c)$$

with boundary conditions for  $n = 0, 1$ , respectively,

$$\psi_0(x, \pm 1) = 0, \quad \psi_0(0, y) = g(y), \quad \varphi_0(x, \pm 1) = 0, \quad \varphi_0(0, y) = 0, \quad (6.193)$$

$$\psi_1(x, \pm 1) = \mp x H'(0) \frac{\partial \psi_0}{\partial y}(x, \pm 1), \quad \psi_1(0, y) = 0, \quad (6.194)$$

$$\varphi_1(x, \pm 1) = \mp x H'(0) \frac{\partial \varphi_0}{\partial y}(x, \pm 1), \quad \varphi_1(0, y) = 0, \dots \quad (6.195)$$

Note that the problem to be solved at each order is the Stokes boundary value problem. Therefore, it is necessary to develop a general theory to solve this problem. This theory, based on operator theory, will be discussed in Chapter III.

## Chapter II

# Analytical approximations to the viscous glass flow problem in the mould–plunger pressing process, including an investigation of boundary conditions

**Abstract.** Industrial glass is produced at temperatures above  $600^{\circ}\text{C}$ , where glass becomes a highly viscous incompressible fluid, usually considered as Newtonian. In the production two phases may be distinguished, namely the pressing phase and the blowing phase. This study will be concerned with glass flow in the pressing phase, which is called this way because a blob of fluid glass (called a gob) is pressed in a mould by a plunger, such that the glass flows between mould and plunger, in order to obtain the preform of a bottle or a jar called a parison. In the blowing phase (not considered here) the parison is subsequently blown into the final shape of the product.

By applying the slender geometry of mould and plunger, and assuming cylindrical symmetry, a form of Reynolds' lubrication flow equations is obtained. These equations are solved by utilizing the incompressibility of the glass, by which the flux at any axial cross section is determined for prescribed plunger velocity, leading to analytical results in closed form for velocity field and pressure gradient. The glass level is implicitly defined by the integral over the varying volume which is to remain constant. The pressure may then be determined by integration.

Special attention is given to the required boundary conditions. It is known that, depending on several problem parameters like temperature, pressure, and smoothness of the wall, the glass flow slips, to some extent, along the wall. Therefore, this study includes a general formulation of the boundary condition of partial slip in the form of a linear relation between shear stress and slip velocity, also known as Navier's slip condition. The coefficient of this relation, a positive number, may vary in our solution with axial position, but depends on the problem and is to be obtained from (for example) experiments.

Two special cases, which seem to be relevant in practice, are considered as examples: (i) no-slip on both plunger and mould; (ii) no-slip on the mould and full slip (zero friction) on the plunger. The results are compared with fully numerical (FEM) solutions of a Stokes flow model, and the agreement is good or excellent.

Since in any practical situation it is not the plunger velocity which is prescribed, but (within practical limits) the force applied by the plunger, the problem of a prescribed plunger force have also been investigated.

## 1 Introduction

Glass is a widely used packing material, for example in the form of jars and bottles in the food industry. The production of glass forms like jars goes more or less along the following lines [57, pp.612-613]. First, grains and additives, like soda, are heated in a tank. Here gas burners or electric heaters provide the heat necessary to warm the material up to some  $1200^{\circ}\text{C}$ . At one end the liquid glass comes out and is led to a pressing or blowing machine. To obtain a glass form a two-stage process is often used. First (Figure 1.1), a blob of hot glass called a *gob* falls into a configuration consisting of a *mould* and *plunger*. As soon as the entire glass drop has fallen into this mould, the plunger starts moving to press the glass. This process is called the *pressing*. At the end, the glass drop is reshaped into a preform of a bottle or a jar called a *parison*. After a short period of time, for cooling purposes (the mould is kept at  $500^{\circ}\text{C}$ ), the *parison* is blown to its final shape in another mould. This process is called *blowing* (see Figure 1.2).

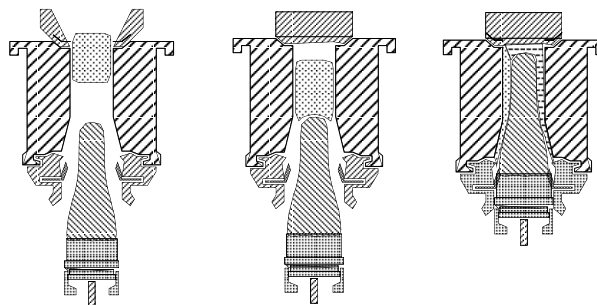


Figure 1.1: Pressing phase

This section is concerning with glass flow in the pressing phase in manufacturing glass jars or parisons. A typical feature of the shape of a parison is the fact that wall thickness and radius vary very slowly (except for the bottom part), see Figure 2.3. Here, this slow variation will be utilized to obtain an explicit, analytical description of velocity and pressure gradient of the glass flow.

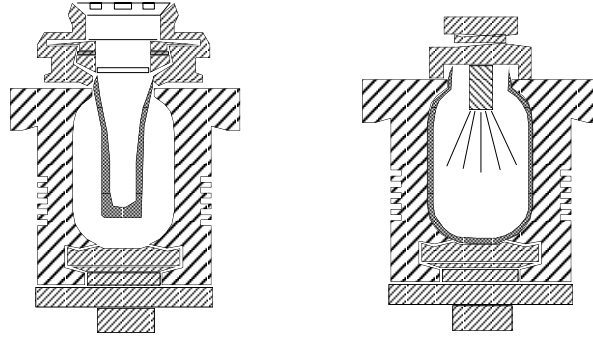


Figure 1.2: Blowing phase

## 2 Governing equations

The motion of glass at temperatures above 600°C can be described by the Navier-Stokes equations for incompressible Newtonian fluids [47, p.3], given by

$$\rho \left( \frac{\partial \mathbf{v}}{\partial t} + \mathbf{v} \cdot \nabla \mathbf{v} \right) = \nabla \cdot \boldsymbol{\sigma}, \quad (2.1a)$$

$$\nabla \cdot \mathbf{v} = 0, \quad (2.1b)$$

where  $\mathbf{v}$  denotes the velocity field,  $\rho$  the density, and  $\boldsymbol{\sigma}$  the fluid stress tensor :

$$\boldsymbol{\sigma} = -p \mathbf{I} + \boldsymbol{\tau}, \quad \text{or} \quad \sigma_{ij} = -p \delta_{ij} + \tau_{ij}, \quad (2.2)$$

with  $p$  the pressure,  $\mathbf{I} = (\delta_{ij})$  the unit tensor defined by  $\delta_{ij} = 1$  if  $i = j$ , and  $= 0$  otherwise, and  $\boldsymbol{\tau}$  is the deviatoric or viscous stress tensor. In Newtonian fluids, a linear relationship is assumed between  $\boldsymbol{\tau}$  and the deformation rate of the fluid element, expressed in the rate-of-strain tensor  $\dot{\boldsymbol{\gamma}} = \nabla \mathbf{v} + (\nabla \mathbf{v})^T$ :

$$\boldsymbol{\tau} = \eta \dot{\boldsymbol{\gamma}} \quad \text{or} \quad \tau_{ij} = \eta \left( \frac{\partial v_i}{\partial x_j} + \frac{\partial v_j}{\partial x_i} \right), \quad (2.3)$$

where  $\eta$  is the dynamic viscosity. In general,  $\eta$  depends on temperature and may vary in space and time, but for a uniform temperature as we have here (approximately; see Section 4),  $\eta$  remains constant. Together with  $\nabla \cdot \mathbf{v} = 0$ ,  $\nabla \cdot \boldsymbol{\sigma}$  reduces to  $-\nabla p + \eta \Delta \mathbf{v}$ . As a result, (2.1a-2.1b) adopt their common form

$$\rho \left( \frac{\partial \mathbf{v}}{\partial t} + \mathbf{v} \cdot \nabla \mathbf{v} \right) = -\nabla p + \eta \Delta \mathbf{v}, \quad (2.4a)$$

$$\nabla \cdot \mathbf{v} = 0. \quad (2.4b)$$

In view of the geometry of plunger and mould, we choose cylindrical coordinates  $(r, \theta, z)$ , while  $v, w, u$  will denote the  $r, \theta, z$  component of the velocity  $\mathbf{v}$ . We assume the problem to be axisymmetric, so that both  $w$  and all  $\theta$ -derivatives vanish, and the problem reduces to a two-dimensional one in the  $(r, z)$ -plane; see Figure 2.3.

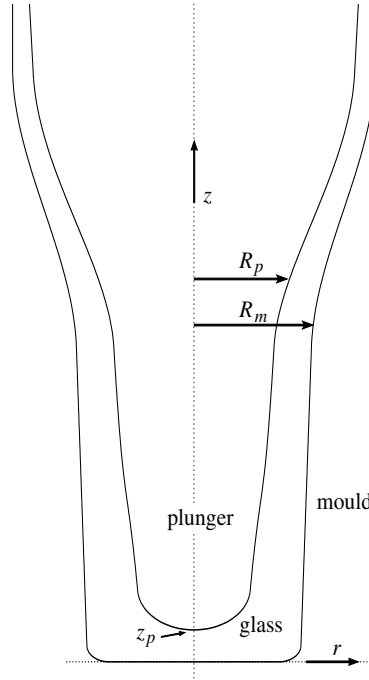


Figure 2.3: Sketch of the configuration. Note that  $R_p = R_p(z - z_p)$  is the surface of the plunger,  $R_m = R_m(z)$  is the surface of the mould, and  $z_p$  is the position of the top of the plunger.

### 3 Slender-geometry approximation

We will concentrate our analysis on the flow in the narrow annular duct between plunger and mould ( $z > z_p$ , see Figure 2.3). This region is very slender, and therefore amenable to asymptotic analysis [26, p.182], while at the same time the flow in the region between mould bottom and plunger top is practically stagnant, and therefore less important.

We will make (2.4a-2.4b) dimensionless by a suitable scaling. From the geometry of plunger and mould, we have 2 relevant length scales, the wall thickness of the parison ( $D$ ) and the length of the plunger ( $L$ ), with  $D \ll L$ . Except near the plunger top, any variation in  $z$  scales on  $L$  and any variation in  $r$  scales on  $D$ . Therefore, we scale  $z$  with  $L$  and  $r$  with  $D$ , while we introduce the small parameter

$$\varepsilon = \frac{D}{L}. \quad (3.5)$$

The axial velocity  $u$  scales on a typical velocity  $V$ , while from the equation of mass conservation it follows that the radial velocity  $v$  has to scale on  $\varepsilon V$ . As density  $\rho$  and viscosity  $\eta$  are constant, they are parameters of the problem. Pressure  $p$  is to be scaled on  $\eta VL/D^2$  (rather than  $\rho V^2$ ), because the glass flow is highly viscous, as we will see below. We have then

$$z = Lz^*, \quad r = Dr^*, \quad u = Vu^*, \quad v = \varepsilon Vv^*, \quad p = \frac{\eta VL}{D^2} p^*, \quad t = \frac{L}{V} t^*.$$

Now we substitute the above scalings into the Navier-Stokes equations and henceforth ignore the asterisks  $*$ , to obtain respectively the dimensionless  $z$ ,  $r$ -components of the Navier-Stokes equations and the continuity equation, *viz.*

$$\varepsilon Re \left( \frac{\partial u}{\partial t} + u \frac{\partial u}{\partial z} + v \frac{\partial u}{\partial r} \right) = -\frac{\partial p}{\partial z} + \varepsilon^2 \frac{\partial^2 u}{\partial z^2} + \frac{1}{r} \frac{\partial}{\partial r} \left( r \frac{\partial u}{\partial r} \right), \quad (3.6a)$$

$$\varepsilon^3 Re \left( \frac{\partial v}{\partial t} + u \frac{\partial v}{\partial z} + v \frac{\partial v}{\partial r} \right) = -\frac{\partial p}{\partial r} + \varepsilon^4 \frac{\partial^2 v}{\partial z^2} + \varepsilon^2 \frac{\partial}{\partial r} \left( \frac{1}{r} \frac{\partial}{\partial r} (rv) \right), \quad (3.6b)$$

$$\frac{\partial u}{\partial z} + \frac{1}{r} \frac{\partial}{\partial r} (rv) = 0, \quad (3.6c)$$

where  $Re = \rho V D / \eta$  is the Reynolds number.

According to [8, p.7], the velocity of the plunger, which can be used as a characteristic velocity if the cross section of the annular channel compared to the plunger cross section is not too small<sup>1</sup>, is typically  $V = 10^{-1}$  m/s. A typical channel width is  $D \approx 10^{-2}$  m. A typical length of the plunger is  $10^{-1}$  m. The dynamic viscosity of glass varies greatly with temperature, but for a temperature around  $800^\circ\text{C}$  it is in the order of  $10^4$  kg/(s m). The density of glass is  $2500$  kg/m<sup>3</sup> [50, p.4]. Therefore, we obtain typically  $\varepsilon = 10^{-1}$ ,  $Re = 2.5 \times 10^{-4}$ ,  $\varepsilon Re = 2.5 \times 10^{-5}$ , and  $\varepsilon^3 Re = 2.5 \times 10^{-7}$ , and we can ignore the inertia and radial friction terms to obtain

$$\frac{\partial p}{\partial z} = \frac{1}{r} \frac{\partial}{\partial r} \left( r \frac{\partial u}{\partial r} \right), \quad (3.7a)$$

$$\frac{\partial p}{\partial r} = 0, \quad (3.7b)$$

$$\frac{\partial u}{\partial z} + \frac{1}{r} \frac{\partial}{\partial r} (rv) = 0. \quad (3.7c)$$

with an assumed error of  $O(\varepsilon^2)$  because  $Re \ll \varepsilon$ . This set of equations may be recognized as Reynold's lubrication-flow equations in cylindrical coordinates [18, p.83].

<sup>1</sup>as follows from an axial mass flux balance; see Section 6.1.



## 4 The temperature problem

Although in viscous flow the energy equation is decoupled from the equation of motion (2.4a) if the flow is incompressible and Newtonian with constant viscosity, the validity of this assumption is not obvious in the present problem. The viscosity is highly temperature-dependent, as is seen from the VFT (Vogel, Fulcher, Tamman)-relation [57, p.936]

$$\log_{10} \eta = A + \frac{B}{T - T_0},$$

where  $A$ ,  $B$ ,  $T_0$  are constants depending on the glass composition (for example  $A = -2.4$ ,  $B = 4032$ , and  $T_0 = 170$  for Soda-Silica Glasses [5]), while  $T$  is in degrees Celsius. In this case  $T = 800$  yields a viscosity of  $\eta = 10^4$  kg/(s m).

The high viscous forces may generate heat by friction, and the walls may supply or absorb heat by conduction, so that the viscosity varies with the temperature along the flow.

To investigate this possibility we will analyse the energy equation and estimate the order of magnitude of the various terms. The energy conservation law for viscous and compressible fluids may be written as [32, p.10]

$$\frac{\partial}{\partial t}(\rho e) + \nabla \cdot (\rho v e) = -p \nabla \cdot \mathbf{v} - \nabla \cdot \mathbf{q} + \boldsymbol{\tau} : \nabla \mathbf{v}, \quad (4.8)$$

where  $e$  denotes the internal energy per unit of mass,  $\mathbf{q}$  the heat flux due to heat conduction, and  $\boldsymbol{\tau}$  the viscous stress tensor. Since we are only interested in an estimate of the order of magnitude, we assume that  $e \simeq c_p T$ , where  $c_p$  is the heat capacity at constant pressure and  $T$  is the absolute temperature [58, p.31], and for  $\mathbf{q}$  we shall use Fourier's law  $\mathbf{q} = -k \nabla T$  where  $k$  is the heat conductivity.

In an incompressible flow with constant  $c_p$  and  $k$  we have

$$\rho c_p \left( \frac{\partial T}{\partial t} + \mathbf{v} \cdot \nabla T \right) = k \Delta T + \eta (\dot{\boldsymbol{\gamma}} : \nabla \mathbf{v}).$$

We make dimensionless like before :

$$r = Dr^*, \quad z = Lz^*, \quad v = \varepsilon V v^*, \quad u = Vu^*, \quad T = T_m + \Delta T T^*, \quad \eta = \eta_g \eta^*, \quad t = \frac{L}{V} t^*,$$

where  $\Delta T = T_g - T_m$  and  $\eta_g$  denotes the glass viscosity at the bulk temperature. Note that in the rest of this section, we shall use a constant viscosity  $\eta = \eta_g$ . We find (ignoring the asterisks \*)

$$\begin{aligned} \varepsilon \left[ \frac{\partial T}{\partial t} + \mathbf{v} \cdot \nabla T \right] &= \frac{1}{Pe} \left[ \frac{1}{r} \frac{\partial}{\partial r} \left( r \frac{\partial T}{\partial r} \right) + \varepsilon^2 \frac{\partial^2 T}{\partial z^2} \right] \\ &+ \frac{Ec}{Re} \eta \left[ \left( \frac{\partial u}{\partial r} + \varepsilon^2 \frac{\partial v}{\partial z} \right)^2 + 2\varepsilon^2 \left( \left[ \frac{\partial v}{\partial r} \right]^2 + \left[ \frac{v}{r} \right]^2 + \left[ \frac{\partial u}{\partial z} \right]^2 \right) \right], \quad (4.9) \end{aligned}$$

with Reynolds number  $Re = \rho V D / \eta_g$ , Eckert number  $Ec = V^2 / c_p \Delta T$ , and Peclet number  $Pe = \rho V D c_p / k$ . Note that  $Pe$  and  $Re$  are related through the Prandtl number as  $Pe = Re Pr$ ,

while  $PeEc/Re = Br$  is called the Brinkman number. When we substitute the following values, typical of glass at 800°C,

$D$ : typical parison length scale = $10^{-2}$ m	$T_g$ : glass temperature = 800°C,
$V$ : typical plunger velocity = $10^{-1}$ m/s	$T_m$ : mould temperature = 500°C,
$\rho$ : glass density = 2500 kg/m <sup>3</sup>	$c_p$ : glass heat capacity = 1100 J/kg°C
$\eta_g$ : glass dynamic viscosity = $10^4$ kg/(s m)	$k$ : glass thermal conductivity = 1.7 W/m°C
$L$ : typical plunger length scale = $10^{-1}$ m	

we get the corresponding dimensionless numbers

$$\varepsilon = 10^{-1}, \quad \frac{1}{Pe} = 6.2 \times 10^{-4}, \quad \frac{Ec}{Re} = 1.2 \times 10^{-4}.$$

Both  $1/(\varepsilon Pe)$  and  $Ec/(\varepsilon Re)$  are very small numbers, so in the bulk of the flow we can ignore the heat conduction and thermal production terms (the second and third term in (4.9)) against the convection (first) term. Hence, the energy equation simplifies to

$$\frac{\partial T}{\partial t} + \mathbf{v} \cdot \nabla T = \frac{dT}{dt} = 0,$$

indicating that the temperature is preserved following the flow. So if we start with a uniform temperature field, it will remain uniform everywhere, and it follows that the viscosity also remains constant.

Note that this is not true in the thin temperature boundary layer along the wall, where the temperature varies from the value at the wall to the bulk temperature, and the conduction term is comparable with the convection term. From this balance

$$\mathbf{v} \cdot \nabla T \sim \frac{1}{\varepsilon Pe} \left[ \frac{\partial^2 T}{\partial r^2} + \frac{1}{r} \frac{\partial T}{\partial r} \right]$$

it follows that the dimensionless boundary layer thickness is of the order of  $O((\varepsilon Pe)^{-1/3})$  (no-slip) or  $O((\varepsilon Pe)^{-1/2})$  (with slip). For the values considered this corresponds to a boundary layer thickness of, respectively,  $\sim 2 \times 10^{-1}$  and  $\sim 0.8 \times 10^{-1}$ , *i.e.* 20% and 8% of the channel width. These values are of course not very small. However, to make progress we will for the moment consider them as small enough to be ignored.

A small counter-effect that may occur is the fact that very close to the wall, where the glass temperature attains the wall temperature, the viscosity increases by several orders of magnitude. For the present example the dimensionless  $\eta(T_m) = 10^{5.8}$ , which leads to  $(Ec/\varepsilon Re)\eta(T_m) = 760$ . So with little or no-slip between glass and wall (otherwise  $\dot{\gamma} : \nabla \mathbf{v}$  is small) the fluid friction very close to the wall is not negligible and will generate some heat. This may increase locally the temperature, and slightly counteract the lower wall temperature. The resulting decrease of viscosity could be called “self-lubrication”.

## 5 Boundary conditions

Depending on problem parameters like wall temperature, fluid pressure, surface tension, or the presence of a lubricant like graphite powder [11],[16],[55],[56], the glass flow slips completely, partly or not at all along the wall. This means that the tangential component of the glass velocity  $\mathbf{v}$  at the wall differs from the wall velocity  $\mathbf{v}_w$ , the difference being called the slip velocity. Since by assumption the glass flows in the  $(r, z)$ -plane and the plunger moves in  $z$ -direction, it is sufficient to consider the tangential component in  $(r, z)$ -plane.

Two slip conditions are commonly used. One is based on Coulomb's friction [16], which is the assumption of a linear relation between tangential (shear) stress and normal stress (pressure), usually with a threshold value. The other is Navier's slip condition [18, p.87], which assumes a linear relation between the slip velocity and the shear stress. Physically, little is known as to which condition is essentially more correct. Therefore, we will take Navier's slip condition, as this one is mathematically more convenient here, since in our theory the pressure is only available as an integral, while the velocities are explicitly known.

The shear stress applied to a surface with unit normal vector  $\mathbf{n}$ , defined *pointing outward* from the fluid, in tangential direction  $\mathbf{t}$ , is given by  $-(\boldsymbol{\sigma} \cdot \mathbf{n}) \cdot \mathbf{t} = -(\boldsymbol{\tau} \cdot \mathbf{n}) \cdot \mathbf{t}$ . The slip velocity  $(\mathbf{v} - \mathbf{v}_w) \cdot \mathbf{t}$  will be proportional to this stress in  $(r, z)$ -plane

$$(\mathbf{v} - \mathbf{v}_w) \cdot \mathbf{t} = -s(\boldsymbol{\tau} \cdot \mathbf{n}) \cdot \mathbf{t}, \quad (5.10)$$

where slip factor  $s$  (a positive number) measures the amount of slip. (A better measure is the dimensionless version of  $s$ ; see below.) There is no slip if  $s = 0$ , while there is no friction if  $s = \infty$ . The inverse,  $s^{-1}$ , might be called the friction factor. In general,  $s$  may be a function of position.

More advanced slip modelling, for example a nonlinear relation with  $s$  depending on pressure, is formally included in this way, if we in some way iteratively adapt  $s$  and the corresponding solution. We have not investigated this possibility here, however.

For reference, we note that in cylindrical coordinates  $\boldsymbol{\sigma}$  is given by

$$\begin{aligned} \sigma_{rr} &= -p + 2\eta \frac{\partial v}{\partial r}, & \sigma_{\theta r} &= \sigma_{r\theta} = 0, & \sigma_{\theta\theta} &= -p + 2\eta \frac{v}{r}, \\ \sigma_{zz} &= -p + 2\eta \frac{\partial u}{\partial z}, & \sigma_{zr} &= \sigma_{rz} = \eta \left( \frac{\partial v}{\partial z} + \frac{\partial u}{\partial r} \right), & \sigma_{\theta z} &= \sigma_{z\theta} = 0. \end{aligned}$$

### 5.1 Boundary conditions on the plunger

To apply the above conditions to the moving plunger surface, we recall that this is defined as:

$$r = R_p(z - z_p(t)),$$

where  $z = z_p(t)$  is the position of the top of the plunger at time  $t$ . Subscript “ $p$ ” denotes the value at the plunger. Unless indicated otherwise, we will write here  $R_p = R_p(z - z_p)$ .

The outward unit normal  $\mathbf{n}_p$  (outward from the fluid at the plunger surface) and the counter clockwise directed unit tangent  $\mathbf{t}_p$  in the  $(r, z)$ -plane are given by

$$\mathbf{n}_p = \frac{R'_p \mathbf{e}_z - \mathbf{e}_r}{\sqrt{1 + R_p'^2}}, \quad \mathbf{t}_p = \frac{-\mathbf{e}_z - R'_p \mathbf{e}_r}{\sqrt{1 + R_p'^2}}. \quad (5.11)$$

From the definition of stress (2.2, 2.3) we have

$$(\boldsymbol{\sigma} \cdot \mathbf{n}_p) \cdot \mathbf{t}_p = \eta \frac{(1 - R_p'^2) \left( \frac{\partial u}{\partial r} + \frac{\partial v}{\partial z} \right) - 2R_p' \left( \frac{\partial u}{\partial z} - \frac{\partial v}{\partial r} \right)}{1 + R_p'^2}. \quad (5.12)$$

To determine the slip velocity, we note that the plunger is going down with speed  $\frac{dz_p}{dt} = u_p$ . So the (dimensional) slip velocity at the plunger surface is

$$(\mathbf{v} - u_p \mathbf{e}_z) \cdot \mathbf{t}_p = ((u - u_p) \mathbf{e}_z + v \mathbf{e}_r) \cdot \frac{-\mathbf{e}_z - R_p' \mathbf{e}_r}{\sqrt{1 + R_p'^2}} = -\frac{(u - u_p) + v R_p'}{\sqrt{1 + R_p'^2}}. \quad (5.13)$$

From (5.10, 5.11, 5.13), we obtain the boundary condition on the plunger

$$\frac{(u - u_p) + v R_p'}{\sqrt{1 + R_p'^2}} = s_p \eta \frac{(1 - R_p'^2) \left( \frac{\partial u}{\partial r} + \frac{\partial v}{\partial z} \right) - 2R_p' \left( \frac{\partial u}{\partial z} - \frac{\partial v}{\partial r} \right)}{1 + R_p'^2}, \quad (5.14)$$

where  $s_p$  is  $s$  at the plunger. The other boundary condition at the plunger is that the wall is solid, so  $(\mathbf{v} - u_p \mathbf{e}_z) \cdot \mathbf{n} = 0$ , or

$$v = (u - u_p) R_p'. \quad (5.15)$$

After introducing the following scaled slip coefficient  $s^*$

$$s = \frac{D}{\eta} s^* \quad (5.16)$$

and using the same scaling as before, we obtain the dimensionless form of (5.14) and (5.15) (with asterisks ignored),

$$\frac{(u - u_p) + \varepsilon^2 v R_p'}{\sqrt{1 + \varepsilon^2 R_p'^2}} = s_p \frac{(1 - \varepsilon^2 R_p'^2) \left( \frac{\partial u}{\partial r} + \varepsilon^2 \frac{\partial v}{\partial z} \right) - 2\varepsilon^2 R_p' \left( \frac{\partial u}{\partial z} - \frac{\partial v}{\partial r} \right)}{1 + \varepsilon^2 R_p'^2}, \quad (5.17)$$

$$v = (u - u_p) R_p'. \quad (5.18)$$

As the wall temperature or the amount of lubricant may vary along the wall, it is practically important to let  $s$  be a function of position. The present solution is perfectly valid for any varying slip factor, as long as axial symmetry is preserved, and  $s$  is a smooth function of position  $z$

$$s = s(z). \quad (5.19)$$

For small  $\varepsilon$  we obtain (with an error  $O(\varepsilon^2)$ ) for the boundary condition (5.17)

$$u - u_p = s_p \frac{\partial u}{\partial r} \quad \text{at } r = R_p, \quad (5.20)$$

where  $s_p$ , if non-constant, is to be interpreted as a property of the moving surface and therefore to be read as  $s_p = s_p(z - z_p)$ . The other boundary condition (5.18) will be left as it is.

## 5.2 Boundary conditions on the mould

The surface of the mould, given by

$$r = R_m(z),$$

(subscript “ $m$ ” denotes the value at the mould) has unit outward normal  $\mathbf{n}_m$  (outward from the fluid) and counter clockwise directed unit tangent  $\mathbf{t}_m$  given by

$$\mathbf{n}_m = \frac{-R'_m \mathbf{e}_z + \mathbf{e}_r}{\sqrt{1 + R_m'^2}}, \quad \mathbf{t}_m = \frac{\mathbf{e}_z + R'_m \mathbf{e}_r}{\sqrt{1 + R_m'^2}}. \quad (5.21)$$

In a similar way as for the boundary conditions on the plunger we obtain the boundary condition on the mould as

$$\frac{u + vR'_m}{\sqrt{1 + R_m'^2}} = -s_m \eta \frac{(1 - R_m'^2) \left( \frac{\partial u}{\partial r} + \frac{\partial v}{\partial z} \right) - 2R'_m \left( \frac{\partial u}{\partial z} - \frac{\partial v}{\partial r} \right)}{1 + R_m'^2}, \quad (5.22)$$

and

$$v = uR'_m. \quad (5.23)$$

In dimensionless form the relations are,

$$\frac{u + \varepsilon^2 v R'_m}{\sqrt{1 + \varepsilon^2 R_m'^2}} = -s_m \frac{(1 - \varepsilon^2 R_m'^2) \left( \frac{\partial u}{\partial r} + \varepsilon^2 \frac{\partial v}{\partial z} \right) - 2\varepsilon^2 R'_m \left( \frac{\partial u}{\partial z} - \frac{\partial v}{\partial r} \right)}{1 + \varepsilon^2 R_m'^2}, \quad (5.24)$$

and

$$v = uR'_m, \quad (5.25)$$

In a similar way as above, boundary condition (5.24) becomes for small  $\varepsilon$

$$u = -s_m \frac{\partial u}{\partial r} \quad \text{at } r = R_m. \quad (5.26)$$

The other condition (5.25) will be left as it is.

## 5.3 The free surface

As the blob of glass does not initially fill the mould completely (see Figure 1.1), there is a free surface of glass moving into the annular duct between mould and plunger. At the free boundary, the normal stress must be equal to the external pressure  $p_0$ , which is assumed to be constant,

$$(\boldsymbol{\sigma} \cdot \mathbf{n}) \cdot \mathbf{n} = -p_0,$$

and the tangential stress must be equal to zero,

$$(\boldsymbol{\sigma} \cdot \mathbf{n}) \cdot \mathbf{t} = 0.$$

In our slender-geometry approximation the exact shape of the free surface cannot be determined. In its neighbourhood, the flow scales both in  $r$  and  $z$  direction on the thickness  $D$  of the annular channel. In other words, the flow is not slowly varying in  $z$  anymore, and the present approximation is not valid.

Without any loss of generality, we can take  $p_0$  zero (that is, we use  $(p - p_0)$  rather than  $p$ ), because only the pressure *gradient* is relevant. Within the present approximation, and with use of the dimensionalization as given in Section (3), we can derive from (2.2)-(2.3) and with (5.21) that, in dimensionless formulation,

$$(\boldsymbol{\sigma} \cdot \mathbf{n}) \cdot \mathbf{n} = -p + O(\varepsilon^2).$$

Therefore, we will deal with the average level  $b$  of the free surface, as follows (in scaled variables)

$$p = 0 \quad \text{at } z = b(t), \quad (5.27)$$

where  $b$  is a function of the time-dependent geometry, implicitly defined in such a way that the (incompressible) glass volume between  $z = 0$  and  $z = b(t)$  is constant for all  $t$ .

## 6 Some auxiliary results

In this section, we derive some expressions (to be used later) for the axial flux and the total force on the plunger.

### 6.1 The flux

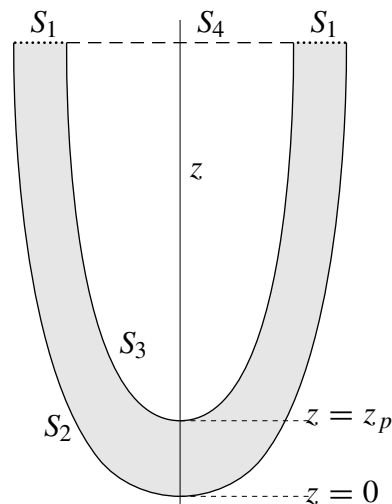


Figure 6.4: Sketch of the control surfaces to calculate the flux.

Consider the flux at some level  $z$  through cross section  $S_1$  (see Figure 6.4). The value of this flux depends on  $z$ , since the plunger goes down and causes the glass to move upward through a varying cross section. We will use this value later to find the pressure gradient.

Since glass is an incompressible fluid, we have with Gauss' divergence theorem

$$0 = \int_{\Omega} \nabla \cdot \mathbf{v} \, dx = \int_{\partial\Omega} \mathbf{v} \cdot \mathbf{n} \, dS = \int_{S_1} \mathbf{v} \cdot \mathbf{n} \, dS + \int_{S_2} \mathbf{v} \cdot \mathbf{n} \, dS + \int_{S_3} \mathbf{v} \cdot \mathbf{n} \, dS \quad (6.28)$$

where  $\mathbf{v} = u\mathbf{e}_z + \varepsilon v\mathbf{e}_r$ . Since the mould is stationary and impermeable we have

$$\int_{S_2} \mathbf{v} \cdot \mathbf{n} \, dS = 0,$$

while the flux through  $S_1$  is given by

$$\int_{S_1} \mathbf{v} \cdot \mathbf{n} \, dS = 2\pi \int_{R_p}^{R_m} r u(r, z) \, dr .$$

To calculate  $\int_{S_3} \mathbf{v} \cdot \mathbf{n} \, dS$ , we note that it would make no difference for the amount of glass displaced by the plunger if the plunger were filled with glass, because glass is just as incompressible as the solid plunger. Therefore, instead of control surface  $S_3$  we can use just as well surface  $S_4$ , which yields more easily the result

$$\int_{S_3} \mathbf{v} \cdot \mathbf{n} \, dS = \int_{S_4} \mathbf{v} \cdot \mathbf{n} \, dS = \pi u_p R_p^2 .$$

It follows that the flux is given by

$$2\pi \int_{R_p}^{R_m} r u(r, z) \, dr = -\pi u_p R_p^2 . \quad (6.29)$$

## 6.2 The total force on the plunger

In this section we discuss the total force on the plunger and use the result to find the velocity of the plunger. We return for a moment to a dimensional formulation. Later, we will turn back to the dimensionless form.

The force (= stress  $\times$  surface) in direction  $\mathbf{e}_k$ , applied to an infinitesimal surface element  $dS$  with outward normal  $\mathbf{n}$ , is by definition

$$-(\boldsymbol{\sigma} \cdot \mathbf{n}) \cdot \mathbf{e}_k \, dS = - \sum_j \sigma_{kj} n_j \, dS.$$

At the plunger surface with unit normal  $\mathbf{n}_p$ , given in (5.11), the stress in the  $z$ -direction is

$$-(\boldsymbol{\sigma} \cdot \mathbf{n}_p) \cdot \mathbf{e}_z = \left\{ \left( p - 2\eta \frac{\partial u}{\partial z} \right) R'_p + \eta \left( \frac{\partial v}{\partial z} + \frac{\partial u}{\partial r} \right) \right\} \frac{1}{\sqrt{1 + R'_p{}^2}},$$

where  $R_p = R_p(z - z_p(t))$ .

A (circular) surface element is given by

$$dS = 2\pi R_p \sqrt{1 + R_p'^2} dz.$$

So the total force on the plunger between top level  $z = z_p(t)$  and glass level  $z = b(t)$  is given by

$$f = 2\pi \int_{z_p}^b \left[ \left( p - 2\eta \frac{\partial u}{\partial z} \right) R_p' + \eta \left( \frac{\partial v}{\partial z} + \frac{\partial u}{\partial r} \right) \right]_{r=R_p} R_p dz. \quad (6.30)$$

Note that this glass level, as a function of time, is yet to be determined (see next section).

We render (6.30) dimensionless by using the same scaling as before, with  $b = Lb^*$ , and scale the force as

$$f = 2\pi \eta V L f^*.$$

This yields (ignoring again the asterisks) :

$$f = \int_{z_p}^b \left[ \left( p - 2\varepsilon^2 \frac{\partial u}{\partial z} \right) R_p' + \varepsilon^2 \frac{\partial v}{\partial z} + \frac{\partial u}{\partial r} \right]_{r=R_p} R_p dz \simeq \int_{z_p}^b \left[ p R_p' + \frac{\partial u}{\partial r} \right]_{r=R_p} R_p dz. \quad (6.31)$$

## 7 Results

### 7.1 The velocity and pressure field

Now we are ready to solve (3.7a-3.7c) with boundary conditions (5.18, 5.20) and (5.25, 5.26). At first, we note that  $p$  is a function of  $z$  only. Then (3.7a)

$$\frac{dp}{dz} = \frac{\partial^2 u}{\partial r^2} + \frac{1}{r} \frac{\partial u}{\partial r} = \frac{1}{r} \frac{\partial}{\partial r} \left( r \frac{\partial u}{\partial r} \right)$$

has solution

$$u = \frac{1}{4} r^2 \frac{dp}{dz} + A(z) \log(r) + B(z).$$

Using boundary conditions (5.20) and (5.26), we obtain:

$$u = \frac{1}{4} \frac{dp}{dz} \left[ r^2 + \frac{\beta_m(\alpha_p - \log r) - \beta_p(\alpha_m - \log r)}{\alpha_m - \alpha_p} \right] + u_p \frac{\alpha_m - \log r}{\alpha_m - \alpha_p}, \quad (7.32)$$

where it has been found convenient to introduce auxiliary parameters  $\alpha_{p,m}$ ,  $\beta_{p,m}$  and  $\gamma_{p,m}$  as follows

$$\sigma_m = s_m/R_m, \quad \sigma_p = -s_p/R_p, \quad \alpha = \log R + \sigma, \quad \beta = R^2(1+2\sigma), \quad \gamma = R^4(1+4\sigma), \quad (7.33)$$

showing at the same time the curious result that the essential slip parameter in a duct is apparently not  $s$  itself, but the product of  $s$  and the wall curvature.



Using the expression for  $u$  (7.32), the relation for the flux (6.29), and the following integral for  $ru$

$$\int ru(r, z) dr = \frac{1}{8}r^2 \frac{dp}{dz} \left[ \frac{1}{2}r^2 + \frac{\beta_m(\alpha_p + \frac{1}{2} - \log r) - \beta_p(\alpha_m + \frac{1}{2} - \log r)}{\alpha_m - \alpha_p} \right] + \dots \\ + \frac{1}{2}r^2 u_p \frac{\alpha_m + \frac{1}{2} - \log r}{\alpha_m - \alpha_p}, \quad (7.34)$$

we can determine the pressure gradient to find

$$\frac{dp}{dz} = -4u_p \frac{\beta_m - \beta_p}{(\beta_m - \beta_p)^2 - (\alpha_m - \alpha_p)(\gamma_m - \gamma_p)} := -m(z), \quad (7.35)$$

leading with (5.27) to

$$p(z) = \int_z^b m(\xi) d\xi. \quad (7.36)$$

Note that it is possible to prove that

$$(\beta_m - \beta_p)^2 - (\alpha_m - \alpha_p)(\gamma_m - \gamma_p) \leq 0,$$

for all  $R_p < R_m$  and  $s_m > 0$ ,  $s_p > 0$ . Furthermore,  $\beta_m - \beta_p > 0$ . So  $\frac{dp}{dz}$  has the sign of  $u_p$ .

Finally we solve (3.7c) with boundary conditions (5.18) or (5.25). We can rewrite (3.7c) as

$$\frac{\partial}{\partial r}(vr) + r \frac{\partial u}{\partial z} = 0,$$

then use (5.25) and Leibnitz rule, to obtain

$$v(r, z) = \frac{1}{r} \left[ R_m v(R_m, z) + \int_r^{R_m} \rho \frac{\partial u}{\partial z}(\rho, z) d\rho \right] = \frac{1}{r} \frac{d}{dz} \int_r^{R_m} \rho u(\rho, z) d\rho. \quad (7.37)$$

Upon substituting (7.34) into (7.37) and subsequent differentiation we obtain a complicated expression for  $v$  (see appendix). It is verified that boundary condition (5.18) indeed is satisfied.

## 7.2 The force on the plunger

By substituting the above results into (6.31), we obtain to leading order (use  $R_p = 0$  at  $z = z_p$ )

$$f = \int_{z_p}^b \left( p \frac{dR_p}{dz} + \left[ \frac{\partial u}{\partial r} \right]_{r=R_p} \right) R_p dz = \int_{z_p}^b \left( -\frac{1}{2} R_p^2 \frac{dp}{dz} + \left[ \frac{\partial u}{\partial r} \right]_{r=R_p} R_p \right) dz = \\ = u_p \int_{z_p}^b \frac{\gamma_m - \gamma_p}{(\beta_m - \beta_p)^2 - (\alpha_m - \alpha_p)(\gamma_m - \gamma_p)} dz. \quad (7.38)$$

Since the integrand is negative, the sign of  $f$  is opposite to the sign of  $u_p$  (as it should be). Although the approximation is strictly speaking not valid anymore at  $z = z_p$ , the integral converges, and it seems that the contribution of the plunger tip area is asymptotically of lower order.

An interesting conserved quantity of the process is the time integral of the plunger force. (Dimensionally equivalent to a net change of momentum, although inertia plays no rôle in the present model). It only depends on the end points  $z_1$  and  $z_2$  and not on the way the plunger moves in time, because  $f$  depends linearly on  $u_p$ .

$$\int_{t_1}^{t_2} f(t) dt = \int_{z_1}^{z_2} \int_{z_p}^b \frac{\gamma_m - \gamma_p}{(\beta_m - \beta_p)^2 - (\alpha_m - \alpha_p)(\gamma_m - \gamma_p)} dz dz_p. \quad (7.39)$$

The quantity is independent of  $u_p$ ,  $t_1$ , and  $t_2$  as long as begin and points,  $z_1$  and  $z_2$ , are kept the same. It may, for example, be used to verify, or compare, numerical methods. The property is not unique of the approximation, but a direct consequence of the fact that in the Stokes equations time is only a parameter, so that velocities may be scaled on  $u_p$ , and the plunger force  $f$  on  $\eta u_p z_p$ .

### 7.3 A prescribed force or velocity of the plunger

Using the condition that the total volume of the glass is constant, we consider the relation between time and velocity of the plunger, assuming either the velocity of, or the force on the plunger to be a prescribed function of  $t$ .

During the pressing phase, the plunger goes down as the glass moves up. So the plunger velocity  $u_p$  or the total force  $f$ , the position of the top of the plunger  $z_p$ , and the glass level  $b$  vary with time. Therefore we have to find a system of three equations for  $z_p$ ,  $b$ , and  $u_p$  or  $f$ .

First, we observe that the (scaled) volume  $\Omega$  of the total amount of glass is for all  $t$  equal to the constant

$$\Omega = \pi \int_0^b R_m^2 dz - \pi \int_{z_p}^b R_p^2 dz = \pi \int_0^b R_m^2 dz - \pi \int_0^{b-z_p} R_p^2(\rho) d\rho. \quad (7.40)$$

So if we could solve this equation explicitly, we would have a functional relation between  $b$  and  $z_p$ . This, however, is only possible in the simplest cases, for example when both  $R_p$  and  $R_m$  are parabola's. In general it has to be solved numerically at each time step. A natural approach is therefore to rewrite this equation into a differential equation in time, that can be solved by standard numerical integration routines.

After differentiating (7.40), using the defining relation between  $z_p$  and  $u_p$ , and the rela-

tion (7.38) between  $f$  and  $u_p$ , we obtain the following system of equations

$$\frac{dz_p}{dt} = u_p, \quad (7.41a)$$

$$\frac{db}{dt} = -u_p \frac{R_p^2(b - z_p)}{R_m^2(b) - R_p^2(b - z_p)}, \quad (7.41b)$$

$$f = u_p \int_{z_p}^b G(z, z_p) dz, \quad G(z, z_p) = \frac{\gamma_m - \gamma_p}{(\beta_m - \beta_p)^2 - (\alpha_m - \alpha_p)(\gamma_m - \gamma_p)}. \quad (7.41c)$$

which can be integrated numerically with either  $f(t)$  or  $u_p(t)$  given. In the simpler case when  $u_p$  is given, (7.41c) only defines  $f$  and is decoupled from the others. Note that  $G(z, z_p) \leq 0$ .

## 8 Examples

In this section we present two examples. In the first one we compare the present analytic expressions for  $u$  and  $\varepsilon v$  with numerical results obtained from a numerical model for glass flow, developed by the TUE Scientific Computing Group of Professor R.M.M. Matheij. We use here simple parabolic profiles for the plunger and mould, and the plots are in non-dimensional quantities.

In the second example we consider the velocity of the plunger, as it results from a given force. In addition, we use a practically more representative geometry of plunger and mould, as given in Figure 8.8. The plots are in dimensional quantities.

### 8.1 A given plunger velocity

Define the geometries and motion of plunger and mould by the following (dimensionless) expressions

$$R_p(z - z_p) = 0.1\sqrt{5}\sqrt{z - z_p}, \quad R_m(z) = 0.8\sqrt{5}\sqrt{z}, \quad z_p(t) = \frac{1}{5}(1 - t),$$

where  $\varepsilon = \frac{1}{5}$  and  $u_p = -1$ , while we will consider  $z = 1$ . Two cases are considered: (i) with no-slip boundary conditions ( $s_p = s_m = 0$ ) and (ii) with mixed boundary conditions ( $s_p = \infty$  and  $s_m = 0$ ). The results will be presented in dimensionless form, although for a proper comparison the velocities will be scaled both on the same (plunger) velocity. In other words, in the figures the axial velocity  $u$  and radial velocity  $\varepsilon v$  are plotted.

In Figure 8.5 we have case (i). Note that the order of magnitude of axial velocity  $u$  is indeed the same as that of the plunger (dimensionless unity), because of the no-slip condition at both sides. It is seen that there is an exceptionally good agreement between the numerical (\*) and the analytic solution (solid line).

Next we consider case (ii), with mixed boundary conditions. By taking  $s_p \rightarrow \infty$  in (5.20), we obtain  $\frac{\partial u}{\partial r} = 0$ . Besides this, we have of course (5.18). On the stationary mould there is no-slip, so here we have simply the boundary condition  $u = v = 0$ . As there is complete slip at the plunger wall, the velocity of the plunger plays no direct role in the problem. The axial

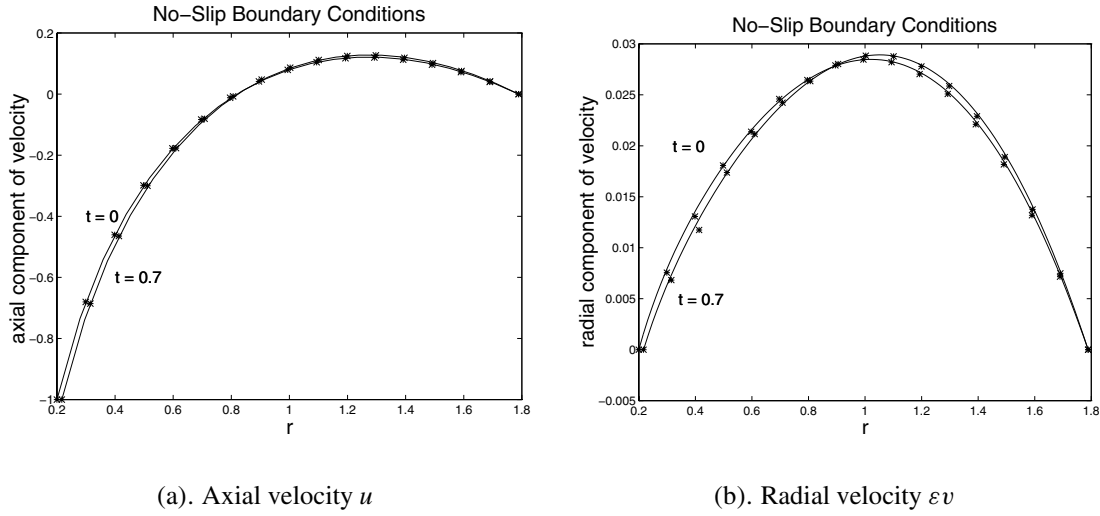


Figure 8.5: Axial and radial velocity. Parabolic geometry, no-slip. (Dimensionless.)

velocity is now determined by the effect of the plunger displacement. As a result the order of magnitude of  $u$  is considerably lower than unity. The results of this case are presented in Figures 8.6. In the axial velocity (Figure 8.6a) the numerical solution (\*) appears to differ a little from the analytical solution (solid line). This is, however, exactly consistent with the (conjectured) error of the asymptotic approximation, which is  $O(\varepsilon^2) \sim 4\%$ . Since  $s_p = \infty$ , (5.10) becomes at the plunger  $(\boldsymbol{\sigma} \cdot \mathbf{n}) \cdot \mathbf{t} = 0$ . This reduces for small  $\varepsilon$  to the approximate value  $\frac{\partial u}{\partial r} = 0 + O(\varepsilon^2)$ . This is different from the no-slip case where the condition  $u = 0$  is not approximate but exact.

Finally, we present a picture of the total force as a function of time for the case of no-slip boundary condition (see Figure 8.7). Here, we consider the no-slip case with the initial condition  $t = 0$ ,  $z_p(0) = 1$ ,  $b(0) = 2$ . As the time evolves, the plunger goes down ( $z_p(t)$  decreases) and the upper level of glass ( $b(t)$ ) increases, so the total wetted surface increases. Therefore, the total force is increasing. Note that the value of  $b(t)$  can be found from (7.40).

This is further illustrated by the following very simple configuration. If we assume both the plunger and the mould are straight cylinders ( $R_p$  and  $R_m$  are constants), we can determine the relation between force  $f(t)$  and velocity  $u_p(t)$  analytically (within the present approximation). Note that since  $R_p$  and  $R_m$  are constants, it follows that  $G(z, z_p)$  in (7.41c) is also constant. Therefore the force  $f(t)$  in (7.41c) becomes

$$f(t) = u_p(t)G(b(t) - z_p(t)), \quad (8.42)$$

where  $b(t)$  can be determined from (7.40) as

$$b(t) = \frac{\Omega/\pi - R_p^2 z_p(t)}{R_m^2 - R_p^2}. \quad (8.43)$$

As a result, we obtain

$$f(t) = G \frac{u_p(t)}{R_m^2 - R_p^2} \left[ \frac{\Omega}{\pi} - R_m^2 z_p(t) \right]. \quad (8.44)$$

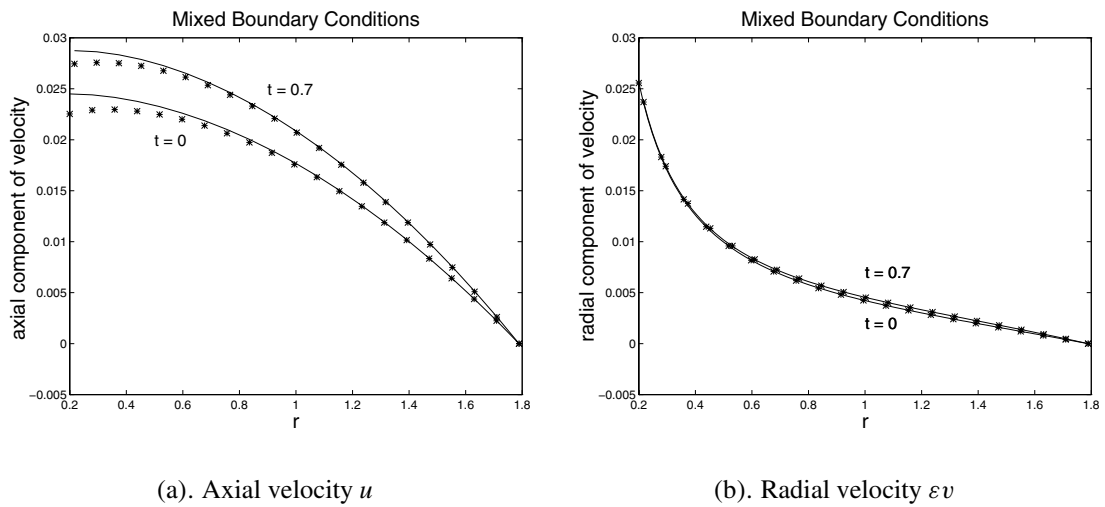


Figure 8.6: Axial and radial velocity. Parabolic geometry, mixed slip. (Dimensionless.)

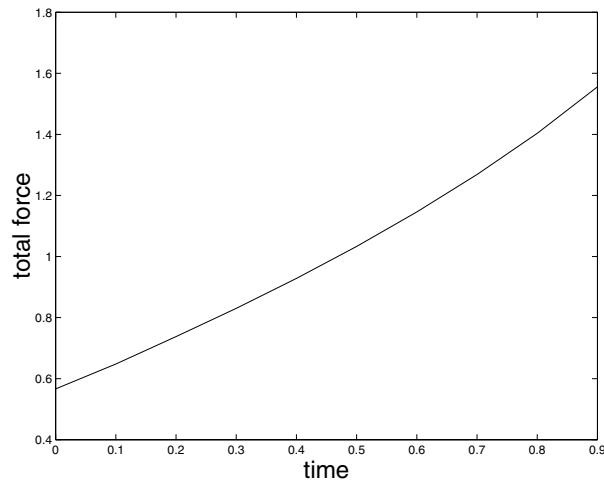


Figure 8.7: Total force as a function of time

For example, if  $u_p(t)$  is constant then  $z_p(t) = z_p(0) + u_p t$ , and  $f(t)$  is a linear function in  $t$ . Note that this expression includes the pressure contribution near the plunger top (see (7.38)).

## 8.2 A given plunger force

In this example we consider a more realistic situation. We will take a geometry of a real parison (Figure 8.8), and we will apply a given force from which the plunger velocity results, using the results of Sections 7.2 and 7.3, all in dimensional units. As in Example 1, we use 2 types of boundary conditions: no-slip ( $s_p = s_m = 0$ ) and mixed ( $s_p = \infty$  and  $s_m = 0$ ). The force on the plunger will be taken constant. Figure 8.8b shows the final position of the plunger in the pressing phase. In order to make the calculation easier, we calculated backwards in time, starting with this final position at  $t = 0$ . Since the Stokes equations do not include inertial effects, the sign of the time is irrelevant, and the results of a forward and a backward calculation are exactly the same.

The problem parameters, related to these cases, are the same as given in the table of Section 4, namely:  $V = 10$  cm/s,  $D = 1$  cm,  $\eta = 10^4$  kg/(s m),  $\varepsilon = 0.1$ , and  $z = 1$ . This suggests that the results are typically correct with an error of the order of 1%. In the case of Figure 8.9 (without slip) the applied plunger force is  $f = 7500$  N, while in the case of Figure 8.10 (with slip) the force is  $f = 5000$  N.

Evidently, when we go further back in time until the very early splash of the plunger in the fluid, and assume that the plunger force is still the same, the absence of resistance leads to unlimited high velocities. This, however, is impossible in practice, as the power ( $\sim$  force  $\times$  velocity) of the equipment is limited, and the inertia of the plunger is nonzero.

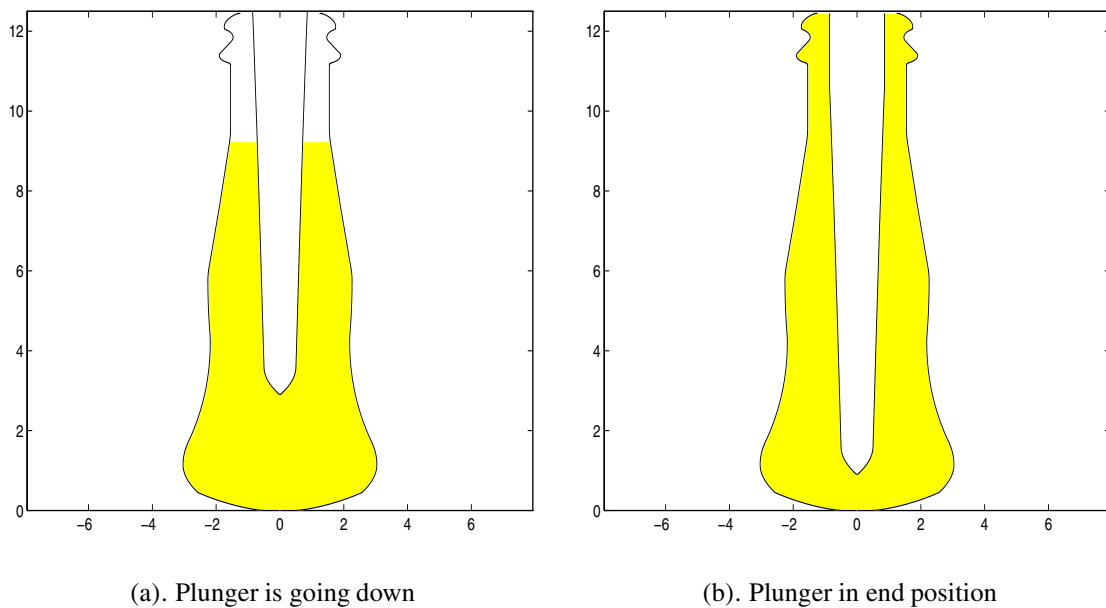


Figure 8.8: Realistic geometry of parison (units: cm)

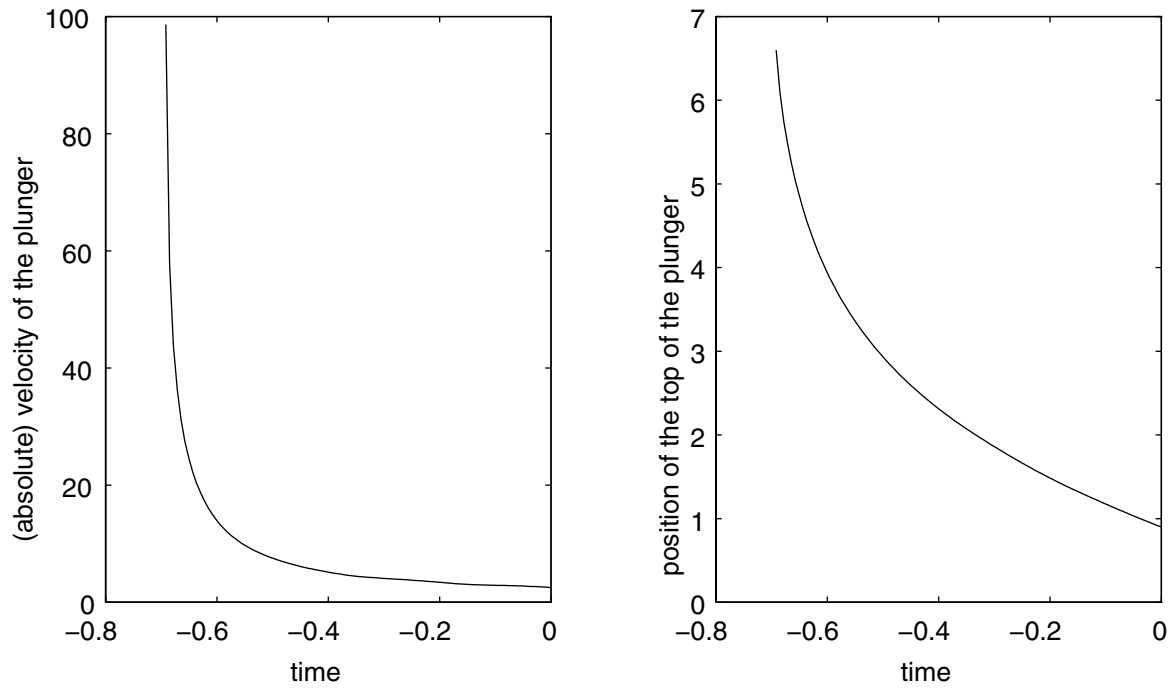


Figure 8.9: Given force = 7500 N, and  $s_p = s_m = 0$  (units: sec and cm/s).

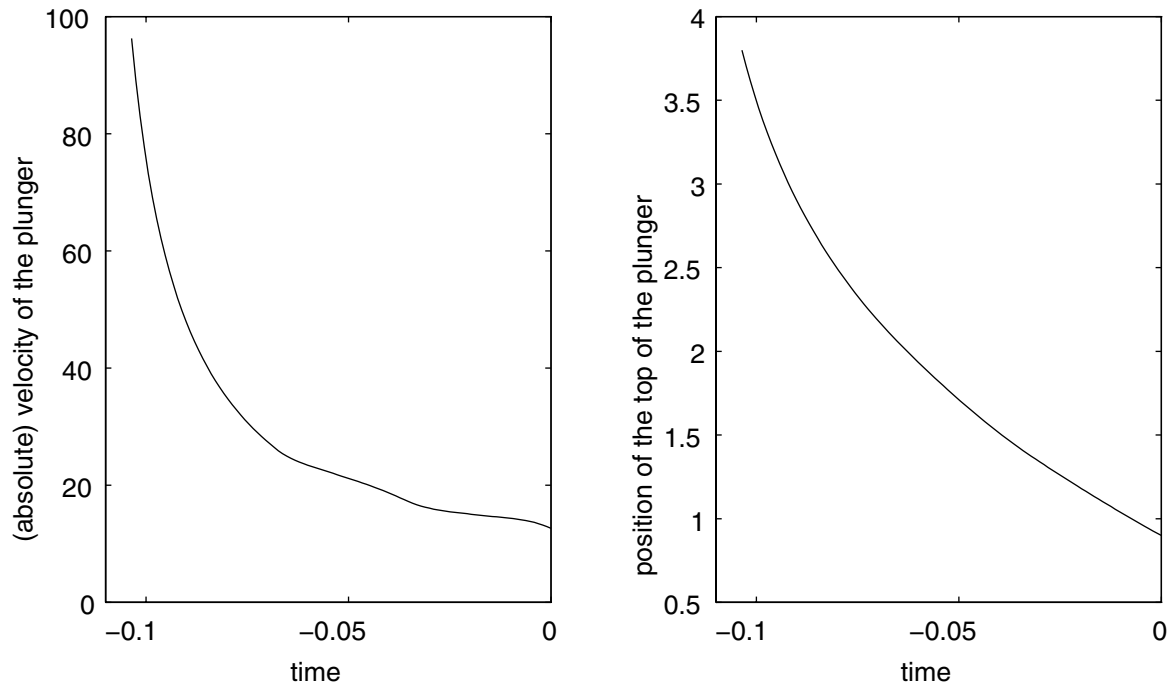


Figure 8.10: Given force = 5000 N,  $s_p = \infty$ , and  $s_m = 0$  (units: sec and cm/s).

For illustration, we consider again the straight cylindrical case with  $R_p$  and  $R_m$  constants. We assume that the force is also constant. Using the definition of  $z_p(t)$  (7.41a), the relation between  $b(t)$  and  $z_p(t)$  (8.43), and  $G(z, z_p)$  is just constant, the total force  $f$  turns into

$$\frac{f}{G} = \frac{\Omega/\pi}{R_m^2 - R_p^2} \frac{dz_p}{dt} - \frac{R_m^2}{R_m^2 - R_p^2} z_p(t) \frac{dz_p}{dt}. \quad (8.45)$$

Integrate (8.45) with respect to  $t$  yields

$$\frac{f}{G} t + K = \frac{\Omega/\pi}{R_m^2 - R_p^2} z_p - \frac{1}{2} \frac{R_m^2}{R_m^2 - R_p^2} z_p^2, \quad (8.46)$$

where  $K = \frac{\Omega/\pi}{R_m^2 - R_p^2} z_p(0) - \frac{1}{2} \frac{R_m^2}{R_m^2 - R_p^2} z_p^2(0)$ . Therefore we obtain (note that  $z_p(t) \leq \frac{\Omega/\pi}{R_m^2}$ )

$$z_p(t) = \frac{\Omega/\pi}{R_m^2} - \left[ \left( \frac{\Omega/\pi}{R_m^2} - z_p(0) \right)^2 - 2 \frac{R_m^2 - R_p^2}{R_m^2} \frac{f}{G} t \right]^{1/2}, \quad (8.47)$$

$$u_p(t) = \frac{f}{G} \frac{R_m^2 - R_p^2}{R_m^2} \left[ \left( \frac{\Omega/\pi}{R_m^2} - z_p(0) \right)^2 - 2 \frac{R_m^2 - R_p^2}{R_m^2} \frac{f}{G} t \right]^{-1/2}. \quad (8.48)$$

Since  $G$  is negative,  $u_p$  is negative for positive  $f$ , and decays as the time evolves. Note that at the initial splash of the plunger, *i.e.* at

$$t = \frac{1}{2} \frac{G}{f} \frac{R_m^2}{R_m^2 - R_p^2} \left( \frac{\Omega/\pi}{R_m^2} - z_p(0) \right)^2, \quad (8.49)$$

the velocity is indeed infinite.

### 8.3 Numerical method

A detailed description of the numerical method used in Example 1 may be found in [30, p.209]. In summary, it is described as follows: the glass flow is modelled by the Stokes equations, *i.e.*, for vanishing Reynolds number. The (self-adaptive) discretization scheme of the domain is based on a triangular mesh, where each triangle has twelve degrees of freedom for the velocity components. On each triangle the pressure is constant and the velocity is piecewise linear. The Finite Element Method (second order with respect to the size of mesh) is used to solve the Stokes equations, with an indicated accuracy of at least three digits. The time evolution of the glass domain  $\Omega$  is found by solving the ordinary differential equation

$$\frac{d\mathbf{x}(t)}{dt} = \mathbf{v}(\mathbf{x}(t)), t \in [t_n, t_{n+1}], \quad (8.50a)$$

$$\mathbf{x}(t_n) \in \Omega_{t_n}. \quad (8.50b)$$



## 9 Conclusions

We described a model for highly viscous incompressible glass flow during the pressing phase of the production. The model includes a general slip boundary condition. By using a perturbation method based on the slender geometry and low Reynolds number, we obtained explicit expressions for flow velocity and pressure gradient.

Based on these results, we calculated the total force on the plunger for given plunger velocity, and the resulting plunger velocity for given the total force. The examples show for the first case that the total force increases as the time evolves and for the second case, the plunger velocity decreases.

Representative examples showed a very good agreement of the flow velocity between the present solution based on the reduced, slender-geometry model and numerically obtained FEM based on the full model. solutions. We conclude that the perturbation method based on the slender geometry is an highly appropriate approach to this problem.

### Appendix : $v(r, z)$

In this appendix, we derive the expression for  $v(r, z)$ . We already got (7.37)

$$v = \frac{1}{r} \frac{d}{dz} \int_r^{R_m} \rho u(\rho, z) d\rho. \quad (9.51)$$

Using (7.34) and (7.35), we obtain

$$\begin{aligned} \int_r^{R_m} \rho u(\rho, z) d\rho &= \frac{u_p}{4} \left( \frac{\beta_m - \beta_p}{\alpha_m - \alpha_p} \right) \left\{ (R_m^4 - r^4)(\alpha_m - \alpha_p) \dots \right. \\ &+ 2(\beta_m - \beta_p)r^2 \log\left(\frac{r}{R_p}\right) - 2(\beta_m R_m^2 - \beta_p r^2) \log\left(\frac{R_m}{R_p}\right) + \frac{\beta_m \beta_p (R_m^2 - R_p^2)(R_m^2 - r^2)}{R_m^2 R_p^2} \left. \right\} \times \dots \\ &\left\{ (R_m^4 - R_p^4)(\alpha_m - \alpha_p) - 2(\beta_m R_m^2 - \beta_p R_p^2) \log\left(\frac{R_m}{R_p}\right) + \beta_m \beta_p \left( \frac{R_m}{R_p} - \frac{R_p}{R_m} \right)^2 \right\}^{-1} \dots \\ &- \frac{u_p}{4} \left[ \frac{\beta_m \left(1 - \frac{r^2}{R_m^2}\right) + 2r^2 \log\left(\frac{R_m}{r}\right)}{\alpha_m - \alpha_p} \right]. \quad (9.52) \end{aligned}$$

From (7.33), we obtain for the  $z$ -derivatives of  $\alpha_{m,p}$  and  $\beta_{m,p}$

$$\alpha' = \frac{R'}{R} (1 - \sigma) \pm \frac{s'}{R}, \quad \beta' = 2RR'(1 + \sigma) \pm 2Rs'. \quad (9.53)$$

By differentiating (9.52) with respect to  $z$  and using (9.53), we will obtain the full expression of  $v$ .

## **Acknowledgement**

We are grateful for the cooperation with the TUE Scientific Computing Group of Professor R.M.M. Mattheij, who generously provided the results from the numerical glass flow simulation. In particular, we want to express our gratitude to ir. Bram van de Broek and L.G.F.C. van Bree. We are grateful for the helpful discussions with Dr.ir. J.K.M. Jansen, Dr.ir. Y. Knops, and K. Laevsky. Especially appreciated are the many suggestions and fruitful ideas from Dr. Peter Howell. Finally, we are grateful for the very constructive remarks made by the referees.



# Chapter III

## On an operator equation for Stokes boundary value problems

**Abstract.** Stokes Boundary Value Problems (SBVP) can be found in many areas of engineering, for example, in fluid mechanics when the Reynolds number is small. This study investigates a method to solve the SBVP by translating the problem into an operator equation on the boundary  $\partial\Omega$  of the domain  $\Omega$  with a tangent vector field  $\alpha$  on the boundary  $\partial\Omega$  as unknown. This operator equation leads to the solutions of SBVP that can be parameterized by  $\alpha_{,x}$ , the *harmonic extension* of  $\alpha$  to the interior of the domain  $\Omega$ . As an application, the full explicit solutions of SBVP are presented for some simple domains such as the interior of the unit disk and of the unit ball.

### 1 Introduction

In recent years, a number of studies have been made to find a method to solve the Stokes equations

$$\begin{cases} \mu\Delta\mathbf{v} - \nabla p = \mathbf{0}, \\ \nabla \cdot \mathbf{v} = 0. \end{cases} \quad (1.1a,b)$$

For example, Padmavathi et al [40] and Sheng and Zhong [46] mention some methods such as the Naghdi-Hsu, the Papkovitch-Neuber, and the Boussinesq-Galerkin approach.

Inspired by these ideas, we develop a general theory of solving the inhomogeneous Stokes boundary value problems (SBVP)

$$\begin{cases} \mu\Delta\mathbf{v} - \nabla p = -\mathbf{f}, & \mathbf{x} \in \Omega, \\ \nabla \cdot \mathbf{v} = h, & \mathbf{x} \in \Omega, \\ \mathbf{v}(\mathbf{x}) = \mathbf{a}(\mathbf{x}), & \mathbf{x} \in \partial\Omega. \end{cases} \quad (1.2a,b,c)$$

Briefly, we solve the inhomogeneous Dirichlet and Neumann problems which lead to an operator equation on the boundary  $\partial\Omega$  of  $\Omega$  with a tangent vector field  $\alpha$  on the boundary  $\partial\Omega$

as unknown. We show that the solution of SBVP (1.2 a-c) can be 'parameterized' by  $\alpha_{\mathcal{H}}$ , the harmonic extension of  $\alpha$  to the interior of  $\Omega$ .

Finally, we give some applications of the method in the case of some simple domains.

## 2 General Theory

On a fixed open domain  $\Omega \subset \mathbb{R}^n$  with piecewise smooth boundary  $\partial\Omega$ , we consider the system of Stokes equations

$$\begin{cases} \mu \Delta \mathbf{v} - \nabla p = -\mathbf{f}, \\ \nabla \cdot \mathbf{v} = h. \end{cases} \quad (2.3a,b)$$

Here  $\mathbf{f} : \Omega \rightarrow \mathbb{R}^n$ ,  $h : \Omega \rightarrow \mathbb{R}$  are given functions.

Without loss of generality, we put  $\mu = 1$  in the sequel. For some given boundary condition  $\mathbf{v} = \mathbf{a}$  on  $\partial\Omega$ , we want to solve  $\mathbf{v}$  and  $p$  from (2.3 a,b). From [40] and [46], we know if the pair  $(\mathbf{v}, p)$  is a solution of (2.3 a,b), then we may decompose  $\mathbf{v}$  and  $p$  as

$$\begin{cases} \mathbf{v} = \boldsymbol{\phi} + \nabla \psi, \\ p = h - \nabla \cdot \boldsymbol{\phi}, \end{cases} \quad (2.4a,b)$$

with  $(\boldsymbol{\phi}, \psi)$  any solution of the system

$$\begin{cases} \Delta \boldsymbol{\phi} = -\mathbf{f}, \\ \Delta \psi + \nabla \cdot \boldsymbol{\phi} = h. \end{cases} \quad (2.5a,b)$$

It will turn out that the boundary condition of the system (2.3 a,b) is related to the boundary condition of (2.5 a,b) through an operator equation. For later convenience, we now split the solution  $(\boldsymbol{\phi}, \psi)$  of (2.5 a,b) into several pieces.

### 2.1 The Dirichlet problem

Here we consider the Dirichlet problem for the function  $\boldsymbol{\phi}$  introduced in (2.5 a)

$$\begin{cases} \Delta \boldsymbol{\phi} = -\mathbf{f}, & \mathbf{x} \in \Omega, \\ \boldsymbol{\phi} = \boldsymbol{\alpha}, & \mathbf{x} \in \partial\Omega, \end{cases} \quad (2.6a,b)$$

where  $\boldsymbol{\alpha} : \partial\Omega \rightarrow \mathbb{R}^n$  is an arbitrary, but fixed tangent vector field on  $\partial\Omega$ . The idea is to split  $\boldsymbol{\phi}$  up into a part  $\mathcal{D}\mathbf{f}$  that satisfies the inhomogeneous Laplace equation (2.6 a) but with vanishing boundary condition, and a part  $\alpha_{\mathcal{H}}$  that satisfies the homogeneous Laplace equation, but with non vanishing boundary condition as follows

$$\begin{cases} \Delta (\mathcal{D}\mathbf{f}) = -\mathbf{f}, & \mathbf{x} \in \Omega, \\ \mathcal{D}\mathbf{f} = \mathbf{0}, & \mathbf{x} \in \partial\Omega, \end{cases} \quad (2.7a,b)$$

and

$$\begin{cases} \Delta \alpha_{\mathcal{H}} = \mathbf{0}, & \mathbf{x} \in \Omega, \\ \alpha_{\mathcal{H}} = \boldsymbol{\alpha}, & \mathbf{x} \in \partial\Omega. \end{cases} \quad (2.8a,b)$$

Note that  $\mathcal{D}\mathbf{f}$  and  $\alpha_{\mathcal{H}}$  can be obtained, at least in principle, by means of Green's function [51, pp. 86-87].

## 2.2 The Neumann problem

Here we consider the Neumann problem for the function  $\psi$  introduced in (2.5 b). Using (2.5 b) and the same decomposition of  $\phi$  as introduced in Section 2.1, we find

$$\begin{cases} \Delta \psi = -\nabla \cdot \phi + h = -\nabla \cdot \alpha_{\mathcal{H}} - \nabla \cdot \mathcal{D}f + h, & \mathbf{x} \in \Omega, \\ \frac{\partial \psi}{\partial n} = \gamma, & \mathbf{x} \in \partial\Omega, \end{cases} \quad (2.9a,b)$$

where  $\gamma : \partial\Omega \rightarrow \mathbb{R}$  is an arbitrary but fixed function. For this Neumann problem, we impose the compatibility condition

$$\int_{\partial\Omega} \gamma d\tau = \int_{\Omega} (-\nabla \cdot \alpha_{\mathcal{H}} - \nabla \cdot \mathcal{D}f + h) d\sigma = \int_{\Omega} h d\sigma = 0. \quad (2.10)$$

Here we have used  $\mathcal{D}f = \mathbf{0}$  on the boundary and

$$\int_{\Omega} \nabla \cdot \alpha_{\mathcal{H}} d\sigma = \int_{\partial\Omega} \alpha_{\mathcal{H}} \cdot \mathbf{n} d\tau = \int_{\partial\Omega} \alpha \cdot \mathbf{n} d\tau = 0, \quad (2.11)$$

since  $\alpha$  is a tangent vector field on  $\partial\Omega$ .

It is convenient to read (2.9 a) as the sum of three Neumann problems. Because of that, we write  $\psi$  as the sum of the solutions of these problems in the following way :

$$\psi = \mathcal{N}(\nabla \cdot \alpha_{\mathcal{H}}) + \mathcal{N}(\nabla \cdot \mathcal{D}f - h) + \gamma_{\mathcal{H},\mathcal{N}},$$

with

$$\begin{cases} \Delta \mathcal{N}(\nabla \cdot \alpha_{\mathcal{H}}) = -\nabla \cdot \alpha_{\mathcal{H}}, & \mathbf{x} \in \Omega, \\ \frac{\partial}{\partial n} \mathcal{N}(\nabla \cdot \alpha_{\mathcal{H}}) = 0, & \mathbf{x} \in \partial\Omega, \end{cases} \quad (2.12a,b)$$

$$\begin{cases} \Delta \mathcal{N}(\nabla \cdot \mathcal{D}f - h) = -\nabla \cdot \mathcal{D}f + h, & \mathbf{x} \in \Omega, \\ \frac{\partial}{\partial n} \mathcal{N}(\nabla \cdot \mathcal{D}f - h) = 0, & \mathbf{x} \in \partial\Omega, \end{cases} \quad (2.13a,b)$$

and

$$\begin{cases} \Delta \gamma_{\mathcal{H},\mathcal{N}} = 0, & \mathbf{x} \in \Omega, \\ \frac{\partial}{\partial n} \gamma_{\mathcal{H},\mathcal{N}} = \gamma, & \mathbf{x} \in \partial\Omega. \end{cases} \quad (2.14a,b)$$

We remark that (2.12), (2.13), and (2.14) have the same structure as (2.7) and (2.8) and are in principle solvable. So, in the following, we may consider  $\phi$  and  $\psi$  to be known as provided that the boundary functions  $\alpha$  and  $\gamma$  are known.

Note that, because of  $\Delta \alpha_{\mathcal{H}} = \mathbf{0}$ , one has

$$\Delta \left( -\frac{1}{2} \mathbf{x} \cdot \alpha_{\mathcal{H}} \right) = -\nabla \cdot \alpha_{\mathcal{H}}, \quad (2.15)$$

where,  $\mathbf{x}$  denotes position. The solution for the inhomogeneous Neumann problem (2.12 a,b) can thus be written as

$$\mathcal{N}(\nabla \cdot \alpha_{\mathcal{H}}) = -\frac{1}{2} \mathbf{x} \cdot \alpha_{\mathcal{H}} + \psi^{(\alpha)}, \quad (2.16)$$

where  $\psi^{(\alpha)}$  is the solution of the homogeneous Neumann boundary value problem

$$\begin{cases} \Delta \psi^{(\alpha)} = 0, & \mathbf{x} \in \Omega, \\ \frac{\partial \psi^{(\alpha)}}{\partial n} = \frac{\partial}{\partial n} \left( \frac{1}{2} \mathbf{x} \cdot \alpha_{\mathcal{H}} \right), & \mathbf{x} \in \partial\Omega. \end{cases} \quad (2.17a,b)$$

### 2.3 A parameterized class of solutions

We may summarize the findings in above as follows. For any tangent vector field  $\boldsymbol{\alpha} : \partial\Omega \rightarrow \mathbb{R}^n$  and any function  $\gamma : \partial\Omega \rightarrow \mathbb{R}$ , the pair  $(\mathbf{v}, p)$  with

$$\begin{cases} \mathbf{v} = \boldsymbol{\alpha}_{\mathcal{H}} + \mathcal{D}\mathbf{f} + \nabla\mathcal{N}(\nabla \cdot \boldsymbol{\alpha}_{\mathcal{H}}) + \nabla\mathcal{N}(\nabla \cdot \mathcal{D}\mathbf{f}) - \nabla\mathcal{N}(h) + \nabla\gamma_{\mathcal{H},\mathcal{N}}, \\ p = h - \nabla \cdot \boldsymbol{\alpha}_{\mathcal{H}} - \nabla \cdot \mathcal{D}\mathbf{f}, \end{cases} \quad (2.18a,b)$$

is a solution of the system (2.3 a,b).

The problem we have to solve now is :

How are  $\boldsymbol{\alpha}$  and  $\gamma$  related to the *prescribed* vector field  $\mathbf{a}$  on  $\partial\Omega$  ?

It will be explained that for  $\boldsymbol{\alpha}$  the solution of an operator equation on the boundary has to be taken. This operator equation involves all the data :  $\mathbf{a}, \mathbf{f}, h$ .

### 2.4 The operator equation on the boundary $\partial\Omega$ .

In this section, we derive an operator equation which relates  $\boldsymbol{\alpha} : \partial\Omega \rightarrow \mathbb{R}^n$  to the prescribed data  $(\mathbf{a}, \mathbf{f}, h)$ . From (2.4 a), we obtain the requirement

$$\mathbf{v} = \mathbf{a} = \boldsymbol{\phi} + \nabla\psi, \text{ on } \partial\Omega, \quad (2.19)$$

or

$$\boldsymbol{\alpha} + \nabla\mathcal{N}(\nabla \cdot \boldsymbol{\alpha}_{\mathcal{H}}) = \mathbf{a} - \nabla\gamma_{\mathcal{H},\mathcal{N}} - \nabla\mathcal{N}(\nabla \cdot \mathcal{D}\mathbf{f}) + \nabla\mathcal{N}(h), \text{ on } \partial\Omega. \quad (2.20)$$

If we take on each  $\mathbf{x} \in \partial\Omega$  the inner product of both sides of identity (2.20) with the normal vector  $\mathbf{n}$ , and using (2.12 b), (2.13 b), (2.14 b), then we get

$$\gamma = \mathbf{a} \cdot \mathbf{n}. \quad (2.21)$$

Therefore, we obtain the operator equation for an unknown *tangent vector field*  $\boldsymbol{\alpha}$  on the boundary

$$\boldsymbol{\alpha} + \nabla\mathcal{N}(\nabla \cdot \boldsymbol{\alpha}_{\mathcal{H}}) = \mathbf{a} - \nabla(\mathbf{a} \cdot \mathbf{n})_{\mathcal{H},\mathcal{N}} - \nabla\mathcal{N}(\nabla \cdot \mathcal{D}\mathbf{f}) + \nabla\mathcal{N}(h), \text{ on } \partial\Omega, \quad (2.22)$$

where the right-hand side is a tangent vector field on  $\partial\Omega$  that can, in principle, be calculated from  $\mathbf{a}, \mathbf{f}$ , and  $h$ . If we can solve  $\boldsymbol{\alpha}$  from the operator equation (2.22), then the solution of the inhomogeneous SBVP

$$\begin{cases} \Delta\mathbf{v} - \nabla p = -\mathbf{f}, & \mathbf{x} \in \Omega, \\ \nabla \cdot \mathbf{v} = h, & \mathbf{x} \in \Omega, \\ \mathbf{v}(\mathbf{x}) = \mathbf{a}(\mathbf{x}), & \mathbf{x} \in \partial\Omega, \end{cases} \quad (2.23a,b,c)$$

is given by (2.18 a,b), or equivalently by

$$\begin{cases} \mathbf{v} = \boldsymbol{\alpha}_{\mathcal{H}} + \mathcal{D}\mathbf{f} + \nabla\left\{-\frac{1}{2}\mathbf{x} \cdot \boldsymbol{\alpha}_{\mathcal{H}} + \psi^{(\boldsymbol{\alpha})}\right\} + \nabla\mathcal{N}(\nabla \cdot \mathcal{D}\mathbf{f}) - \nabla\mathcal{N}(h) + \nabla(\mathbf{a} \cdot \mathbf{n})_{\mathcal{H},\mathcal{N}}, \\ p = h - \nabla \cdot \boldsymbol{\alpha}_{\mathcal{H}} - \nabla \cdot \mathcal{D}\mathbf{f}. \end{cases} \quad (2.24a,b)$$

Next, as an application, we present full explicit solutions of homogeneous SBVP for some simple domains such as the interior of the unit disk and of the unit ball.

### 3 Applications

#### 3.1 The interior of the unit disk

Here, we consider the homogeneous SBVP with as domain the interior of the unit disk  $D = \{(x, y) \mid x^2 + y^2 < 1\}$ ,

$$\begin{cases} \Delta \mathbf{v} - \nabla p = \mathbf{0}, & \mathbf{x} \in D, \\ \nabla \cdot \mathbf{v} = 0, & \mathbf{x} \in D, \\ \mathbf{v}(\mathbf{x}) = \mathbf{a}(\mathbf{x}), & \mathbf{x} \in \partial D = \{(x, y) \mid x^2 + y^2 = 1\}. \end{cases} \quad (3.25a,b,c)$$

We assume that the prescribed boundary condition  $\mathbf{a}(\mathbf{x})$  can be expanded into a Fourier series

$$\mathbf{a}(\mathbf{x}) = \sum_{n=-\infty}^{\infty} \left\{ a_n \begin{pmatrix} -\sin(\theta) \\ \cos(\theta) \end{pmatrix} e^{in\theta} + b_n \begin{pmatrix} \cos(\theta) \\ \sin(\theta) \end{pmatrix} e^{in\theta} \right\}.$$

The compatibility condition  $0 = \int_{\Omega} \nabla \cdot \mathbf{v} \, d\sigma = \int_{\partial\Omega} \mathbf{a} \cdot \mathbf{n} \, d\tau$  implies  $b_0 = 0$ .

According to the theory, we have to solve the boundary operator equation (2.22)

$$\boldsymbol{\alpha} + \nabla \mathcal{N}(\nabla \cdot \boldsymbol{\alpha}_{\mathcal{H}}) = \mathbf{a} - \nabla(\mathbf{a} \cdot \mathbf{n})_{\mathcal{H}\mathcal{N}}, \quad (3.26)$$

since  $\mathbf{f} = \mathbf{0}$ , and  $h = 0$ . Therefore, at first, we study the action of the operator

$$\boldsymbol{\alpha} \longmapsto \boldsymbol{\alpha} + \nabla \mathcal{N}(\nabla \cdot \boldsymbol{\alpha}_{\mathcal{H}}), \quad (3.27)$$

on the 'basic' tangent vector fields :

$$\mathbf{t}_n = \begin{pmatrix} -\sin(\theta) \\ \cos(\theta) \end{pmatrix} e^{in\theta}, \quad n \in \mathbb{Z}. \quad (3.28)$$

We would like to calculate  $\mathbf{t}_{n,\mathcal{H}}$ , the harmonic extension of  $\mathbf{t}_n$ ,

$$\begin{cases} \Delta \mathbf{t}_{n,\mathcal{H}} = \mathbf{0}, & \mathbf{x} \in D, \\ \mathbf{t}_{n,\mathcal{H}} = \mathbf{t}_n, & \mathbf{x} \in \partial D. \end{cases} \quad (3.29a,b)$$

Using the notations  $z = x + iy$ ,  $\bar{z} = x - iy$ , and  $\Delta = 4 \frac{\partial}{\partial z} \frac{\partial}{\partial \bar{z}}$  we obtain

$$\mathbf{t}_{n,\mathcal{H}} = \begin{cases} \frac{1}{2} \begin{pmatrix} i \\ 1 \end{pmatrix} z^{(n+1)} + \frac{1}{2} \begin{pmatrix} -i \\ 1 \end{pmatrix} z^{(n-1)}, & n \in \mathbb{N}, \\ \frac{1}{2} \begin{pmatrix} i \\ 1 \end{pmatrix} z + \frac{1}{2} \begin{pmatrix} -i \\ 1 \end{pmatrix} \bar{z}, & n = 0, \\ \frac{1}{2} \begin{pmatrix} i \\ 1 \end{pmatrix} \bar{z}^{(|n|-1)} + \frac{1}{2} \begin{pmatrix} -i \\ 1 \end{pmatrix} \bar{z}^{(|n|+1)}, & -n \in \mathbb{N}, \end{cases} \quad (3.30)$$



that leads to

$$\nabla \mathcal{N}(\nabla \cdot \mathbf{t}_{n_{\mathcal{H}}})|_{r=1} = \begin{cases} -\frac{1}{2}\mathbf{t}_n, & n \in \mathbb{Z}/\{0\}, \\ 0, & n = 0. \end{cases} \quad (3.31)$$

We conclude that the left-hand side of the boundary operator equation (3.26) is a mapping

$$\boldsymbol{\alpha} \mapsto \boldsymbol{\alpha} + \nabla \mathcal{N}(\nabla \cdot \boldsymbol{\alpha}_{\mathcal{H}}), \quad (3.32)$$

that maps

$$\begin{cases} \mathbf{t}_n \mapsto \frac{1}{2}\mathbf{t}_n, & n \in \mathbb{Z}/\{0\}, \\ \mathbf{t}_0 \mapsto \mathbf{t}_0, & n = 0. \end{cases} \quad (3.33)$$

Therefore, given the boundary condition  $\mathbf{a}$ , we can solve the boundary operator equation (3.26) for  $\boldsymbol{\alpha}_{\mathcal{H}}$ . For example, given the 'basic' boundary condition  $\mathbf{a} = \begin{pmatrix} \cos(\theta) \\ \sin(\theta) \end{pmatrix} e^{in\theta}$ ,  $n \in \mathbb{N}$ , we obtain

$$\mathbf{a} - \nabla(\mathbf{a} \cdot \mathbf{n})_{\mathcal{H}\mathcal{N}} = \frac{1}{2} \begin{pmatrix} 1 \\ -i \end{pmatrix} z^{n+1} - \frac{1}{2} \begin{pmatrix} 1 \\ i \end{pmatrix} z^{n-1}. \quad (3.34)$$

Hence,  $\boldsymbol{\alpha}_{\mathcal{H}} = 2(\mathbf{a} - \nabla(\mathbf{a} \cdot \mathbf{n})_{\mathcal{H}\mathcal{N}}) = \begin{pmatrix} 1 \\ -i \end{pmatrix} z^{n+1} - \begin{pmatrix} 1 \\ i \end{pmatrix} z^{n-1}$ .

### 3.1.1 Solution

Since  $\mathbf{f} = \mathbf{0}$  and  $h = 0$ , we obtain from (2.18 *a,b*) the solution of the homogeneous SBVP :

$$\mathbf{v} = \boldsymbol{\alpha}_{\mathcal{H}} + \nabla \mathcal{N}(\nabla \cdot \boldsymbol{\alpha}_{\mathcal{H}}) + \nabla(\mathbf{a} \cdot \mathbf{n})_{\mathcal{H}\mathcal{N}}, \quad p = -\nabla \cdot \boldsymbol{\alpha}_{\mathcal{H}}. \quad (3.35)$$

Below, we present a table of solutions for various 'basic' boundary conditions.

boundary condition ( $\mathbf{a}$ )	velocity ( $\mathbf{v}$ )	pressure ( $p$ )
$\begin{pmatrix} -\sin(\theta) \\ \cos(\theta) \end{pmatrix} e^{in\theta}, n \in \mathbb{N}$	$\frac{1}{2} \begin{pmatrix} i \\ 1 \end{pmatrix} z^{n+1} + \frac{1}{2} \begin{pmatrix} -i \\ 1 \end{pmatrix} z^n \bar{z}$ $+ \frac{n}{2} \begin{pmatrix} i \\ -1 \end{pmatrix} z^{n-1} (1 - z\bar{z})$	$-2i(n+1)z^n$
$\begin{pmatrix} -\sin(\theta) \\ \cos(\theta) \end{pmatrix} e^{-in\theta}, n \in \mathbb{N}$	$\frac{1}{2} \begin{pmatrix} -i \\ 1 \end{pmatrix} \bar{z}^{n+1} + \frac{1}{2} \begin{pmatrix} i \\ 1 \end{pmatrix} \bar{z}^n z$ $- \frac{n}{2} \begin{pmatrix} i \\ 1 \end{pmatrix} \bar{z}^{n-1} (1 - z\bar{z})$	$2i(n+1)\bar{z}^n$
$\begin{pmatrix} -\sin(\theta) \\ \cos(\theta) \end{pmatrix}$	$\frac{1}{2} \begin{pmatrix} i \\ 1 \end{pmatrix} z + \frac{1}{2} \begin{pmatrix} -i \\ 1 \end{pmatrix} \bar{z}$	0

boundary condition ( $\mathbf{a}$ )	velocity ( $\mathbf{v}$ )	pressure ( $p$ )
$\begin{pmatrix} \cos(\theta) \\ \sin(\theta) \end{pmatrix} e^{in\theta}, n \in \mathbb{N}$	$\frac{1}{2} \begin{pmatrix} 1 \\ -i \end{pmatrix} z^{n+1} + \frac{1}{2} \begin{pmatrix} 1 \\ i \end{pmatrix} z^{n-1} + \left(\frac{n+1}{2}\right) \begin{pmatrix} 1 \\ i \end{pmatrix} z^{n-1} (1 - z\bar{z})$	$-2(n+1)z^n$
$\begin{pmatrix} \cos(\theta) \\ \sin(\theta) \end{pmatrix} e^{-in\theta}, n \in \mathbb{N}$	$\frac{1}{2} \begin{pmatrix} 1 \\ i \end{pmatrix} \bar{z}^{n+1} + \frac{1}{2} \begin{pmatrix} 1 \\ -i \end{pmatrix} \bar{z}^{n-1} + \left(\frac{n+1}{2}\right) \begin{pmatrix} 1 \\ -i \end{pmatrix} \bar{z}^{n-1} (1 - z\bar{z})$	$-2(n+1)\bar{z}^n$

In view of the linearity of the problem, each solution  $(\mathbf{v}, p)$  of the homogeneous SBVP in the interior of the unit disk is a linear superposition of these elementary solutions. Note that for every fixed  $|z| < 1$ , the value of the basic solutions decreases exponentially if  $|n| \rightarrow \infty$ . This implies that any linear superposition of basic solution with coefficients  $\{c_n\}$ , not increasing faster than polynomially, leads to a solution of the homogeneous SBVP on the open disk  $D$ . If, in addition, one assumes that  $\sum_{n=1}^{\infty} |nc_n| < \infty$ , then both the velocity  $\mathbf{v}$  and the pressure field  $p$  extend continuously to the closed disk  $\bar{D}$ .

### 3.2 The interior of the unit ball

In this section, we consider the homogeneous SBVP with as domain the interior of the unit ball  $B = \{(x, y, z) \mid x^2 + y^2 + z^2 < 1\}$ ,

$$\begin{cases} \Delta \mathbf{v} - \nabla p = \mathbf{0}, & \mathbf{x} \in B, \\ \nabla \cdot \mathbf{v} = 0, & \mathbf{x} \in B, \\ \mathbf{v}(\mathbf{x}) = \mathbf{a}(\mathbf{x}), & \mathbf{x} \in \partial B = \{(x, y, z) \mid x^2 + y^2 + z^2 = 1\}, \end{cases} \quad (3.36a,b,c)$$

with  $\mathbf{a} : \partial B \rightarrow \mathbb{R}^3$  the prescribed velocity field on the boundary.

#### 3.2.1 Some notations and preliminaries

In this section, we introduce some notations that will be used later. The closure of  $B$  is denoted by  $\bar{B} = B \cup \partial B$ . For a tangent vector field  $\boldsymbol{\alpha}$ , one has for all  $\mathbf{x} \in \partial B : \boldsymbol{\alpha} \cdot \mathbf{x} = 0$ . We will use bold greek lower case symbols for tangent vector fields. Extensive use will be made of the usual vector algebra and vector calculus in  $\mathbb{R}^3$  applying the usual nabla notations :

$$\nabla f = \text{grad } f, \quad \nabla \cdot \mathbf{v} = \text{div } \mathbf{v}, \quad \nabla \times \mathbf{v} = \text{rot } \mathbf{v}. \quad (3.37)$$

Also the Euler operator  $\mathcal{E} = \mathbf{x} \cdot \nabla = x \frac{\partial}{\partial x} + y \frac{\partial}{\partial y} + z \frac{\partial}{\partial z}$ , and its resolvents  $(\mathcal{E} + s)^{-1}$ ,  $s \geq 0$ , given by

$$(\mathcal{E} + s)^{-1} f(\mathbf{x}) = \int_0^1 \lambda^{s-1} f(\lambda \mathbf{x}) d\lambda, \quad (3.38)$$

play an important role. For vector fields  $\mathbf{v}$  the operators  $\mathcal{E}\mathbf{v}$  and  $(\mathcal{E} + s)^{-1}\mathbf{v}$  are defined componentwise. We mention some commutator properties for  $\mathcal{E}$  and its resolvents. They follow from straightforward computation :

$$\nabla\mathcal{E} = \nabla + \mathcal{E}\nabla, \quad \Delta\mathcal{E} = 2\Delta + \mathcal{E}\Delta, \quad \nabla\left((\mathcal{E} + s)^{-1}f\right)(\mathbf{x}) = (\mathcal{E} + s + 1)^{-1}\nabla f(\mathbf{x}). \quad (3.39)$$

Next, we discuss some lemmas.

**Lemma 3.1.** If a continuous vector function  $\boldsymbol{\phi} : \bar{B} \rightarrow \mathbb{R}^3$  satisfies

$$\begin{cases} \Delta\boldsymbol{\phi}(\mathbf{x}) = \mathbf{0}, & \mathbf{x} \in B, \\ \nabla \cdot \boldsymbol{\phi}(\mathbf{x}) = 0, & \mathbf{x} \in B, \\ \mathbf{x} \cdot \boldsymbol{\phi} = 0, & \mathbf{x} \in \partial B, \end{cases}$$

then  $\boldsymbol{\phi}$  can be written as  $\boldsymbol{\phi} = \mathbf{x} \times \nabla\varphi$ , with  $\Delta\varphi = 0$  and  $\varphi$  is unique if we require  $\varphi(\mathbf{0}) = 0$ .

**Proof.** First we find a necessary condition on  $\nabla\varphi$  by taken the curl of both sides of  $\boldsymbol{\phi} = \mathbf{x} \times \nabla\varphi$ ,

$$\nabla \times \boldsymbol{\phi} = \nabla \times (\mathbf{x} \times \nabla\varphi) = (\nabla \cdot \nabla\varphi)\mathbf{x} + (\nabla\varphi \cdot \nabla)\mathbf{x} - (\nabla \cdot \mathbf{x})\nabla\varphi - (\mathbf{x} \cdot \nabla)\nabla\varphi = -(\mathcal{E} + 2)\nabla\varphi. \quad (3.40)$$

So, a candidate for  $\nabla\varphi$  is given by  $-(\mathcal{E} + 2)^{-1}(\nabla \times \boldsymbol{\phi})$  which can be rewritten as  $-(\mathcal{E} + 2)^{-1}(\nabla \times \boldsymbol{\phi}) = -\nabla \times ((\mathcal{E} + 1)^{-1}\boldsymbol{\phi})$ . We shall show that this field is rotation free :

$$\begin{aligned} \nabla \times \left( (\mathcal{E} + 2)^{-1}(\nabla \times \boldsymbol{\phi}) \right) &= \nabla \times \left( \nabla \times (\mathcal{E} + 1)^{-1}\boldsymbol{\phi} \right) \\ &= \nabla \left( \nabla \cdot \left( (\mathcal{E} + 1)^{-1}\boldsymbol{\phi} \right) \right) - \Delta(\mathcal{E} + 1)^{-1}\boldsymbol{\phi} \\ &= \nabla(\mathcal{E} + 2)^{-1}(\nabla \cdot \boldsymbol{\phi}) - (\mathcal{E} + 3)^{-1}\Delta\boldsymbol{\phi} = \mathbf{0}. \end{aligned}$$

So, the vector field  $-(\mathcal{E} + 2)^{-1}(\nabla \times \boldsymbol{\phi})$  has a potential  $\varphi$ , say, and we may write  $-(\mathcal{E} + 2)^{-1}(\nabla \times \boldsymbol{\phi}) = \nabla\varphi$ . Further, note that  $\Delta\varphi = \nabla \cdot \nabla\varphi = -\nabla \cdot \nabla \times (\mathcal{E} + 1)^{-1}\boldsymbol{\phi} = 0$ . So,  $\varphi$  is harmonic.

Finally, we prove that the vector field  $\mathbf{u} = \boldsymbol{\phi} + (\mathbf{x} \times (\nabla \times (\mathcal{E} + 1)^{-1}\boldsymbol{\phi})) = \boldsymbol{\phi} - (\mathbf{x} \times \nabla\varphi)$  is identically zero. Observe that

1.  $\nabla \times \mathbf{u} = \mathbf{0}$ . See above.
2.  $\nabla \cdot \mathbf{u} = \nabla \cdot \boldsymbol{\phi} + (\nabla \times \mathbf{x}) \cdot (\nabla \times (\mathcal{E} + 1)^{-1}\boldsymbol{\phi}) - (\nabla \times (\nabla \times (\mathcal{E} + 1)^{-1}\boldsymbol{\phi})) \cdot \mathbf{x} = 0$ .
3.  $\mathbf{u} = \nabla\sigma$ , with  $\Delta\sigma = 0$ . Since  $\mathbf{x} \cdot \mathbf{u} = \mathcal{E}\sigma = 0$  on the boundary  $\partial B$  and  $\Delta\mathcal{E}\sigma = 2\Delta\sigma + \mathcal{E}\Delta\sigma = 0$ , we obtain  $\mathcal{E}\sigma = 0$  for the whole region  $B$ . Expand  $\sigma$  in spherical harmonics  $\sigma = \sum_{n=0}^{\infty} \sigma_n$ . Then  $\mathcal{E}\sigma = \sum_{n=0}^{\infty} n\sigma_n$ . We conclude that  $\sigma_n = 0$  if  $n = 1, 2, \dots$ . Therefore  $\sigma$  must be constant and hence  $\mathbf{u} = \mathbf{0}$ .

Finally, note that until now  $\varphi$  is fixed up to an additive constant. By taking  $\varphi(\mathbf{0}) = 0$ , this arbitrariness is removed.  $\square$

**Lemma 3.2.** If a continuous vector function  $\boldsymbol{\phi} : \bar{B} \rightarrow \mathbb{R}^3$  satisfies

$$\begin{cases} \Delta \boldsymbol{\phi}(\mathbf{x}) = 0, & \mathbf{x} \in B, \\ \mathbf{x} \cdot \boldsymbol{\phi} = 0, & \mathbf{x} \in \partial B, \end{cases}$$

then  $\boldsymbol{\phi}$  can be written as  $\boldsymbol{\phi} = \boldsymbol{\phi}_0 + \boldsymbol{\phi}_1$ , with

$$\boldsymbol{\phi}_0 = \mathbf{x} \times \nabla \varphi, \quad (3.41)$$

$$\boldsymbol{\phi}_1 = \nabla \chi - (\mathcal{E} \chi) \mathbf{x} + \frac{1}{2}(|\mathbf{x}|^2 - 1) \nabla \left[ (\mathcal{E} + \frac{1}{2})^{-1} \mathcal{E} \right] \chi, \quad (3.42)$$

where both  $\varphi : \bar{B} \rightarrow \mathbb{R}$  and  $\chi : \bar{B} \rightarrow \mathbb{R}$  are harmonic. If we require  $\varphi(\mathbf{0}) = \chi(\mathbf{0}) = 0$ , then both  $\varphi$  and  $\chi$  are unique. Moreover,  $\chi$  satisfies  $\left[ -(\mathcal{E} + 1)^2 + \frac{1}{2} + \frac{1}{4}(\mathcal{E} + \frac{1}{2})^{-1} \right] \chi = \nabla \cdot \boldsymbol{\phi} = \nabla \cdot \boldsymbol{\phi}_1$ .

**Proof.** First, construct  $\chi$  from  $\nabla \cdot \boldsymbol{\phi}$ , i.e.  $\chi = \left[ -(\mathcal{E} + 1)^2 + \frac{1}{2} + \frac{1}{4}(\mathcal{E} + \frac{1}{2})^{-1} \right]^{-1} \nabla \cdot \boldsymbol{\phi}$ , and define  $\boldsymbol{\phi}_1$  according to (3.42). Put  $\boldsymbol{\phi}_0 = \boldsymbol{\phi} - \boldsymbol{\phi}_1$ . Observe that  $\nabla \cdot \boldsymbol{\phi}_0 = 0$ . Next, we obtain  $\mathbf{x} \cdot \boldsymbol{\phi}_1 = (1 - |\mathbf{x}|^2) \mathcal{E} \left[ I - \frac{1}{2}(\mathcal{E} + \frac{1}{2})^{-1} \mathcal{E} \right] \chi$ . Therefore, we get  $\mathbf{x} \cdot \boldsymbol{\phi}_0 = 0$  on the boundary. Further, since  $\Delta \boldsymbol{\phi}_1 = 0$ , also  $\Delta \boldsymbol{\phi}_0 = 0$ . Hence, according to Lemma 3.1, we obtain  $\boldsymbol{\phi}_0 = \mathbf{x} \times \nabla \varphi$ . Finally, note that until now  $\varphi$  and  $\chi$  are fixed up to an additive constant. By taking  $\varphi(\mathbf{0}) = \chi(\mathbf{0}) = 0$ , this arbitrariness is removed.  $\square$

**Lemma 3.3.** Let  $\vartheta : \bar{B} \rightarrow \mathbb{R}$  be continuous and such that  $\Delta \vartheta(\mathbf{x}) = 0$ ,  $\mathbf{x} \in B$ ,  $\vartheta(\mathbf{0}) = 0$ . If the vector function  $\mathbf{w} : \bar{B} \rightarrow \mathbb{R}^3$  satisfies

$$\begin{cases} \Delta \mathbf{w}(\mathbf{x}) = \mathbf{0}, & \mathbf{x} \in B, \\ \mathbf{w}(\mathbf{x}) = \mathbf{x} \vartheta(\mathbf{x}) + c \mathbf{x}, & \mathbf{x} \in \partial B, c \in \mathbb{R}, \end{cases}$$

then  $\mathbf{w}$  can be written as  $\mathbf{w} = \nabla \mathcal{E}^{-1} \vartheta + c \mathbf{x}$ , where  $c = \frac{1}{4\pi} \int_{\partial B} \mathbf{w}(\mathbf{x}) \cdot \mathbf{x} \, d\tau$ .

**Proof.** Straightforward computation yields  $\Delta \mathbf{w} = \Delta(\nabla \mathcal{E}^{-1} \vartheta + c \mathbf{x}) = \mathbf{0}$ . Next, by taking the inner product  $\mathbf{w}(\mathbf{x}) \cdot \mathbf{x}$  on the boundary, one finds

$$\mathbf{x} \cdot \mathbf{w} = \mathbf{x} \cdot \nabla \mathcal{E}^{-1} \vartheta + \mathbf{x} \cdot c \mathbf{x} = \vartheta(\mathbf{x}) + c,$$

which is equal to  $\mathbf{x} \cdot \mathbf{w} = \mathbf{x} \cdot \mathbf{x} \vartheta + \mathbf{x} \cdot c \mathbf{x} = \vartheta(\mathbf{x}) + c$ . Finally, if we take the inner product  $\mathbf{w}(\mathbf{x}) \cdot \mathbf{x}$  on the boundary, calculate the integral over the boundary, and use the mean value theorem for harmonic functions, then we obtain

$$\int_{\partial B} \mathbf{w} \cdot \mathbf{x} \, d\tau = \int_{\partial B} \mathbf{x} \cdot \mathbf{x} \vartheta(\mathbf{x}) \, d\tau + \int_{\partial B} c \mathbf{x} \cdot \mathbf{x} \, d\tau = 4\pi \vartheta(\mathbf{0}) + 4\pi c,$$

or

$$c = \frac{1}{4\pi} \int_{\partial B} \mathbf{w} \cdot \mathbf{x} \, d\tau. \quad \square$$

In the preceding lemmas, we gave three different recipes for constructing harmonic vector fields from harmonic functions. For later convenience we introduce a notation for these recipes.

**Definition 3.4.** Let  $\mathbf{h}_j[\varphi] : B \rightarrow \mathbb{R}$ ,  $j = 0, 1, 2$ , denote the harmonic vector fields defined by

$$\begin{aligned}\mathbf{h}_0[\varphi] &: \mathbf{x} \mapsto \mathbf{x} \times \nabla\varphi(\mathbf{x}), \\ \mathbf{h}_1[\chi] &: \mathbf{x} \mapsto \nabla\chi - (\mathfrak{E}\chi)\mathbf{x} + \frac{1}{2}(|\mathbf{x}|^2 - 1)\nabla\left[(\mathfrak{E} + \frac{1}{2})^{-1}\mathfrak{E}\right]\chi, \\ \mathbf{h}_2[\vartheta] &: \mathbf{x} \mapsto \nabla\mathfrak{E}^{-1}\vartheta.\end{aligned}$$

Remember that  $\varphi$ ,  $\chi$ , and  $\vartheta$  are supposed to be harmonic. We gather the recipes of this section in the following theorem.

**Theorem 3.5.** Consider the continuous vector field  $\mathbf{a} : \partial B \rightarrow \mathbb{R}^3$ . Let  $\mathbf{a}_{\mathcal{H}} : \bar{B} \rightarrow \mathbb{R}^3$  be the harmonic extension of  $\mathbf{a}$ . Then there exist unique harmonic functions  $\varphi, \chi, \vartheta : B \rightarrow \mathbb{R}$ , with  $\varphi(\mathbf{0}) = \chi(\mathbf{0}) = \vartheta(\mathbf{0}) = 0$  such that

$$\mathbf{a}_{\mathcal{H}} = \mathbf{h}_0[\varphi] + \mathbf{h}_1[\chi] + \mathbf{h}_2[\vartheta] + c\mathbf{x},$$

with  $c = \frac{1}{4\pi} \int_{\partial B} (\mathbf{a} \cdot \mathbf{x}) \, d\tau$ . Note that if  $\vartheta = 0$  and  $c = 0$ , then  $\mathbf{a}$  is a tangential vector field.

**Proof.** The proof is divided into several steps.

1. Split the vector field  $\mathbf{a}$  into a tangential and two normal parts as follows :  $\mathbf{a} = \mathbf{a}_t + \mathbf{a}_n + c\mathbf{n}$ , with  $c = \frac{1}{4\pi} \int_{\partial B} (\mathbf{a} \cdot \mathbf{n}) \, d\tau$ ,  $\mathbf{a}_n = (\mathbf{a} \cdot \mathbf{n} - c)\mathbf{n}$  and  $\mathbf{a}_t = \mathbf{a} - \mathbf{a}_n - c\mathbf{n}$ . Note that  $\mathbf{a}_t$  is tangential and that  $\mathbf{a}_n$  is parallel to  $\mathbf{n}$ .
2. Define  $\vartheta$  as the solution of the Dirichlet problem

$$\begin{cases} \Delta\vartheta(\mathbf{x}) = 0, & \mathbf{x} \in B, \\ \vartheta(\mathbf{x}) = \mathbf{a} \cdot \mathbf{n} - c, & \mathbf{x} \in \partial B. \end{cases}$$

3. Note that for any  $\mathbf{x} \in \partial B$ , the vector field  $\mathbf{a} - \nabla\mathfrak{E}^{-1}\vartheta(\mathbf{x}) - c\mathbf{x}$  is tangential.
4. The harmonic extension  $\mathbf{x} \mapsto \mathbf{a}_{\mathcal{H}}(\mathbf{x}) - \nabla\mathfrak{E}^{-1}\vartheta(\mathbf{x}) - c\mathbf{x}$  satisfies the conditions of Lemma 3.2. This means it can be uniquely written as  $\mathbf{h}_0[\varphi] + \mathbf{h}_1[\chi]$  for suitable harmonic  $\varphi$  and  $\chi$ .  $\square$

Note : Keep in mind that  $\mathbf{h}_0$  and  $\mathbf{h}_1$  also depend on  $\mathbf{a} \cdot \mathbf{n}$ . In our case,  $\nabla \cdot \mathbf{v} = 0$  (3.36 b) implies  $c = 0$ .

### 3.2.2 Solution

In a similar way as in Section 3.1 for the unit disk, we have to solve the boundary operator equation (2.22)

$$\boldsymbol{\alpha} + \nabla \mathcal{N}(\nabla \cdot \boldsymbol{\alpha}_{\mathcal{H}}) = \mathbf{a} - \nabla(\mathbf{a} \cdot \mathbf{n})_{\mathcal{H}\mathcal{N}}, \quad (3.43)$$

and, at first, we study the operator

$$\boldsymbol{\alpha} \longmapsto \boldsymbol{\alpha} + \nabla \mathcal{N}(\nabla \cdot \boldsymbol{\alpha}_{\mathcal{H}}). \quad (3.44)$$

Based on Theorem 3.5, we know that any tangent vector field on the boundary  $\boldsymbol{\alpha}$  can be split into  $\mathbf{h}_0[\varphi] + \mathbf{h}_1[\chi]$ . Therefore,

1. if  $\boldsymbol{\alpha} = \mathbf{h}_0[\varphi] = \mathbf{x} \times \nabla \varphi$ , then we get

$$\boldsymbol{\alpha} + \nabla \mathcal{N}(\nabla \cdot \boldsymbol{\alpha}_{\mathcal{H}}) = \mathbf{h}_0[\varphi] = \mathbf{x} \times \nabla \varphi, \quad (3.45)$$

or on the boundary ( $|\mathbf{x}| = 1$ ),

$$\mathbf{h}_0[\varphi] \longmapsto \mathbf{h}_0[\varphi]. \quad (3.46)$$

2. if  $\boldsymbol{\alpha} = \mathbf{h}_1[\chi]|_{|\mathbf{x}|=1} = \nabla \chi - \mathbf{x} \mathcal{E} \chi$ , then we get

$$\begin{aligned} \boldsymbol{\alpha} + \nabla \mathcal{N}(\nabla \cdot \boldsymbol{\alpha}_{\mathcal{H}}) &= \mathbf{h}_1[\chi]|_{|\mathbf{x}|=1} + \mathbf{h}_1 \left[ -\chi + \frac{1}{2} \mathcal{E} (\mathcal{E} + \frac{1}{2})^{-1} \chi \right] |_{|\mathbf{x}|=1} \\ &= \mathbf{h}_1 \left[ \frac{1}{2} \mathcal{E} (\mathcal{E} + \frac{1}{2})^{-1} \chi \right] |_{|\mathbf{x}|=1}, \end{aligned} \quad (3.47)$$

or on the boundary ( $|\mathbf{x}| = 1$ ),

$$\mathbf{h}_1[\chi] \longmapsto \mathbf{h}_1 \left[ \frac{1}{2} \mathcal{E} (\mathcal{E} + \frac{1}{2})^{-1} \chi \right]. \quad (3.48)$$

Hence, given the boundary condition  $\mathbf{a}$ , we can solve the boundary operator equation (3.43) for  $\boldsymbol{\alpha}_{\mathcal{H}}$ . For example, if  $\mathbf{a} = \vartheta \mathbf{x}$ , with  $\Delta \vartheta = \mathbf{0}$ ,  $\vartheta(\mathbf{0}) = 0$ , then we have

$$(\mathbf{a} \cdot \mathbf{n})_{\mathcal{H}\mathcal{N}} = \mathcal{E}^{-1} \vartheta, \quad \mathbf{a} - \nabla(\mathbf{a} \cdot \mathbf{n})_{\mathcal{H}\mathcal{N}} = \vartheta \mathbf{x} - \nabla \mathcal{E}^{-1} \vartheta = \mathbf{h}_1[-\mathcal{E}^{-1} \vartheta]|_{|\mathbf{x}|=1}. \quad (3.49)$$

Therefore, according to (3.47),  $\boldsymbol{\alpha}_{\mathcal{H}} = \mathbf{h}_1 \left[ -2(\mathcal{E} + \frac{1}{2}) \mathcal{E}^{-2} \vartheta \right]$ .

Below, we present the solution of the boundary operator equation (3.43) for various boundary conditions  $\mathbf{a}$  :

boundary condition ( $\mathbf{a}$ )	$\boldsymbol{\alpha}_{\mathcal{H}}$
$\mathbf{x} \times \nabla \varphi$	$\mathbf{x} \times \nabla \varphi$
$\nabla \chi - \mathbf{x} \mathcal{E} \chi$	$\mathbf{h}_1 \left[ 2(\mathcal{E} + \frac{1}{2}) \mathcal{E}^{-1} \chi \right]$
$\vartheta \mathbf{x}$	$\mathbf{h}_1 \left[ -2(\mathcal{E} + \frac{1}{2}) \mathcal{E}^{-2} \vartheta \right]$

Next, we make some special choices for the right-hand side  $\mathbf{a}$  of the boundary operator equation. These special choices involve harmonic homogen polynomials ( $Q_m$ ) of degree  $m$  on which the Euler Operator  $\mathcal{E}$  acts as a simple multiplication :  $\mathcal{E} Q_m = m Q_m$ . Using solutions (2.18 *a,b*),

$$\mathbf{v} = \boldsymbol{\alpha}_{\mathcal{H}} + \nabla \mathcal{N} (\nabla \cdot \boldsymbol{\alpha}_{\mathcal{H}}) + \nabla \gamma_{\mathcal{H}\mathcal{N}}, \quad p = -\nabla \cdot \boldsymbol{\alpha}_{\mathcal{H}}, \quad (3.50)$$

we obtain the following table of solutions

boundary condition ( $\mathbf{a}$ )	solutions
$\mathbf{x} \times \nabla Q_m$	$\mathbf{v} = \mathbf{x} \times \nabla Q_m,$ $p = 0.$
$\nabla Q_m - m Q_m \mathbf{x}$	$\mathbf{v} = \nabla Q_m - m Q_m \mathbf{x} + \frac{1}{2}(m+3)( \mathbf{x} ^2 - 1)\nabla Q_m,$ $p = (2m+3)(m+1)Q_m.$
$Q_m \mathbf{x}$	$\mathbf{v} = Q_m \mathbf{x} - \left(\frac{m+3}{2m}\right)( \mathbf{x} ^2 - 1)\nabla Q_m,$ $p = -\frac{(2m+3)(m+1)}{m}Q_m.$

In view of the linearity of the problem, each solution  $(\mathbf{v}, p)$  of the homogeneous SBVP in the unit ball is a linear superposition of the elementary solutions. The remarks similar to those given directly below the table in Section 3.1.1 apply here as well.

For functional analysis considerations (also for the general case) we refer to [20].

# Chapter IV

## Further illustrations of the operator method

### 1 Introduction

In chapter III, we presented full explicit solutions of the homogeneous Stokes Boundary Value Problem (SBVP) with as domain the interior of the unit disk and of the unit ball. Here, we consider the same problem with as domain the exterior of the unit disk and of the unit ball, an upper half space, an infinite strip, and an infinite wedge. Also, we give an example of an inhomogeneous SBVP with as domain the interior of the unit disk. For convenience, from now on, we change the symbol  $\gamma_{\mathcal{N}}$  that is introduced in Chapter III with  $\mathcal{N}(0; \mathbf{a} \cdot \mathbf{n})$ .

### 2 The exterior of the unit disk

In this section, we consider a homogeneous SBVP with as domain the exterior of the unit disk  $D^c = \{ (x, y) \mid x^2 + y^2 > 1 \}$ ,

$$\Delta \mathbf{v} - \nabla p = \mathbf{0}, \quad \mathbf{x} \in D^c, \quad (2.1a)$$

$$\nabla \cdot \mathbf{v} = 0, \quad \mathbf{x} \in D^c, \quad (2.1b)$$

$$\mathbf{v}(\mathbf{x}) = \mathbf{a}(\mathbf{x}), \quad \mathbf{x} \in \partial D^c, \quad (2.1c)$$

$$\mathbf{v} \rightarrow \mathbf{0} \text{ and } p \rightarrow 0, \text{ as } |\mathbf{x}| \rightarrow \infty. \quad (2.1d)$$

We assume that the prescribed boundary condition  $\mathbf{a}(\mathbf{x})$  can be expanded into a Fourier Series

$$\mathbf{a}(\mathbf{x}) = \sum_{n=-\infty}^{\infty} \left\{ a_n \begin{pmatrix} -\sin(\theta) \\ \cos(\theta) \end{pmatrix} e^{in\theta} + b_n \begin{pmatrix} \cos(\theta) \\ \sin(\theta) \end{pmatrix} e^{in\theta} \right\},$$

with  $b_0 = 0$  to satisfy the compatibility condition  $\int_{\Omega} \nabla \cdot \mathbf{v} \, d\sigma = \int_{\partial\Omega} \mathbf{a} \cdot \mathbf{n} \, d\tau = 0$ .



## 2.1 The operator equation

According to the general procedure in Chapter III, we have to solve the operator equation on the boundary

$$\alpha + \nabla \mathcal{N}(\nabla \cdot \alpha_{\mathcal{H}}) = \mathbf{a} - \nabla \mathcal{N}(0; \mathbf{a} \cdot \mathbf{n}). \quad (2.2)$$

We study this operator equation in the following lemma.

**Lemma 2.1.** The solution of the operator equation (2.2)

1. for  $\mathbf{a} = \begin{pmatrix} -\sin(\theta) \\ \cos(\theta) \end{pmatrix}$  is  $\alpha_{\mathcal{H}} = \frac{1}{2} \begin{pmatrix} i \\ 1 \end{pmatrix} \frac{1}{\bar{z}} + \frac{1}{2} \begin{pmatrix} -i \\ 1 \end{pmatrix} \frac{1}{z}$ ,
2. for  $\mathbf{a} = \begin{pmatrix} -\sin(\theta) \\ \cos(\theta) \end{pmatrix} e^{in\theta}$ ,  $n \in \mathbb{N}$  is  $\alpha_{\mathcal{H}} = \begin{pmatrix} i \\ 1 \end{pmatrix} \left(\frac{1}{\bar{z}}\right)^{n+1} + \begin{pmatrix} -i \\ 1 \end{pmatrix} \left(\frac{1}{z}\right)^{n-1}$ ,
3. for  $\mathbf{a} = \begin{pmatrix} \cos(\theta) \\ \sin(\theta) \end{pmatrix} e^{in\theta}$ ,  $n \in \mathbb{N}$  is  $\alpha_{\mathcal{H}} = \begin{pmatrix} -1 \\ i \end{pmatrix} \left(\frac{1}{\bar{z}}\right)^{n+1} + \begin{pmatrix} 1 \\ i \end{pmatrix} \left(\frac{1}{z}\right)^{n-1}$ .

**Proof.** Similar as in the disk case in Chapter III, we study the action for the operator

$$\alpha \longmapsto \alpha + \nabla \mathcal{N}(\nabla \cdot \alpha_{\mathcal{H}}), \quad (2.3)$$

on the 'basic' tangent vector fields :

$$\mathbf{t}_n = \begin{pmatrix} -\sin(\theta) \\ \cos(\theta) \end{pmatrix} e^{in\theta}, \quad n \in \mathbb{N}. \quad (2.4)$$

Using the notations  $z = x + iy$ ,  $\bar{z} = x - iy$ , and  $\Delta = 4 \frac{\partial}{\partial z} \frac{\partial}{\partial \bar{z}}$ , we obtain the harmonic extension  $\mathbf{t}_{n\mathcal{H}}$  of  $\mathbf{t}_n$  as

$$\mathbf{t}_{n\mathcal{H}} = \begin{cases} \frac{1}{2} \begin{pmatrix} i \\ 1 \end{pmatrix} \left(\frac{1}{\bar{z}}\right)^{(n+1)} + \frac{1}{2} \begin{pmatrix} -i \\ 1 \end{pmatrix} \left(\frac{1}{z}\right)^{(n-1)}, & n \in \mathbb{N}, \\ \frac{1}{2} \begin{pmatrix} i \\ 1 \end{pmatrix} \frac{1}{\bar{z}} + \frac{1}{2} \begin{pmatrix} -i \\ 1 \end{pmatrix} \frac{1}{z}, & n = 0, \\ \frac{1}{2} \begin{pmatrix} i \\ 1 \end{pmatrix} \left(\frac{1}{z}\right)^{(|n|+1)} + \frac{1}{2} \begin{pmatrix} -i \\ 1 \end{pmatrix} \left(\frac{1}{\bar{z}}\right)^{(|n|-1)}, & -n \in \mathbb{N}, \end{cases} \quad (2.5)$$

that leads to

$$\nabla \mathcal{N}(\nabla \cdot \mathbf{t}_{n\mathcal{H}})|_{r=1} = \begin{cases} -\frac{1}{2} \mathbf{t}_n, & n \in \mathbb{Z}/\{0\}, \\ 0, & n = 0. \end{cases} \quad (2.6)$$

We conclude that the left-hand side of the boundary operator equation (2.2) is a mapping

$$\alpha \longmapsto \alpha + \nabla \mathcal{N}(\nabla \cdot \alpha_{\mathcal{H}}), \quad (2.7)$$

that maps

$$\begin{cases} \mathbf{t}_n \mapsto \frac{1}{2}\mathbf{t}_n, & n \in \mathbb{Z}/\{0\}, \\ \mathbf{t}_0 \mapsto \mathbf{t}_0, & n = 0. \end{cases} \quad (2.8)$$

Therefore, given the boundary condition  $\mathbf{a}$  and using (2.8) we can determine  $\alpha_{\mathcal{H}}$ . Lemma 2.1.1 and Lemma 2.1.2 are direct consequence of (2.8), since  $\mathbf{a} \cdot \mathbf{n} = 0$ . For Lemma 2.1.3, at first we calculate

$$\mathbf{a} - \nabla \mathcal{N}(0; \mathbf{a} \cdot \mathbf{n}) = \frac{1}{2} \begin{pmatrix} -1 \\ i \end{pmatrix} \left(\frac{1}{\bar{z}}\right)^{n+1} + \frac{1}{2} \begin{pmatrix} 1 \\ i \end{pmatrix} \left(\frac{1}{\bar{z}}\right)^{n-1}. \quad (2.9)$$

Therefore,  $\alpha_{\mathcal{H}} = \begin{pmatrix} -1 \\ i \end{pmatrix} \left(\frac{1}{\bar{z}}\right)^{n+1} + \begin{pmatrix} 1 \\ i \end{pmatrix} \left(\frac{1}{\bar{z}}\right)^{n-1}$ . □

## 2.2 Solution

Based on the Lemma 2.1, we present the solution of the SBVP (2.1) for various boundary conditions  $\mathbf{a}$  as follows :

boundary condition ( $\mathbf{a}$ )	solutions
$\begin{pmatrix} -\sin(\theta) \\ \cos(\theta) \end{pmatrix}$	$\mathbf{v} = \frac{1}{2} \begin{pmatrix} i \\ 1 \end{pmatrix} \frac{1}{\bar{z}} + \frac{1}{2} \begin{pmatrix} -i \\ 1 \end{pmatrix} \frac{1}{z},$ $p = 0.$
$\begin{pmatrix} -\sin(\theta) \\ \cos(\theta) \end{pmatrix} e^{in\theta}, n \in \mathbb{N}$	$\mathbf{v} = \frac{1}{2} \begin{pmatrix} i \\ 1 \end{pmatrix} \left(\frac{1}{\bar{z}}\right)^n z + \frac{1}{2} \begin{pmatrix} -i \\ 1 \end{pmatrix} \left(\frac{1}{\bar{z}}\right)^{n-1}$ $+ \frac{n}{2} \begin{pmatrix} i \\ 1 \end{pmatrix} \left(\frac{1}{\bar{z}}\right)^{n+1} (1 - z\bar{z}),$ $p = -2i(n-1) \left(\frac{1}{\bar{z}}\right)^n.$
$\begin{pmatrix} -\sin(\theta) \\ \cos(\theta) \end{pmatrix} e^{-in\theta}, n \in \mathbb{N}$	$\mathbf{v} = \frac{1}{2} \begin{pmatrix} -i \\ 1 \end{pmatrix} \left(\frac{1}{z}\right)^n \bar{z} + \frac{1}{2} \begin{pmatrix} i \\ 1 \end{pmatrix} \left(\frac{1}{z}\right)^{n-1}$ $+ \frac{n}{2} \begin{pmatrix} -i \\ 1 \end{pmatrix} \left(\frac{1}{z}\right)^{n+1} (1 - z\bar{z}),$ $p = 2i(n-1) \left(\frac{1}{z}\right)^n.$

boundary condition ( <b>a</b> )	solutions
$\begin{pmatrix} \cos(\theta) \\ \sin(\theta) \end{pmatrix} e^{in\theta}, n \in \mathbb{N}$	$\mathbf{v} = \begin{pmatrix} 1 \\ -i \end{pmatrix} \left(\frac{1}{z}\right)^{n+1} + \frac{1}{2} \begin{pmatrix} 1 \\ i \end{pmatrix} \left(\frac{1}{z}\right)^{n-1}$ $- \frac{1}{2} \begin{pmatrix} 1 \\ -i \end{pmatrix} \left(\frac{1}{z}\right)^n z - \frac{n}{2} \begin{pmatrix} 1 \\ -i \end{pmatrix} \left(\frac{1}{z}\right)^{n+1} (1 - z\bar{z}),$ $p = 2(n-1) \left(\frac{1}{z}\right)^n.$
$\begin{pmatrix} \cos(\theta) \\ \sin(\theta) \end{pmatrix} e^{-in\theta}, n \in \mathbb{N}$	$\mathbf{v} = \begin{pmatrix} 1 \\ i \end{pmatrix} \left(\frac{1}{z}\right)^{n+1} + \frac{1}{2} \begin{pmatrix} 1 \\ -i \end{pmatrix} \left(\frac{1}{z}\right)^{n-1}$ $- \frac{1}{2} \begin{pmatrix} 1 \\ i \end{pmatrix} \left(\frac{1}{z}\right)^n \bar{z} - \frac{n}{2} \begin{pmatrix} 1 \\ i \end{pmatrix} \left(\frac{1}{z}\right)^{n+1} (1 - z\bar{z}),$ $p = 2(n-1) \left(\frac{1}{z}\right)^n.$

In view of the linearity of the problem, each solution  $(\mathbf{v}, p)$  of the homogeneous SBVP on the exterior of the unit disk is a linear superposition of these elementary solutions.

### 3 The exterior of the unit ball

In this section, we consider a homogeneous SBVP with as domain the exterior of the unit ball  $B^c = \{(x, y, z) \mid x^2 + y^2 + z^2 > 1\}$ ,

$$\Delta \mathbf{v} - \nabla p = \mathbf{0}, \quad \mathbf{x} \in B^c, \quad (3.10a)$$

$$\nabla \cdot \mathbf{v} = 0, \quad \mathbf{x} \in B^c, \quad (3.10b)$$

$$\mathbf{v}(\mathbf{x}) = \mathbf{a}(\mathbf{x}), \quad \mathbf{x} \in \partial B^c, \quad (3.10c)$$

$$\mathbf{v} \rightarrow \mathbf{0} \text{ and } p \rightarrow 0, \text{ as } |\mathbf{x}| \rightarrow \infty. \quad (3.10d)$$

Similar as the ball case in Chapter III, we introduce the harmonic functions  $\mathbf{h}_j$  as follows.

**Definition 3.1.** Let  $\mathbf{h}_j[\varphi] : B^c \rightarrow \mathbb{R}$ ,  $j = 0, 1, 2$ , denote the harmonic vector fields defined by

$$\mathbf{h}_0[\varphi] : \mathbf{x} \mapsto \mathbf{x} \times \nabla \varphi(\mathbf{x}),$$

$$\mathbf{h}_1[\chi] : \mathbf{x} \mapsto \nabla \chi - (\mathcal{E}\chi)\mathbf{x} + \frac{1}{2}(|\mathbf{x}|^2 - 1)\nabla \left[ (\mathcal{E} + \frac{1}{2})^{-1} \mathcal{E} \right] \chi,$$

$$\mathbf{h}_2[\vartheta] : \mathbf{x} \mapsto \nabla \mathcal{E}^{-1} \vartheta.$$

Remember that  $\varphi$ ,  $\chi$ , and  $\vartheta$  are supposed to be harmonic and tends to 0 as  $|\mathbf{x}| \rightarrow \infty$ . Also, recall that the boundary condition can be written as  $\mathbf{a}_{\mathcal{H}} = \mathbf{h}_0[\varphi] + \mathbf{h}_1[\chi] + \mathbf{h}_2[\vartheta]$ .

Next, we study the operator equation on the boundary

$$\boldsymbol{\alpha} + \nabla \mathcal{N} (\nabla \cdot \boldsymbol{\alpha}_{\mathcal{H}}) = \mathbf{a} - \nabla \mathcal{N}(0; \mathbf{a} \cdot \mathbf{n}) \quad (3.11)$$

in the following lemma.

### 3.1 The operator equation

**Lemma 3.2.** The solution of the operator equation (3.11) on the boundary ( $|\mathbf{x}| = 1$ )

1. for  $\mathbf{a} = \mathbf{h}_0[\varphi] = \mathbf{x} \times \nabla \varphi$  is  $\boldsymbol{\alpha}_{\mathcal{H}} = \mathbf{x} \times \nabla \varphi$ ,
2. for  $\mathbf{a} = \nabla \chi - (\mathcal{E} \chi) \mathbf{x} = \mathbf{h}_1[\chi]_{|\mathbf{x}|=1}$  is  $\boldsymbol{\alpha}_{\mathcal{H}} = \mathbf{h}_1 \left[ 2(\mathcal{E} + \frac{1}{2}) \mathcal{E}^{-1} \chi \right]$ ,
3. for  $\mathbf{a} = \vartheta \mathbf{x}$  is  $\boldsymbol{\alpha}_{\mathcal{H}} = \mathbf{h}_1 \left[ -2(\mathcal{E} + \frac{1}{2}) \mathcal{E}^{-2} \vartheta \right]$ .

**Proof.**

1. Follows from  $\nabla \cdot \mathbf{h}_0[\varphi] = 0$ .
2. On  $\partial B^c$ , we have  $\mathbf{x} \cdot \mathbf{h}_1[\chi] = 0$ . We calculate  $\mathcal{N} \left( 0; \frac{1}{2} \frac{\partial}{\partial n} (\mathbf{x} \cdot \boldsymbol{\alpha}_{\mathcal{H}}) \right)$  for  $\boldsymbol{\alpha} = \mathbf{h}_1[\chi]$ . For  $\mathbf{x} \in \partial B^c$ , we obtain

$$\begin{aligned} \frac{1}{2} \frac{\partial}{\partial n} (\mathbf{x} \cdot \boldsymbol{\alpha}_{\mathcal{H}}) &= \frac{1}{2} \{ \mathcal{E} (\mathbf{x} \cdot \mathbf{h}_1[\chi]) \} = \frac{1}{2} \mathcal{E} \left\{ (|\mathbf{x}|^2 - 1) (-\mathcal{E} \chi + \frac{1}{2} \mathcal{E}^2 (\mathcal{E} + \frac{1}{2})^{-1} \chi) \right\} \\ &= \mathcal{E} \left( -\chi + \frac{1}{2} \mathcal{E} (\mathcal{E} + \frac{1}{2})^{-1} \chi \right). \end{aligned} \quad (3.12)$$

Therefore,  $\mathcal{N} \left( 0; \frac{1}{2} \frac{\partial}{\partial n} (\mathbf{x} \cdot \boldsymbol{\alpha}_{\mathcal{H}}) \right) = -\chi + \frac{1}{2} \mathcal{E} (\mathcal{E} + \frac{1}{2})^{-1} \chi$ . Hence, we obtain

$$\begin{aligned} \mathcal{N}(\nabla \cdot \boldsymbol{\alpha}_{\mathcal{H}}) &= -\frac{1}{2} \mathbf{x} \cdot \boldsymbol{\alpha}_{\mathcal{H}} + \mathcal{N} \left( 0; \frac{1}{2} \frac{\partial}{\partial n} (\mathbf{x} \cdot \boldsymbol{\alpha}_{\mathcal{H}}) \right) \\ &= \frac{1}{2} (1 - |\mathbf{x}|^2) \mathcal{E} \left( -\chi + \frac{1}{2} \mathcal{E} (\mathcal{E} + \frac{1}{2})^{-1} \chi \right) - \chi + \frac{1}{2} \mathcal{E} (\mathcal{E} + \frac{1}{2})^{-1} \chi, \end{aligned} \quad (3.13)$$

and on the boundary ( $|\mathbf{x}| = 1$ )

$$\begin{aligned} \boldsymbol{\alpha} + \nabla \mathcal{N}(\nabla \cdot \boldsymbol{\alpha}_{\mathcal{H}}) &= \mathbf{h}_1[\chi]_{|\mathbf{x}|=1} - \mathcal{E} \left( -\chi + \frac{1}{2} \mathcal{E} (\mathcal{E} + \frac{1}{2})^{-1} \chi \right) \mathbf{x} \\ &\quad + \nabla \left( -\chi + \frac{1}{2} \mathcal{E} (\mathcal{E} + \frac{1}{2})^{-1} \chi \right) \\ &= \mathbf{h}_1[\chi]_{|\mathbf{x}|=1} + \mathbf{h}_1 \left[ -\chi + \frac{1}{2} \mathcal{E} (\mathcal{E} + \frac{1}{2})^{-1} \chi \right]_{|\mathbf{x}|=1} \\ &= \mathbf{h}_1 \left[ \frac{1}{2} \mathcal{E} (\mathcal{E} + \frac{1}{2})^{-1} \chi \right]_{|\mathbf{x}|=1}. \end{aligned} \quad (3.14)$$

Therefore, the solution of the operator equation (3.11) is  $\boldsymbol{\alpha}_{\mathcal{H}} = \mathbf{h}_1 \left[ 2(\mathcal{E} + \frac{1}{2}) \mathcal{E}^{-1} \chi \right]$ .

3. For  $\mathbf{a} = \vartheta \mathbf{x}$  we obtain

$$\mathcal{N}(0; \mathbf{a} \cdot \mathbf{n}) = \mathcal{E}^{-1} \vartheta, \quad \mathbf{a} - \nabla \mathcal{N}(0; \mathbf{a} \cdot \mathbf{n}) = \vartheta \mathbf{x} - \nabla \mathcal{E}^{-1} \vartheta = \mathbf{h}_1 \left[ -\mathcal{E}^{-1} \vartheta \right]_{|\mathbf{x}|=1}. \quad (3.15)$$

Therefore, according to previous result,  $\boldsymbol{\alpha}_{\mathcal{H}} = \mathbf{h}_1 \left[ -2(\mathcal{E} + \frac{1}{2}) \mathcal{E}^{-2} \vartheta \right]$ .  $\square$

Similar as the ball case, we make some special choices for the boundary condition  $\mathbf{a}$  that involves the harmonic homogeneous function  $\left(\frac{Q_m(\mathbf{x})}{|\mathbf{x}|^{2m+1}}\right)$  of degree  $-(m+1)$  on which the Euler operator  $\mathcal{E}$  acts as a simple multiplication. Note that  $\frac{Q_m(\mathbf{x})}{|\mathbf{x}|^{2m+1}}$  is the Kelvin Transform<sup>1</sup> of  $Q_m(\mathbf{x})$ .

Below, we present some properties of the Euler operator acting on harmonic homogeneous function  $\left(\frac{Q_m(\mathbf{x})}{|\mathbf{x}|^{2m+1}}\right)$  of degree  $-(m+1)$ .

**Lemma 3.3.**

1.  $\mathcal{E} \left( \frac{Q_m(\mathbf{x})}{|\mathbf{x}|^{2m+1}} \right) = -(m+1) \left( \frac{Q_m(\mathbf{x})}{|\mathbf{x}|^{2m+1}} \right)$ .
2.  $\Delta \left( \frac{Q_m(\mathbf{x})}{|\mathbf{x}|^{2m+1}} \right) = 0$ .
3.  $\mathcal{E} \nabla \left( \frac{Q_m(\mathbf{x})}{|\mathbf{x}|^{2m+1}} \right) = -(m+2) \nabla \left( \frac{Q_m(\mathbf{x})}{|\mathbf{x}|^{2m+1}} \right)$ .

**Proof.** Followed by straightforward calculation. □

Using Lemma 3.2 and Lemma 3.3, we obtain the solution of the operator equation (3.11) for various boundary conditions  $\mathbf{a}$  as follows :

boundary condition ( $\mathbf{a}$ )	$\alpha_{\mathcal{H}}$
$\mathbf{x} \times \nabla \left( \frac{Q_m(\mathbf{x})}{ \mathbf{x} ^{2m+1}} \right) = \mathbf{h}_0 \left[ \frac{Q_m(\mathbf{x})}{ \mathbf{x} ^{2m+1}} \right]_{ \mathbf{x} =1}$ $\nabla \left( \frac{Q_m(\mathbf{x})}{ \mathbf{x} ^{2m+1}} \right) + (m+1)\mathbf{x} \left( \frac{Q_m(\mathbf{x})}{ \mathbf{x} ^{2m+1}} \right) = \mathbf{h}_1 \left[ \frac{Q_m(\mathbf{x})}{ \mathbf{x} ^{2m+1}} \right]_{ \mathbf{x} =1}$ $\mathbf{x} \left( \frac{Q_m(\mathbf{x})}{ \mathbf{x} ^{2m+1}} \right)$	$\mathbf{x} \times \nabla \left( \frac{Q_m(\mathbf{x})}{ \mathbf{x} ^{2m+1}} \right)$ $\mathbf{h}_1 \left[ 2\left(\mathcal{E} + \frac{1}{2}\right)\mathcal{E}^{-1} \left( \frac{Q_m(\mathbf{x})}{ \mathbf{x} ^{2m+1}} \right) \right]$ $\mathbf{h}_1 \left[ -2\left(\mathcal{E} + \frac{1}{2}\right)\mathcal{E}^{-2} \left( \frac{Q_m(\mathbf{x})}{ \mathbf{x} ^{2m+1}} \right) \right]$

### 3.2 Solution

Using the above  $\alpha_{\mathcal{H}}$  and the solution

$$\mathbf{v} = \alpha_{\mathcal{H}} + \nabla \mathcal{N}(\nabla \cdot \alpha_{\mathcal{H}}) + \nabla \mathcal{N}(0; \mathbf{a} \cdot \mathbf{n}), \quad (3.16)$$

$$p = -\nabla \cdot \alpha_{\mathcal{H}}. \quad (3.17)$$

we obtain the solution of SBVP (3.10) as follows :

<sup>1</sup>The Kelvin Transform of  $f(\mathbf{x})$  is  $\frac{1}{|\mathbf{x}|} f\left(\frac{\mathbf{x}}{|\mathbf{x}|^2}\right)$ ,  $\mathbf{x} \in \mathbb{R}^3 / \{0\}$ .

boundary condition ( $\mathbf{a}$ )	solutions
$\mathbf{x} \times \nabla \left( \frac{Q_m(\mathbf{x})}{ \mathbf{x} ^{2m+1}} \right)$	$\mathbf{v} = \mathbf{x} \times \nabla \left( \frac{Q_m(\mathbf{x})}{ \mathbf{x} ^{2m+1}} \right),$ $p = 0.$
$\nabla \left( \frac{Q_m(\mathbf{x})}{ \mathbf{x} ^{2m+1}} \right) + (m+1)\mathbf{x} \left( \frac{Q_m(\mathbf{x})}{ \mathbf{x} ^{2m+1}} \right)$	$\mathbf{v} = \nabla \left( \frac{Q_m(\mathbf{x})}{ \mathbf{x} ^{2m+1}} \right) + (m+1)\mathbf{x} \left( \frac{Q_m(\mathbf{x})}{ \mathbf{x} ^{2m+1}} \right)$ $+ \left( \frac{2-m}{2} \right) ( \mathbf{x} ^2 - 1) \nabla \left( \frac{Q_m(\mathbf{x})}{ \mathbf{x} ^{2m+1}} \right),$ $p = (2m-1)m \left( \frac{Q_m(\mathbf{x})}{ \mathbf{x} ^{2m+1}} \right).$
$\mathbf{x} \left( \frac{Q_m(\mathbf{x})}{ \mathbf{x} ^{2m+1}} \right)$	$\mathbf{v} = \mathbf{x} \left( \frac{Q_m(\mathbf{x})}{ \mathbf{x} ^{2m+1}} \right) + \left( \frac{2-m}{2(m+1)} \right) ( \mathbf{x} ^2 - 1) \nabla \left( \frac{Q_m(\mathbf{x})}{ \mathbf{x} ^{2m+1}} \right),$ $p = \frac{(2m-1)m}{m+1} \left( \frac{Q_m(\mathbf{x})}{ \mathbf{x} ^{2m+1}} \right).$

In view of the linearity of the problem, each solution  $(\mathbf{v}, p)$  of the homogeneous SBVP on the exterior of the unit ball is a linear superposition of these elementary solutions.

## 4 An inhomogeneous SBVP in the unit disk

In this section, we consider an inhomogeneous SBVP with as domain the unit disk  $D = \{(x, y) \mid x^2 + y^2 < 1\}$  with a singularity point  $\mathbf{s} = (\xi, \eta)$  inside the disk,

$$\Delta \mathbf{v} - \nabla p = -\mathbf{f}, \quad \mathbf{f} = \begin{pmatrix} 0 \\ \delta(\mathbf{x}) \end{pmatrix}, \quad \mathbf{x} \in D, \quad (4.18a)$$

$$\nabla \cdot \mathbf{v} = \delta(\mathbf{x} - \mathbf{s}), \quad \mathbf{x} \in D, \quad (4.18b)$$

$$\mathbf{v}(\mathbf{x}) = \mathbf{a}(\mathbf{x}), \quad \mathbf{x} \in \partial D. \quad (4.18c)$$

Since the problem (4.18) is inhomogeneous, it is instructive to solve the problem by splitting into 3 subproblems, one is an homogeneous problem and the others still inhomogeneous, as follows

### 4.1 Subproblems

The first subproblem is a homogeneous SBVP

$$\Delta \mathbf{v}_1 - \nabla p_1 = \mathbf{0}, \quad \mathbf{x} \in D, \quad (4.19a)$$

$$\nabla \cdot \mathbf{v}_1 = 0, \quad \mathbf{x} \in D, \quad (4.19b)$$

$$\mathbf{v}_1(\mathbf{x}) = \mathbf{a}_1(\mathbf{x}), \quad \mathbf{x} \in \partial D, \quad (4.19c)$$

with  $\int_D \nabla \cdot \mathbf{v}_1 \, d\sigma = \int_{\partial D} \mathbf{a}_1 \cdot \mathbf{n} \, d\tau = \int_{\partial D} \mathbf{v}_1 \cdot \mathbf{n} \, d\tau = 0$ . We assume the boundary condition  $\mathbf{a}_1(\mathbf{x})$  can be expanded into a Fourier series

$$\mathbf{a}_1(\mathbf{x}) = \sum_{n=-\infty}^{\infty} \left\{ a_n \begin{pmatrix} -\sin(\theta) \\ \cos(\theta) \end{pmatrix} e^{in\theta} + b_n \begin{pmatrix} \cos(\theta) \\ \sin(\theta) \end{pmatrix} e^{in\theta} \right\}, \quad (4.20)$$

with  $b_0 = 0$ . Note that this subproblem is similar as the disk case in Chapter III. Therefore we have the same solution as that in the disk case.

The second subproblem is an inhomogeneous and divergence free SBVP.

$$\Delta \mathbf{v}_2 - \nabla p_2 = -\mathbf{f}, \quad \mathbf{x} \in D, \quad (4.21a)$$

$$\nabla \cdot \mathbf{v}_2 = 0, \quad \mathbf{x} \in D, \quad (4.21b)$$

$$\mathbf{v}_2(\mathbf{x}) = \mathbf{0}, \quad \mathbf{x} \in \partial D. \quad (4.21c)$$

Finally, the third subproblem is

$$\Delta \mathbf{v}_3 - \nabla p_3 = \mathbf{0}, \quad \mathbf{x} \in D, \quad (4.22a)$$

$$\nabla \cdot \mathbf{v}_3 = \delta(\mathbf{x} - \mathbf{s}), \quad \mathbf{x} \in D, \quad (4.22b)$$

$$\mathbf{v}_3(\mathbf{x}) = \mathbf{a}_3(\mathbf{x}), \quad \mathbf{x} \in \partial D, \quad (4.22c)$$

with  $\int_{\partial D} \mathbf{a}_3 \cdot \mathbf{n} \, d\tau = \int_{\partial D} \mathbf{v}_3 \cdot \mathbf{n} \, d\tau = \int_D \nabla \cdot \mathbf{v}_3 \, d\sigma = \int_D \delta(\mathbf{x} - \mathbf{s}) \, d\sigma = 1$ . Therefore, we choose  $\mathbf{a}_3(\mathbf{x}) = \frac{1}{2\pi} \mathbf{x}$ . Finally, the solutions of (4.18a-4.18c) are  $\mathbf{v} = \mathbf{v}_1 + \mathbf{v}_2 + \mathbf{v}_3$  and  $p = p_1 + p_2 + p_3$ .

Since we have already discussed and got the solutions of the first subproblem, now we consider the second subproblem (4.21) and the third subproblem (4.22).

#### 4.1.1 Subproblem 2

We will study the operator equation on the boundary ( $|\mathbf{x}| = 1$ ). Since  $\mathbf{a} = \mathbf{0}$  and  $h = 0$ , the operator equation on the boundary is

$$\boldsymbol{\alpha} + \nabla \mathcal{N}(\nabla \cdot \boldsymbol{\alpha}_{\mathcal{H}}) = -\nabla \mathcal{N}(\nabla \cdot \mathcal{D} \mathbf{f}). \quad (4.23)$$

The solution of (4.23) is discussed in the following theorem.

**Theorem 4.1.** The solution of the operator equation (4.23) is

$$\boldsymbol{\alpha}_{\mathcal{H}} = \frac{1}{8\pi} \left\{ \begin{pmatrix} i \\ 1 \end{pmatrix} z^2 + \begin{pmatrix} -i \\ 1 \end{pmatrix} \bar{z}^2 + \begin{pmatrix} 0 \\ 2 \end{pmatrix} \right\}. \quad (4.24)$$

**Proof.** Consider the right-hand side of the operator equation (4.23). First, we determine  $\mathcal{D} \mathbf{f}$  by solving the Dirichlet problem

$$\Delta \mathcal{D} \mathbf{f} = -\mathbf{f} = - \begin{pmatrix} 0 \\ \delta(\mathbf{x}) \end{pmatrix}, \quad \mathbf{x} \in D, \quad (4.25a)$$

$$\mathcal{D} \mathbf{f} = \mathbf{0}, \quad \mathbf{x} \in \partial D. \quad (4.25b)$$

Since  $\Delta \left( \frac{1}{2\pi} \ln |\mathbf{x}| \right) = \delta(\mathbf{x})$ , the solution of (4.25) is  $\mathcal{D} \mathbf{f} = \begin{pmatrix} 0 \\ -\frac{1}{2\pi} \ln |\mathbf{x}| \end{pmatrix}$ .

Next we determine  $\mathcal{N}(\nabla \cdot \mathcal{D} \mathbf{f})$  by solving the Neumann problem

$$\Delta \mathcal{N}(\nabla \cdot \mathcal{D} \mathbf{f}) = -\nabla \cdot \mathcal{D} \mathbf{f} = \frac{1}{2\pi} \frac{y}{|\mathbf{x}|^2}, \quad \mathbf{x} \in D, \quad (4.26a)$$

$$\frac{\partial}{\partial n} \mathcal{N}(\nabla \cdot \mathcal{D} \mathbf{f}) = 0, \quad \mathbf{x} \in \partial D. \quad (4.26b)$$

We split the Neumann problem (4.26) into 2 parts. One which solve the Poisson equation (4.26a) without considering the boundary condition (4.26b) and the other solve the Laplace equation with an inhomogeneous boundary condition in order to satisfy the boundary condition (4.26b). This splitting can be written as  $\mathcal{N}(\nabla \cdot \mathcal{D}f) = \mathcal{N}_0(\mathbf{x}) + \mathcal{N}_1(\mathbf{x})$ , where  $\mathcal{N}_0(\mathbf{x})$  is the solution of

$$\Delta \mathcal{N}_0(\mathbf{x}) = -\nabla \cdot \mathcal{D}f = \frac{1}{2\pi} \frac{y}{|\mathbf{x}|^2}, \quad (4.27)$$

and  $\mathcal{N}_1(\mathbf{x})$  is the solution of

$$\Delta \mathcal{N}_1(\mathbf{x}) = 0, \quad \mathbf{x} \in D, \quad (4.28a)$$

$$\frac{\partial \mathcal{N}_1}{\partial n} = -\frac{\partial \mathcal{N}_0}{\partial n}, \quad \mathbf{x} \in \partial D. \quad (4.28b)$$

First consider (4.27). Note that the solution of

$$\frac{\partial^2 \psi}{\partial r^2} + \frac{1}{r} \frac{\partial \psi}{\partial r} = \frac{1}{2\pi} \ln(r), \quad (4.29)$$

is

$$\psi(r) = \frac{1}{8\pi} r^2 \ln(r) - \frac{1}{8\pi} r^2, \quad (4.30)$$

or

$$\psi(|\mathbf{x}|) = \frac{1}{8\pi} |\mathbf{x}|^2 \ln |\mathbf{x}| - \frac{1}{8\pi} |\mathbf{x}|^2. \quad (4.31)$$

Therefore we obtain

$$\mathcal{N}_0(\mathbf{x}) = \frac{\partial \psi(\mathbf{x})}{\partial y} = \frac{1}{4\pi} y \ln |\mathbf{x}| - \frac{1}{8\pi} y. \quad (4.32)$$

Next, consider (4.28). Using (4.32), the boundary condition (4.28b) turns into

$$\frac{\partial \mathcal{N}_1}{\partial n} = -\frac{\partial \mathcal{N}_0}{\partial n} = -\mathcal{E} \mathcal{N}_0 = -\frac{1}{8\pi} y. \quad (4.33)$$

Therefore the solution of (4.28) is  $\mathcal{N}_1(\mathbf{x}) = -\frac{1}{8\pi} y$ . Finally the solution of the Neumann problem (4.26) is

$$\mathcal{N}(\nabla \cdot \mathcal{D}f) = \mathcal{N}_0(\mathbf{x}) + \mathcal{N}_1(\mathbf{x}) = \frac{1}{4\pi} y \ln |\mathbf{x}| - \frac{1}{4\pi} y. \quad (4.34)$$

Taking the gradient of (4.34) yields

$$\nabla \mathcal{N}(\nabla \cdot \mathcal{D}f) = \frac{1}{4\pi} \ln |\mathbf{x}| \begin{pmatrix} 0 \\ 1 \end{pmatrix} + \frac{1}{4\pi} \frac{x}{|\mathbf{x}|^2} \begin{pmatrix} y \\ -x \end{pmatrix}, \quad (4.35)$$

and on the boundary ( $|\mathbf{x}| = 1$ ) we have

$$\nabla \mathcal{N}(\nabla \cdot \mathcal{D}f) = \frac{1}{4\pi} x \begin{pmatrix} y \\ -x \end{pmatrix} = -\frac{1}{8\pi} \begin{pmatrix} -\sin(\theta) \\ \cos(\theta) \end{pmatrix} e^{i\theta} - \frac{1}{8\pi} \begin{pmatrix} -\sin(\theta) \\ \cos(\theta) \end{pmatrix} e^{-i\theta}. \quad (4.36)$$

Recall that the solution of the operator equation (4.23) has already been discussed in the disk case. The left-hand side of the operator equation (4.23) is a mapping

$$\alpha \longmapsto \alpha + \nabla \mathcal{N}(\nabla \cdot \alpha_{\mathcal{N}}) = \frac{1}{2} \alpha. \quad (4.37)$$



Therefore, using the notations  $z = x + iy$  and  $\bar{z} = x - iy$ , the solution of the operator equation (4.23) is

$$\alpha_{\mathcal{H}} = \frac{1}{8\pi} \left\{ \begin{pmatrix} i \\ 1 \end{pmatrix} z^2 + \begin{pmatrix} -i \\ 1 \end{pmatrix} \bar{z}^2 + \begin{pmatrix} 0 \\ 2 \end{pmatrix} \right\}. \quad (4.38)$$

□

Using the above result, we obtain the solutions of the second subproblem (4.21a-4.21c) as

$$\begin{aligned} v_2 &= \alpha_{\mathcal{H}} + \nabla \mathcal{N}(\nabla \cdot \alpha_{\mathcal{H}}) + \mathcal{D}f + \nabla \mathcal{N}(\nabla \cdot \mathcal{D}f) \\ &= \frac{1}{8\pi} (1 - z\bar{z}) \begin{pmatrix} 0 \\ -1 \end{pmatrix} + \frac{1}{16\pi} \begin{pmatrix} i \\ 1 \end{pmatrix} z^2 + \frac{1}{16\pi} \begin{pmatrix} -i \\ 1 \end{pmatrix} \bar{z}^2 + \frac{1}{8\pi} \begin{pmatrix} 0 \\ 1 \end{pmatrix} z\bar{z} \\ &\quad - \frac{1}{2\pi} \ln |\mathbf{x}| \begin{pmatrix} 0 \\ 1 \end{pmatrix} + \frac{1}{4\pi} \frac{x}{|\mathbf{x}|^2} \begin{pmatrix} y \\ -x \end{pmatrix} + \frac{1}{4\pi} \ln |\mathbf{x}| \begin{pmatrix} 0 \\ 1 \end{pmatrix}, \end{aligned} \quad (4.39)$$

$$p_2 = -\nabla \cdot \alpha_{\mathcal{H}} - \nabla \cdot \mathcal{D}f = -\frac{i}{2\pi} z + \frac{i}{2\pi} \bar{z} + \frac{1}{2\pi} \frac{y}{|\mathbf{x}|^2}. \quad (4.40)$$

Now we consider the third subproblem.

### 4.1.2 Subproblem 3

We would like to solve

$$\Delta \mathbf{v}_3(\mathbf{x}) - \nabla p_3(\mathbf{x}) = \mathbf{0}, \quad \mathbf{x} \in D, \quad (4.41a)$$

$$\nabla \cdot \mathbf{v}_3(\mathbf{x}) = \delta(\mathbf{x} - s), \quad \mathbf{x} \in D, \quad (4.41b)$$

$$\mathbf{v}_3(\mathbf{x}) = \frac{1}{2\pi} \mathbf{x}, \quad \mathbf{x} \in \partial D. \quad (4.41c)$$

We split the problem (4.41) into 2 parts. One which solve only (4.41a)-(4.41b) without considering the boundary condition (4.41c), and the other solve the homogeneous SBVP with an inhomogenous boundary condition in order to satisfy the boundary condition (4.41c). This splitting can be written as  $\mathbf{v}_3 = \mathbf{v}_{30} + \mathbf{v}_{31}$  and  $p_3 = p_{30} + p_{31}$ , where  $\mathbf{v}_{30}$ ,  $p_{30}$ ,  $\mathbf{v}_{31}$ , and  $p_{31}$  are, respectively, the solutions of

$$\Delta \mathbf{v}_{30} - \nabla p_{30} = \mathbf{0}, \quad \mathbf{x} \in D, \quad (4.42a)$$

$$\nabla \cdot \mathbf{v}_{30} = \delta(\mathbf{x} - s), \quad \mathbf{x} \in D, \quad (4.42b)$$

and

$$\Delta \mathbf{v}_{31} - \nabla p_{31} = \mathbf{0}, \quad \mathbf{x} \in D, \quad (4.43a)$$

$$\nabla \cdot \mathbf{v}_{31} = 0, \quad \mathbf{x} \in D, \quad (4.43b)$$

$$\mathbf{v}_{31}(\mathbf{x}) = \frac{1}{2\pi} \mathbf{x} - \frac{1}{2\pi} \frac{\mathbf{x}-s}{|\mathbf{x}-s|^2}, \quad \mathbf{x} \in \partial D, \quad (4.43c)$$

with  $\int_{\partial D} \mathbf{v}_{31} \cdot \mathbf{n} \, d\sigma = 0$ .

First, consider (4.42). Since  $\Delta \frac{1}{2\pi} \ln |\mathbf{x} - \mathbf{s}| = \delta(\mathbf{x} - \mathbf{s})$ , we obtain

$$\mathbf{v}_{30} = \nabla \left( \frac{1}{2\pi} \ln |\mathbf{x} - \mathbf{s}| \right) = \frac{1}{2\pi} \frac{\mathbf{x} - \mathbf{s}}{|\mathbf{x} - \mathbf{s}|^2}, \quad (4.44)$$

$$p_{30} = \delta(\mathbf{x} - \mathbf{s}). \quad (4.45)$$

Next, consider (4.43). Similar as the disk case, we expand the boundary condition (4.43c) into Fourier series as follows

$$\begin{aligned} \frac{1}{2\pi} \frac{\mathbf{x} - \mathbf{s}}{|\mathbf{x} - \mathbf{s}|^2} &= \frac{1}{2\pi} \frac{1 - \mathbf{x} \cdot \mathbf{s}}{|\mathbf{x} - \mathbf{s}|^2} \mathbf{x} + \frac{1}{2\pi} \frac{(\mathbf{x} \cdot \mathbf{s})\mathbf{x} - \mathbf{s}}{|\mathbf{x} - \mathbf{s}|^2} \\ &= \frac{1}{2\pi} \begin{pmatrix} \cos(\theta) \\ \sin(\theta) \end{pmatrix} + \frac{1}{4\pi} \begin{pmatrix} \cos(\theta) \\ \sin(\theta) \end{pmatrix} \left\{ \sum_{n=1}^{\infty} (\xi - i\eta)^n e^{in\theta} + \sum_{n=1}^{\infty} (\xi + i\eta)^n e^{-in\theta} \right\} \\ &\quad + \frac{i}{4\pi} \begin{pmatrix} -\sin(\theta) \\ \cos(\theta) \end{pmatrix} \left\{ \sum_{n=1}^{\infty} -(\xi - i\eta)^n e^{in\theta} + \sum_{n=1}^{\infty} (\xi + i\eta)^n e^{-in\theta} \right\} \\ &= \frac{1}{2\pi} \begin{pmatrix} \cos(\theta) \\ \sin(\theta) \end{pmatrix} + \frac{1}{4\pi} \frac{(\xi - i\eta) e^{i2\theta}}{1 - (\xi - i\eta) e^{i\theta}} \begin{pmatrix} 1 \\ -i \end{pmatrix} + \frac{1}{4\pi} \frac{(\xi + i\eta) e^{-i2\theta}}{1 - (\xi + i\eta) e^{-i\theta}} \begin{pmatrix} 1 \\ i \end{pmatrix}. \end{aligned}$$

Therefore, the boundary condition (4.43c) turns into

$$\begin{aligned} \mathbf{v}_{31}(\mathbf{x}) = \mathbf{b}(\mathbf{x}) &= \frac{1}{2\pi} \mathbf{x} - \frac{1}{2\pi} \frac{\mathbf{x} - \mathbf{s}}{|\mathbf{x} - \mathbf{s}|^2} \\ &= -\frac{1}{4\pi} \frac{(\xi - i\eta) e^{i2\theta}}{1 - (\xi - i\eta) e^{i\theta}} \begin{pmatrix} 1 \\ -i \end{pmatrix} - \frac{1}{4\pi} \frac{(\xi + i\eta) e^{-i2\theta}}{1 - (\xi + i\eta) e^{-i\theta}} \begin{pmatrix} 1 \\ i \end{pmatrix}. \end{aligned} \quad (4.46)$$

According to the general procedure, we study the operator equation on the boundary ( $|\mathbf{x}| = 1$ )

$$\boldsymbol{\alpha} + \nabla \mathcal{N}(\nabla \cdot \boldsymbol{\alpha}_{\mathcal{N}}) = \mathbf{b} - \nabla \mathcal{N}(0; \mathbf{b} \cdot \mathbf{n}). \quad (4.47)$$

Consider the right-hand side of (4.47). We determine  $\mathcal{N}(0; \mathbf{b} \cdot \mathbf{n})$  by solving the Neumann problem

$$\Delta \mathcal{N}(0; \mathbf{b} \cdot \mathbf{n}) = 0, \quad \mathbf{x} \in D, \quad (4.48)$$

$$\frac{\partial}{\partial n} \mathcal{N}(0; \mathbf{b} \cdot \mathbf{n}) = \mathbf{b} \cdot \mathbf{n}, \quad \mathbf{x} \in \partial D. \quad (4.49)$$

Using the notations  $z = x + iy$ ,  $\bar{z} = x - iy$ ,  $w = \xi + i\eta$ , and  $\bar{w} = \xi - i\eta$ , the solution of (4.48) is

$$\mathcal{N}(0; \mathbf{b} \cdot \mathbf{n}) = \frac{1}{4\pi} \ln(1 - \bar{w}z) + \frac{1}{4\pi} \ln(1 - w\bar{z}). \quad (4.50)$$

Taking the gradient of (4.50), we obtain the right-hand side of (4.47) as

$$\begin{aligned} \mathbf{b} - \nabla \mathcal{N}(0; \mathbf{b} \cdot \mathbf{n}) &= -\frac{1}{4\pi} \frac{\bar{w} e^{i2\theta}}{1 - \bar{w} e^{i\theta}} \begin{pmatrix} 1 \\ -i \end{pmatrix} + \frac{1}{4\pi} \frac{w}{1 - w e^{-i\theta}} \begin{pmatrix} 1 \\ -i \end{pmatrix} \\ &\quad - \frac{1}{4\pi} \frac{w e^{-i2\theta}}{1 - w e^{-i\theta}} \begin{pmatrix} 1 \\ i \end{pmatrix} + \frac{1}{4\pi} \frac{\bar{w}}{1 - \bar{w} e^{i\theta}} \begin{pmatrix} 1 \\ i \end{pmatrix}. \end{aligned} \quad (4.51)$$

Using a similar way as in the disk case, we obtain the solution of (4.47) as

$$\boldsymbol{\alpha}_{\mathcal{H}} = -\frac{1}{2\pi} \frac{\bar{w}z^2}{1-\bar{w}z} \begin{pmatrix} 1 \\ -i \end{pmatrix} + \frac{1}{2\pi} \frac{w}{1-w\bar{z}} \begin{pmatrix} 1 \\ -i \end{pmatrix} + \frac{1}{2\pi} \frac{\bar{w}}{1-\bar{w}z} \begin{pmatrix} 1 \\ i \end{pmatrix} - \frac{1}{2\pi} \frac{w\bar{z}^2}{1-w\bar{z}} \begin{pmatrix} 1 \\ i \end{pmatrix}. \quad (4.52)$$

This leads to

$$\begin{aligned} \nabla \mathcal{N}(\nabla \cdot \boldsymbol{\alpha}_{\mathcal{H}}) &= \frac{1}{4\pi} \frac{\bar{w}(|z|^2-1)}{(1-\bar{w}z)^2} \begin{pmatrix} 1 \\ i \end{pmatrix} + \frac{1}{4\pi} \frac{\bar{w}(|z|^2-2)}{1-\bar{w}z} \begin{pmatrix} 1 \\ i \end{pmatrix} + \frac{1}{4\pi} \frac{w\bar{z}^2}{1-w\bar{z}} \begin{pmatrix} 1 \\ i \end{pmatrix} \\ &+ \frac{1}{4\pi} \frac{w(|z|^2-1)}{(1-w\bar{z})^2} \begin{pmatrix} 1 \\ -i \end{pmatrix} + \frac{1}{4\pi} \frac{w(|z|^2-2)}{1-w\bar{z}} \begin{pmatrix} 1 \\ -i \end{pmatrix} + \frac{1}{4\pi} \frac{\bar{w}z^2}{1-\bar{w}z} \begin{pmatrix} 1 \\ -i \end{pmatrix}. \end{aligned} \quad (4.53)$$

Finally, the full solutions of (4.43a-4.43c) are

$$\begin{aligned} \boldsymbol{v}_{31} &= \frac{1}{4\pi} \frac{\bar{w}(|z|^2-1)}{(1-\bar{w}z)^2} \begin{pmatrix} 1 \\ i \end{pmatrix} + \frac{1}{4\pi} \frac{\bar{w}(|z|^2-1)}{1-\bar{w}z} \begin{pmatrix} 1 \\ i \end{pmatrix} - \frac{1}{4\pi} \frac{w\bar{z}^2}{1-w\bar{z}} \begin{pmatrix} 1 \\ i \end{pmatrix} \\ &+ \frac{1}{4\pi} \frac{w(|z|^2-1)}{(1-w\bar{z})^2} \begin{pmatrix} 1 \\ -i \end{pmatrix} + \frac{1}{4\pi} \frac{w(|z|^2-1)}{1-w\bar{z}} \begin{pmatrix} 1 \\ -i \end{pmatrix} - \frac{1}{4\pi} \frac{\bar{w}z^2}{1-\bar{w}z} \begin{pmatrix} 1 \\ -i \end{pmatrix}, \end{aligned} \quad (4.54)$$

$$p_{31} = \frac{1}{\pi} \frac{\bar{w}z(2-\bar{w}z)}{(1-\bar{w}z)^2} + \frac{1}{\pi} \frac{w\bar{z}(2-w\bar{z})}{(1-w\bar{z})^2}. \quad (4.55)$$

Therefore the solutions of subproblem 3 (4.41) are

$$\boldsymbol{v}_3 = \boldsymbol{v}_{30} + \boldsymbol{v}_{31} = \frac{1}{2\pi} \frac{\boldsymbol{x} - \boldsymbol{s}}{|\boldsymbol{x} - \boldsymbol{s}|^2} + \boldsymbol{v}_{31}, \quad (4.56)$$

$$p_3 = p_{30} + p_{31} = \delta(\boldsymbol{x} - \boldsymbol{s}) + p_{31}, \quad (4.57)$$

with  $\boldsymbol{v}_{31}$  and  $p_{31}$  as in (4.54) and (4.55).

## 4.2 Solution

In this section, we present the solution of the SBVP (4.18) for various boundary conditions  $\boldsymbol{a}$  as follows :

boundary condition ( $\mathbf{a}$ )	solutions
$\begin{pmatrix} -\sin(\theta) \\ \cos(\theta) \end{pmatrix} e^{in\theta} + \frac{1}{2\pi} \mathbf{x}, n \in \mathbb{N}$	$\mathbf{v} = \frac{1}{2} \begin{pmatrix} i \\ 1 \end{pmatrix} z^{n+1} + \frac{1}{2} \begin{pmatrix} -i \\ 1 \end{pmatrix} z^n \bar{z}$ $- \frac{n}{2} \begin{pmatrix} -i \\ 1 \end{pmatrix} z^{n-1} (1 - z\bar{z}) + \mathbf{v}_2 + \mathbf{v}_3,$ $p = -2i(n+1)z^n + p_2 + p_3.$
$\begin{pmatrix} -\sin(\theta) \\ \cos(\theta) \end{pmatrix} e^{-in\theta} + \frac{1}{2\pi} \mathbf{x}, n \in \mathbb{N}$	$\mathbf{v} = \frac{1}{2} \begin{pmatrix} -i \\ 1 \end{pmatrix} \bar{z}^{n+1} + \frac{1}{2} \begin{pmatrix} i \\ 1 \end{pmatrix} \bar{z}^n z$ $- \frac{n}{2} \begin{pmatrix} i \\ 1 \end{pmatrix} \bar{z}^{n-1} (1 - z\bar{z}) + \mathbf{v}_2 + \mathbf{v}_3,$ $p = 2i(n+1)\bar{z}^n + p_2 + p_3.$
$\begin{pmatrix} -\sin(\theta) \\ \cos(\theta) \end{pmatrix} + \frac{1}{2\pi} \mathbf{x}$	$\mathbf{v} = \frac{1}{2} \begin{pmatrix} i \\ 1 \end{pmatrix} z + \frac{1}{2} \begin{pmatrix} -i \\ 1 \end{pmatrix} \bar{z} + \mathbf{v}_2 + \mathbf{v}_3,$ $p = p_2 + p_3.$
$\begin{pmatrix} \cos(\theta) \\ \sin(\theta) \end{pmatrix} e^{in\theta} + \frac{1}{2\pi} \mathbf{x}, n \in \mathbb{N}$	$\mathbf{v} = \frac{1}{2} \begin{pmatrix} 1 \\ -i \end{pmatrix} z^{n+1} + \frac{1}{2} \begin{pmatrix} 1 \\ i \end{pmatrix} z^{n-1}$ $+ \left( \frac{n+1}{2} \right) \begin{pmatrix} 1 \\ i \end{pmatrix} z^{n-1} (1 - z\bar{z}) + \mathbf{v}_2 + \mathbf{v}_3,$ $p = -2(n+1)z^n + p_2 + p_3.$
$\begin{pmatrix} \cos(\theta) \\ \sin(\theta) \end{pmatrix} e^{-in\theta} + \frac{1}{2\pi} \mathbf{x}, n \in \mathbb{N}$	$\mathbf{v} = \frac{1}{2} \begin{pmatrix} 1 \\ i \end{pmatrix} \bar{z}^{n+1} + \frac{1}{2} \begin{pmatrix} 1 \\ -i \end{pmatrix} \bar{z}^{n-1}$ $+ \left( \frac{n+1}{2} \right) \begin{pmatrix} 1 \\ -i \end{pmatrix} \bar{z}^{n-1} (1 - z\bar{z}) + \mathbf{v}_2 + \mathbf{v}_3,$ $p = -2(n+1)\bar{z}^n + p_2 + p_3.$
$\frac{1}{2\pi} \mathbf{x}$	$\mathbf{v} = \mathbf{v}_2 + \mathbf{v}_3,$ $p = p_2 + p_3.$

In view of the linearity of the problem, each solution  $(\mathbf{v}, p)$  of the inhomogeneous SBVP on the interior of the unit disk is a linear superposition of these elementary solutions.

## 5 A Half-space

In this section, we consider a homogeneous SBVP with as domain the half-space  $H = \{(x, y, z) \in \mathbb{R}^3 \mid z > 0\}$ ,

$$\Delta \mathbf{v} - \nabla p = \mathbf{0}, \quad \mathbf{x} \in H, \quad \mathbf{v} = (u, v, w), \quad (5.58a)$$

$$\nabla \cdot \mathbf{v} = 0, \quad \mathbf{x} \in H, \quad (5.58b)$$

$$\mathbf{v}(x, y, 0) = \mathbf{a}(x, y) = (a_1(x, y), a_2(x, y), a_3(x, y)), \quad (5.58c)$$

$$\mathbf{v} \rightarrow \mathbf{0} \text{ and } p \rightarrow 0, \text{ as } z \rightarrow \infty \text{ and } |x|, |y| \rightarrow \infty. \quad (5.58d)$$

Note that we require  $\int_{-\infty}^{\infty} \int_{-\infty}^{\infty} a_3(x, y) dx dy = 0$  to satisfy the compatibility condition

$$\int_{\Omega} \nabla \cdot \mathbf{v} d\sigma = \int_{\partial\Omega} \mathbf{a} \cdot \mathbf{n} d\tau = 0.$$

N. Tanaka in (see [38]) solved the SBVP (5.58) by applying the two-dimensional Fourier transform<sup>2</sup> directly into (5.58) to obtain a system of ordinary differential equations. Considering the boundary conditions, his results are the same as the solutions (5.73-5.76).

### 5.1 The operator equation

Similar as the previous sections, we study the operator equation on the boundary  $z = 0$

$$\boldsymbol{\alpha} + \nabla \mathcal{N}(\nabla \cdot \boldsymbol{\alpha}_{\mathcal{H}}) = \mathbf{a} - \nabla \mathcal{N}(0; \mathbf{a} \cdot \mathbf{n}). \quad (5.59)$$

Applying the two-dimensional Fourier transform, we can determine the solution of (5.59).

**Theorem 5.1.** The solution of the operator equation (5.59) is

$$\begin{aligned} \boldsymbol{\alpha}_{\mathcal{H}} &= \frac{1}{2\pi} \int_{-\infty}^{\infty} \int_{-\infty}^{\infty} \hat{\alpha}(\xi, \eta) e^{i(x\xi + y\eta)} e^{-|\xi'|z} d\xi d\eta \begin{pmatrix} 1 \\ 0 \\ 0 \end{pmatrix} \\ &+ \frac{1}{2\pi} \int_{-\infty}^{\infty} \int_{-\infty}^{\infty} \hat{\beta}(\xi, \eta) e^{i(x\xi + y\eta)} e^{-|\xi'|z} d\xi d\eta \begin{pmatrix} 0 \\ 1 \\ 0 \end{pmatrix}, \end{aligned} \quad (5.60)$$

with  $|\xi'| = \sqrt{\xi^2 + \eta^2}$ , and

$$\hat{\alpha}(\xi, \eta) = \frac{\hat{a}_1(\eta^2 + 2\xi^2) + \hat{a}_2\xi\eta}{|\xi'|^2} + \frac{2i\hat{a}_3\xi}{|\xi'|}, \quad (5.61)$$

$$\hat{\beta}(\xi, \eta) = \frac{\hat{a}_2(2\eta^2 + \xi^2) + \hat{a}_1\xi\eta}{|\xi'|^2} + \frac{2i\hat{a}_3\eta}{|\xi'|}. \quad (5.62)$$

---

<sup>2</sup>  $\hat{f}(\xi, \eta) = \frac{1}{2\pi} \int_{-\infty}^{\infty} \int_{-\infty}^{\infty} f(x, y) e^{-i(x\xi + y\eta)} dx dy$ ,  $f(x, y) = \frac{1}{2\pi} \int_{-\infty}^{\infty} \int_{-\infty}^{\infty} \hat{f}(\xi, \eta) e^{i(x\xi + y\eta)} d\xi d\eta$ .

Note that  $\boldsymbol{\alpha}_{\mathcal{H}}(x, y, 0) = \alpha(x, y) \begin{pmatrix} 1 \\ 0 \\ 0 \end{pmatrix} + \beta(x, y) \begin{pmatrix} 0 \\ 1 \\ 0 \end{pmatrix}$  is a tangent vector fields on the boundary  $z = 0$ .

**Proof.** At first, we consider the left-hand side of (5.59). We have to determine  $\boldsymbol{\alpha}_{\mathcal{H}}$  the harmonic extension of  $\boldsymbol{\alpha}$ , by solving the following Dirichlet problem

$$\Delta \boldsymbol{\alpha}_{\mathcal{H}} = \mathbf{0}, \quad \boldsymbol{x} \in H, \quad (5.63a)$$

$$\boldsymbol{\alpha}_{\mathcal{H}} = \boldsymbol{\alpha} = \alpha(x, y) \begin{pmatrix} 1 \\ 0 \\ 0 \end{pmatrix} + \beta(x, y) \begin{pmatrix} 0 \\ 1 \\ 0 \end{pmatrix}, \quad \boldsymbol{x} \in \partial H, \quad (5.63b)$$

$$\boldsymbol{\alpha}_{\mathcal{H}} \rightarrow \mathbf{0} \text{ as } z \rightarrow \infty \text{ and } |x|, |y| \rightarrow \infty. \quad (5.63c)$$

Using the two-dimensional Fourier transform with respect to  $(x, y) \rightarrow (\xi, \eta)$ , the solution of (5.63) is

$$\begin{aligned} \boldsymbol{\alpha}_{\mathcal{H}} &= \frac{1}{2\pi} \int_{-\infty}^{\infty} \int_{-\infty}^{\infty} \hat{\alpha}(\xi, \eta) e^{i(x\xi+y\eta)} e^{-|\xi'|z} d\xi d\eta \begin{pmatrix} 1 \\ 0 \\ 0 \end{pmatrix} \\ &+ \frac{1}{2\pi} \int_{-\infty}^{\infty} \int_{-\infty}^{\infty} \hat{\beta}(\xi, \eta) e^{i(x\xi+y\eta)} e^{-|\xi'|z} d\xi d\eta \begin{pmatrix} 0 \\ 1 \\ 0 \end{pmatrix}. \end{aligned} \quad (5.64)$$

Next, we determine  $\mathcal{N}(\nabla \cdot \boldsymbol{\alpha}_{\mathcal{H}}) = -\frac{1}{2} \boldsymbol{x} \cdot \boldsymbol{\alpha}_{\mathcal{H}} + \mathcal{N}\left(0; \frac{1}{2} \frac{\partial}{\partial n} (\boldsymbol{x} \cdot \boldsymbol{\alpha}_{\mathcal{H}})\right)$ . Using (5.64), we obtain

$$\begin{aligned} \frac{1}{2} \boldsymbol{x} \cdot \boldsymbol{\alpha}_{\mathcal{H}} &= \frac{i}{2} \frac{1}{2\pi} \int_{-\infty}^{\infty} \int_{-\infty}^{\infty} \left[ \frac{\partial \hat{\alpha}}{\partial \xi} - \hat{\alpha}(\xi, \eta) \frac{\xi z}{|\xi'|} \right] e^{i(x\xi+y\eta)} e^{-|\xi'|z} d\xi d\eta \\ &+ \frac{i}{2} \frac{1}{2\pi} \int_{-\infty}^{\infty} \int_{-\infty}^{\infty} \left[ \frac{\partial \hat{\beta}}{\partial \eta} - \hat{\beta}(\xi, \eta) \frac{\eta z}{|\xi'|} \right] e^{i(x\xi+y\eta)} e^{-|\xi'|z} d\xi d\eta. \end{aligned} \quad (5.65)$$

Now, we determine  $\mathcal{N}\left(0; \frac{1}{2} \frac{\partial}{\partial n} (\boldsymbol{x} \cdot \boldsymbol{\alpha}_{\mathcal{H}})\right)$  by solving the Neumann problem

$$\Delta \mathcal{N}\left(0; \frac{1}{2} \frac{\partial}{\partial n} (\boldsymbol{x} \cdot \boldsymbol{\alpha}_{\mathcal{H}})\right) = 0, \quad \boldsymbol{x} \in H, \quad (5.66a)$$

$$\frac{\partial}{\partial n} \mathcal{N}\left(0; \frac{1}{2} \frac{\partial}{\partial n} (\boldsymbol{x} \cdot \boldsymbol{\alpha}_{\mathcal{H}})\right) = -\frac{1}{2} \frac{\partial}{\partial z} (\boldsymbol{x} \cdot \boldsymbol{\alpha}_{\mathcal{H}}), \quad \boldsymbol{x} \in \partial H. \quad (5.66b)$$

In a similar way as the Dirichlet problem (5.63), we obtain the solution of (5.66) as

$$\begin{aligned} \mathcal{N}\left(0; \frac{1}{2} \frac{\partial}{\partial n} (\boldsymbol{x} \cdot \boldsymbol{\alpha}_{\mathcal{H}})\right) &= \frac{i}{2} \frac{1}{2\pi} \int_{-\infty}^{\infty} \int_{-\infty}^{\infty} \left[ \frac{\partial \hat{\alpha}}{\partial \xi} + \hat{\alpha}(\xi, \eta) \frac{\xi}{|\xi'|^2} \right] e^{i(x\xi+y\eta)} e^{-|\xi'|z} d\xi d\eta \\ &+ \frac{i}{2} \frac{1}{2\pi} \int_{-\infty}^{\infty} \int_{-\infty}^{\infty} \left[ \frac{\partial \hat{\beta}}{\partial \eta} + \hat{\beta}(\xi, \eta) \frac{\eta}{|\xi'|^2} \right] e^{i(x\xi+y\eta)} e^{-|\xi'|z} d\xi d\eta. \end{aligned} \quad (5.67)$$

Therefore,

$$\begin{aligned}
\mathcal{N}(\nabla \cdot \boldsymbol{\alpha}_{\mathcal{H}}) &= -\frac{1}{2} \mathbf{x} \cdot \boldsymbol{\alpha}_{\mathcal{H}} + \mathcal{N}\left(0; \frac{1}{2} \frac{\partial}{\partial n} (\mathbf{x} \cdot \boldsymbol{\alpha}_{\mathcal{H}})\right) \\
&= \frac{i}{2} \frac{1}{2\pi} \int_{-\infty}^{\infty} \int_{-\infty}^{\infty} \hat{\alpha}(\xi, \eta) \left[ \frac{\xi z}{|\xi'|} + \frac{\xi}{|\xi'|^2} \right] e^{i(x\xi+y\eta)} e^{-|\xi'|z} d\xi d\eta \\
&\quad + \frac{i}{2} \frac{1}{2\pi} \int_{-\infty}^{\infty} \int_{-\infty}^{\infty} \hat{\beta}(\xi, \eta) \left[ \frac{\eta z}{|\xi'|} + \frac{\eta}{|\xi'|^2} \right] e^{i(x\xi+y\eta)} e^{-|\xi'|z} d\xi d\eta. \tag{5.68}
\end{aligned}$$

Finally, taking the gradient of (5.68) and adding  $\boldsymbol{\alpha}$  yields the left-hand side of the operator equation (5.59) at  $z = 0$

$$\begin{pmatrix} \frac{1}{2} \frac{1}{2\pi} \int_{-\infty}^{\infty} \int_{-\infty}^{\infty} \left[ \hat{\alpha}(\xi, \eta) \frac{\xi^2 + 2\eta^2}{|\xi'|^2} - \hat{\beta}(\xi, \eta) \frac{\eta\xi}{|\xi'|^2} \right] e^{i(x\xi+y\eta)} d\xi d\eta \\ \frac{1}{2} \frac{1}{2\pi} \int_{-\infty}^{\infty} \int_{-\infty}^{\infty} \left[ -\hat{\alpha}(\xi, \eta) \frac{\xi\eta}{|\xi'|^2} + \hat{\beta}(\xi, \eta) \frac{2\xi^2 + \eta^2}{|\xi'|^2} \right] e^{i(x\xi+y\eta)} d\xi d\eta \\ 0 \end{pmatrix}. \tag{5.69}$$

Now, we consider the right-hand side of the operator equation (5.59). At first, we determine  $\mathcal{N}(0; \mathbf{a} \cdot \mathbf{n})$  by solving the Neumann problem

$$\Delta \mathcal{N}(0; \mathbf{a} \cdot \mathbf{n}) = 0, \quad \mathbf{x} \in H, \tag{5.70a}$$

$$\frac{\partial}{\partial n} \mathcal{N}(0; \mathbf{a} \cdot \mathbf{n}) = \mathbf{a} \cdot \mathbf{n} = -a_3(x, y), \quad \mathbf{x} \in \partial H. \tag{5.70b}$$

Applying the two-dimensional Fourier transform, the solution of (5.70) is

$$\mathcal{N}(0; \mathbf{a} \cdot \mathbf{n}) = \frac{1}{2\pi} \int_{-\infty}^{\infty} \int_{-\infty}^{\infty} \frac{\hat{a}_3(\xi, \eta)}{|\xi'|} e^{i(x\xi+y\eta)} e^{-|\xi'|z} d\xi d\eta. \tag{5.71}$$

Next, taking the gradient of (5.71) and using  $\mathbf{a}$  yields the right-hand side of the operator equation (5.59) at  $z = 0$

$$\begin{pmatrix} \frac{1}{2\pi} \int_{-\infty}^{\infty} \int_{-\infty}^{\infty} \left[ \hat{a}_1 + i\hat{a}_3 \frac{\xi}{|\xi'|} \right] e^{i(x\xi+y\eta)} d\xi d\eta \\ \frac{1}{2\pi} \int_{-\infty}^{\infty} \int_{-\infty}^{\infty} \left[ \hat{a}_2 + i\hat{a}_3 \frac{\eta}{|\xi'|} \right] e^{i(x\xi+y\eta)} d\xi d\eta \\ 0 \end{pmatrix}. \tag{5.72}$$

Now we are ready to solve the operator equation (5.59). Solving the system of equations (5.69) and (5.72) yields  $\hat{\alpha}(\xi, \eta)$  and  $\hat{\beta}(\xi, \eta)$  as in (5.61) and (5.62).  $\square$

## 5.2 Solution

Substituting  $\hat{\alpha}(\xi, \eta)$  (5.61) and  $\hat{\beta}(\xi, \eta)$  (5.62) into  $\boldsymbol{\alpha}_{\mathcal{H}}$ ,  $\mathcal{N}(\nabla \cdot \boldsymbol{\alpha}_{\mathcal{H}})$ , and  $\mathcal{N}(0; \mathbf{a} \cdot \mathbf{n})$  and using

$$\mathbf{v} = \boldsymbol{\alpha}_{\mathcal{H}} + \nabla \mathcal{N}(\nabla \cdot \boldsymbol{\alpha}_{\mathcal{H}}) + \nabla \mathcal{N}(0; \mathbf{a} \cdot \mathbf{n}), \quad p = -\nabla \cdot \boldsymbol{\alpha}_{\mathcal{H}},$$

we obtain the solutions of (5.58) as

$$u = \frac{1}{2\pi} \int_{-\infty}^{\infty} \int_{-\infty}^{\infty} \left[ \hat{a}_1 - (\hat{a}_1 \xi + \hat{a}_2 \eta) \frac{z \xi}{|\xi'|} - i z \hat{a}_3 \xi \right] e^{i(x\xi + y\eta)} e^{-|\xi'|z} d\xi d\eta, \quad (5.73)$$

$$v = \frac{1}{2\pi} \int_{-\infty}^{\infty} \int_{-\infty}^{\infty} \left[ \hat{a}_2 - (\hat{a}_1 \xi + \hat{a}_2 \eta) \frac{z \eta}{|\xi'|} - i z \hat{a}_3 \eta \right] e^{i(x\xi + y\eta)} e^{-|\xi'|z} d\xi d\eta, \quad (5.74)$$

$$w = \frac{1}{2\pi} \int_{-\infty}^{\infty} \int_{-\infty}^{\infty} [\hat{a}_3 - (i\hat{a}_1 \xi + i\hat{a}_2 \eta - \hat{a}_3 |\xi'|) z] e^{i(x\xi + y\eta)} e^{-|\xi'|z} d\xi d\eta, \quad (5.75)$$

$$p = \frac{1}{\pi} \int_{-\infty}^{\infty} \int_{-\infty}^{\infty} [-i\hat{a}_1 \xi - i\hat{a}_2 \eta + \hat{a}_3 |\xi'|] e^{i(x\xi + y\eta)} e^{-|\xi'|z} d\xi d\eta. \quad (5.76)$$

## 6 An infinite strip

In this section, we consider a homogeneous SBVP with as domain the infinite strip  $I = \{(x, y) | -\infty < x < \infty, -1 < y < 1\}$ ,

$$\Delta \mathbf{v} - \nabla p = \mathbf{0}, \quad \mathbf{x} \in I, \quad \mathbf{v} = (u, v), \quad (6.77a)$$

$$\nabla \cdot \mathbf{v} = 0, \quad \mathbf{x} \in I, \quad (6.77b)$$

$$\mathbf{v}(x, -1) = \mathbf{a}(x) = \begin{pmatrix} a_1(x) \\ a_2(x) \end{pmatrix}, \quad (6.77c)$$

$$\mathbf{v}(x, 1) = \mathbf{b}(x) = \begin{pmatrix} b_1(x) \\ b_2(x) \end{pmatrix}, \quad (6.77d)$$

$$\mathbf{v} \rightarrow \mathbf{0} \text{ and } p \rightarrow 0 \text{ as } |\mathbf{x}| \rightarrow \infty. \quad (6.77e)$$

Note that we require  $\int_{-\infty}^{\infty} (b_2(x) - a_2(x)) dx = 0$  to satisfy the compatibility condition

$$\int_{\Omega} \nabla \cdot \mathbf{v} d\sigma = \int_{\partial\Omega} \mathbf{a} \cdot \mathbf{n} d\tau = 0.$$



## 6.1 The operator equation

As in the previous sections, we study the operator equations on the boundaries  $y = 1$  and  $y = -1$ . Since there are two boundaries, we write the operator equation as

$$\boldsymbol{\alpha} + \nabla \mathcal{N}(\nabla \cdot \boldsymbol{\alpha}_{\mathcal{H}}) = \mathbf{c} - \nabla \mathcal{N}(0; \mathbf{c} \cdot \mathbf{n}), \quad (6.78)$$

with

$$\mathbf{c}(x) = \begin{cases} \mathbf{a}(x), & y = -1, \\ \mathbf{b}(x), & y = 1. \end{cases} \quad (6.79)$$

We investigate the solution of (6.78) in the following theorem.

**Theorem 6.1.** The solution of the operator equations (6.78) is

$$\boldsymbol{\alpha}_{\mathcal{H}}(\mathbf{x}) = \frac{1}{\sqrt{2\pi}} \int_{-\infty}^{\infty} \left( \frac{\sinh((1-y)\xi)}{\sinh(2\xi)} \hat{\boldsymbol{\alpha}}(\xi) + \frac{\sinh((1+y)\xi)}{\sinh(2\xi)} \hat{\boldsymbol{\beta}}(\xi) \right) e^{i\xi x} d\xi \begin{pmatrix} 1 \\ 0 \end{pmatrix}, \quad (6.80)$$

with

$$\begin{aligned} \hat{\boldsymbol{\alpha}}(\xi) = & \left( \frac{2 \sinh^2(2\xi)}{\sinh^2(2\xi) - 4\xi^2} \right) \hat{a}_1(\xi) + i \left( \frac{\sinh(4\xi) + 4\xi}{\sinh^2(2\xi) - 4\xi^2} \right) \hat{a}_2(\xi) + \left( \frac{4\xi \sinh(2\xi)}{\sinh^2(2\xi) - 4\xi^2} \right) \hat{b}_1(\xi) \\ & - 2i \left( \frac{2\xi \cosh(2\xi) + \sinh(2\xi)}{\sinh^2(2\xi) - 4\xi^2} \right) \hat{b}_2(\xi), \end{aligned} \quad (6.81)$$

and

$$\begin{aligned} \hat{\boldsymbol{\beta}}(\xi) = & \left( \frac{2 \sinh^2(2\xi)}{\sinh^2(2\xi) - 4\xi^2} \right) \hat{b}_1(\xi) - i \left( \frac{\sinh(4\xi) + 4\xi}{\sinh^2(2\xi) - 4\xi^2} \right) \hat{b}_2(\xi) + \left( \frac{4\xi \sinh(2\xi)}{\sinh^2(2\xi) - 4\xi^2} \right) \hat{a}_1(\xi) \\ & + 2i \left( \frac{2\xi \cosh(2\xi) + \sinh(2\xi)}{\sinh^2(2\xi) - 4\xi^2} \right) \hat{a}_2(\xi). \end{aligned} \quad (6.82)$$

Note that  $\boldsymbol{\alpha}_{\mathcal{H}}(x, 1) = \beta(x) \begin{pmatrix} 1 \\ 0 \end{pmatrix}$  and  $\boldsymbol{\alpha}_{\mathcal{H}}(x, -1) = \alpha(x) \begin{pmatrix} 1 \\ 0 \end{pmatrix}$  are tangent vector fields at  $y = 1$  and  $y = -1$ , respectively.

**Proof.** At first, we consider the left-hand side of (6.78). We have to determine  $\boldsymbol{\alpha}_{\mathcal{H}}$  the harmonic extension of  $\boldsymbol{\alpha}$ , by solving the Dirichlet problem

$$\Delta \boldsymbol{\alpha}_{\mathcal{H}}(x, y) = \mathbf{0}, \quad \mathbf{x} \in I, \quad (6.83a)$$

$$\boldsymbol{\alpha}_{\mathcal{H}}(x, 1) = \beta(x) \begin{pmatrix} 1 \\ 0 \end{pmatrix}, \quad (6.83b)$$

$$\boldsymbol{\alpha}_{\mathcal{H}}(x, -1) = \alpha(x) \begin{pmatrix} 1 \\ 0 \end{pmatrix}, \quad (6.83c)$$

$$\boldsymbol{\alpha}_{\mathcal{H}} \rightarrow \mathbf{0}, \quad \text{as } |x| \rightarrow \infty. \quad (6.83d)$$

Using the Fourier transform with respect to  $x(x \rightarrow \xi)$ , the solution of (6.83) is

$$\alpha_{\mathcal{H}}(\mathbf{x}) = \frac{1}{\sqrt{2\pi}} \int_{-\infty}^{\infty} \left( \frac{\sinh((1-y)\xi)}{\sinh(2\xi)} \hat{\alpha}(\xi) + \frac{\sinh((1+y)\xi)}{\sinh(2\xi)} \hat{\beta}(\xi) \right) e^{i\xi x} d\xi \begin{pmatrix} 1 \\ 0 \end{pmatrix}. \quad (6.84)$$

Next, we determine  $\mathcal{N}(\nabla \cdot \alpha_{\mathcal{H}}) = -\frac{1}{2} \mathbf{x} \cdot \alpha_{\mathcal{H}} + \mathcal{N}(0; \frac{1}{2} \frac{\partial}{\partial n} (\mathbf{x} \cdot \alpha_{\mathcal{H}}))$ . Using (6.84), we obtain

$$\begin{aligned} \frac{1}{2} \mathbf{x} \cdot \alpha_{\mathcal{H}} &= \frac{i}{2} \frac{1}{\sqrt{2\pi}} \int_{-\infty}^{\infty} \frac{d}{d\xi} \left( \frac{\hat{\alpha}(\xi)}{\sinh(2\xi)} \right) \sinh(\xi(1-y)) e^{i\xi x} d\xi \\ &\quad + \frac{i}{2} \frac{(1-y)}{\sqrt{2\pi}} \int_{-\infty}^{\infty} \hat{\alpha}(\xi) \frac{\cosh(\xi(1-y))}{\sinh(2\xi)} e^{i\xi x} d\xi \\ &\quad + \frac{i}{2} \frac{1}{\sqrt{2\pi}} \int_{-\infty}^{\infty} \frac{d}{d\xi} \left( \frac{\hat{\beta}(\xi)}{\sinh(2\xi)} \right) \sinh(\xi(1+y)) e^{i\xi x} d\xi \\ &\quad + \frac{i}{2} \frac{(1+y)}{\sqrt{2\pi}} \int_{-\infty}^{\infty} \hat{\beta}(\xi) \frac{\cosh(\xi(1+y))}{\sinh(2\xi)} e^{i\xi x} d\xi. \end{aligned} \quad (6.85)$$

Now, we determine  $\mathcal{N}(0; \frac{1}{2} \frac{\partial}{\partial n} (\mathbf{x} \cdot \alpha_{\mathcal{H}}))$  by solving the Neumann problem

$$\Delta \mathcal{N} \left( 0; \frac{1}{2} \frac{\partial}{\partial n} (\mathbf{x} \cdot \alpha_{\mathcal{H}}) \right) (x, y) = 0, \quad \mathbf{x} \in I, \quad (6.86a)$$

$$\frac{\partial}{\partial n} \mathcal{N} \left( 0; \frac{1}{2} \frac{\partial}{\partial n} (\mathbf{x} \cdot \alpha_{\mathcal{H}}) \right) (x, 1) = \frac{1}{2} \frac{\partial}{\partial y} (\mathbf{x} \cdot \alpha_{\mathcal{H}}), \quad (6.86b)$$

$$\frac{\partial}{\partial n} \mathcal{N} \left( 0; \frac{1}{2} \frac{\partial}{\partial n} (\mathbf{x} \cdot \alpha_{\mathcal{H}}) \right) (x, -1) = -\frac{1}{2} \frac{\partial}{\partial y} (\mathbf{x} \cdot \alpha_{\mathcal{H}}). \quad (6.86c)$$

In a similar way as the Dirichlet problem (6.83), the solution of (6.86) is

$$\begin{aligned} \mathcal{N} \left( 0; \frac{1}{2} \frac{\partial}{\partial n} (\mathbf{x} \cdot \alpha_{\mathcal{H}}) \right) &= \\ &\frac{i}{2} \frac{1}{\sqrt{2\pi}} \int_{-\infty}^{\infty} \left\{ \frac{d}{d\xi} \left( \hat{\beta}(\xi) \frac{\xi \cosh(2\xi)}{\sinh(2\xi)} \right) - \frac{d}{d\xi} \left( \hat{\alpha}(\xi) \frac{\xi}{\sinh(2\xi)} \right) \right\} \frac{\cosh((1+y)\xi)}{\xi \sinh(2\xi)} e^{i\xi x} d\xi \\ &\quad + \frac{i}{2} \frac{1}{\sqrt{2\pi}} \int_{-\infty}^{\infty} \left\{ \frac{d}{d\xi} \left( \hat{\alpha}(\xi) \frac{\xi \cosh(2\xi)}{\sinh(2\xi)} \right) - \frac{d}{d\xi} \left( \hat{\beta}(\xi) \frac{\xi}{\sinh(2\xi)} \right) \right\} \frac{\cosh((1-y)\xi)}{\xi \sinh(2\xi)} e^{i\xi x} d\xi. \end{aligned} \quad (6.87)$$

Adding  $(-\frac{1}{2}\mathbf{x} \cdot \boldsymbol{\alpha}_{\mathcal{N}})$  (6.85) and  $\mathcal{N}(0; \frac{1}{2}\frac{\partial}{\partial n}(\mathbf{x} \cdot \boldsymbol{\alpha}_{\mathcal{N}}))$  (6.87), we have  $\mathcal{N}(\nabla \cdot \boldsymbol{\alpha}_{\mathcal{N}})$ . Finally, calculating  $\nabla \mathcal{N}(\nabla \cdot \boldsymbol{\alpha}_{\mathcal{N}})$  and using  $\boldsymbol{\alpha}_{\mathcal{N}}$  (6.84), we obtain the left-hand side of the operator equation (6.78) at  $y = 1$  and  $y = -1$ , respectively,

$$\begin{pmatrix} \frac{1}{2} \frac{1}{\sqrt{2\pi}} \int_{-\infty}^{\infty} \hat{\beta}(\xi) e^{i\xi x} d\xi - \frac{1}{\sqrt{2\pi}} \int_{-\infty}^{\infty} \frac{\xi}{\sinh(2\xi)} \hat{\alpha}(\xi) e^{i\xi x} d\xi \\ 0 \end{pmatrix}, \quad (6.88)$$

and

$$\begin{pmatrix} \frac{1}{2} \frac{1}{\sqrt{2\pi}} \int_{-\infty}^{\infty} \hat{\alpha}(\xi) e^{i\xi x} d\xi - \frac{1}{\sqrt{2\pi}} \int_{-\infty}^{\infty} \frac{\xi}{\sinh(2\xi)} \hat{\alpha}(\xi) e^{i\xi x} d\xi \\ 0 \end{pmatrix}. \quad (6.89)$$

Now, we consider the right-hand side of the operator equation (6.78). At first, we determine  $\mathcal{N}(0; \mathbf{c} \cdot \mathbf{n})$  by solving the Neumann problem

$$\Delta \mathcal{N}(0; \mathbf{c} \cdot \mathbf{n})(x, y) = 0, \quad \mathbf{x} \in I, \quad (6.90a)$$

$$\frac{\partial}{\partial n} \mathcal{N}(0; \mathbf{c} \cdot \mathbf{n})(x, 1) = b_2(x), \quad (6.90b)$$

$$\frac{\partial}{\partial n} \mathcal{N}(0; \mathbf{c} \cdot \mathbf{n})(x, -1) = -a_2(x). \quad (6.90c)$$

Using the Fourier transform, the solution of (6.90) is

$$\mathcal{N}(0; \mathbf{c} \cdot \mathbf{n}) = \frac{1}{\sqrt{2\pi}} \int_{-\infty}^{\infty} \left\{ \frac{\cosh((1+y)\xi)}{\xi \sinh(2\xi)} \hat{b}_2(\xi) - \frac{\cosh((1-y)\xi)}{\xi \sinh(2\xi)} \hat{a}_2(\xi) \right\} e^{i\xi x} d\xi. \quad (6.91)$$

Next, taking the gradient of (6.91) yields the right-hand side of (6.78) at  $y = 1$  and  $y = -1$ , respectively,

$$\begin{pmatrix} \frac{1}{2} \frac{1}{\sqrt{2\pi}} \int_{-\infty}^{\infty} \left\{ \hat{b}_1(\xi) - \frac{i \cosh(2\xi)}{\sinh(2\xi)} \hat{b}_2(\xi) + \frac{i}{\sinh(2\xi)} \hat{a}_2(\xi) \right\} e^{i\xi x} d\xi \\ 0 \end{pmatrix}, \quad (6.92)$$

and

$$\begin{pmatrix} \frac{1}{2} \frac{1}{\sqrt{2\pi}} \int_{-\infty}^{\infty} \left\{ \hat{a}_1(\xi) + \frac{i \cosh(2\xi)}{\sinh(2\xi)} \hat{a}_2(\xi) - \frac{i}{\sinh(2\xi)} \hat{b}_2(\xi) \right\} e^{i\xi x} d\xi \\ 0 \end{pmatrix}. \quad (6.93)$$

Now we are ready to solve the operator equation (6.78). Solving the system of equations (6.78) using (6.88), (6.89), (6.92), and (6.93), yields  $\hat{\alpha}(\xi)$  and  $\hat{\beta}(\xi)$  as in (6.81) and (6.82).  $\square$

## 6.2 Solution

Using the above results and

$$\mathbf{v} = \boldsymbol{\alpha}_{,x} + \nabla \mathcal{N}(\nabla \cdot \boldsymbol{\alpha}_{,x}) + \nabla \mathcal{N}(0; \mathbf{c} \cdot \mathbf{n}), \quad p = -\nabla \cdot \boldsymbol{\alpha}_{,x}, \quad (6.94)$$

the solutions of (6.77) are

$$\begin{aligned} u(x, y) &= \frac{1}{2} \frac{1}{\sqrt{2\pi}} \int_{-\infty}^{\infty} \left\{ \frac{\sinh((1-y)\xi) - (1+y)\xi \cosh((1-y)\xi)}{\sinh(2\xi)} \right\} \hat{\alpha}(\xi) e^{i\xi x} d\xi \\ &+ \frac{1}{2} \frac{1}{\sqrt{2\pi}} \int_{-\infty}^{\infty} \left\{ \frac{\sinh((1+y)\xi) - (1-y)\xi \cosh((1+y)\xi)}{\sinh(2\xi)} \right\} \hat{\beta}(\xi) e^{i\xi x} d\xi \\ &+ \frac{i}{\sqrt{2\pi}} \int_{-\infty}^{\infty} \left\{ \frac{\cosh((1+y)\xi)}{\sinh(2\xi)} \hat{b}_2(\xi) - \frac{\cosh((1-y)\xi)}{\sinh(2\xi)} \hat{a}_2(\xi) \right\} e^{i\xi x} d\xi, \quad (6.95) \end{aligned}$$

$$\begin{aligned} v(x, y) &= -\frac{1}{2} \frac{i}{\sqrt{2\pi}} \int_{-\infty}^{\infty} \left\{ \frac{2\xi \sinh((1-y)\xi) - (1-y)\xi \sinh((1-y)\xi)}{\sinh(2\xi)} \right\} \hat{\alpha}(\xi) e^{i\xi x} d\xi \\ &+ \frac{1}{2} \frac{i}{\sqrt{2\pi}} \int_{-\infty}^{\infty} \left\{ \frac{2\xi \sinh((1+y)\xi) - (1+y)\xi \sinh((1+y)\xi)}{\sinh(2\xi)} \right\} \hat{\beta}(\xi) e^{i\xi x} d\xi \\ &+ \frac{1}{\sqrt{2\pi}} \int_{-\infty}^{\infty} \left\{ \frac{\sinh((1+y)\xi)}{\sinh(2\xi)} \hat{b}_2(\xi) + \frac{\sinh((1-y)\xi)}{\sinh(2\xi)} \hat{a}_2(\xi) \right\} e^{i\xi x} d\xi, \quad (6.96) \end{aligned}$$

$$p(x, y) = -\frac{i}{\sqrt{2\pi}} \int_{-\infty}^{\infty} \left\{ \frac{\sinh((1-y)\xi)}{\sinh(2\xi)} \hat{\alpha}(\xi) + \frac{\sinh((1+y)\xi)}{\sinh(2\xi)} \hat{\beta}(\xi) \right\} \xi e^{i\xi x} d\xi. \quad (6.97)$$

## 7 An infinite wedge

In this section, we consider a homogeneous SBVP with as domain the infinite wedge  $W = \{(r, \theta) \mid 0 < r < \infty, 0 < \theta < \omega\}$ ,

$$\frac{\partial}{\partial r} \left( \frac{1}{r} \frac{\partial}{\partial r} (r v_r) \right) + \frac{1}{r^2} \frac{\partial^2 v_r}{\partial \theta^2} - \frac{2}{r^2} \frac{\partial v_\theta}{\partial \theta} - \frac{\partial p}{\partial r} = \mathbf{0}, \quad \mathbf{x} \in W, \quad (7.98a)$$

$$\frac{\partial}{\partial r} \left( \frac{1}{r} \frac{\partial}{\partial r} (r v_\theta) \right) + \frac{1}{r^2} \frac{\partial^2 v_\theta}{\partial \theta^2} + \frac{2}{r^2} \frac{\partial v_r}{\partial \theta} - \frac{1}{r} \frac{\partial p}{\partial \theta} = \mathbf{0}, \quad \mathbf{x} \in W, \quad (7.98b)$$

$$\frac{1}{r} \frac{\partial}{\partial r} (r v_r) + \frac{1}{r} \frac{\partial v_\theta}{\partial \theta} = 0, \quad \mathbf{x} \in W, \quad (7.98c)$$

$$\mathbf{v}(r, 0) = \mathbf{a}(r) = \begin{pmatrix} a_1(r) \\ a_2(r) \end{pmatrix}, \quad (7.98d)$$

$$\mathbf{v}(r, \omega) = \mathbf{b}(r) = \begin{pmatrix} b_1(r) \\ b_2(r) \end{pmatrix}, \quad (7.98e)$$

$$\mathbf{v} \rightarrow \mathbf{0}, p \rightarrow 0, \text{ as } r \rightarrow \infty. \quad (7.98f)$$

According to the general procedure, we will investigate the operator equations on the boundaries  $\theta = 0$  and  $\theta = \omega$

$$\boldsymbol{\alpha} - \nabla \mathcal{N}(\nabla \cdot \boldsymbol{\alpha}_{\mathcal{H}}) = \mathbf{c} - \nabla \mathcal{N}(0; \mathbf{c} \cdot \mathbf{n}), \quad (7.99)$$

with

$$\mathbf{c}(r) = \begin{cases} \mathbf{a}(r), & \theta = 0, \\ \mathbf{b}(r), & \theta = \omega. \end{cases} \quad (7.100)$$

Consider the left-hand side of (7.99). To find the harmonic extension  $\boldsymbol{\alpha}_{\mathcal{H}}$  and  $\mathcal{N}(\nabla \cdot \boldsymbol{\alpha}_{\mathcal{H}})$  we have to solve the Dirichlet and the Neumann problem respectively. First, we discuss the former problem.

### 7.1 The Dirichlet problem

Let  $\boldsymbol{\alpha}_{\mathcal{H}}(r, \theta) = \begin{pmatrix} \alpha_r(r, \theta) \\ \alpha_\theta(r, \theta) \end{pmatrix}$ . We would like to solve the Dirichlet problem

$$\frac{\partial}{\partial r} \left( \frac{1}{r} \frac{\partial}{\partial r} (r \alpha_r) \right) + \frac{1}{r^2} \frac{\partial^2 \alpha_r}{\partial \theta^2} - \frac{2}{r^2} \frac{\partial \alpha_\theta}{\partial \theta} = \mathbf{0}, \quad \mathbf{x} \in W, \quad (7.101a)$$

$$\frac{\partial}{\partial r} \left( \frac{1}{r} \frac{\partial}{\partial r} (r \alpha_\theta) \right) + \frac{1}{r^2} \frac{\partial^2 \alpha_\theta}{\partial \theta^2} + \frac{2}{r^2} \frac{\partial \alpha_r}{\partial \theta} = \mathbf{0}, \quad \mathbf{x} \in W, \quad (7.101b)$$

$$\boldsymbol{\alpha}_{\mathcal{H}}(r, 0) = \alpha(r) \begin{pmatrix} 1 \\ 0 \end{pmatrix}, \quad (7.101c)$$

$$\boldsymbol{\alpha}_{\mathcal{H}}(r, \omega) = \beta(r) \begin{pmatrix} 1 \\ 0 \end{pmatrix}, \quad (7.101d)$$

$$\boldsymbol{\alpha}_{\mathcal{H}}(r, \theta) \rightarrow \mathbf{0} \text{ as } |R| \rightarrow \infty. \quad (7.101e)$$

Note that  $\alpha_r$  and  $\alpha_\theta$  in (7.101a, 7.101b) are not decouple. Therefore to simplify the problem, we change the polar coordinates into alternative polar coordinates by using a transformation  $r = e^R$ ,

$-\infty < R < +\infty$  (see [37], p. 13). From now on, we will consider  $(R, \theta)$  coordinates. Using this coordinates, the Dirichlet problem (7.101) turn into

$$\frac{\partial^2 \alpha_r}{\partial R^2} + \frac{\partial^2 \alpha_r}{\partial \theta^2} - 2 \frac{\partial \alpha_\theta}{\partial \theta} - \alpha_r = 0, \text{ in } W', \quad (7.102a)$$

$$\frac{\partial^2 \alpha_\theta}{\partial R^2} + \frac{\partial^2 \alpha_\theta}{\partial \theta^2} - 2 \frac{\partial \alpha_r}{\partial \theta} - \alpha_\theta = 0, \text{ in } W', \quad (7.102b)$$

$$\alpha_{\mathcal{H}}(R, 0) = \alpha(R) \begin{pmatrix} 1 \\ 0 \end{pmatrix}, \quad (7.102c)$$

$$\alpha_{\mathcal{H}}(R, \omega) = \beta(R) \begin{pmatrix} 1 \\ 0 \end{pmatrix}, \quad (7.102d)$$

$$\alpha_{\mathcal{H}}(R, \theta) \rightarrow \mathbf{0} \text{ as } |R| \rightarrow \infty. \quad (7.102e)$$

Although  $\alpha_r$  and  $\alpha_\theta$  still are not decouple, the problem is easier than (7.101) and it is possible to solve using the Fourier transform with respect to  $R$  ( $R \rightarrow \xi$ ). We obtain a system of ordinary differential equations

$$\frac{d^2 \hat{\alpha}_r}{d\theta^2} - 2 \frac{d\hat{\alpha}_\theta}{d\theta} - (\xi^2 + 1)\hat{\alpha}_r = 0, \quad (7.103a)$$

$$\frac{d^2 \hat{\alpha}_\theta}{d\theta^2} + 2 \frac{d\hat{\alpha}_r}{d\theta} - (\xi^2 + 1)\hat{\alpha}_\theta = 0. \quad (7.103b)$$

We change the system (7.103) by multiplying (7.103b) with  $i$  and adding to (7.103a). Next, multiplying (7.103b) with  $(-i)$  and adding to (7.103a), we arrive at

$$\frac{d^2}{d\theta^2} (\hat{\alpha}_r + i\hat{\alpha}_\theta) + 2i \frac{d}{d\theta} (\hat{\alpha}_r + i\hat{\alpha}_\theta) - (\xi^2 + 1)(\hat{\alpha}_r + i\hat{\alpha}_\theta) = 0, \quad (7.104a)$$

$$\frac{d^2}{d\theta^2} (\hat{\alpha}_r - i\hat{\alpha}_\theta) - 2i \frac{d}{d\theta} (\hat{\alpha}_r - i\hat{\alpha}_\theta) - (\xi^2 + 1)(\hat{\alpha}_r - i\hat{\alpha}_\theta) = 0. \quad (7.104b)$$

Solving the system (7.104) and applying the boundary conditions (7.102c) and (7.102d) yielding

$$\alpha_{\mathcal{H}}(R, \theta) = \begin{pmatrix} \frac{1}{\sqrt{2\pi}} \int_{-\infty}^{\infty} \left\{ \frac{\cos(\theta) \sinh((\omega - \theta)\xi)}{\sinh(\omega\xi)} \hat{\alpha}(\xi) + \frac{\cos(\omega - \theta) \sinh(\theta\xi)}{\sinh(\omega\xi)} \hat{\beta}(\xi) \right\} e^{i\xi R} d\xi \\ \frac{1}{\sqrt{2\pi}} \int_{-\infty}^{\infty} \left\{ -\frac{\sin(\theta) \sinh((\omega - \theta)\xi)}{\sinh(\omega\xi)} \hat{\alpha}(\xi) + \frac{\sin(\omega - \theta) \sinh(\theta\xi)}{\sinh(\omega\xi)} \hat{\beta}(\xi) \right\} e^{i\xi R} d\xi \end{pmatrix}. \quad (7.105)$$

Note that  $\alpha_{\mathcal{R}}(R, 0) = \alpha(R) \begin{pmatrix} 1 \\ 0 \end{pmatrix}$  and  $\alpha_{\mathcal{R}}(R, \omega) = \beta(R) \begin{pmatrix} 1 \\ 0 \end{pmatrix}$  are tangent vector fields at  $\theta = 0$  and  $\theta = \omega$  respectively.

Later we will determine  $\hat{\alpha}(\xi)$  and  $\hat{\beta}(\xi)$  by solving the operator equation (7.99) in  $(R, \theta)$ . Now we determine  $\mathcal{N}(\nabla \cdot \alpha_{\mathcal{R}})$  by solving the following Neumann problem.

## 7.2 The Neumann problem

Since  $\mathcal{N}(\nabla \cdot \alpha_{\mathcal{R}}) = -\frac{1}{2} \mathbf{x} \cdot \alpha_{\mathcal{R}} + \mathcal{N}\left(0; \frac{1}{2} \frac{\partial}{\partial n}(\mathbf{x} \cdot \alpha_{\mathcal{R}})\right)$ , we consider the Neumann problem

$$\left(\frac{\partial^2}{\partial R^2} + \frac{\partial^2}{\partial \theta^2}\right) \mathcal{N}\left(0; \frac{1}{2} \frac{\partial}{\partial n}(\mathbf{x} \cdot \alpha_{\mathcal{R}})\right) = 0, \quad \mathbf{x} \in W', \quad (7.106a)$$

$$\frac{\partial}{\partial n} \mathcal{N}\left(0; \frac{1}{2} \frac{\partial}{\partial n}(\mathbf{x} \cdot \alpha_{\mathcal{R}})\right)(R, 0) = \frac{1}{2} e^R \frac{\partial}{\partial \theta} \alpha_r(r, 0), \quad (7.106b)$$

$$\frac{\partial}{\partial n} \mathcal{N}\left(0; \frac{1}{2} \frac{\partial}{\partial n}(\mathbf{x} \cdot \alpha_{\mathcal{R}})\right)(R, \omega) = \frac{1}{2} e^R \frac{\partial}{\partial \theta} \alpha_r(r, \omega). \quad (7.106c)$$

Using the Fourier transform with respect to  $R$  ( $R \rightarrow \xi$ ), the solution of (7.106) is

$$\begin{aligned} \mathcal{N}\left(0; \frac{1}{2} \frac{\partial}{\partial n}(\mathbf{x} \cdot \alpha_{\mathcal{R}})\right)(R, \theta) = & \\ \frac{1}{2} \frac{1}{\sqrt{2\pi}} \int_{-\infty}^{\infty} & \left\{ \frac{\cosh(\omega(\xi + i)) \cosh((\omega - \theta)\xi) - \cos(\omega) \cosh(\theta\xi)}{\xi \sinh(\omega\xi) \sinh(\omega(\xi + i))} \right\} (\xi + i) \hat{\alpha}(\xi + i) e^{i\xi R} d\xi \\ + \frac{1}{2} \frac{1}{\sqrt{2\pi}} \int_{-\infty}^{\infty} & \left\{ \frac{\cosh(\omega(\xi + i)) \cosh(\theta\xi) - \cos(\omega) \cosh((\omega - \theta)\xi)}{\xi \sinh(\omega\xi) \sinh(\omega(\xi + i))} \right\} (\xi + i) \hat{\beta}(\xi + i) e^{i\xi R} d\xi. \end{aligned} \quad (7.107)$$

Using the above results, we can solve the operator equation (7.99) to obtain  $\hat{\alpha}(\xi)$  and  $\hat{\beta}(\xi)$ .

## 7.3 The operator equation

**Theorem 7.1.** The solution of the operator equations (7.99) is  $\alpha_{\mathcal{R}}(R, \theta)$  (7.105), with

$$\begin{aligned} \hat{\alpha}(\xi) = & \frac{2 \sinh(\omega\xi) [\sinh(\omega\xi) \hat{b}_1(\xi) + \xi \sin(\omega) \hat{a}_1(\xi)]}{\sinh^2(\omega\xi) - \xi^2 \sin^2(\omega)} \\ + & \frac{2i \sinh(\omega\xi) [\sinh(\omega\xi) \cosh(\omega(\xi - i)) + \xi \sin(\omega)]}{\sinh(\omega(\xi - i)) (\sinh^2(\omega\xi) - \xi^2 \sin^2(\omega))} \hat{b}_2(\xi) \\ - & \frac{2i \sinh(\omega\xi) [\sinh(\omega\xi) + \xi \sin(\omega) \cosh(\omega(\xi - i))]}{\sinh(\omega(\xi - i)) (\sinh^2(\omega\xi) - \xi^2 \sin^2(\omega))} \hat{a}_2(\xi), \end{aligned} \quad (7.108)$$

and

$$\begin{aligned}\hat{\beta}(\xi) &= \frac{2 \sinh(\omega\xi)[\sinh(\omega\xi)\hat{a}_1(\xi) + \xi \sin(\omega)\hat{b}_1(\xi)]}{\sinh^2(\omega\xi) - \xi^2 \sin^2(\omega)} \\ &\quad - \frac{2i \sinh(\omega\xi)[\sinh(\omega\xi) \cosh(\omega(\xi - i)) + \xi \sin(\omega)]}{\sinh(\omega(\xi - i))(\sinh^2(\omega\xi) - \xi^2 \sin^2(\omega))} \hat{a}_2(\xi) \\ &\quad + \frac{2i \sinh(\omega\xi)[\sinh(\omega\xi) + \xi \sin(\omega) \cosh(\omega(\xi - i))]}{\sinh(\omega(\xi - i))(\sinh^2(\omega\xi) - \xi^2 \sin^2(\omega))} \hat{b}_2(\xi).\end{aligned}\quad (7.109)$$

**Proof.** First consider the left-hand side of operator equation (7.99). We have found  $\alpha_{\mathcal{N}}$ . Using this  $\alpha_{\mathcal{N}}$  (7.105) and  $\mathcal{N}(0; \frac{1}{2} \frac{\partial}{\partial n}(\mathbf{x} \cdot \alpha_{\mathcal{N}}))$  (7.107), we obtain the left-hand side of the operator equation (7.99) at  $\theta = 0$  and  $\theta = \omega$ , respectively

$$\left( \begin{array}{c} \frac{1}{2} \frac{1}{\sqrt{2\pi}} \int_{-\infty}^{\infty} \left\{ \hat{\alpha}(\xi) - \frac{\xi \sin(\omega)}{\sinh(\omega\xi)} \hat{\beta}(\xi) \right\} e^{i\xi R} d\xi \\ 0 \end{array} \right) \quad (7.110)$$

and

$$\left( \begin{array}{c} \frac{1}{2} \frac{1}{\sqrt{2\pi}} \int_{-\infty}^{\infty} \left\{ -\frac{\xi \sin(\omega)}{\sinh(\omega\xi)} \hat{\alpha}(\xi) + \hat{\beta}(\xi) \right\} e^{i\xi R} d\xi \\ 0 \end{array} \right). \quad (7.111)$$

Now, we determine the right-hand side of the operator equation (7.99). First, we determine  $\mathcal{N}(0; \mathbf{c} \cdot \mathbf{n})$  by solving the Neumann problem

$$\left( \frac{\partial^2}{\partial R^2} + \frac{\partial^2}{\partial \theta^2} \right) \mathcal{N}(0; \mathbf{c} \cdot \mathbf{n}) = 0, \quad (7.112a)$$

$$\frac{\partial}{\partial n} \mathcal{N}(0; \mathbf{c} \cdot \mathbf{n})(R, 0) = e^{-R} \frac{\partial}{\partial \theta} \mathcal{N}(0; \mathbf{c} \cdot \mathbf{n})(R, 0) = b_2(R), \quad (7.112b)$$

$$\frac{\partial}{\partial n} \mathcal{N}(0; \mathbf{c} \cdot \mathbf{n})(R, \omega) = e^{-R} \frac{\partial}{\partial \theta} \mathcal{N}(0; \mathbf{c} \cdot \mathbf{n})(R, \omega) = a_2(R). \quad (7.112c)$$

Using the Fourier transform, the solution of (7.112) is

$$\mathcal{N}(0; \mathbf{c} \cdot \mathbf{n}) = \frac{1}{\sqrt{2\pi}} \int_{-\infty}^{\infty} \left\{ \frac{\cosh(\theta\xi)}{\xi \sinh(\omega\xi)} \hat{a}_2(\xi + i) - \frac{\cosh((\omega - \theta)\xi)}{\xi \sinh(\omega\xi)} \hat{b}_2(\xi + i) \right\} e^{i\xi R} d\xi, \quad (7.113)$$

Next, taking the gradient of (7.113) yields the right-hand side of (7.99) at  $\theta = 0$  and  $\theta = \omega$  are respectively

$$\left( \begin{array}{c} \frac{1}{\sqrt{2\pi}} \int_{-\infty}^{\infty} \left\{ \hat{b}_1(\xi) - \frac{i}{\sinh(\omega(\xi - i))} \hat{a}_2(\xi) + \frac{i \cosh(\omega(\xi - i))}{\sinh(\omega(\xi - i))} \hat{b}_2(\xi) \right\} e^{i\xi R} d\xi \\ 0 \end{array} \right) \quad (7.114)$$



and

$$\begin{pmatrix} \frac{1}{\sqrt{2\pi}} \int_{-\infty}^{\infty} \left\{ \hat{a}_1(\xi) + \frac{i}{\sinh(\omega(\xi - i))} \hat{b}_2(\xi) - \frac{i \cosh(\omega(\xi - i))}{\sinh(\omega(\xi - i))} \hat{a}_2(\xi) \right\} e^{i\xi R} d\xi \\ 0 \end{pmatrix}. \quad (7.115)$$

Now we are ready to solve the operator equation (7.99). Solving the system of equations (7.110), (7.111), (7.114), and (7.115), yielding  $\hat{\alpha}(\xi)$  and  $\hat{\beta}(\xi)$  as in (7.108) and (7.109).  $\square$

## 7.4 Solution

Using the above results and

$$\mathbf{v} = \boldsymbol{\alpha}_{\mathcal{H}} + \nabla \mathcal{N}(\nabla \cdot \boldsymbol{\alpha}_{\mathcal{H}}) + \nabla \mathcal{N}(0; \mathbf{c} \cdot \mathbf{n}), \quad p = -\nabla \cdot \boldsymbol{\alpha}_{\mathcal{H}}, \quad (7.116)$$

the solutions of SBVP are

$$\begin{aligned} v_r &= \frac{1}{2} \frac{1}{\sqrt{2\pi}} \int_{-\infty}^{\infty} \left\{ \frac{\cos(\theta) \sinh((\omega - \theta)\xi)}{\sinh(\omega\xi)} - \frac{\xi \sin(\theta) \cosh((\omega - \theta)\xi)}{\sinh(\omega\xi)} \right\} \hat{\alpha}(\xi) e^{i\xi R} d\xi \\ &+ \frac{1}{2} \frac{1}{\sqrt{2\pi}} \int_{-\infty}^{\infty} \left\{ \frac{\cos(\omega - \theta) \sinh(\theta\xi)}{\sinh(\omega\xi)} - \frac{\xi \sin(\omega - \theta) \cosh(\theta\xi)}{\sinh(\omega\xi)} \right\} \hat{\beta}(\xi) e^{i\xi R} d\xi \\ &+ \frac{i}{\sqrt{2\pi}} \int_{-\infty}^{\infty} \left\{ \frac{\cosh(\theta(\xi - i))}{\sinh(\omega(\xi - i))} \hat{a}_2(\xi) - \frac{\cosh((\omega - \theta)(\xi - i))}{\sinh(\omega(\xi - i))} \hat{b}_2(\xi) \right\} e^{i\xi R} d\xi, \end{aligned} \quad (7.117)$$

$$\begin{aligned} v_\theta &= -\frac{1}{2} \frac{1}{\sqrt{2\pi}} \int_{-\infty}^{\infty} \left\{ \frac{(1 + i\xi) \sin(\theta) \sinh((\omega - \theta)\xi)}{\sinh(\omega\xi)} \right\} \hat{\alpha}(\xi) e^{i\xi R} d\xi \\ &+ \frac{1}{2} \frac{1}{\sqrt{2\pi}} \int_{-\infty}^{\infty} \left\{ \frac{(1 + i\xi) \sin(\omega - \theta) \sinh(\theta\xi)}{\sinh(\omega\xi)} \right\} \hat{\beta}(\xi) e^{i\xi R} d\xi \\ &+ \frac{i}{\sqrt{2\pi}} \int_{-\infty}^{\infty} \left\{ \frac{\sinh(\theta(\xi - i))}{\sinh(\omega(\xi - i))} \hat{a}_2(\xi) - \frac{\sinh((\omega - \theta)(\xi - i))}{\sinh(\omega(\xi - i))} \hat{b}_2(\xi) \right\} e^{i\xi R} d\xi, \end{aligned} \quad (7.118)$$

$$\begin{aligned} p &= \frac{i}{\sqrt{2\pi}} e^{-R} \int_{-\infty}^{\infty} \left\{ \frac{-\xi \cos(\theta) \sinh((\omega - \theta)\xi) + i\xi \sin(\theta) \cosh((\omega - \theta)\xi)}{\sinh(\omega\xi)} \right\} \hat{\alpha}(\xi) e^{i\xi R} d\xi \\ &+ \frac{i}{\sqrt{2\pi}} e^{-R} \int_{-\infty}^{\infty} \left\{ \frac{-\xi \cos(\omega - \theta) \sinh(\theta\xi) + i\xi \sin(\omega - \theta) \cosh(\theta\xi)}{\sinh(\omega\xi)} \right\} \hat{\beta}(\xi) e^{i\xi R} d\xi. \end{aligned} \quad (7.119)$$

# Chapter V

## The effect of spatial inhomogeneity in thermal conductivity on the formation of hot-spots

**Abstract.** The steady-state microwave heating of a unit slab consisting of three layers of materials with different thermal conductivities is examined. The governing equations are a damped wave equation derived from Maxwell's equations and a heat-force equation for the temperature. As the primary concern is to investigate the dependence of the steady-state on the thermal-conductivity parameter, a simplifying assumption is made, namely that the electrical conductivity is temperature independent. Under this assumption, the damped wave equation governing the electric field may be solved separately. An eigenfunction expansion for the problem based on the Galerkin method is described and a fundamental-mode approximation is presented. If this approximation is applied to a unit slab composed of three layers with different thermal conductivities, the hot-spots formation can be addressed and a global steady-state solution is found for the whole domain. Numerical results for some different cases of the three-layer combinations are interpreted to gain some insight in parameter dependence and the position of the low-thermal-conductivity inner layer related to hot-spots formation.

### 1 Introduction

In recent years there has been a growing interest in the use of microwave radiation for industrial processing such as drying, melting, smelting, and sintering. This heating technique is proved to have some advantages over the use of a conventional oven. In the sintering of ceramics, for example, the use of a conventional oven for prolonged periods of time is required to achieve high equilibrium temperatures in a processes that are controlled by thermal conductivity [27]. Generating heat internally by means of microwave energy can significantly reduce the time as required in conventional sintering [4], [6], [7], [54]. The widespread industrial applications of microwave heating have also created a number of problems. Forthmost

of these problems there is the formation of hot-spots, which is a small region of very high temperature relative to the surroundings. Such a phenomenon can either be desirable, such as in metal melting, or undesirable, such as in ceramic sintering.

In general, the microwave heating of a material are coupling of electromagnetic and thermal phenomena. These phenomena can be expressed mathematically as a couple of a damped wave equation derived from Maxwell's equations governing the propagation of the microwave radiation and a forced heat equation governing the resultant of heat flow. The forcing term in the last equation is proportional to the square amplitude of the microwave field. General analysis of this kind of microwave heating of a material is not easy. Until recently, the mathematical analysis of the problem was divided into two main streams [34]. First, under assumption that the properties of the heated material are slowly varying with the temperature, the effects of the electromagnetic field are of interest. In this case, perturbation solutions are found for both the electric field and the temperature. Such studies have been carried out by a number of authors such as Kriegsmann *et al.* [27], Kriegsmann [28], Marchant and Picombe [34], Picombe and Smyth [42], and Smyth [48]. When the thermal aspects are isolated, a simplifying assumption can be made, namely that the microwave radiation has a constant amplitude, [10], [22], [44], leading to a single heat-force equation for the temperature  $\theta_t = \nu \Delta \theta + f(\theta)$ . Here,  $f(\theta)$  is the temperature-dependent rate of energy absorption by the material.

Using the second approach, Coleman [10] investigated the hot-spots formation for different functions of temperature-dependent reaction rate  $f(\theta)$ . In the case of an Arrhenius dependency of the form  $f(\theta) = \delta e^{-\gamma/\theta}$ , he found numerically that, for sufficiently small  $\nu$ ,  $\theta$  becomes large in finite time, signifying the formation of hot-spots. For a dependency of the form  $f(\theta) = \delta e^{-\gamma/\theta}$ , Hill and Smyth [22] found the steady-state solutions in planar and cylindrical geometries with constant  $\nu$  and constant temperature on the boundary of the body. For a quadratic dependence in temperature of the reaction rate  $f(\theta)$  and a connective heat-lost boundary condition, for a cylindrical body, Roussy *et al.* [44] found numerically an approximate criterion for hot-spots to form. It is noted that based on an analysis of the experiment data collected for various materials, Hill and Jennings [23] found that linear, quadratic and exponential temperature dependencies of the reaction rate  $f(\theta)$  are valid for many materials.

Recently Palesko and Kriegsmann [41] studied the microwave heating of a one-dimensional ceramic laminate composed of three layers of two different types of material (identical outer layers and an inside layer). These two materials have widely disparate effective electrical conductivities. The governing equations considered are a couple of the damped wave equation governing the propagation of the microwave radiation and the forced-heat equation governing the resultant of heat flow. An asymptotic theory was set up based on the assumption that the ratio the two conductivities is small. This approach yields simplified equations which were then analyzed numerically. Marchant and Liu in [35] used a Galerkin method to find the steady-state microwave heating of a one dimensional finite slab with electrical conductivity and thermal absorptivity governed by the Arrhenius function which, in this paper, was approximated by a rational cubic function. The boundary conditions took account of both connective and radiative heat losses. For small thermal absorptivity, approximate analytical solutions were found for the steady-state temperature as well as the electric

field amplitude. Multi-valued steady-state temperatures were found at the S-shaped curve of temperature-versus-power relationship. The thermal runaway was described as when the temperature jumps from the lower to the upper branch of the curve.

The present paper is concerned with a finite slab consisting three layers. Contrary to the three layers in the work of Palesko and Kriegsmann [41] where the electrical conductivity is of the interest, here we assume that the layers have different thermal conductivities (thermal diffusivities). An Arrhenius-type of temperature dependency of the reaction rate of the form  $f(\theta) = e^{\frac{\alpha\theta}{\alpha+\theta}}$  for some  $\alpha > 0$  is used. Using the approach in [49] that is, assuming a temperature independent of the electrical conductivity of the material and microwave speed, we may solve the damped wave equation separately which leads to a single forced heat equation governing the resulting heat flow. The forcing term in the last equation is proportional to the spatially dependent squared amplitude of the microwave field. The technique exploited is a one-term Galerkin approximation. It is investigated in [1] and [53] that such an approximation makes sense to obtain the salient features of the solution. In this paper, we address the hot-spots formation by finding a global steady-state solution for the whole domain of different thermal conductivities. Although the paper is concerned with hot-spots formation, the approach may be applied to a three-layer configuration of a finite slab. The novelty of this approach lies in its simplicity.

In the next section, we present the governing equations for the microwave heating of a material which consists of a damped wave equation that is derived from Maxwell's equations and a heat-force equation for the temperature. As our primary concern is to investigate the influence of the spatial dependence of the thermal conductivity of the material, the simplifying assumption is made that the electrical conductivity is temperature-independent. Under this assumption, the equation governing the electrical field may be solved separately. In Section 3 some preliminary results and an eigenfunction expansion based on a Galerkin approximation are presented. For some geometries (unit sphere, finite cylinder, and rectangular block) with Dirichlet boundary conditions, it is numerically shown in [1], [3] that the fundamental mode is dominant. The critical parameters obtained by using this single mode approximate the critical parameters of the solution. For this reason, we focus on this fundamental mode. The formulation of the problem for a unit slab consisting three layers of different thermal conductivities is presented in Section 4. An analysis based on the one-term Galerkin approximation is presented in the same section. In Section 5, we present some numerical results for some different cases of the three-layer combinations. In the last section concluding remarks are given.

## 2 Governing equations

The equations governing the microwave heating of a material are the damped wave equation derived from Maxwell's equations governing the propagation of the microwave radiation and the forced heat equation governing flow of heat [49],

$$E_{tt} + \sigma(\theta)E_t = c^2\Delta E, \quad (2.1)$$

$$\theta_t = \nabla \cdot (k(\theta)\nabla\theta) + \delta|E|^2 f(\theta). \quad (2.2)$$

Here,  $E$  and  $\theta$  are the electric field associated with the microwave heating radiation and the temperature, respectively. The temperature-dependent parameter  $\sigma$  is the electrical conductivity of the material and  $c$  is the microwave speed. The parameter  $\delta$  is a positive parameter related to the intensity of electric field. While,  $|E|$  is the amplitude of the electric field,  $k(\theta)$  is thermal conductivity of the material with the properties  $k(\theta) > 0, k'(\theta) > 0$ . Here, we assume  $k(\theta) = \mu(x) e^{\gamma\theta}$ . While  $f(\theta)$  is the rate of the microwave energy absorption by the material with properties  $f(\theta) > 0, f'(\theta) > 0$ . Here, we take  $f(\theta)$  to be Arrhenius-type of the form  $f(\theta) = e^{\frac{\alpha\theta}{\alpha+\theta}}$  for some  $\alpha > 0$ . The damped wave equation (2.1) may derived from the Maxwell's equations under the assumption that  $\sigma$  is small and that the microwave speed  $c$  is temperature-independent.

It is difficult to solve (2.1) and (2.2) with temperature-dependent  $\sigma$ . In this work we make the simplifying assumption that  $\sigma$  is constant. Although this creates an unphysical temperature variation in  $\sigma$ , our primary concern is to investigate the spatial dependence of the thermal conductivity of the material  $k(\theta)$ . Under this assumption, in the one-dimensional domain, (2.1) and (2.2) become

$$E_{tt} + \sigma E_t = c^2 E_{xx}, \quad (2.3)$$

$$\frac{\partial \theta}{\partial t} = \frac{\partial}{\partial x} \left( k(\theta) \frac{\partial \theta}{\partial x} \right) + \delta |E|^2 f(\theta). \quad (2.4)$$

The damped wave equation (2.3) has a travelling-wave solution in the form

$$E = e^{-k_1 x} e^{i(kx - \omega t)}, \quad (2.5)$$

where

$$k^2 = \frac{\omega^2}{2c^2} \left[ 1 + \left( 1 + \frac{\sigma^2}{\omega^2} \right)^{1/2} \right] \quad (2.6)$$

and

$$k_1^2 = \frac{\omega^2}{2c^2} \left[ -1 + \left( 1 + \frac{\sigma^2}{\omega^2} \right)^{1/2} \right]. \quad (2.7)$$

Using the above assumption, we can write the force-heat equation (2.2) in the form

$$\frac{\partial \theta}{\partial t} = \frac{\partial}{\partial x} \left[ k(\theta) \frac{\partial \theta}{\partial x} \right] + \delta R(x) f(\theta), \quad (2.8)$$

where  $R(x) = |E|^2$  and the expression for  $E$  is of the form (2.5). Note that for  $k(\theta) = 1$  and  $R(x) = 1$ , (2.8) features prominently in combustion theory and has been studied by many authors such as in [2], [19](Chapters 2-4), [29], [52], and many others.

In the above model the conductivity parameter  $\mu$ , which measures the magnitude of thermal conductivity of material, is constant throughout the medium D. In this work, however, we intend to investigate the effect of inhomogeneity of  $\mu$  on the formation of a hot-spots, which is a small region in the heated medium where the temperature is much higher than elsewhere.

For the domain  $D$  we take a unit slab  $[0,1]$  and the conductivity is given by  $k(\theta) = \mu(x) e^{\gamma x}$ , where  $\mu(x)$  is a function of the spatial variable  $x$ , namely

$$k(\theta) = \begin{cases} \mu_1 e^{\gamma \theta} & \text{if } 0 \leq x \leq x_0, \\ \mu_2 e^{\gamma \theta} & \text{if } x_0 \leq x \leq x_0 + \varepsilon, \\ \mu_3 e^{\gamma \theta} & \text{if } x_0 + \varepsilon \leq x \leq 1, \end{cases} \quad (2.9)$$

where  $\mu_2 < \mu_1$  and  $\mu_2 < \mu_3$ . Here, we address hot-spots formation by finding a global steady-state solution for the whole region  $[0,1]$  in which this formation appears which is in the region  $[x_0, x_0 + \varepsilon]$ .

### 3 Analysis of the reduced equation

We consider a model

$$\frac{\partial \theta}{\partial t} = \nabla \cdot (k(\theta) \nabla \theta) + \delta R(\mathbf{x}) f(\theta). \quad (3.10)$$

Using the transformation

$$v = \int_0^\theta k(s) ds, \quad (3.11)$$

we may write (3.10) as follows

$$\frac{\partial v}{\partial t} = K(v) \{ \Delta v + \delta R(\mathbf{x}) F(v) \}, \quad (3.12)$$

where  $K(v) = k(\theta(v))$  and  $F(v) = f(\theta(v))$ . Since  $v(\theta)$  is monotonically increasing, we observe that both  $K(u)$  and  $F(u)$  have the same features as  $k(\theta)$  and  $f(\theta)$ , respectively. We can remove the function  $K(v)$  by letting  $\tau$  to be such that  $d\tau/dt = K(v(\mathbf{x}, t))$  and  $u(\mathbf{x}, \tau) = v(\mathbf{x}, t)$  giving

$$\frac{\partial u}{\partial \tau} = \Delta u + \delta R(\mathbf{x}) F(u). \quad (3.13)$$

#### 3.1 Behaviour of solutions

We will now study the behaviour of the solution of the equation

$$\frac{\partial u}{\partial t} = \Delta u + \delta R(\mathbf{x}) F(u), \quad (3.14)$$

subject the initial and Dirichlet boundary conditions

$$u(\mathbf{x}, 0) = H(\mathbf{x}), \quad u(\mathbf{x}, t) = 0 \text{ on } \partial D. \quad (3.15)$$

From the transformation (3.11) the function  $F$  in (3.14) can be written in the form

$$F(u) = f(\theta(u)) = \exp \left\{ \frac{\frac{\alpha}{\gamma} \log(1 + \gamma u / \mu)}{\alpha + \frac{1}{\gamma} \log(1 + \gamma u / \mu)} \right\}. \quad (3.16)$$

The following results are summarized from [1] for completeness. First, we consider the following boundary value problem

$$\frac{\partial U}{\partial t} = \Delta U + \delta R(\mathbf{x})F(m), \quad (3.17)$$

$$U(\mathbf{x}, 0) = H(\mathbf{x}), \quad U(\mathbf{x}, t) = 0 \text{ on } \partial D. \quad (3.18)$$

for some parameter  $m \geq 0$ . Let  $\bar{u}$  and  $\bar{U}$  denote the steady-state solution of (3.14), (3.15) and (3.17), (3.18), respectively. If  $m = \max_{\mathbf{x}} \bar{u}(\mathbf{x})$ , then, by the minimum principle, we can show that  $\max_{\mathbf{x}} \bar{U}(\mathbf{x}, m) \geq m$ .

We assume that we can expand  $U(\mathbf{x}, t) = \sum_i a_i(t)\varphi_i(\mathbf{x})$ , with  $\varphi_n$  and  $\lambda_n$  be the normalized eigenfunctions and eigenvalues of the boundary value problem

$$\Delta \varphi_n = -\lambda_n^2 \varphi_n, \quad (3.19)$$

$$\varphi_n = 0 \text{ on } \partial D, \quad (3.20)$$

where  $\lambda_1 < \lambda_2 \leq \lambda_3 \leq \dots$

Using (3.19) and the normalized eigenfunctions, the steady-state solution of (3.17) may be written in the form  $\bar{U}(\mathbf{x}, m) = \delta F(m) \sum_i \frac{B_i}{\lambda_i^2} \varphi_i(\mathbf{x})$ , where  $B_i = \int_D R(\mathbf{x})\varphi_i(\mathbf{x}) \, d\mathbf{x}$ . If we

write  $M = \max_{\mathbf{x}} \sum_i \frac{B_i}{\lambda_i^2} \varphi_i(\mathbf{x})$  then  $\max_{\mathbf{x}} \bar{U}(\mathbf{x}, m) = \delta M F(m)$ . Taking  $\mu = 1$ , we note that

$$F'(m) = \frac{(\alpha\gamma)^2 F(m)}{[1 + \gamma m][\alpha\gamma + \log(1 + \gamma m)]^2}, \quad (3.21)$$

while

$$F''(m) = \frac{\alpha^2 \gamma^3 G(\alpha, \gamma, m) F(m)}{[1 + \gamma m]^2 [\alpha\gamma + \log(1 + \gamma m)]^3}, \quad (3.22)$$

where

$$G(\alpha, \gamma, m) = \alpha\gamma(\alpha - 2 - \alpha\gamma) - \log(1 + \gamma m)[2 + 2\gamma\alpha + \log(1 + \gamma m)], \quad (3.23)$$

giving  $F'(m) > 0$  for  $m \geq 0$  and, if  $\alpha(1 - \gamma) \leq 2$ , then  $F''(m) < 0$ , for  $m > 0$  and so the graph of  $F(m)$  vs.  $m$  intersects the line  $m$  at one and only one point for any value of  $\delta$ . For  $\mu = 1$ , a necessary condition such that the graph of  $F(m)$  vs.  $m$  is in the form of an S-shaped curve is that  $\alpha(1 - \gamma) > 2$ . This analysis will still hold later for the one-term Galerkin approximation provided that the first mode  $\varphi_1(\mathbf{x})$  is non-negative throughout the region  $D$ . For some values of  $\alpha$  and  $\gamma$  such that the graph  $F(m)$  vs.  $m$  has an S-shaped curve, Figure 3.1 (a) shows the graph of  $\max_{\mathbf{x}} \bar{U}(\mathbf{x}, m)$  vs.  $m$  for different values of  $\delta$ .

When the graph of  $F(m)$  vs.  $m$  has an S-shaped curve, for which is necessary that  $\alpha(1 - \gamma) > 2$ , using the minimum principle, we can show (see [1]) that

1. If  $\delta$  is such that  $\max_x \bar{U}(x, m) - m = 0$  has a single root, say  $m_0$ , then  $\max_x \bar{u}(x) \leq m_0$ .
2. If  $\delta$  is such that  $\max_x \bar{U}(x, m) - m = 0$  has three roots, say  $m_1, m_2, m_3$ , where  $m_1 < m_2 < m_3$ , [see Figure 3.1 (b)], then  $0 \leq \max_x \bar{u}(x) \leq m_1$  or  $m_2 \leq \max_x \bar{u}(x) \leq m_3$ . Here we note that  $m_1$  is  $O(1)$  while  $m_3$  is  $O(e^\alpha)$ .

Let  $\delta^{U_{cr}}$  and  $\delta_{U_{cr}}$  be the largest and the smallest value of  $\delta$  such that the line  $m$  is tangent to the lower and upper portion of the graph  $\max_x \bar{U}(x, m)$  vs  $m$ , respectively [see Figure 3.1 (c) and (d)]. Let  $\delta$  be such that  $\delta^{U_{cr}} < \delta < \delta_{U_{cr}}$ . Then for these values of  $\delta$ ,  $\max_x \bar{U}(x, m) - m = 0$  has three roots. Since  $\bar{U}(x, m)$  is an upper solution of  $\bar{u}(x)$  then, if  $H(x) = 0$ ,  $u(x, t)$  will be  $O(1)$  for all  $t$ .

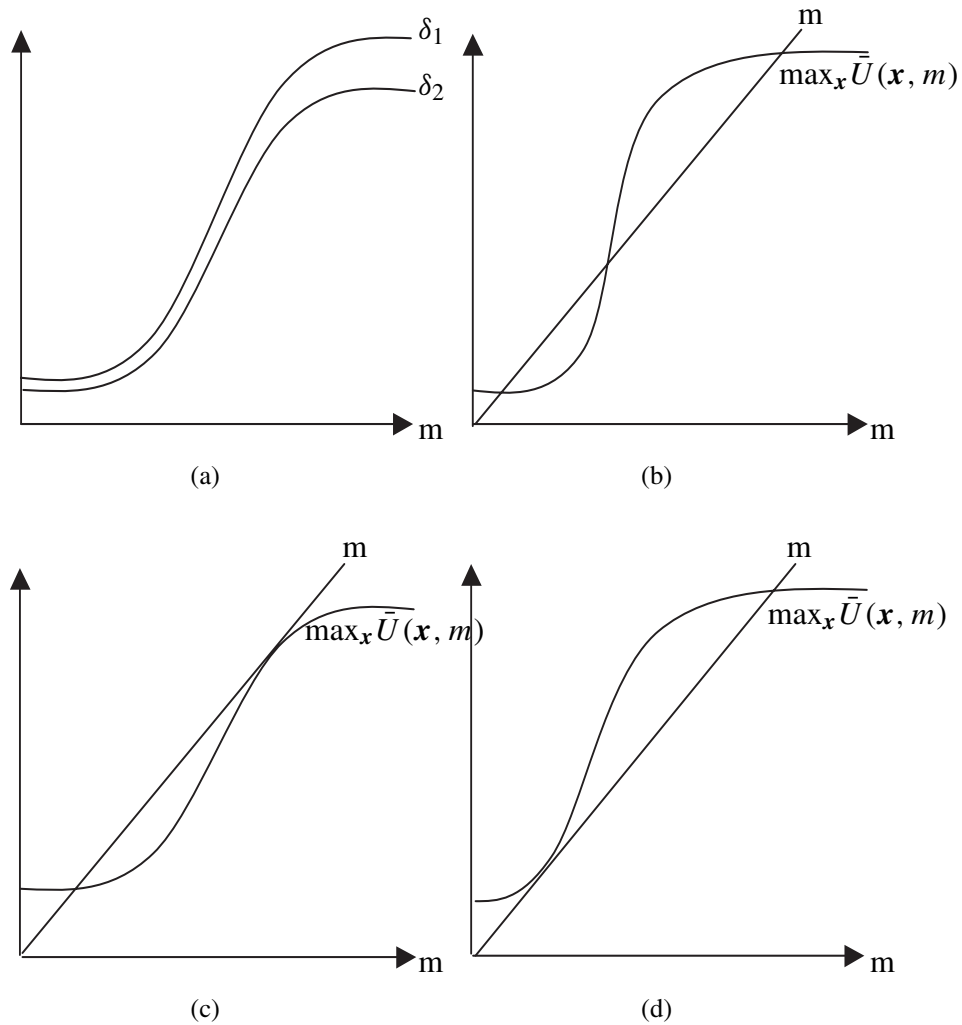


Figure 3.1: (a)  $\max_x \bar{U}(x, m)$  vs.  $m$  for different  $\delta$ ,  $\delta_1 > \delta_2$ , (b) Intersections of  $\max_x \bar{U}(x, m)$  vs.  $m$  and the line  $m$ , (c)  $\max_x \bar{U}(x, m)$  vs.  $m$  for  $\delta = \delta_{U_{cr}}$ , (d)  $\max_x \bar{U}(x, m)$  vs.  $m$  for  $\delta = \delta^{U_{cr}}$ .



### 3.2 Fundamental mode approximation

Let us return to the boundary value problem (3.14), (3.15). Adopting the following approximation procedure, which can be attributed to Galerkin, let us write

$$s_N(\mathbf{x}, t) = \sum_{i=1}^N A_i^{(N)}(t) \varphi_i(\mathbf{x}), \quad (3.24)$$

where  $A_i^{(N)}(t)$  is the solution of the integral equation

$$\frac{dA_i^{(N)}}{dt} = -\lambda_i^2 A_i^{(N)} + \delta \int_D R(\mathbf{x}) F\left(\sum_{i=1}^N A_i^{(N)} \varphi_i(\mathbf{x})\right) \varphi_i(\mathbf{x}) dv(\mathbf{x}), \quad (3.25)$$

for  $1 \leq i \leq N$ . The above equations constitute  $N$  integral equations with  $N$  unknowns.

From the behaviour of the solution as studied above and assuming that the first eigenfunction  $\varphi_1(\mathbf{x})$  is non-negative, we conclude that it makes sense to adopt a fundamental-mode approximation,  $s_1(\mathbf{x}, t) = A(t)\varphi_1(\mathbf{x})$ . This  $A(t)$  is obtained from the integral equation

$$\frac{dA}{dt} = -\lambda_1^2 A + \delta \int_D R(\mathbf{x}) F(A\varphi_1(\mathbf{x})) \varphi_1(\mathbf{x}) dv(\mathbf{x}), \quad (3.26)$$

Let

$$I(A) = \int_D R(\mathbf{x}) F(A\varphi_1(\mathbf{x})) \varphi_1(\mathbf{x}) dv(\mathbf{x}). \quad (3.27)$$

The equilibrium values of  $A$  can be obtained graphically from the intersection of the straight line  $\lambda_1^2 A / \delta$  vs.  $A$  and the curve of the graph  $I(A)$  vs.  $A$ . Similar to the result found in the previous subsection, it is not difficult to see that for  $\mu = 1$  a necessary condition for the graph  $I(A)$  vs.  $A$  to have an S-shaped curve is

$$\alpha(1 - \gamma) > 2. \quad (3.28)$$

For  $\alpha(1 - \gamma) \leq 2$  there is only one possible steady-state solution for  $A$ . In combustion this phenomenon is often called 'loss of criticality' which occurs for the critical values of  $\alpha$  and  $\gamma$  such that  $\alpha(1 - \gamma) \leq 2$ . Lacey and Wake [29] showed that for a simpler equation  $\nabla \cdot (e^{\gamma\theta} \nabla\theta) + \delta e^\theta = 0$ , the solution does not exhibit a critical phenomenon when  $\gamma \geq 1$ . Tam in [52] showed that for a sphere of unit radius with  $\alpha = 100$ , loss of criticality occur when  $\gamma = 0.9$ . From the simple analysis above for  $\alpha = 100$ , loss of criticality occurs when  $\gamma = 0.98$ .

When the graph  $I(A)$  vs.  $A$  has an S-shape, there are two critical parameters of  $\delta$ , say  $\delta^{cr}$  and  $\delta_{cr}$ . The critical value  $\delta^{cr}$ , where the steady-state of (3.26) is  $O(e^\alpha)$  for  $\delta > \delta^{cr}$ , is obtained when the straight line  $\lambda_1^2 A / \delta$  vs.  $A$  is tangent to the lower portion of the S-shape curve. On the other hand, the critical value  $\delta_{cr}$ , where the steady-state of (3.26) is  $O(1)$  for  $\delta < \delta_{cr}$ , is obtained when the straight line  $\lambda_1^2 A / \delta$  vs.  $A$  is tangent to the upper portion of the S-shaped curve. For  $\delta$ ,  $\delta_{cr} < \delta < \delta^{cr}$ , for some critical values  $\delta_{cr}$  and  $\delta^{cr}$ , depending on the initial condition  $A(0) = C_1$ , there are three possible steady-state solutions for (3.26), say

$A_1$ ,  $A_2$ , and  $A_3$ , where  $A_1 < A_2 < A_3$  and  $A_1$  is of  $O(1)$ ,  $A_3$  is of  $O(e^\alpha)$ . We note that the middle solution  $A_2$  is unstable, whereas, the other two are stable.

For a few different configurations of the medium, *viz.* a unit sphere, a finite cylinder and a rectangular block, it is shown in [1], [3], that it is not only the first mode which is dominant, but also the critical values  $\delta_{cr}$  and  $\delta^{cr}$  obtained by using a single mode, close to the critical values  $\delta$  of  $u$ .

### 3.3 Steady-state solution for a unit slab geometry

To illustrate the method described above, let us consider a unit slab geometry  $[0, 1]$ . For this slab, we have the first eigenvalue  $\lambda_1 = \pi^2$  corresponding to the normalized eigenfunction  $\varphi_1 = \sqrt{1/2\pi} \sin(\pi x)$ . Taking an exponential function of  $R(x) = |E|^2$ , with  $k = 1$  in (2.5), we may obtain the steady-state solutions  $A$  from

$$\frac{\lambda_1^2}{\delta} A = \int_D R(\mathbf{x}) F(A\varphi_1(\mathbf{x})) \varphi_1(\mathbf{x}) dv(\mathbf{x}). \quad (3.29)$$

The critical parameter  $\delta^{cr}$  can be approximated as follows. Let  $A_1$  be the smallest  $A$  satisfying  $I(A_1) = \lambda_1^2 A_1 / \delta^{cr}$  then

$$\frac{d}{dA} \left[ I(A) - \frac{\lambda_1^2 A}{\delta^{cr}} \right]_{A=A_1} = 0, \quad (3.30)$$

or

$$I'(A_1) = \frac{\lambda_1^2}{\delta^{cr}}. \quad (3.31)$$

Thus, we can calculate  $\delta^{cr}$  by first obtaining the value of  $A_1$  from

$$I(A_1) - A_1 I'(A_1) = 0 \quad (3.32)$$

and then

$$\delta^{cr} = \frac{\lambda_1^2 A_1}{I(A_1)}. \quad (3.33)$$

For  $\alpha = 10$ ,  $\mu = 1$ ,  $\gamma = 0.1$ , Figure 3.2 shows a bifurcation diagram for the temperature  $\theta$  as obtained from the inverse of the transformation (3.11) and the fundamental-mode approximation, that is  $\theta \approx \frac{1}{\gamma} \log(1 + \gamma A \varphi_1 / \mu)$ . The parameter  $\delta$  can be seen as the magnitude of the square amplitude of the electric field  $R(x)$ . The bifurcation diagram shows that there is a critical parameter  $\delta_{cr}$  such that, for  $\delta < \delta_{cr}$ , there is only one steady-state solution  $\theta$  for which the corresponding  $A$  is  $O(1)$  and there is a critical parameter  $\delta^{cr}$  such that, for  $\delta > \delta^{cr}$ , again there is only one steady-state solution  $\theta$ , but  $A$  is  $O(e^\alpha)$ . The critical value  $\delta^{cr}$ , in this computation  $\delta^{cr} = 6.869$ , plays an important role in hot-spots formation. Here a slight change in the magnitude of the electric field near  $\delta^{cr}$  produces a substantial difference in the temperature, that is, there is a temperature jump from  $O(1)$  to  $O(e^\alpha)$ . A similar result can be found in [35].

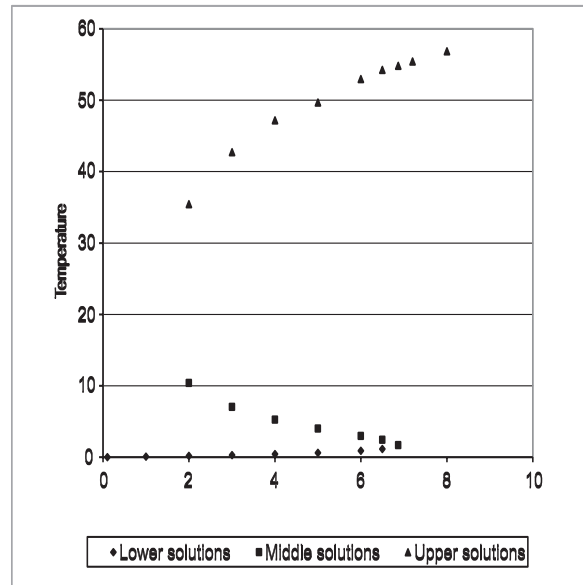


Figure 3.2: Bifurcation diagram of the temperature  $\theta$  vs  $\delta$  evaluated at  $x = 0.5$ .

Although it is not fully justified, this simple analysis may be applied to the case of a unit slab composed of three layers of two different materials (identical outer layers and an inside layer) as was done in [41] where the two materials have widely disparate effective electrical conductivities. The magnitude of the electric field produced is a function of the electrical conductivity of the material. Thermal runaway can be experienced if the magnitude of electric field exceeds the critical value. Locally (the layers are considered as three isolated layers) thermal runaway can happen in one of the layers, but not in the others, depending on the effective electrical conductivity of the materials considered.

## 4 Formation of hot-spots in a three-layer finite slab

In this section, we consider a unit slab composed of three layers of three different materials. As we are concerned in this work with hot-spots formation, the inside layer considered has a thermal conductivity which differs considerably from that of the outer layers. Homogeneous Dirichlet boundary conditions will be used. Although these conditions are very idealized, they have the advantage of making the investigation more manageable, thus leading to a better understanding of the thermal conductivity. Future work will be done to extend this approach by including more general boundary conditions.

Let us first consider a domain  $D$  with a constant conductivity parameter  $\mu$  throughout  $D$ . From the transformation (3.11), we obtain

$$\theta = \frac{1}{\gamma} \log \left( 1 + \frac{\gamma u}{\mu} \right), \quad (4.34)$$

where the conductivity  $k(\theta) = \mu e^{\gamma\theta}$ . Here  $u(x, t) \approx A(t)\varphi_1(x)$ , where  $A(t)$  satisfies

$$\frac{dA}{dt} = -\lambda_1^2 A + \delta I(A), \quad (4.35)$$

$$A(0) = C_1, \quad (4.36)$$

$$I(A) = \int_D R(x)F(A\varphi_1(x))\varphi_1(x)dx, \quad (4.37)$$

and  $\varphi_1, \lambda_1$  are the first eigenfunction and eigenvalue of the boundary value problem

$$\Delta\varphi_n = -\lambda_n^2\varphi_n \quad , \quad \varphi_n = 0 \quad \text{on} \quad \partial D . \quad (4.38)$$

Thus

$$\theta \approx \frac{1}{\gamma} \log \left( 1 + \frac{\gamma A \varphi_1(x)}{\mu} \right). \quad (4.39)$$

If we consider two separate domains with conductivity  $k_1 = \mu_1 e^{\gamma\theta}$  and  $k_2 = \mu_2 e^{\gamma\theta}$ , respectively, where  $\mu_1 > \mu_2$ , it is clear that the domain with the lower conductivity  $\mu$  reaches a higher temperature, independently of the value of  $\gamma$ . This simple analysis suggests that non-homogeneity of thermal conductivity may contribute to the formation of hot-spots.

#### 4.1 Formulation of the problem

Let us consider a unit slab  $[0,1]$  composed of three layers having thermal conductivity  $k(\theta)$  expressed in the form

$$k(\theta) = \begin{cases} \mu_1 e^{\gamma\theta} & \text{if } 0 \leq x < x_0 \\ \mu_2 e^{\gamma\theta} & \text{if } x_0 \leq x \leq x_0 + \varepsilon \\ \mu_3 e^{\gamma\theta} & \text{if } x_0 + \varepsilon < x \leq 1 . \end{cases} \quad (4.40)$$

We formulate the problem by dividing the interval  $[0, 1]$  into three parts, that is  $[0, x_0]$ ,  $[x_0, x_0 + \varepsilon]$  and  $[x_0 + \varepsilon, 1]$ , for small  $\varepsilon$ . Let  $\theta_1, \theta_2$ , and  $\theta_3$  be the temperature in the intervals  $[0, x_0]$ ,  $[x_0, x_0 + \varepsilon]$  and  $[x_0 + \varepsilon, 1]$ , respectively. For simplification we will consider the steady-state solution only. We can obtain steady-state temperature  $\theta_1, \theta_2$ , and  $\theta_3$  by solving

$$\theta_i = \frac{1}{\gamma} \log \left( 1 + \frac{\gamma u_i}{\mu_i} \right) \quad , \quad i = 1, 2, 3 , \quad (4.41)$$

where  $u_i$  is the solution of

$$\frac{d^2 u_i}{dx^2} + \delta R(x)F_i(u_i) = 0 \quad , \quad i = 1, 2, 3 , \quad (4.42)$$

$$F_i(u_i) = \exp \left\{ \frac{\frac{\alpha}{\gamma} \log \left( 1 + \frac{\gamma u_i}{\mu_i} \right)}{\alpha + \frac{1}{\gamma} \log \left( 1 + \frac{\gamma u_i}{\mu_i} \right)} \right\} \quad , \quad i = 1, 2, 3 . \quad (4.43)$$

Across the interfaces, the temperature  $\theta$  as well as the heat flux  $k(\theta) d\theta/dx$  are continuous (see [39]). Using (4.41) and the requirement that  $\theta$  is continuous on the interfaces, that is  $\theta_1(x_0) = \theta_2(x_0)$  and  $\theta_2(x_0 + \varepsilon) = \theta_3(x_0 + \varepsilon)$ , we have the conditions

$$u_1(x_0) = \mu_1 a, \quad u_2(x_0) = \mu_2 a, \quad (4.44)$$

and

$$u_2(x_0 + \varepsilon) = \mu_2 b, \quad u_3(x_0 + \varepsilon) = \mu_3 b, \quad (4.45)$$

where  $a$  and  $b$  have to be determined as a part of the problem. Together with homogeneous Dirichlet boundary conditions, this continuity of the temperature yields boundary conditions for each layer

$$u_1(0) = 0, \quad u_1(x_0) = \mu_1 a, \quad (4.46)$$

$$u_2(x_0) = \mu_2 a, \quad u_2(x_0 + \varepsilon) = \mu_2 b, \quad (4.47)$$

$$u_3(x_0 + \varepsilon) = \mu_3 b, \quad u_3(1) = 0. \quad (4.48)$$

The heat flux in each layer may be written as

$$k(\theta_i) \frac{d\theta_i}{dx} = \frac{e^{\gamma\theta_i}}{1 + \frac{\gamma u_i}{\mu_i}} \frac{du_i}{dx}. \quad (4.49)$$

Noting that  $\theta$  is continuous on the interfaces  $x = x_0, x_0 + \varepsilon$  and using the conditions for  $u_i(x_0)$  and  $u_i(x_0 + \varepsilon)$  above, we see that the continuity of the heat flux across the interfaces may be written in the form

$$\left. \frac{du_1}{dx} \right|_{x=x_0^-} = \left. \frac{du_2}{dx} \right|_{x=x_0^+} \quad (4.50)$$

and

$$\left. \frac{du_2}{dx} \right|_{x=x_0+\varepsilon^-} = \left. \frac{du_3}{dx} \right|_{x=x_0+\varepsilon^+}. \quad (4.51)$$

## 4.2 Steady-state solutions

To solve the problem defined by (4.42), (4.46), (4.47), and (4.48), for all the intervals  $[0, x_0]$ ,  $[x_0, x_0 + \varepsilon]$ , and  $[x_0 + \varepsilon, 1]$ , we introduce the following transformations.

$$u_1 = \varphi + \mu_1 a \frac{x}{x_0}, \quad u_2 = \psi + \mu_2 \frac{(b-a)(x-x_0)}{\varepsilon} + \mu_2 a, \quad (4.52)$$

and

$$u_3 = \chi + \mu_3 b \left( 1 - \frac{x-x_0-\varepsilon}{1-x_0-\varepsilon} \right), \quad (4.53)$$

where  $\varphi$ ,  $\psi$ , and  $\chi$  satisfy

$$\frac{d^2\varphi}{dx^2} + \delta R(x) F_1(u_1) = 0, \quad \varphi(0) = \varphi(x_0) = 0, \quad (4.54)$$

$$\frac{d^2\psi}{dx^2} + \delta R(x) F_2(u_2) = 0, \quad \psi(x_0) = \psi(x_0 + \varepsilon) = 0, \quad (4.55)$$

$$\frac{d^2\chi}{dx^2} + \delta R(x) F_3(u_3) = 0, \quad \chi(x_0 + \varepsilon) = \chi(1) = 0. \quad (4.56)$$

In the first interval,  $[0, x_0]$ , using the above transformation and the the fundamental-mode approximation, we obtain  $\varphi \approx A\phi_1$ , where  $\phi_1(x) = \sqrt{\frac{2}{x_0}} \sin\left(\frac{\pi}{x_0}x\right)$  is the eigenfunction corresponding to the smallest eigenvalue  $\lambda_1 = \pi^2/x_0^2$  of the eigenvalue problem

$$\frac{d^2\phi}{dx^2} = -\lambda^2\phi, \quad \phi(0) = \phi(x_0) = 0. \quad (4.57)$$

The parameter A in this approximation satisfies

$$-A + \frac{\delta}{\lambda_1^2} \int_0^{x_0} E(x)F_1(u_1)\phi_1 dx = 0, \quad (4.58)$$

and

$$u_1 \approx A\sqrt{\frac{2}{x_0}} \sin\left(\frac{\pi}{x_0}x\right) + \mu_1 a \frac{x}{x_0}. \quad (4.59)$$

For the second interval,  $[x_0, x_0 + \varepsilon]$ , we make a transformation  $\xi = x - x_0$  and so  $\psi = \psi(\xi)$ . Again, using the fundamental-mode approximation we obtain  $\psi_1 \approx B\vartheta_1$ , where  $\vartheta_1 = \sqrt{\frac{2}{\varepsilon}} \sin\left(\frac{\pi}{\varepsilon}\xi\right)$  is the eigenfunction corresponding to the smallest eigenvalue  $\nu_1 = \pi^2/\varepsilon^2$  of the eigenvalue problem

$$\frac{d^2\vartheta}{d\xi^2} = -\nu^2\vartheta, \quad \vartheta(0) = \vartheta(\varepsilon) = 0. \quad (4.60)$$

Here, B satisfies

$$-B + \frac{\delta}{\nu_1^2} \int_{x_0}^{x_0+\varepsilon} R(x)F_2(u_2)\vartheta_1 dx = 0, \quad (4.61)$$

and

$$u_2 \approx B\sqrt{\frac{2}{\varepsilon}} \sin\left(\frac{\pi}{\varepsilon}(x - x_0)\right) + \mu_2 \frac{(b - a)(x - x_0)}{\varepsilon} + \mu_2 a. \quad (4.62)$$

For the last interval,  $[x_0 + \varepsilon, 1]$ , we use a transformation  $\eta = x - x_0 - \varepsilon$ , so that  $\chi = \chi(\eta)$ . Again, using the fundamental-mode approximation we obtain  $\chi \approx Cv_1$ , where  $v_1 = \sqrt{\frac{2}{1-x_0-\varepsilon}} \sin\left(\frac{\pi}{1-x_0-\varepsilon}\eta\right)$  is the eigenfunction corresponding to the smallest eigenvalue  $\tau_1 = \pi^2/(1 - x_0 - \varepsilon)^2$  of the eigenvalue problem

$$\frac{d^2v}{d\eta^2} = -\tau^2v, \quad v(0) = v(1 - x_0 - \varepsilon) = 0. \quad (4.63)$$

In this approximation, C satisfies

$$-C + \frac{\delta}{\tau_1^2} \int_{x_0+\varepsilon}^1 R(x)F_3(u_3)v_1 dx = 0, \quad (4.64)$$

and

$$u_3 \approx C \sqrt{\frac{2}{1-x_0-\varepsilon}} \sin\left(\pi \frac{x-x_0-\varepsilon}{1-x_0-\varepsilon}\right) + \mu_3 b \left(1 - \frac{x-x_0-\varepsilon}{1-x_0-\varepsilon}\right). \quad (4.65)$$

From (4.58), (4.61), and (4.64), we obtain three equations and five independent variables A, B, C, a, dan b. To solve them, we use the interface conditions (4.50) and (4.51) to obtain two additional equations

$$-A \left(\frac{\pi}{x_0}\right) \sqrt{\frac{2}{x_0}} + \mu_1 \frac{a}{x_0} = B \left(\frac{\pi}{\varepsilon}\right) \sqrt{\frac{2}{\varepsilon}} + \mu_2 \frac{b-a}{\varepsilon} \quad (4.66)$$

and

$$-B \left(\frac{\pi}{\varepsilon}\right) \sqrt{\frac{2}{\varepsilon}} + \mu_2 \frac{b-a}{\varepsilon} = C \left(\frac{\pi}{1-x_0-\varepsilon}\right) \sqrt{\frac{2}{1-x_0-\varepsilon}} - \mu_3 \frac{b}{1-x_0-\varepsilon}. \quad (4.67)$$

Equations (4.66) dan (4.67) may be written in the matrix form  $\mathbf{A}[a \ b]^T = [c_1 \ c_2]^T$ ,

$$\begin{bmatrix} \frac{\mu_1}{x_0} + \frac{\mu_2}{\varepsilon} - \frac{\mu_2}{\varepsilon} & \\ -\frac{\mu_2}{\varepsilon} & \frac{\mu_2}{\varepsilon} + \frac{\mu_3}{1-x_0-\varepsilon} \end{bmatrix} \begin{bmatrix} a \\ b \end{bmatrix} = \begin{bmatrix} A \frac{\pi}{x_0} \sqrt{\frac{2}{x_0}} + B \frac{\pi}{\varepsilon} \sqrt{\frac{2}{\varepsilon}} \\ B \frac{\pi}{\varepsilon} \sqrt{\frac{2}{\varepsilon}} + C \frac{\pi}{1-x_0-\varepsilon} \sqrt{\frac{2}{1-x_0-\varepsilon}} \end{bmatrix}. \quad (4.68)$$

The solutions  $a$  and  $b$  (4.68) can be expressed in the following

$$a = \frac{A_{22}c_1 - A_{12}c_2}{\text{Det}(\mathbf{A})}, \quad (4.69)$$

$$b = \frac{A_{11}c_2 - A_{21}c_1}{\text{Det}(\mathbf{A})}, \quad (4.70)$$

where  $\text{Det}(\mathbf{A})$  is the determinant of the matrix  $\mathbf{A}$  in (4.68).

Substituting (4.69) and (4.70) into (4.58), (4.61) and (4.64) we obtain three equations with three unknowns: A, B, and C. Using these values, we may then compute  $a$  and  $b$  from (4.69) and (4.70). Further, from (4.59), (4.62) and (4.65) we calculate  $u_1$ ,  $u_2$ , and  $u_3$  and finally, using

$$\theta_i = \frac{1}{\gamma} \log\left(1 + \frac{\gamma u_i}{\mu_i}\right), \quad i = 1, 2, 3, \quad (4.71)$$

we obtain the temperature  $\theta_i$ ,  $i = 1, 2, 3$ .

## 5 Numerical results

In the following we will present results for the smallest steady-state solutions  $A$ ,  $B$ , and  $C$  whenever there is more than one steady-state solution of (4.58), (4.61) and (4.64). This solution can be seen as the steady-state temperature having the initial condition equal to 0 (the normalized ambient temperature). In all computations, we have taken  $\alpha = 10$ ,  $\varepsilon = 0.1$ ,  $\gamma = 0.1$ , and  $\delta = 1$ . Based on a simplifying assumption described in Section 2, we take  $R(x) = e^{-|x-0.5|}$ .

First, we take  $\mu_1 = \mu_3 = 1$  and  $\mu_2 = 1, 10^{-1}, 10^{-2}, 10^{-3}$  in Figure 5.3 (a), (b), (c), and (d), respectively. The middle part of the slab is located at  $x_0 = 0.45$  in the interval  $[0,1]$ . Figure 5.3 (a) simply shows that the conductivity parameter  $\mu$  is constant throughout the region  $[0,1]$ . As expected by using a fundamental-mode approximation, the temperature profile in Figure 5.3 (a) is zero on the boundaries  $x = 0$  and  $x = 1$  and reaches a maximum value in the middle of the slab. By taking smaller  $\mu_2$  in the region  $[x_0, x_0 + \varepsilon]$ , we find that the temperature in this region is higher than elsewhere. Figures 5.3 (b), (c), (d) show that, the smaller the value  $\mu_2$ , the larger will be the discrepancy of the temperature between  $[x_0, x_0 + \varepsilon]$  and the rest of the region. These figures show an interesting feature. The change in the parameter  $\mu$  from  $10^{-1}$  to  $10^{-2}$  does not lead to a significant change in the temperature of the inner layer. However, the change of  $\mu$  from the  $10^{-2}$  to  $10^{-3}$  results in a drastic change in the temperature of the inner layer, suggesting the existence of a critical value  $\mu$  below which thermal runaway is experienced pointing the formation of a hot-spots.

We further calculate the temperature of the middle interval of the inner layer  $[x_0, x_0 + \varepsilon]$  with the same parameters as in Figure 5.3, but we change the values of  $\mu$  from  $\mu = 10^{-2}$  to  $\mu = 10^{-3}$ . This produce the following results

$\mu$	0.01	0.009	0.008	0.007	0.006	0.005	0.004	0.003	0.002	0.001
$\theta$	0.221	0.238	0.261	0.291	0.333	0.399	0.511	0.767	56.898	65.568

It shows that there is a jump in the temperature of the inner layer that occurs for the values of  $\mu$  in the range  $0.003 < \mu < 0.002$ .

In Section 3, we made an investigation of the bifurcation diagram of  $\theta$  vs. the parameter  $\delta$  where this  $\delta$  measures the magnitude (power) of the square amplitude of the electric field. The thermal runaway is investigated through an S-shaped curve of an Arrhenius-type reaction rate of the microwave-energy absorption vs. temperature. There, we found a critical value  $\delta^{cr}$  where a slight change in  $\delta$  near this critical value results in a substantial change in the temperature. Several authors have made similar investigations, *e.g.* in [22], [35], [41], and elsewhere. The numerical investigation above calls for further investigations into the effect of the parameter  $\mu$  and its critical value(s).



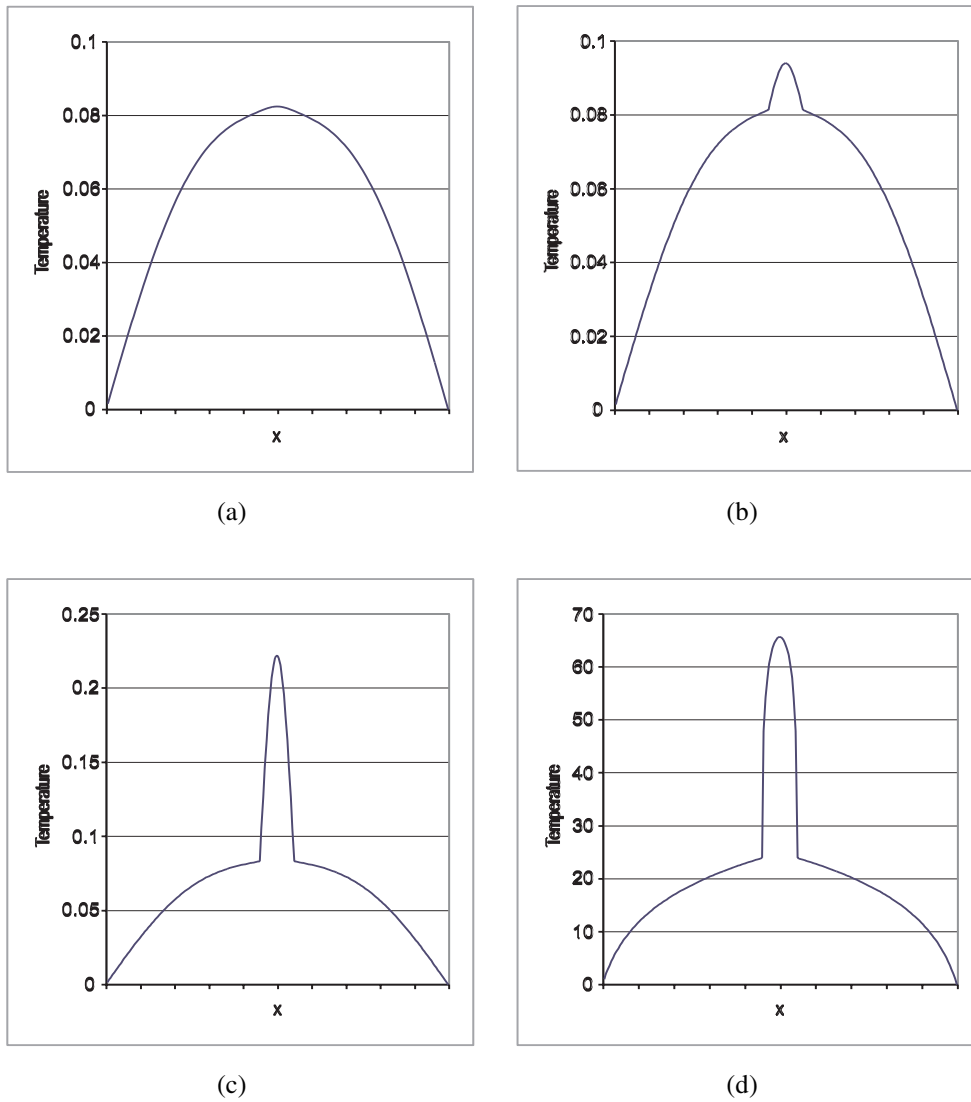


Figure 5.3: The steady-state temperature with a constant parameter  $\gamma = 0.1$ , and for the thermal conductivity parameter  $\mu_1 = \mu_3 = 1$  in outer layers while in the inner layer (a)  $\mu_2 = 1$ , (b)  $\mu_2 = 10^{-1}$ , (c)  $\mu_2 = 10^{-2}$ , (d)  $\mu_2 = 10^{-3}$ . Notice the temperature jump from the value computed for  $\mu_2 = 10^{-2}$  to that computed for  $\mu_2 = 10^{-3}$ .

In Figure 5.4, we show the steady-state temperature in the center of each of the subintervals  $[0, x_0]$ ,  $[x_0, x_0 + \varepsilon]$  and  $[x_0 + \varepsilon, 1]$  as a function of the position  $x_0$  where  $\mu_1 = \mu_3 = 1$ ,  $\mu_2 = 10^{-2}$ . A similar computation is carried out in Figure 5.4 (b), but now for  $\mu_2 = 10^{-3}$ . Comparing these figures, for any position  $x_0$ , there is a jump in temperature from the values computed for  $\mu_2 = 10^{-2}$  in Figure 5.4 (a) to those for  $\mu_2 = 10^{-3}$  in Figure 5.4 (b). These jumps, again, suggest the existence of the critical value(s) of  $\mu$ .

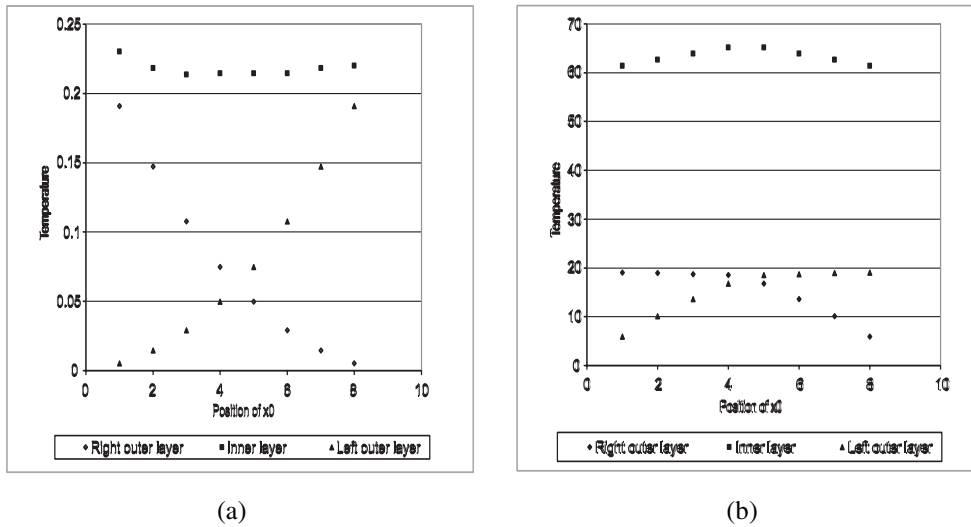


Figure 5.4: (a) The steady-state temperature in the middle of each of the subintervals  $[0, x_0]$ ,  $[x_0, x_0 + \varepsilon]$  and  $[x_0 + \varepsilon, 1]$  as a function of the position  $x_0$ , where  $\mu_1 = \mu_3 = 1$ ,  $\mu_2 = 10^{-2}$  and  $\gamma = 0.1$ . (b) Same as in Figure (a), but now for  $\mu_1 = \mu_3 = 1$ ,  $\mu_2 = 10^{-3}$ . Notice the temperature jump from the values computed for  $\mu_2 = 10^{-2}$  in Figure (a) and those for  $\mu_2 = 10^{-3}$  in Figure (b).

## 6 Concluding remarks

We have considered a simplified model of the microwave heating of a one-dimensional unit slab. We have described an eigenfunction expansion for the problem based on the Galerkin method and have used a fundamental-mode approximation. We have made an investigation of the bifurcation diagram of the temperature  $\theta$  vs. the parameter  $\delta$  where this  $\delta$  measures the magnitude (power) of the square amplitude of the electric field. The thermal runaway has been investigated through an S-shaped curve of an Arrhenius-type reaction rate of the microwave-energy absorption vs. temperature. Critical values  $\delta^{cr}$  has been found. The critical value  $\delta^{cr}$  is of the interest, where slight changes in  $\delta$  near this critical value result in substantial changes in the temperature. Similar investigations and results can be found in [22], [35], [41], and elsewhere.

We have further applied the approximation to a unit slab consisting of three layers of material with different thermal conductivities. We have taken the thermal conductivity to be

of the form  $k(\theta) = \mu e^{\gamma\theta}$ , where  $\theta$  is the temperature, while the parameter  $\mu$  has different values in each of the three layers. This  $\mu$  measures the magnitude of the thermal conductivity of the material. We have addressed the hot-spots formation by finding the global steady-state solution for the whole domain of different thermal conductivities in which the inner layer has a smaller value of the parameter  $\mu$ .

By making  $\mu$  smaller in the inner layer than in the outer layers, according to prediction, we find a temperature in this region that is higher than in the rest. The larger the difference of  $\mu$  in the inner and outer layers, the larger will be the discrepancy of the temperature between the inner layer and the rest of the region. It is very interesting to see that given a fixed value of  $\delta$ , there is a temperature jump of the inner layer near some value of  $\mu$ . This jump shows that there is a critical value of the parameter  $\mu$  below which thermal runaway is experienced, thus signifying the formation of hot-spots.

We remark that, although the paper is concerned with hot-spots formation, the approach may be applied to a three-layer configuration of a finite slab. Further, the use of Dirichlet boundary conditions, which is very idealistic, allows a more manageable investigation into the parameter dependence of the problem. Future work will include more realistic heat-flux conditions on the boundaries and further study on the effects of the parameter  $\mu$  and its critical value(s) will be done.

## Acknowledgments

This research was initiated during a research workshop at Pusat Matematika (P4M-ITB) in August/September 1996 in cooperation with the University of Twente, The Netherlands. Funding for this research was partly provided by the Center Grant (P4M-ITB) and the Royal Netherlands Academy of Arts and Sciences, KNAW. The authors are very grateful to Prof K.K. Tam, Dr. Edy Soewono, Prof. E. van Groesen and Mr. Toto Nusantara for discussions, suggestions, and encouragement during the writing of this paper. They would like to thank the referees whose comments lead to a significant change and expanded version of the original manuscript.

## Bibliography

- [1] ANDONOWATI, *A study of some problems arising from combustion and the microwave heating*. Ph.D. thesis, McGill University, Montreal, Canada, 1995.
- [2] ANDONOWATI, A two-sided shooting method in computation of travelling combustion waves of a solid material. *J. Austral. Math. Soc. Ser. B.*, 38:220-228, 1996.
- [3] ANDONOWATI, Microwave heating: Critical dependence on data and parameters. In: E. van Groesen and E. Soewono (eds.), *Differential Equations: Theory, Numeric, and Applications*, Dordrecht: Kluwer, 189–210, 1997.
- [4] J.C. ARANETA, M.E. BRODWIN, and G.A. KRIEGSMANN, High temperature characterization of dielectric rods. *IEEE MTT*, 32:1328–1334, 1984.
- [5] C.L. BABCOCK, Viscosity and electrical conductivity of molten glasses. *Journal of the American Ceramic Society*, 17:329–342, 1934.
- [6] A.J. BERTRAN and J.C. BADOT, High temperature microwave heating in refractory materials. *J. Microwave Power*, 11:315–320, 1976.
- [7] M.E. BRODWIN, and D.L. JOHNSON, Microwave sintering of ceramics. *MIT-S*, K5:287–288, 1988.
- [8] W.A. VAN DEN BROEK, *Glass Morphology in Manufacturing Jars*. Master's Thesis. Eindhoven University of Technology, 1996.
- [9] A.W. BUSH, *Perturbation Methods for Engineers and Scientists*. CRC Press, London, 1992.
- [10] C.J. COLEMAN, On the microwave hot-spot problem. *J. Austral. Math. Soc. Ser. B*, 33:1–8, 1991.
- [11] W.C. DOWLING, H.V. FAIRBANKS, and W.A. KOEHLER. A study of the effect of lubricants on molten glass to heated metals. *Journal of the American Ceramic Society*, 33:269–273, 1950.
- [12] M. VAN DYKE, *Perturbation Methods in Fluid Mechanics*. The Parabolic Press, California, 1975.
- [13] M. VAN DYKE, Slow Variations in Continuum Mechanics. *Advances in Applied Mechanics*, 25:1–45, 1987.
- [14] M. VAN DYKE, Slow Variations in Fluid Mechanics. *Applied Mathematics in Aerospace Science and Engineering* (Erice, 1991), pp. 3-12, in *Mathematical Concepts and Methods in Science and Engineering* 44, Plenum, New York, 1994.
- [15] W. ECKHAUS, *Asymptotic Analysis of Singular Perturbation*. North Holland Publishing Company, Amsterdam, 1979.
- [16] M. FALIPOU, F. SICLOROFF, and C. DONNET, New method for measuring the friction between hot viscous glass and metals. *Glastechnische Berichte* 72:59–66, 1999.
- [17] R. FRISCH-FAY, *Flexible Bars*. Butterworths & Co, London, 1962.
- [18] A.C. FOWLER, *Mathematical Models in the Applied Sciences*. Cambridge University Press, Cambridge, 1998.
- [19] D.A. FRANK-KAMENETSKII and J.P. APPLETON, *Diffusion and Heat Transfer in Chemical Kinetics*. Plenum, New York, 1969

- [20] J. DE. GRAAF, T.D. CHANDRA, and R. DUIJS, On A Boundary Operator Equation For Stokes Flow (article in preparation).
- [21] I.S. GRADSHTEYN and I.M. RYZHIK, *Table of Integrals, Series, and Products*. Academic Press, San Diego, 2000.
- [22] J.M. HILL and N.F. SMYTH, On the mathematical analysis of hotspots arising from microwave heating. *Math. Engng. Ind.*, 2:267–278, 1990.
- [23] J.M. HILL and M.J. JENNINGS, Formulation of model equations for heating by microwave radiation. *Appl. Math. Modelling*, 17:1823–1834, 1993.
- [24] E.J. HINCH, *Perturbation Methods*. Cambridge University Press, Cambridge, 1991.
- [25] M.H. HOLMES, *Introduction to Perturbation Methods*. Springer Verlag, Berlin, 1995.
- [26] J. KEVORKIAN and J.D. COLE, *Multiple Scale and Singular Perturbation Methods*. Springer-Verlag, New York, 1996.
- [27] G.A. KRIEGSMANN, M.E. BRODWIN, and D.G. WATTER, Microwave heating of ceramic half-space. *SIAM J. Appl. Math.*, 50:1088–1098, 1990.
- [28] G.A. KRIEGSMANN, Thermal runaway in microwave heated ceramics: a one-dimensional model. *J. Appl. Phys*, 71:1960–1966, 1992.
- [29] A. LACEY and G.C. WAKE, Thermal ignition with variable thermal conductivity. *IMA J. Appl. Math.*, 28:23–39, 1982.
- [30] K. LAEVSKY and R.M.M. MATTHEIJ, Mathematical modeling of some glass problems. In: A. FASANO(ed.), *Complex Flows in Industrial Processes*. Birkhäuser, Boston, 2000.
- [31] P.A. LAGERSTROM, *Matched Asymptotic Expansions*. Springer Verlag, Berlin, 1980.
- [32] L.D. LANDAU and E.M. LIFSHITZ, *Fluid Mechanics*. Pergamon Press, Oxford, 2<sup>nd</sup> edition, 1987.
- [33] T.R. MARCHANT, Microwave heating of materials with impurities. *J. Engng. Math.*, 28: 379–400, 1994.
- [34] T.R. MARCHANT and A.H. PICOMBE, Microwave heating of materials with temperature dependent properties. *Wave Motion*, 19:67–81, 1994.
- [35] T.R. MARCHANT and B. LIU, The steady-state microwave heating of slabs with small Arrhenius absorptivity. *J. Engng. Math.*, 33:219–236, 1998.
- [36] B.S. MASSEY, *Mechanics of Fluids*. Van Nostrand Reinhold (International) Co. Ltd., London, 1989.
- [37] P. MOON and D.E. SPENCER, *Field Theory Handbook*. Springer-Verlag, Berlin, 1961.
- [38] NAOTO TANAKA, On the Boundary Value Problem for the Stationary Stokes System in the Half-Space. *Journal of Differential Equations* 115:70–74, 1995.
- [39] N. OEZISIK, *Heat Conduction*. Wiley Interscience, New York, 1980.
- [40] B.S. PADMAVATHI, G.P. RAJA SEK HAR, and T. AMARANATH, A Note on Complete General Solutions of the Stokes Equations. *Quarterly Journal of Mechanics and Applied Mathematics*, 51:383–388, 1998.
- [41] J.A. PALESKO and J.A. KRIEGSMANN, Microwave heating of ceramic laminates. *J. Engng. Math.*, 32:1–18, 1997.

- [42] A.H. PICOMBE and N.F. SMYTH, Microwave heating of materials with low conductivity. *Proc. R. Soc. London. A*, 433:479–498, 1991.
- [43] A.D. PIERCE, *Acoustics: An Introduction to its Physical Principles and Applications*. McGraw-Hill Book Company, New York, 1989.
- [44] G. ROUSSY, A. BENNANI, and J. THIEBAUT, Temperature runaway of microwave irradiated materials. *J. Appl. Phys.*, 62:1167–1170, 1987.
- [45] B.P. RYNNE and M.A. YOUNGSON, *Linear Functional Analysis*. Springer-Verlag, London, 2000.
- [46] X.X. SHENG and W.M. ZHONG, General Complete Solutions of the Equations of Spatial and Axisymmetric Stokes Flow. *Quarterly Journal of Mechanics and Applied Mathematics* 44:537–548, 1991.
- [47] PH. SIMONS and R.M.M. MATTHEIJ, *The Cooling of Molten Glass In a Mould*. Rana 95-21, Eindhoven University of Technology, 1995.
- [48] N.F. SMYTH, Microwave heating of bodies with temperature dependent properties. *Wave Motion*, 12:171–186, 1990.
- [49] N.F. SMYTH, The effect of conductivity on hotspots. *J. Austral. Math. Soc. Ser. B*, 33:403–413, 1992.
- [50] S.L. DE SNOO, R.M.M. MATTHEIJ, and G.A.L. VAN DE VORST, *Modelling of Glass, in Particular Small Scale Surface Changes*. Rana 96-11, Eindhoven University of Technology, 1996.
- [51] I. STAKGOLD, *Green's Functions and Boundary Value Problem*. John Wiley & Sons, Inc., Toronto, 1998.
- [52] K. K. TAM, Criticality dependence on data and parameters for a problem in combustion theory, with temperature-dependent conductivity. *J. Austral. Math. Soc. B.*, 31:76–80, 1989.
- [53] K.K. TAM, ANDONOWATI, and M.T. KIANG, Nonlinear eigenfunction expansion for a problem in microwave heating. *Canad. Appl. Math. Q.* 4:311–325, 1996.
- [54] Y.L. TIAN, M.E. BRODWIN, and D.L. JOHNSON, Ultra-fine microstructure of  $Al_2O_3$  produced by microwave sintering. *Ceramic Transactions*, 1:925–931, 1987.
- [55] W. TRIER, and F. HASSOUN, Mechanik des Gleitens Heißen, Zähflüssigen Glases auf Metalloberflächen. *Glastechnische Berichte*, 45:271–276, 1972.
- [56] W. TRIER, Gleitverhalten von Heißem, Zähflüssigem Glas auf Metalloberflächen. *Glastechnische Berichte*, 51:240–243, 1978.
- [57] F.V. TOOLEY, *The Handbook of Glass Manufacture Vol II*. Books For Industry, Inc, and Glass Industry Magazine, New York, 1974.
- [58] Y. YENER and S. KAKAC, *Heat Conduction*, Taylor & Francis, Washington DC, 3<sup>rd</sup> edition, 1993.

# Index

- Arrhenius-type, 113, 114
- asymptotic expansion, 11
  - Poincaré expansion, 11, 13, 39
  - regular perturbation expansion, 13, 40
  - singular perturbation expansion, 13
- asymptotic sequence, 11, 12
- bifurcation diagram, 119
- blowing, 50
- boundary layer, 15
  - composite expansion, 18
  - distinguished limit, 17
  - inner expansion, 16, 30, 36, 47
  - inner region, 16
  - inner solutions, 36
  - matching by an intermediate variable, 17, 22
  - matching by Van Dyke's rule, 18, 21
  - nonuniformity, 15
  - outer expansion, 16, 28, 45
  - outer region, 16
  - outer solution, 36
  - principle of the least degeneracy, 17
  - thickness of the boundary layer, 16
- boundary value problem, 116, 121
- conductivity
  - conductivity parameter, 114, 120
  - thermal conductivity, 114, 121
- cylindrical coordinates, 52, 53, 56
  - axisymmetric, 52
- damped wave equation, 113, 114
  - travelling-wave solution, 114
- Dirichlet problem, 74
- eigenfunction, 31
- eigenfunctions, 116
  - first eigenfunction, 121
- eigenvalues, 116
  - smallest eigenvalue, 123
- energy equation, 54, 55
- exponentially small term, 9
- exterior of the unit ball, 88
- exterior of the unit disk, 85
- flux, 60
  - heat flux, 38, 39
  - volume flux, 44
- Fourier Sine Transform, 33
- Fourier's law, 54
- free boundary, 58
- fundamental-mode approximation, 118, 123
- glass, 50
  - density, 53
  - incompressible, 51, 54, 59, 60
  - Newtonian, 54
  - velocity, 56
- Green's function, 33
- Green's second identity, 34
- half-space, 98
- harmonic
  - harmonic extension, 73, 74
  - harmonic function, 82, 88
  - harmonic homogen polynomials, 84
  - harmonic vector fields, 82
- heat conduction, 24, 27, 40
  - insulated boundary condition, 27
- heat flux, 122
- hot-spots, 112, 114, 119–121, 125, 128
- infinite strip, 101
- interior of the unit ball, 79
- interior of the unit disk, 77

- Laplace equation, 74
- Large  $O$ , 8
  - uniformly, 8
- microwave heating, 113
- mould, 50, 52
  - boundary condition, 58
  - impermeable, 60
  - stationary, 60, 64
  - straight cylinders, 65, 69
- Navier-Stokes equations, 42, 51, 53
- Neumann problem, 75
- number
  - Brinkman number, 55
  - Eckert number, 54
  - Peclet number, 54
  - Prandtl number, 54
  - Reynolds number, 43, 53, 54
- operator equation, 76, 77, 83, 86, 89, 92, 95, 98, 102, 106
- parison, 50
- plunger, 50, 52
  - boundary condition, 57
  - force, 60, 61, 65, 67
  - straight cylinders, 65, 69
  - top of the plunger, 56, 63
  - velocity, 53, 63, 64
- pressing, 50
- pressure gradient, 62
- resolvents, 79
- Reynold's lubrication-flow, 53
- S-shaped curve, 116
- slight variation
  - slightly varying geometry, 39, 47
- slip
  - Coulomb's friction, 56
  - friction factor, 56
  - mixed boundary conditions, 64, 67
  - Navier's slip condition, 56
  - no friction, 56
  - no-slip boundary conditions, 64, 67
  - slip coefficient, 57
  - slip factor, 56
  - slip velocity, 56, 57
- slow variation
  - slender-geometry approximation, 52, 59
  - slowly varying geometry, 24
- Small  $o$ , 8
  - uniformly, 9
- steady-state solution, 116
- Stokes equations, 42, 47, 74
  - inhomogeneous SBVP, 73
  - solution, 76
  - Stokes boundary value problems (SBVP), 73
- stress, 60
  - shear stress, 56
- Sturm-Liouville, 32
- tangent vector field, 76, 83
- temperature, 114, 121, 122
  - absolute temperature, 54
  - bulk temperature, 54
- tensor
  - fluid stress tensor, 51
  - rate-of-strain tensor, 51
  - unit tensor, 51
  - viscous stress tensor, 51, 54
- theorem
  - Gauss' divergence theorem, 60
- transcendentally small term, 9
- transversal gradient, 27
- velocity, 52
  - wall velocity, 56
- viscosity, 54
  - constant viscosity, 54
  - dynamic viscosity, 52, 53
  - temperature-dependent, 54
  - uniform temperature, 52
- wedge, 106



# Summary

This research investigates a number of problems, related to Stokes flow and to heat flow. The Stokes flow is inspired by glass flow in the process of making bottles or jars. The heat flow is related to a heat conduction model problem, and a problem about hot-spots formation in the microwave heating. We will discuss the first problem.

There are two phases during the industrial process of making glass, *viz.* the pressing phase and the blowing phase. We consider some mathematical aspects of the pressing phase. The motion of glass at temperatures above  $600^{\circ}C$  can be described by the Navier-Stokes equations. Since glass is a highly viscous fluid, those equations can be simplified to the Stokes equations. We use two different methods to solve these equations, *viz.* perturbation and operator methods. The perturbation method is based on the geometry being slowly varying. As a result, we obtain the velocity analytically. This result has a good agreement with numerical results based on finite element modelling. Using the velocity obtained we derive the formula for the force on the plunger.

Next, we consider the operator method. Using this method, the Stokes equations can be transformed into an operator equation on the boundary  $\partial\Omega$  with a tangent vector field  $\alpha$  on the boundary  $\partial\Omega$  as unknown. Solving this operator equation shows, that the solutions of the Stokes equations can be parameterized by  $\alpha_{\mathcal{H}}$ , the *harmonic extension* of  $\alpha$  to the interior of the domain  $\Omega$ . As an application, we present some full explicit solutions of the Stokes equations for several domains such as the interior and exterior of the unit ball and of the unit disk, an infinite strip, a half space, and a wedge.

In the second problem, we consider the heat conduction problem inside two types of geometry, *viz.* slowly and slightly varying geometry. Using this problem, we show the difference between those geometries. An example that involves the boundary layers at the ends is presented.

Finally, we consider a simplified model of the microwave heating of a one-dimensional unit slab. This slab consists of three layers that have different thermal conductivities. We consider only the steady state problem with Dirichlet boundary conditions and continuity of heat flux across the layers. Using a fundamental-mode approximation of eigenfunction expansion, we investigate the effect of thermal conductivity on the formation of hot-spots where the temperature increases catastrophically as a function of  $\delta$ , the amplitude of the applied electric field. First, we consider a unit slab geometry. In this geometry, we find the critical value  $\delta^{cr}$ , for which slight changes in  $\delta$  yields a sudden jump to another stable solution, now with a much higher temperature. Next, we consider a unit slab consisting of three layers of material with different thermal conductivity ( $\mu$ ). We assume the inner layer has the smallest value of  $\mu$ . We find the temperature in this layer is much higher than that in other layers. Then, we consider only the inner layer. For a given value of  $\delta$  and changing values of  $\mu$ , we get a temperature jump near some values of  $\mu$ . This jump shows that there is a critical value of  $\mu$  and signifies the formation of a hot-spot.

# Acknowledgements

I would like to thank all the people who give a lot of contributions to the realization of this thesis. In the first place, my thanks to the corporation among Secondary School Teacher Development Project in Jakarta, Eindhoven University of Technology, and Delft University of Technology that give me the opportunity and financial support to do the doctorate research at Eindhoven University of Technology.

I would like to express my deepest gratitude to my promotor prof.dr.ir. J. de Graaf and my copromotor dr. S.W. Rienstra for their patience and helpful discussion during this research. Without their helps, this thesis will not be published.

My warm thanks go to Remco who helps a lot in studying the operator theory. I had many useful discussions with him. Special thanks to dr. Andonowati for the joined research about the hot-spot formation in microwave heating. During my study, I am lucky to work with wonderful colleagues in the Applied Analysis Group. I thank them all especially to Emilia and Agus Yodi Gunawan.

Additionally, I am indebted to all my friends at TUE, church, and 4U2 group for their kindly friendship. Also to Mrs. van Amsterdam and Koos who provided a nice room during my stay in Eindhoven.

Finally, many thanks to my dearest wife Juli and our beloved son Albert for their love, support, patience, and understanding throughout the many long years during the study.

# Curriculum Vitae

Tjang Daniel Chandra was born on December 8, 1965 in Malang, Indonesia. After finishing his senior high school in 1984, he studied Mathematics Education at the Institute of Teacher Training and Education at Malang and graduated in 1990. Subsequently, from 1991 he studied Mathematics at the Institut Teknologi Bandung and graduated in 1994. From January 1998 till May 2002 he carried out a doctoral research project at the Department of Mathematics and Computer Science, Eindhoven University of Technology. Until now, he is a lecturer at the Department of Mathematics, State University of Malang, Indonesia. He is married and has got one lovely son.

# Stellingen

behorende bij het proefschrift

## Perturbation and Operator Methods for Solving Stokes Flow and Heat Flow Problems

door

**Tjang Daniel Chandra**

### I

The entrance boundary layer representation of the heat conduction problem in a slowly varying geometry (Chapter I, section 4.1.2 of this Thesis) is essentially the same for its generalisation to the same problem but with a slowly varying conductivity

$$\nabla \cdot (\alpha(\varepsilon x, y, z) \nabla T) = 0,$$

and for the problem of long acoustic wave propagation in a slowly varying duct

$$\Delta \phi + \varepsilon^2 \kappa^2 \phi = 0,$$

of which the outer solution leads to Webster's equation.

### II

Stokes Boundary Value Problem (SBVP) can be transformed into an operator equation on the boundary  $\partial\Omega$  of the domain  $\Omega$  with a tangent vector field  $\alpha$  on  $\partial\Omega$  as unknown. Then, the solutions of SBVP can be calculated from  $\alpha_{\mathcal{H}}$ , the *harmonic extension* of  $\alpha$  to the interior of the domain  $\Omega$ .

(Chapter III of this thesis).

### III

Fundamental mode approximation is a simple but effective method to investigate the hot-spot formation in microwave heating.

(Chapter V of this thesis).

### IV

Perturbation and numerical methods are not contradictory but complementary to each other. Numerical methods produce primarily numbers, from which functional relationships may be derived. Perturbation methods produce primarily functional relationships, from which numbers may be derived.

### V

It is disappointing that the computer algebra package Maple (version 7) is still not able to produce Taylor series and asymptotic expansions of Bessel functions of arbitrary order.

## VI

The Runge-Kutta method can be used as an alternative method of finding roots of the equation  $f(x) = 0$  by considering the steady state solution of  $\frac{dx}{dt} = f(x)$ .

## VII

In [1], I.N. Herstein said that *25% of our Ph.D.'s go on to become researchers. While most of the other 75% end up teaching in the university.* In view of this it is desirable to introduce two types of Ph.D, one for those who want to be a researcher, and the other for those who want to be a lecturer.

## VIII

In [2], Weil states that *university teaching in mathematics should : (a) answer the requirements of all those who need mathematics for practical purposes; (b) train specialists in the subject; (c) give to all students that intellectual and moral training which any University has the duty to impart.* Those statements agree with the situation nowadays that the role of mathematics for industry is growing.

## IX

Mathematical software packages such as Mathematica, Maple, and MatLab can serve as a bridge between mathematics and engineering.

## References

- [1] I. N. HERSTEIN. On the Ph.D in Mathematics. *American Mathematical Monthly*, 76:818-824, 1969.
- [2] A. WEIL. Mathematical teaching in universities. *American Mathematical Monthly*, 61:34-36, 1954.